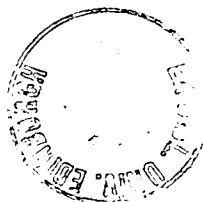


**Design of a Leg Mechanism with Controlled Phase,
Variable Stroke and Energy Storage Capability
for High Speed Locomotion**

Hamid Alper Oral

Doctor of Philosophy

**The University of Edinburgh
Mechanical Engineering Department
November 1992**



Abstract

To achieve high speeds with legs, a hybrid leg mechanism, which has been named Buraq, is designed. Buraq is actuated by a motor driven crank in longitudinal direction, and by a hydraulic ram in vertical direction. The crank radius and the phase can be adjusted during operation to allow legs driven by the same shaft to change phase and longitudinal stroke, so that gait shift and steering can take place. Also a force analysis of the leg mechanism has shown that, when the vehicle is running, the Buraq legs can act like the spring of a bouncing mass-spring model. Using the method of energy storage and retrieval, it should be possible to travel at high speeds by saving considerable energy.

Acknowledgements

For more than three years many groups and individuals have helped in various ways to provide the necessary support which enabled me to complete this thesis.

I would like to start by praising God Almighty who is taken for granted by so many of us, and yet without His Will nothing could be achieved.

I would like to thank my parents who bore with my absence for more than five long years so that I could increase in knowledge.

Throughout the completion of this work, my wife and children have been always understanding, and meeting my needs even though that often meant the sacrifice of their comfort and pleasure. Therefore they deserve very special thanks.

From the academic point of view, I greatly appreciated Dr. Jack Todd, who continually supported me with great patience despite his illness and discomfort. Due to the great loss of Dr. Jack Todd, Dr. Alan Linnett has expended a lot of effort during my final six months so that the work could be presented in "the best logical way." I would like to thank him for his valuable support in these crucial times.

I would like to thank the workshop staff for their help and encouragement.

Also my sincere thanks to the Head of the Department, Dr. George Alder, and his best helpers Isabel Duncan and Isobel Drummond for making everything smooth in the Department through their administrative efforts.

Last but not the least, I would like to thank the Turkish Republic Ministry of Education for providing the necessary financial support throughout my post graduate education.

***I declare that this thesis has been composed by myself
and, except where stated, the work is my own.***

Hamid Alper Oral

Design of a Leg Mechanism with Controlled Phase, Variable Stroke and Energy Storage Capability for High Speed Locomotion

Contents

Chapter 1

Introduction

1.1	Introduction	12
1.2	Why a Legged Vehicle?	12
1.2.1	Problems of Traditional Off-road Vehicles Compared to Legged Vehicles	12
1.2.2	Comparison of a Legged Vehicle with Wheeled and Tracked Ones	13
1.3	What is a Legged Vehicle?	14
1.3.1	Definitions	15
1.3.2	Specifications	17
1.3.2.1	Terrain and Performance Characteristics	17
1.3.2.2	Locomotion	18
1.3.2.3	Control	19
1.4	Previous Research	19
1.4.1	Brief History	19
1.4.2	Locomotion Studies of Biological Systems	21
1.4.2.1	Optimisation of Gaits During Locomotion	21
1.4.2.2	Dynamic Similarity in Locomotion	21
1.4.2.3	Use of Springs in Animal Locomotion	22
1.4.3	Design of a Leg and Its Drive Units	22
1.4.3.1	Leg Type	22
1.4.3.2	Number of Legs	23
1.4.3.3	Leg Geometry	24
1.4.3.4	Drive Units and Joint Types	25

1.4.3.5	Elastic Energy Storage in a Leg Mechanism	25
1.4.4	Ground Reaction Forces	26
1.4.5	Some Legged Vehicles Built Up to Date	28
1.4.6	Expectations from a Legged Vehicle	31
1.5	Where Research is Needed	32
1.6	Objectives	34

Chapter 2

Development of a New Leg Mechanism for Running Legged Vehicles

2.1	Introduction	40
2.2	Some Leg Mechanisms Used in the Previous Research	40
2.2.1	Amplified Sweep Mechanism	40
2.2.2	Four Bar Mechanism	40
2.2.3	Pantograph Mechanism	41
2.2.4	Seven Bar Leg Mechanism	42
2.3	Leg Geometry of Mammals for Elastic Energy Storage	42
2.4	Development of Evaluation Criteria for Leg Mechanisms and Their Actuation	43
2.4.1	Terrain Adaptability	43
2.4.2	Load Handling	43
2.4.3	Dynamic Characteristics	44
2.4.4	Joint Type	44
2.4.5	Geometric Work	44
2.4.6	Straight Line Foot Trajectory at Walking Speeds	45
2.4.7	Inertial Forces	45
2.4.8	Elastic Energy Storage	46
2.5	Development of a New Leg Design	46
2.6	Actuation of the Buraq Leg Mechanism	46
2.7	Evaluation of the Buraq Leg Mechanism	47
2.8	Conclusions	49

Chapter 3

Computer Simulation Studies of the Buraq Leg

3.1	Introduction	57
3.2	Definitions	57
3.3	Simulation Study	58
3.3.1	The Initial Position and Values	58
3.3.2	The Support Period	58
3.3.3	The Lower Actuator Positions	59
3.3.4	The Transfer Period	60
3.3.5	Crank-Rocker Mechanism Design	61
3.4	Effects of The Drive Parameters on the Leg Mechanism Motion	62
3.5	Kinematical Analysis of the Buraq Leg Mechanism	62
3.6	Simulation Results	63
3.7	Conclusions	65

Chapter 4

Experimental Study of the Buraq Leg Mechanism

4.1	Introduction	87
4.2	Design of a Model	87
4.2.1	Mechanical Design	87
4.2.2	Power System	88
4.2.2.1	Longitudinal Drive	88
4.2.2.2	Vertical Drive	88
4.2.3	Control	88
4.2.3.1	Logic Control	89
4.2.3.2	Computer Control	90
4.3	Experiments to Calculate Specific Resistance	91
4.3.1	Initial Assumptions and Instrumentation	91
4.3.2	Calibration of the Instruments	91

4.3.2.1	Strain-gauge calibration	91
4.3.2.2	Current transducer calibration	92
4.3.3	DC Motor Characteristics	93
4.3.3.1	Measuring stall torque	93
4.3.3.2	No load speed	93
4.3.3.3	Evaluations	93
4.3.4	Calculation of the Specific Resistance	94
4.3.5	Load Sensitivity of the Specific Resistance	97
4.4	Foot Trajectory	97
4.4.1	A Mechanical Constraint on the Foot Trajectory	97
4.4.2	Calibration of the Straight Line Potentiometer	97
4.4.3	Measurement of the Foot Trajectory	98
4.5	Observations	98
4.6	Conclusions	99

Chapter 5

Design and Application of a Mechanical Drive Mechanism with a Variable Stroke and Phase

5.1	Introduction	125
5.2	Change of The Foot Stroke	125
5.3	Change of Phase Between Two Parallel Driven Legs	126
5.4	The Proposed Method for Change of The Foot Stroke and Change of Phase	126
5.4.1	The Relation Between the Crank Point Position and the Crank Effective Length	127
5.4.2	The Relation Between the Crank Point Position and the Phase between Parallel Driven Legs	127
5.4.3	The Relation Between Phase and Gait	128
5.4.4	The Effect of the Crank Effective Length Variation on the Gait of the Vehicle	129
5.5	Characteristics of a Variable Crank Mechanism	130

5.5.1	A Mechanical Constraint	130
5.5.2	A Point to Consider in Control	130
5.5.3	The Crank Point Position on the Disk and Manouerebility of the Vehicle	130
5.5.4	Maximum Time to Change Phase	131
5.6	Simulation Results	131
5.7	Conclusions	132

Chapter 6

Elastic Energy Storage in the Buraq Leg Mechanism for High Speed Legged Locomotion

6.1	Introduction	152
6.2	How Elastic Energy is Stored and Contributed Into the Leg Energy Cycle	152
6.3	Ground Reaction Forces During High Speed Legged Locomotion and the Need for the Elastic Energy Storage	152
6.4	Force Analysis of the Buraq Leg Mechanism for Elastic Energy Storage	154
6.5	Evaluation of Results and Conclusions	155

Chapter 7

Proposed Mechanical Design for a Legged Vehicle with the Buraq Legs

7.1	Introduction	168
7.2	Setting the Terrain and the Performance Characteristics	168
7.3	A Mechanical Design Proposal	169
7.3.1	Leg Mechanism	169
7.3.2	Vehicle Body	171
7.3.3	Steering	172
7.3.4	Brake and Suspension Systems	174
7.3.5	Foot Design	174

7.4	Power Transmission	175
7.4.1	Longitudinal Drive	175
7.4.2	Vertical Drive	176
7.4.3	Steering	176
7.5	Conclusions	176

Chapter 8

A Summary and Evaluation of the Overall Research

8.1	Introduction	194
8.2	A Summary and Evaluation of the Overall Research	194
8.2.1	Design of the New Leg Mechanism	194
8.2.2	Choice of the Actuation Method	195
8.2.3	The Leg Unit Consisting of the Buraq Leg and Actuators	195
8.2.4	The Legged Vehicle with Prescribed Leg Units	196
8.2.5	Future Study	197
	References	199
	Appendices	209

Chapter 1

Introduction

1.1 Introduction

1.2 Why a Legged Vehicle?

1.2.1 Problems of Traditional Off-road Vehicles Compared to Legged Vehicles

1.2.2 Comparison of a Legged Vehicle with Wheeled and Tracked Ones

1.3 What is a Legged Vehicle?

1.3.1 Definitions

1.3.2 Specifications

1.3.2.1 Terrain and Performance Characteristics

1.3.2.2 Locomotion

1.3.2.3 Control

1.4 Previous Research

1.4.1 Brief History

1.4.2 Locomotion Studies of Biological Systems

1.4.2.1 Optimisation of Gaits During Locomotion

1.4.2.2 Dynamic Similarity in Locomotion

1.4.2.3 Use of Springs in Animal Locomotion

1.4.3 Design of a Leg and Its Drive Units

1.4.3.1 Leg Type

1.4.3.2 Number of Legs

1.4.3.3 Leg Geometry

1.4.3.4 Drive Units and Joint Types

1.4.3.5 Elastic Energy Storage in a Leg Mechanism

1.4.4 Ground Reaction Forces

1.4.5 Some Legged Vehicles Built Up to Date

1.4.6 Expectations from a Legged Vehicle

1.5 Where Research is Needed

1.6 Objectives

1.1 Introduction

A vehicle which can adopt itself to various terrain conditions has great importance from a military-logistic support point of view. Wheeled and tracked vehicles have been used when terrain conditions are convenient. In case of rough terrain conditions, animals such as mules and horses are used. Using legged vehicles is proposed as an alternative to using animals.

This research investigates some new methods which can enable the present level of science approach towards building an artificial horse.

1.2 Why a Legged Vehicle?

1.2.1 Problems of Traditional Off-road Vehicles

Traditional off-road vehicles which are those with wheels and tracks face various problems during operation. These problems can be summarised as follows:

Problems in operating in paddy fields - In military and agricultural applications sometimes off-road vehicles are expected to operate on paddy fields where the surface conditions are very difficult for locomotion due to the water content of the soil. In paddy fields four-wheel-drive and tracked vehicles become handicapped (Tanaka 1984). The nominal pressure between the ground and the vehicle should not be more than a few hundred kPa, otherwise the vehicle cannot operate on such a soft ground (Larminie 1988).

Problems of travelling on sand - Off-road vehicles require low pressure distribution on the ground contact of the wheel to travel on sand. Otherwise the wheels either spin or the motor is stalled from the lack of torque (Dwyer 1984), (Kemp 1990). An example in relation to this problem can be seen in both photographs 1.1 and 1.2 (Moorehead 1965).

Problems from environmental point of view - Tracked and wheeled vehicles interact very vigorously with the terrain, and more importantly they leave a continuous track which induces erosion and reduces vegetation recovery (Abele et al 1984), (Baldwin and Stoddard 1973), (Braunack 1986),

(Coates 1981), (McGhee, 1981).

1.2.2 Comparison of a Legged Vehicle with Wheeled and Tracked Ones

The first question that comes to mind is why legs rather than wheels or tracks? Is not the symbol of the modern society wheels? As it was shown in the previous section, wheeled and tracked vehicles suffer from mobility and environmental factors. A legged vehicle can remedy the problems about wheeled and tracked vehicles. The studies show the following facts.

First of all more than half of the landscape is inaccessible by wheeled vehicles. And if it is carefully examined, it can be seen that highway technology is the backbone of wheeled transportation. However, for a legged vehicle there is no such dependence (McGhee 1981).

Second, from the mobility point of view, there is a fundamental difference between the ways a traditional off-road vehicle and a legged vehicle interact with the terrain. When a wheel is put on soft soil it creates a hole that continuously it has to climb out from during its motion. That is a waste of energy. Whereas the working principle of a legged vehicle is different, and that wasted energy can be saved. A leg, unlike a wheel or a track, does not push the soil forward, but backward, and the depression caused by the leg helps the vehicle to move forward since the foot pushes towards the ground during locomotion unlike a wheel or a track which depend on friction of the surface (McGhee 1981). Hence the mobility of a legged vehicle in paddy fields and on sand is quite high compared to wheeled and tracked off-road vehicles. Animals use %10 as much energy as wheeled or tracked vehicles over rough terrain (Song et al 1981).

Third, a wheeled vehicle definitely needs gravity force to be able to roll without slippage on any surface. In space applications, where human labour cost is tremendously expensive, wheeled vehicles cannot be used due to lack of gravity. However a legged vehicle moves by pushing the surface, that way there is a potential for legged vehicles in future space

applications (McGhee 1981).

Fourth, for military logistic support legged vehicles are much more preferable than stubborn mules or wheeled vehicles (McGhee 1981).

Fifth, the manoeuvrability of a wheeled vehicle on uneven ground is very poor compared to a legged vehicle due to the suspension function of the legs.

Sixth, when a wheeled vehicle travels on uneven ground the body sways excessively. However a legged vehicle can move on the same ground without swaying, because of active function of its legs. Some work machines are designed to have the same active function to adapt to terrain variations. However, comparing to a legged vehicle, this adaptability is relatively small.

Seventh, from the environmental point of view, the wheeled vehicles interact more vigorously with soil than the legged vehicles, and they leave a continuous track inducing erosion. The legs leave discrete foot prints on the terrain unlike wheeled or tracked off-road vehicles. When the damage caused by hundreds of thousands of caribou, which are quite large animals, can heal over within a year, the damage caused by a single passage of a caterpillar tractor on the same area may take up to 100 years to heal, and it may not heal at all (McGhee 1981).

There can be many more advantages of legged vehicles that are not mentioned here, however, on level and hard surfaces the wheeled vehicles are ideal. This disadvantage of the legged vehicle can be solved by adding wheels to the system to be used as an additional operational mode of the vehicle. In fact, Titan III is an example to such a hybrid type legged vehicle (Hirose et al 1984).

1.3 What is a Legged Vehicle?

A legged vehicle is a conveyance with the ability to move on its legs for a specified purpose such as transportation of goods and passengers on land, patrolling an area for safety reasons, etc. Further definitions and

specifications about legged vehicles are given in the following sub-sections.

1.3.1 Definitions

Support Period: The time during which the foot supports the vehicle body through ground contact.

Transfer Period: The time during which the foot travels in the air.

Leg Cycle Time: The time spent to complete a support and a transfer period.

Duty Factor: The ratio of the support period to the leg cycle time.

Leg Stroke: Relative disposition of the foot with respect to the body.

Froude Number: A non-dimensional number which is used to compare dynamic systems. It is expressed as u^2/gh where u is the speed at a particular time, h is the characteristic length, and g is the gravitational acceleration. In case of a mammal, h refers to the distance between the ground and the hip joint while the foot is supporting.

Gait: Set of leg motions which help a legged system to move. A gait is called *periodic* (or *regular*) when all legs repeats the same pattern of states at the same leg cycle times (McKerrow 1990).

Support Pattern: A two dimensional point set in a horizontal plane which is a polygon formed by the vertical projection of all foot points during support period (Song and Waldron 1987 (b)).

Statically Stable Locomotion: A legged system is said to be adopting statically stable legged locomotion when its support pattern has at least three corners at all times.

Dynamically Stable Locomotion: A legged system is said to be adopting dynamically stable legged locomotion when its support pattern is a line, a point or does not exist at any time during locomotion.

Hybrid Type of Locomotion: A legged vehicle is said to be adopting a hybrid type of locomotion when both statically and dynamically stable locomotion are adopted interchangeably. For example, most mammals use statically stable gaits while walking, and they use dynamically stable gaits

during running.

Relative Phase: When a periodic gait is adopted by a legged vehicle, all the legs have the same leg cycle time regardless of the value of the duty factor. Let a leg cycle be assumed to take place between time 0 and time 1. If a particular foot placement on the ground is taken as a reference with the relative phase value of 0, then all the other foot placements have to take relative phase values between 0 and 1. (Alexander 1984(a)) explains the use of a similar representation as beneficial because "it avoids making gaits that are mirror images of each other seem grossly different." See figure 1.1 for diagram of quadruped running gaits showing typical relative phases of the feet of a horse. The adapted figure is reproduced in a different format from (Alexander 1984(a)).

Geometric Work: Geometric work is a factor that effects the mechanical efficiency of a legged vehicle (Waldron and Kinzel 1981). The studies done by Waldron and Kinzel show that low efficiencies of legged vehicles are largely due to the actuators "acting as brakes"; that is they are driven backwards. Geometric work is further explained in figure 1.2. It can be observed that early in the support period the torque generated by the actuator and the angular velocity of the joint are both in the same direction. Therefore the work done by the actuator is positive. Whereas later in the support period the actuator torque direction is opposite to that of angular velocity. In that case there is a negative work done, and the other actuators have to compensate for that energy lost. The energy converted into heat energy during this cycle is called geometric work.

This phenomenon occurs when each joint is driven by a separate actuator. Therefore the suggestion of Waldron and Kinzel to minimise the geometric work is to operate actuators across more than one joint.

Specific Resistance: Specific resistance of a legged vehicle is a non-dimensional value through which the performance of a legged vehicle can be evaluated. It is defined as the ratio of (the input power to the vehicle) to (the product of vehicle speed and total weight) (Todd 1985). The higher

the value of the specific resistance value, the worse the performance of a legged vehicle.

Virtual Legs: This concept is developed by Dr. Raibert (Raibert, p92 1986 (a)) to ease the control task. The leg pairs with the same relative phases are defined as virtual legs. For example, looking at figure 1.1, it can be seen that in cases of trot, pace and bound, virtual leg concept can be applied to the leg pairs with the same relative phase values. In case of pronk during which all legs act together with zero relative phase, theoretically, virtual leg concept can even be used for four legs. That way, the total number of legs are reduced from four to two and to even one in case of pronk. The concept eases the control and analysis of multi-legged vehicles.

1.3.2 Specifications

1.3.2.1 Terrain and Performance Characteristics

Terrain characteristics are predicted according to the physical environment in which the vehicle operates. Since the environment may vary for various applications, these characteristics will change a great deal from one design to another. For example a legged vehicle designed to search for radiation leakage has to be able to adapt itself to various obstacles and gradients. On the other hand, a legged vehicle designed to act as a means of transport -which is the ultimate purpose of this research-, has a choice about the terrain that it wants to follow. Therefore it does not have to deal with a terrain with many obstacles.

Performance characteristics are predicted according to the desired locomotion response of a legged vehicle. The performance characteristics are closely related to terrain characteristics. A legged vehicle searching for radiation leakage has to travel at low speeds since searching requires low speed. Also it is practically impossible to travel at high speeds due to too many obstacles. On the other hand, a legged vehicle acting as a means of transport has to travel at high speeds because the time is always an

important factor especially in transportation.

A recent study done by R.A.Bryson (1988) defines tactical mobility for a battle tank as shown in figure 1.3. As the figure shows, tactical mobility covers terrain and performance characteristics. These characteristics can be applied to any off-road vehicle such as 4WD's, agricultural vehicles, etc. However some vehicles perform better than others. A battle tank deals with obstacles better than any other off-road vehicle. Whereas a motorcycle with lightest weight and highest power/weight ratio deals with ground traverse and performance characteristics better than other off-road vehicles (see the data in (Larminie 1988)).

1.3.2.2 Locomotion

The type of locomotion can be estimated by evaluation of terrain and performance characteristics. The type of locomotion can be either statically stable locomotion, or dynamically stable locomotion, or both. The type of locomotion is closely related to the number of legs of the whole vehicle and also its gait structures.

A legged vehicle adopting statically stable legged locomotion always keeps its statical balance by using at least three legs on the ground. For example, a four legged vehicle can carry out statically stable locomotion by moving one foot at a time while the other three legs support the body in a statical balance condition. The minimum number of legs for a legged vehicle adopting statically stable legged locomotion is therefore four.

A legged vehicle adopting dynamically stable locomotion is never statically stable. It continuously moves on its legs, and keeps a dynamical balance. A one legged hopping machine is a typical example (Raibert 1986 (a)). By controlling the thrust force towards the end of the support period and the leg swing angle, the hopping machine can travel at low speeds as well as at high speeds.

A legged vehicle adopting a hybrid type of locomotion is a vehicle adopting both locomotion types. Biological systems such as mammals

adopt statically stable legged locomotion at low speeds, and dynamically stable locomotion at high speeds.

The type of stability, gaits, number of legs of a legged vehicle all affect its locomotion.

1.3.2.3 Control

Various control techniques have been used for legged vehicles. Control of legged vehicles adopting statically stable legged locomotion was first achieved after 1967 by Dr. Andrew Frank and Dr. Robert McGhee using basic flip flops (McGhee 1981). Control of legged vehicles adopting dynamically stable legged locomotion was first achieved in 1986 by Dr. Raibert (Raibert 1986 (a)). More complex control schemes have been developed since then for both types of locomotion purposes (Lapskin et al 1991), (Tsai et al 1987). Especially having three degrees of freedom per foot makes the control very complicated for conventional walking machines.

1.4 Previous Research

1.4.1 A Brief History

(Liston 1967) presents a brief history of studies in the field of legged vehicles; starting in 1954, a series of studies were conducted towards building a legged vehicle for off-road transport by U.S. Army. The first trial was made by Prof. Bernhard of Rutgers University, which proposed a walking and running vehicle, however the control during the flight period posed serious drawbacks.

Therefore a comparatively slower machine was proposed by the University of Michigan. The work was taken over by Prof. Shigley, and a mechanical model was built with mechanical linkages to fulfil a set of requirements. Even though inertial forces from the legs were absorbed by a set of non-circular gears, the manufacture and operation of the gears posed the prime trouble. Also, due to having completely mechanical actuators, the vehicle was not terrain adaptive.

Numerous investigations were carried out, and a hydraulically controlled walking machine using 16 pantograph-like leg mechanisms was declared to be the optimum selection. Even when operating at speeds up to 20 mph, the inertial forces were tolerable. However, the control process was lacking force feedback. To remedy this problem, General Electric's Company developed a quadruped with force feedback control system.

(McGhee 1981) gives an account for the following years; a quadruped vehicle controlled by a master slave mechanism was constructed during the period between 1964 and 1967. The vehicle was operated by a human being. The operation principle was simply the magnification of the signals given by a human operator. Even though the force magnification ratio was as high as 1 to 100, it was a very difficult task to coordinate 12 joints, three in each leg. Therefore, even the designer of the machine was not able to control it for more than 10 minutes a day. Then the main interest of legged vehicle research began to centre around the computer control problem of the vehicle. A later attempt was made by Dr. Andrew Frank and Dr. Robert McGhee to prove that human intelligence is not necessarily required for walking motion. That fact was shown by using only 16 flip flops, and the joint motions were coordinated electronically. Afterwards several legged vehicles were built.

There are mainly two types of legged vehicle (Kaneko et al 1985) ;

First type: Each leg has three degrees of freedom. The vehicle can adapt its feet to irregular terrain, and that kind of motion requires a tremendously complex control scheme.

Second type: Legged vehicles with a fixed walking gait. All legs are linked mechanically by employing machine elements such as linkages and cams. This type lacks the most important function; active terrain adaptability.

Also, only a few of these machines could be *self-sufficient*, that is carrying their own power and computing supplies on board. The Adaptive Suspension Vehicle (Waldron and McGhee 1986 (a)) is one of the exceptions which carries its own supplies on board, however it has a very

poor payload to weight ratio of less than 0.1. Nevertheless it deals with uneven terrain quite successfully.

Odex I (Russell 1983) is a self-sufficient six legged vehicle with a significant 1.1 payload to weight ratio.

The one legged hopping machine of Raibert is a good example to show that control problem of the vehicle during the flight period has been solved.

1.4.2 Locomotion Studies of Biological Systems

Biological systems, especially mammals, have been studied extensively to find a relation between energy expenditure, the means and the patterns of locomotion. Some of the results are mentioned briefly in the following sub-sections.

1.4.2.1 Optimisation of Gaits During Locomotion

The gaits of biological systems have been studied extensively in the past (Alexander 1980 1989), (Alexander and Jayes 1983), (Alexander et al 1980). Also, the gaits of articulated systems have been studied (Raibert 1986 (a) and 1990), (Song and Waldron 1987 (b)), (Song and Chen 1991).

The research studies have shown that animals follow the most economical gaits during locomotion. The experiments conducted on a horse on a treadmill can be given as an example; horses change their gaits while increasing their speed. Hence they walk, trot and gallop keeping their energy expenditure always at minimum (Hoyt and Taylor 1981). Also other mammals follow the same minimum energy expenditure strategy by changing their gait during locomotion (Alexander 1980), (Alexander 1984(a)).

1.4.2.2 Dynamic Similarity in Locomotion

A wide range of experiments conducted on animals have shown that mammals move in a dynamically similar fashion while travelling at equal froude numbers. Speeds of gait changes, leg strokes, duty factors, shapes

of force records and rates of performance of work all can be predicted fairly well using this dynamic similarity (Alexander and Jayes 1983), (Alexander 1984(a)), (McMahon 1984).

Studies have also shown that animals follow a symmetrical pattern of motion while running. In terms of balance and stability the concept of symmetry seems quite significant (Raibert 1986 (a)).

1.4.2.3 Use of Springs in Animal Locomotion

Studies have shown that animals use spring motions in locomotion in three different ways. They use their bodies as pogo sticks and save energy in their tendons, hence reducing unwanted energy loss in the form of heat and increasing the efficiency (Alexander and Vernon 1975), (Alexander and Goldspink 1977), (Jayes and Alexander 1982), (McMahon 1984), (Alexander 1984 (b)), (Alexander et al 1985), (Ker et al 1986), (Bennett 87), (Alexander 1988). During leg swing, tendons of the leg are used to transfer energy at the end of the forward and the backward stride (Alexander 1982), (Dimery and Alexander 1985), (Dimery et al 1986 (a)), (Dimery et al 1986 (b)). And also on the foot, springs are used as compliant pads. Especially during running at high speeds this padding is essential, those pads are actually paw pads in animal structure (Alexander et al 1986), (Salathe et al 1990). A collection of literature can be found in Alexander (1988), and a review specifically for robotics applications can be reviewed in Alexander (1990).

1.4.3 Design of a Leg and Its Drive Units

1.4.3.1 Leg Type

Definitions of leg types are given in (Hirose and Umetani 1978) as following;

The mammal type leg (Horse type) : The configuration of a leg in which the knee joint is always situated under the hip joint as in most mammals.

The insect type leg (Spider type) : The configuration in which the knee joint is situated laterally or higher than the hip joint as in most insects.

The insect type leg is considered superior for walking robots by Hirose and Umetani (1978) for the following reasons:

- The insect type leg can extend the toe (the far end of the foot) very effectively permitting the vehicle to locomote in quite rough environment.
- The insect type leg requires less energy compared to the horse type leg under the same conditions.

The studies of Hirose and Umetani (1980) also point out the advantage of the insect type. The insect type leg is advised because long legs are applicable to this type, hence keeping the gravity centre of the body lower and maintaining high stability. The long legs are considered to enable the body to move faster and to be adaptable to comparatively large unevenness of the ground.

In Waldron and Kinzel (1981) the mammalian type leg geometry is considered effective in avoiding power drain due to kinetic energy absorption. However it is also considered as being potentially subject to the more serious power loss mechanism that is geometric work.

According to the author the mammal type leg has higher locomoting energy efficiency if geometric work is prevented. However to get use of the above advantages, insect type legs should be included in the leg geometry by a flexible design. Actually TITANIII (Hirose et al 1984) is the most hybrid vehicle built up to date, because not only does it include both of wheels and legs attached to its body, but also it has the flexibility for operating with both type of legs.

1.4.3.2 Number of Legs

According to Hirose and Umetani (1978) the fundamental considerations about the number of legs are as follows:

- The factors which are beneficial when the number of legs increases are
- the stability to keep a standing posture

- the adaptability toward the roughness of the ground
- the reduction of the total kinetic energy
- the reduction of the load which each leg should support and resultant simplification of each leg.

The factors which are beneficial when the number of legs decreases are ;

- The simplicity of the total driving mechanism
- The simplicity of control devices

The simplicity of the total driving mechanism is considered as the biggest barrier to overcome in the development of a legged vehicle.

1.4.3.3 Leg Geometry

Studies done in Song et al (1981) indicate that the importance of the leg geometry for a legged vehicle as the most crucial aspect of the design, since it strongly influences the efficiency. Furthermore the most important property of the leg geometry was realised by (Hirose and Umetani 1978), (Song et al 1981) and (Kaneko et al 1985). That is, in order to have good efficiency only one actuator per leg should be active during the support phase of the leg while ensuring the motion of the body is on a horizontal straight line, because most of the power has been wasted in the early generation of legged vehicles due to the up and down motion of the body causing potential energy losses. In addition to that, the leg should be simple in structure.

The studies done in Orin et al (1976) indicate a trade off about leg geometry. The specific question raised is the effective length of a leg. The effective length of a leg is preferred to be large for the following reasons:

- Adequate reach in moving over rocky or pock-marked terrain,
- To climb over large obstacles,
- To clear wide ditches,
- For higher speed.

However there is a trade off between the leg length and joint torque required for a given ground reaction force. The ground reaction force

directly depends on the vehicle weight and the payload. From the practical point of view the operating conditions of a vehicle have to be defined to find the optimum solution.

1.4.3.4 Drive Units and Joint Types

While mechanical drives suffer from the lack of terrain adaptability (Liston 1968), hydraulic drives also have some disadvantages. The study done in Gardner et al (1983) indicates that one of the biggest trade offs of hydraulic circuit design, namely the trade off between good dynamic response and energy efficiency which must both be provided by the drive system. However the hydraulic circuit equipments fall short of satisfying both of these requirements together. To improve the characteristics a by-pass configuration is advised by Gardner et al (1983), however it is admitted that the valves and sliding joints are undesirable features of the drive system.

McGhee (1981) clearly describes the disadvantages of hydraulic drives; "...The actuation mechanism is likely to be hydraulic, although that is a very serious problem. The efficiency of conventional hydraulic actuators is unacceptable, we must find something better ..." and "conventional hydraulic actuators are very inefficient," due in fact to the existence of sliding joints. Motion discontinuances in hydraulically driven mechanisms also cause undesired vibrations (Jones 1983). Also the mechanical reliability of drive systems with sliding joints is admitted to be less reliable (Song et al 1983). Hirose et al (1984) make a comparison between rotating and sliding joints as following; "Generally speaking, it has been maintained thus far that one should use rotating joints as much as possible when designing any component of the machine, and that it is better not to use sliding elements of linear movements because of the strength, low friction and reliability of ball bearings."

1.4.3.5 Elastic Energy Storage in a Leg Mechanism

In this section, some of the research carried out to accommodate flexible

linkages and springs in leg mechanisms are cited.

For biped locomotion, a mathematical model of the swing period is developed during walking in Mochon and McMahon (1980(a)). An improved model is further presented in Mochon and McMahon (1980(b)). The model is justified by comparing the results with experimental data relating to kinematic measurements and gaits in human walking.

Alexander, in his book titled "Elastic Mechanisms in Animal Locomotion" (Alexander 1988), sets aside a whole chapter to explain the basic knowledge about suspension springs and shock absorbers in relation to biological structures such as paw pads and animal skeletons.

McGeer (1989 (a)) discusses a leg swing motion based on the natural mode of a pendulum. An experimental walking model is developed with torsional springs at the hip joints using only gravitational power to locomote downhill. The study further investigates the application of the same principles for level and uphill locomotion (see also (McGeer 1989 (b)) for further details about "Passive Running").

A study investigating the dynamic model of a mechanism with a flexible linkage declares that adding flexibility to a mechanism means only a slight variation in the existing rigid-link dynamic model (Bodner 1989).

The relation between the running speed and the stiffness of a leg mechanism has been also investigated (McMahon and Cheng 1990). A mathematical model of a leg for terrestrial running is developed with similar properties of a simple spring, and results are compared with experimental force platform data.

Three different ways of incorporating springy structures into a legged vehicle derived from the study of biological systems are discussed in Alexander (1990). One of these ways are further discussed in Brown and Raibert (1987) for an artificial leg mechanism.

1.4.4 Ground Reaction Forces

Legged locomotion involves force interaction between the legs and the

ground. Ground reaction force is the reaction of the ground acting on the body through the legs. Much research has been carried out about the subject since the results can be used in various fields such as medicine, locomotion and control. While building an artificial leg, all the results are valuable to an engineer.

(Bobbert et al 1991), (Bryant et al 1987), (Cavanagh and LaFortune 1980), (Dickinson et al 1985), (Elftman 1939), (Greene 1985) and (Hay and Nohara 1990) are representative of the research carried out to investigate the reaction forces due to walking, running and jumping.

Munro et al (1987) measured the ground reaction forces on the legs of some running human objects. Also Ozguven and Berne (1988) have studied the impact forces for human jumping following experimental and analytical methods. For a different running technique (Groucho running), the variation in ground reaction forces has been measured by using force platforms (McMahon et al 1987). Also the effect of locomotion speed on the pressure of particular muscles has been studied by (Kirby et al 1988). Vertical movements in walking and running and coordination of body parts in vertical jumping have investigated in Alexander and Jayes (1978) and Bobbert and Schenare (1988) respectively. Fourier analysis of ground reaction forces are carried out in Alexander and Jayes (1980) and relations between the Fourier coefficients and locomotion characteristics were investigated. Some researchers have used the ground reaction forces to estimate the body size (Cavagna 1985). Also some have developed mathematical models for force evaluation (Seireg and Arvikar 1973).

To investigate the internal reactions in the legs and body due to ground reaction forces, various studies have been carried out by testing specific organic parts to collect data such as, Ackland et al (1988) providing data about inertial characteristics of body parts, Weiss et al (1988) providing data about ankle joint stiffness, and Ashman and Rho (1988) providing data about the elastic modulus of a trabecular bone.

For balanced locomotion, the distribution of ground reaction forces is a

key point. Therefore many researchers have contributed to the area of force control using different methods under various terrain conditions. Some representative references are (Gorinevsky and Shneider 1990), (Klein and Briggs 1980), (Klein et al 1983), (Majeed 1990), (McGhee and Orin 1976), (Waldron 1986) and (Waldron and Kinzel 1981).

1.4.5 Some Legged Vehicles Built Up to Date

Those Adopting Statically Stable Legged Locomotion:

OSU HEXAPOD

Several experiments have been done with the OSU Hexapod (Orin et al 1976), (McGhee 1977), (McGhee et al 1978). The OSU Hexapod has six legs with 3 joints each, each individually powered by an electric motor. Its most significant property could be shown as the maximum joint output torque, which is about 275 Nm. Computer and power supplies are off board. The vehicle is able to climb over obstacles comparable to its own size. The leg mechanism is not efficiently designed, hence there are power losses and dynamical disturbance in the form of vibration. The speed of the vehicle is very low, about 0.75 m/s. Force feedback is implemented on the vehicle by attaching strain gauges on its legs, and the necessity of force feedback is proven for the vehicle by the following experimental results:

With force feedback the vehicle consumes 0.75 kW power and walks with a speed of 0.2 m/s.

Without force feedback the vehicle consumes 3 kW power and walks with a speed of 0.2 m/s.

The most significant disadvantages of this vehicle are

- not using a straight line generating leg design, hence causing potential energy losses,
- having serially articulated joints which also causes energy losses (McCloy 1990).

KUMO I (Hirose and Umetani 1978)

KUMO I was a legged vehicle for which the importance of the pantograph mechanism was realised, and the result is a more efficient legged vehicle. It has four legs with three joints each. The leg mechanism is a planar pantograph leg. Spider type legs are realised to save geometric work, however speed is sacrificed. Also, as a further step, kinetic energy of the leg is carried over to the other legs. However the walking speed is only 1.5 m/min. It weighs about 14 kg. and the leg is 1.5 m. long. Computer and power supplies are off board.

TITAN III (Hirose et al 1984)

This vehicle is a hybrid type with four legs. The driving mechanism is a 3D pantomec. The leg type is hybrid and both mammal and insect type legs can be realised. Linear actuators are used and computer and power supplies are off board. The maximum walking velocity is 3 m/min.

MELWALK MARK III (Kaneko et al 1985)

This vehicle has six legs and uses a special four bar mechanism. The drive mechanism is able to produce an approximate straight line by rotating one joint. Thus it enjoys mechanical efficiency. The main advantage of the vehicle is the usage of the decoupled freedom control approximation, hence simpler control hardware. The study results also indicate that a hexapod vehicle with fewer independently actuated degrees of freedom will be essentially faster, more energy efficient, and less expensive compared to the machine without mechanical actuators. The machine is limited to a one single gait.

The model is admitted not to have sufficient freedom for terrain adaptability - in the sense that it cannot select the foot placement point in 3D space freely. To compensate with this disadvantage 2 solutions are given :

- More freedoms per leg for terrain adaptability

- One more freedom to change stride length

Some experimental data are given. The body mass is 35 kg, and it can carry a load of 24 kg. It has a specific resistance of 0.4 without payload and 0.2 with three times machine weight, both at a speed of 0.3 m/s.

ADAPTIVE SUSPENSION VEHICLE (ASV)

This vehicle has six legs each with three joints powered by linear hydraulic actuators. The driving mechanism is a 3D pantograph mechanism. High level control with one microprocessor per leg is adopted. The computer and power supply is on board. The design goals of the vehicle are given as follows (Gardner et al 1983), (Pugh et al 1990), (Waldron and McGhee 1986 (a) and (b)), (Waldron et al 1984 (a) and (b));

Weight	260 kg
Payload	225 kg
Speed	2.25 m/s cruise, 3.6 m/s dash
Grade Climbing Ability	> 60 % , 70 %
Length	5.2 m
Width	2.4 m
Height	3 m
Endurance	10 h.
Leg Stroke	1.80 m
Vertical Foot Height Variation	1.22 m
Lateral Leg Swing	20 °
Vertical Step Negotiation	2.1 m
Horizontal Ditch Negotiation	2.7 m

Compared to the Melwalk Mark III, this design has a higher specific resistance of about 0.3 (Waldron et al 1984 (a)). The control structure is very complex and the cost of production is extremely high. Most of all, having sliding joints in the structure is a big disadvantage. Also another drawback of the design is having a rectangular foot trajectory which could be smoothed to increase efficiency (Choi and Song 1988), (McCloy 1989).

ODEX I

Odex I (Russell 1983) has six legs and a mass of 168 kg. Each leg can lift about 180 kg. The robot can travel at about 1.5 m/s. The robot raises three legs to advance, and uses a tripod gait. It is capable of climbing steps as high as 845 mm. The robot has 18 motors on board. It is completely self-sufficient. Further versions of the same robot have been built later (Byrd and DeVries 1990).

Those Adopting Dynamically Stable Legged Locomotion:

ONE LEGGED HOPPING MACHINE

A one legged hopping machine (Raibert 1986 (a)) has a single leg hinged to a body carrying electronics, sensors and valves. The leg is a double-acting pneumatic cylinder with a padded foot. Four electronic solenoid valves control the flow of air to the leg cylinder. It is possible to regulate the air pressure to adjust the speed. Peak amplitude of the body can be varied between 0.04 and 0.3 m with corresponding hopping frequencies of 3 and 1.5 hops per second. The total mass of the machine is 8.6 kg. Two legged and four legged versions of the same machine were built using the same basic control approach which consists of three parts; control of hopping height, forward speed and body attitude (Raibert et al 1989), (Raibert 1990).

1.4.6 Expectations From a Legged Vehicle

Some requirements of a legged vehicle are listed in Liston (1967) :

- The machine must have a uniform velocity while the feet are in contact with the ground,
- The stride must be long in relation to the physical dimensions of the machine to achieve adequate speeds,
- The height and length of the stride must be controllable by the operator,

- The height of the step should be large compared with the dimensions of the machine.
- The feet should have a high stride-to-return-time ratio,
- A mechanism integral to the legs must be provided for steering the vehicle,
- The vehicle must be able to move forward and in reverse,
- The inertia torques and forces must be balanced,
- The energy lost in lifting the foot should be recoverable in lowering the foot,
- The height of the body of the machine above the ground should be controllable by the operator.

Hirose and Umetani (1978) comment that legged vehicles should be able to get over and stride over big obstacles sometimes higher than the vehicles own height, and move on such uneven terrain with minimum swaying and jumping movement.

Hirose et al (1984) describe the design objectives of a legged vehicle; To develop a machine that can move freely on the uneven ground of the natural environment (rugged and irregular surfaces and/or soft soil texture) with high energy efficiency and high adaptability to surface topography.

1.5 Where Research is Needed

Most research in the field of legged vehicles has been concentrated on walking vehicles. Some legged vehicles adopting dynamically stable legged locomotion at high speeds have been designed during the past five years. However their main emphasise has been the control of the dynamically stable legged locomotion rather than the performance. Also, some research has been carried out relating to biological systems. The research has suggested energy storage mechanisms for legged vehicles to enable more efficient locomotion. In this study, the findings of the above research are incorporated into one unified body with a specific purpose which is to design a leg mechanism with energy storage capacity for high

speed legged locomotion. The following areas have been identified to be studied:

A Leg Mechanism:

Even though the superiority of revolute (rotary) joints is accepted compared to sliding joints, present technology has concentrated on the pantograph leg design with sliding joints. Therefore there is a need for a leg mechanism with revolute joints and with similar positive properties of a pantograph mechanism such as avoiding geometric work, and producing a straight line during walking while only the longitudinal actuator is operating. However straight line foot trajectory during support period is significant only at walking speeds. Also, for high speed locomotion, the ratio of leg stroke to leg height is preferred to be relatively high in magnitude.

A Drive Mechanism

Mechanical actuators have the potential to reduce geometric work since they can be driven across more than one joint (Waldron and Kinzel 1981). If a compromise was to be made between using a hydraulic and a mechanical actuator, the control duty would be easier as well as the possibility of achieving very high speeds. Also a mechanical actuator would have the additional advantage of being more reliable and balancing inertial forces when all legs are driven through the same drive shaft. However electrical and hydraulic actuators are usually preferred due to their superiority in control. Therefore a mechanical actuator needs to be developed with more flexibility and control. In this way a mechanical actuator can be used especially for longitudinal motion directly to contribute to the speed of the vehicle.

Elastic Energy Storage

There have been various studies on elastic energy storage in legged locomotion (see section 1.4.3.5). However its practical application are

severely lacking. One legged hopping machine and its multi-legged versions are basically built as control applications, therefore the efficiency of the locomotion is not the main concern. Therefore there is a need to further study about elastic energy usage in legged vehicle locomotion.

A Hybrid Type Legged Vehicle

Previous research has been limited to two separate approaches to legged vehicles from the locomotion point of view. There has been no study investigating the possibility of a legged vehicle adopting both statically and dynamically stable legged locomotion with respect to the locomotion speed.

1.6 Objectives

The objectives of this research have been set out as follows;

- 1- To design a leg mechanism
 - free from sliding joints
 - with straight line foot trajectory during the support period
 - better than previously designed leg mechanisms for high speed legged locomotion such as with higher leg stroke to leg height ratio.
- 2- To develop an actuation strategy
 - free from geometric work
 - with full control in the vertical direction for terrain adaptability
 - with longitudinal mechanical actuation for fast locomotion
 - with steering and gait shift capacity during locomotion
- 3- To study elastic energy storage by carrying out
 - an application method
 - a feasibility study
- 4- To study a hybrid type legged vehicle by
 - setting the design parameters by using present off-road vehicles' experimental data
 - developing some proposals for mechanical design.



Photograph 1.1 "A Valentine tank badly bogged in a soft flat near the coast." (Moorehead 1965)



Photograph 1.2 "Often they had to dig their vehicles out of the soft sand." (Moorehead 1965)

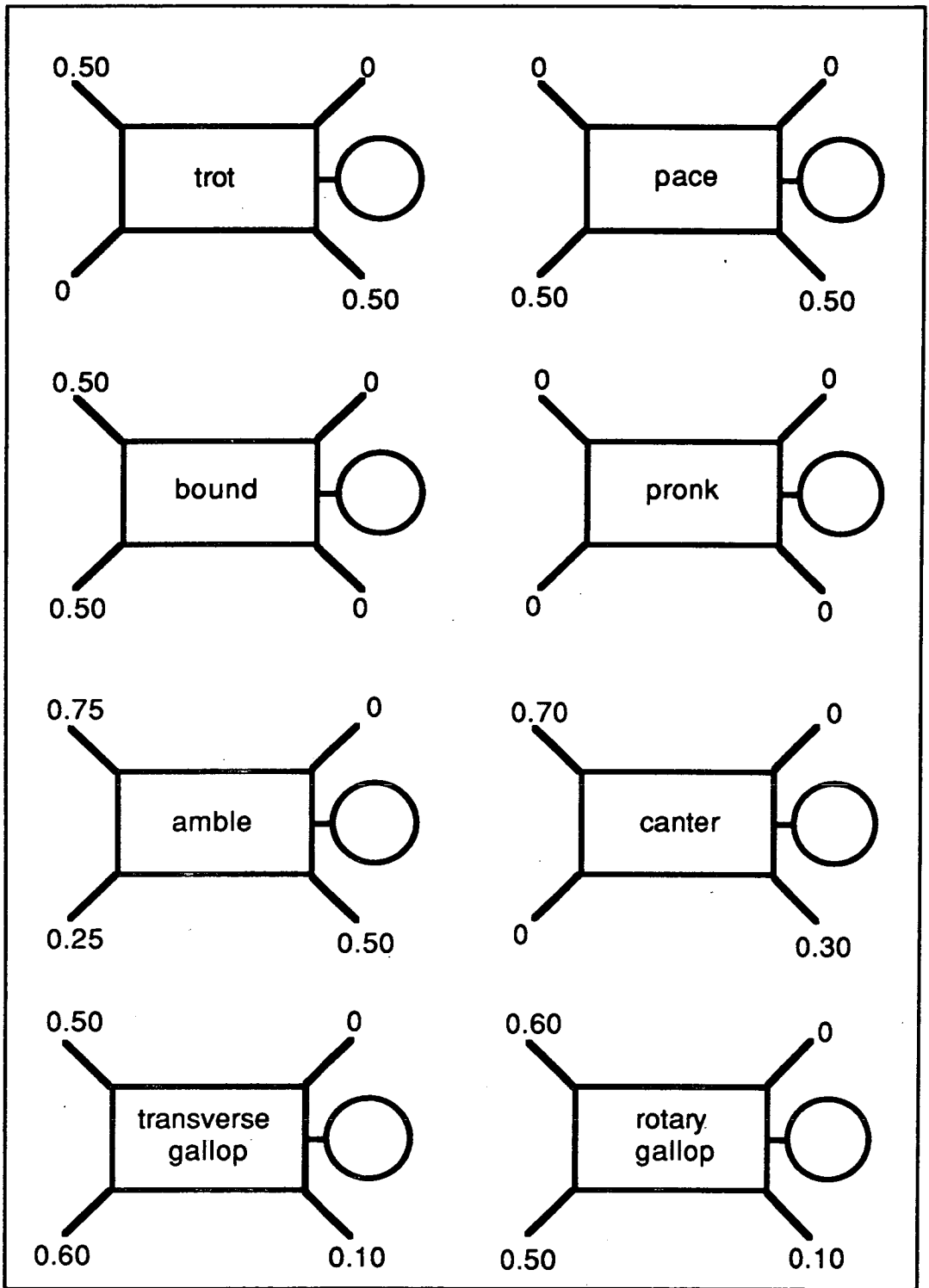


Figure 1.1 Quadruped running gaits with typical relative phases (adapted from Alexander, 1984(a)).

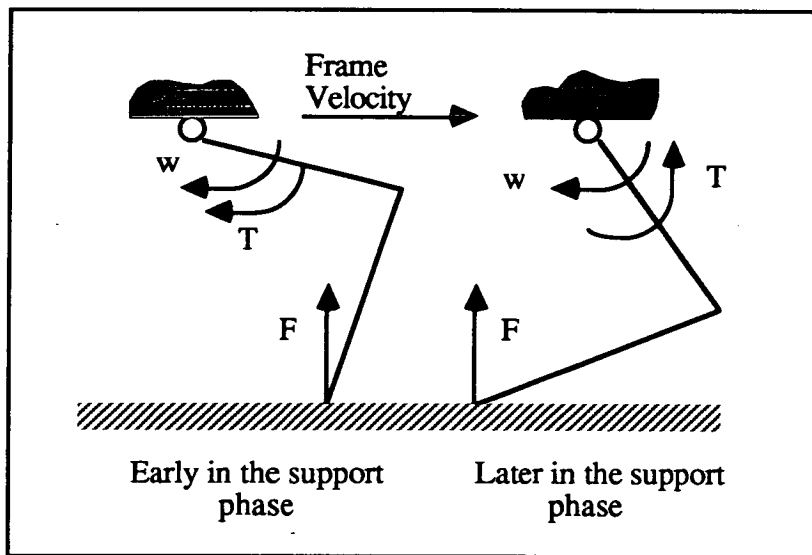


Figure 1.2 Description of geometric work (adapted from Waldron and Kinzel, 1981).

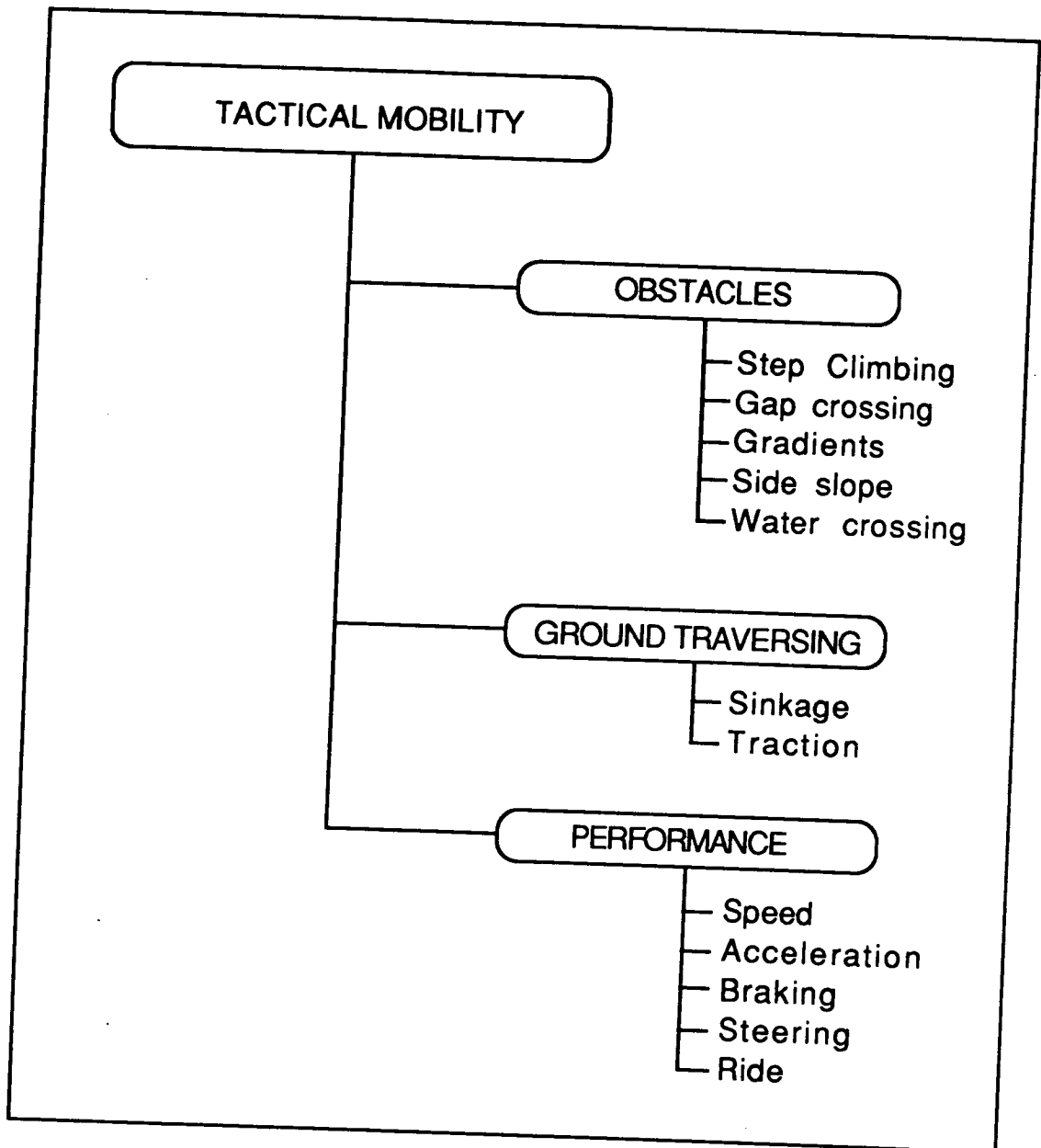


Figure 1.3 Tactical Mobility for a battle tank
(Adapted from (Bryson, 1988)).

Chapter 2

Development of a New Leg Mechanism for Running Legged Vehicles

Contents

2.1 Introduction

2.2 Some Leg Mechanisms Used in the Previous Research

2.2.1 Amplified Sweep Mechanism

2.2.2 Four Bar Mechanism

2.2.3 Pantograph Mechanism

2.2.4 Seven Bar Leg Mechanism

2.3 Leg Geometry of Mammals for Elastic Energy Storage

2.4 Development of Evaluation Criteria for Leg Mechanisms and Their Actuation

2.4.1 Terrain Adaptability

2.4.2 Load Handling

2.4.3 Dynamic Characteristics

2.4.4 Joint Type

2.4.5 Geometric Work

2.4.6 Straight Line Foot Trajectory at Walking Speeds

2.4.7 Inertial Forces

2.4.8 Elastic Energy Storage

2.5 Development of A New Leg Design

2.6 Actuation of the Buraq Leg Mechanism

2.7 Evaluation of the Buraq Leg Mechanism

2.8 Conclusions

2.1 Introduction

To design a new leg mechanism satisfying some specified conditions has been set as the first objective of this research. Also, this leg mechanism is expected to have elastic energy storage capacity. The following procedure is proposed to achieve the desired leg design.

Some of the leg mechanisms studied in previous research are evaluated. In addition to artificial leg mechanisms, some biological leg mechanisms are examined, since mammals especially use elastic energy quite efficiently during running. These investigations lead to the production of performance criteria especially for leg mechanisms operating at high speeds. A new leg mechanism is then designed and evaluated according to a set of performance criteria.

2.2 Some Leg Mechanisms Used in Previous Research

Some leg mechanisms used in previous research in the field of legged vehicles are evaluated in an order, starting from a simple mechanism towards the most recent one. That way the evolution of leg mechanisms according to the needs of researchers can be observed.

2.2.1 Amplified Sweep Mechanism

First, an amplified sweep mechanism was used (figure 2.1(a)); There is no linear relation between actuators and the foot movement. In addition, the mechanism which helps to move the foot is a major constraint keeping the working envelope of the mechanism small.

2.2.2 Four Bar Mechanism

The four bar leg is the leg design used by some early generation legged vehicles. When the importance of the mechanical efficiency question raised, more research was directed towards improving leg mechanisms. One study states that the four bar mechanism is found to be deficient and very difficult in mechanical design (Song et al, 1983).

Roberts mechanism (figure 2.1(b)) and Hoecken (figure 2.1(c)) mechanism are some examples of four bar mechanisms. According to (McCloy 1989) these two mechanisms can not generate a satisfactory horizontal straight line motion.

Basically Hoecken mechanism and Four bar mechanism with a hinge joint (figure 2.1(d)) are the same designs except the way the foot linkage is actuated. Both mechanisms, similar to Robert's mechanism, decouple up and down motion of the foot, gaining some degree of controllability on the foot trajectory. That way terrain adaptability of a legged vehicle can be improved. Song's four bar mechanism (figure 2.1(e)) was an even higher achievement. The working envelope of a foot can be improved drastically by using Song's four bar mechanism.

2.2.3 Pantograph Mechanism

The real breakthrough in leg mechanism design came with the introduction of a pantograph mechanism (figure 2.1(f)) to legged vehicles. A pantograph leg has one of the most important properties required of a legged vehicle, that is only one actuator is active during the support phase, and the body moves on horizontal line. That property of a pantograph leg paves the way for its wide usage. The horizontal motion and vertical motions of the foot can be arranged so that they are either decoupled or can be achieved by moving the same joint. The design is simple because of the basic properties of the leg geometry. The force calculations also become very easy, therefore it is easy to control.

The advantages and disadvantages of a pantograph leg are also given in (Song et al, 1983) as follows;

Advantages:

- It is more compact in the vertical direction.
- It generates an exact straight line.
- It has better energy efficiency.
- The actuators can be placed high on the leg minimising rotating inertia.

- ° Simpler coordination control algorithm.

Disadvantages :

- The two linear slides are hard to design and may have less mechanical reliability.

Like a pantograph mechanism, a later design, the Odex leg mechanism (figure 2.1(g)) proved to have a high performance. The odex leg mechanism shown in the figure is only another version of a pantograph mechanism which is actuated by electrical linear actuators instead of the more common hydraulic type of actuation (Russell 1983).

2.2.4 Seven Bar Leg Mechanism

Song (1983) came up with an alternative mechanism, a seven bar leg (2.1(h)). Even though the mechanism consists of only revolute joints, some of the linkages included hydraulic actuators to change the length of the linkages for actuation. However these actuators increase the inertial forces of the mechanism. It is a combination of two four bar mechanisms. Linkages are compact enough and linear actuators should be used. The design is produced by using a software package called RECSYN (Song 1983), and computer simulation studies are carried out on the design. The advantages and disadvantages of the seven bar leg are given as follows;

Advantages :

- The mechanism is composed of rotary joints only. This makes the mechanical design easier and the mechanism more reliable.

Disadvantages :

- It requires longer total mechanism to produce desired walking envelope.
- It generates an approximate straight line foot path when only the drive actuator is used.
- It is likely to have less energy efficiency because a linear motion is converted to a rotary motion and is converted back to a linear motion.

2.3 Leg Geometry of Mammals for Elastic Energy Storage

In figure 2.2, the leg limbs of a horse and a cheetah are roughly shown at the beginning and at the end of the support period. Both front and rear legs are shown during running (Gray 1968). As can be seen from the figure, straight line foot trajectory is not a concern during running. Whereas large longitudinal stroke compared to the leg height is significant in a cheetah compared to a horse. The limb movements not only serve to push the body forward but also help to preserve energy in the muscles and tendons to be used for locomotion.

2.4 Development of Evaluation Criteria for Leg Mechanisms and Their Actuation

Evaluation criteria are developed by explaining desired specifications at each item as follows;

2.4.1 Terrain Adaptability

Terrain adaptability is what distinguishes a legged vehicle from other types of vehicle. To achieve terrain adaptability, the stroke or rotation of the actuators driving a leg mechanism should be able to be controlled in addition to timing and speed characteristics. While mechanical actuators fall short in complying with terrain adaptability requirements, the hydraulic and electrical actuators perform very well from the control point of view.

For a legged vehicle travelling at high speeds, the terrain conditions can be specified assuming that an obstacle free path is always available. Hence the terrain adaptability in the longitudinal direction is not seen as a serious concern. However in the vertical direction, terrain adaptability is required.

2.4.2 Load Handling

A legged vehicle which is going to be used for off-road transport should be designed in such a way that it can handle considerable load compared to its weight. Therefore load handling is considered to be a desired

characteristic for an actuator. The hydraulic actuators are considered to be superior to electrical and mechanical actuators from the load handling point of view. In a leg mechanism, the following factors affect the load handling characteristics;

1- The number of connections between the vehicle body and the leg mechanism (see figure 2.3(a)).

2- The number of linkages with three or more connections (see figure 2.3(b)).

Since the number of connections and the linkages vary greatly in leg mechanisms, the ratio of these quantities should be used to the overall number in the leg mechanism. Hence these ratios are represented by L_1 and L_2 respectively. The higher are these ratios, the better are the load handling characteristics as shown in the figures.

2.4.3 Dynamic Characteristics

A leg mechanism for off-road transport is required to operate at various speeds. Especially it is necessary to operate at high speeds and to be able to incorporate the inertial forces of the mechanism into the leg cycle. Mechanical actuators are therefore considered to be superior than other types of actuators from dynamical point of view because they can operate at high speeds while balancing the inertial forces.

2.4.4 Joint Type

The leg mechanism can have the following joint types;

- Sliding joints
- Revolute joints
- A point contact

From the reliability point of view revolute joints are preferred.

2.4.5 Geometric Work

The significance of geometric work from the actuation point of view can

be explained as follows; Geometric work can be removed or reduced by actuating joints in pairs. In case of revolute joints, all joints can be arranged in such a way that one single drive can be used for all rotating parts. Whereas, in case of sliding joints each joint has to be driven by a separate actuator. Therefore actuators with revolute joints are preferable such as cranks.

The significance of geometric work from the leg mechanism's point of view can be explained as follows; Geometric work in a mechanism can be avoided by decoupling the longitudinal and vertical actuator motions. In that way ground reaction forces can only effect the vertical actuator, hence avoiding geometric work. For example, all leg mechanisms which accommodate a pantograph mechanism in their structure avoid geometric work regardless of the way in which they are actuated.

2.4.6 Straight Line Foot Trajectory At Walking Speeds

Some leg mechanisms can produce a straight line foot trajectory during walking, hence avoiding potential energy losses due to body swing. This property is considered to be valuable during locomotion at low speeds (Cavagna and Kaneko 1977), (Hirose and Kunieda 1991), (Hirose and Umetani 1978), (Kaneko et al 1985), (Song and Lee 1988), (Song et al 1981). However, at high speeds straight line foot trajectory characteristic has no role to play for energy efficiency, since the potential energy of the body significantly changes due to bouncing motion. In that case, the potential energy can be converted into elastic energy for storage during the support period as mammals do.

2.4.7 Inertial Forces

From the actuation point of view, rotary actuators such as crank-rocker and slider-crank are superior compared to the other type of actuation methods, since they absorb the inertial forces by keeping a constant rotation speed. Whereas in a hydraulic ram example, the backward and forward

motions brought to a halt at the end of each half cycle.

From the leg mechanism point of view, having telescopic limbs in the structure of a leg mechanism increases inertial loads during leg swing and destabilises the motion. Therefore applications causing similar effects are undesirable in leg mechanisms. The closer the telescoping linkages are to the foot, the worse the inertial forces become.

2.4.8 Elastic Energy Storage

The leg mechanism should be able to store elastic energy during the support period so that it can use it during the transfer period to increase the potential energy of the vehicle. There has been no application involving storing energy in a hydraulic or pneumatic circuit, even though theoretically this is possible. Also the energy can be stored mechanically in a leg mechanism itself by using springy linkages.

2.5 Development of A New Leg Design

A pantograph leg geometry has been shown to be very advantageous among the previously designed leg mechanisms. Therefore its advantages should be benefited by incorporating its structure to the new leg design. When mammal leg geometries are examined, they can be assumed to be a pantograph with an extra limb attached to the end. The limbs of the front and rear legs of a cat are shown in figure 2.4(a) (Gray 1968). Figure 2.4(b) further shows how a pantograph leg can be substituted for the right upper limbs. The additional linkage can be supported by being connected to the extended linkage as shown in figure 2.4(c). This new leg design is called *Buraq**. As it can be seen in figure 2.5, the Buraq leg can be used either as an insect type or as a mammal type leg.

2.6 Actuation of the Buraq Leg Mechanism

A compromise has to be made between adaptability and dynamic characteristic when a mechanical actuator is to be used. Moreover, the

(*) In the Islamic tradition, Buraq refers to the horse-like animal with wings which took the Prophet of Islam from Makka to Jerusalem in no time.

adaptability of a legged vehicle for off-road transport is not so crucial in the longitudinal direction since the terrain is mostly obstacle-free, and steering around the obstacles can be done by the driver (see section 2.4.1). For longitudinal drive, dynamic characteristics bear much greater importance due to the need to travel at high speeds. Hence, a mechanical actuator can be used for longitudinal drive. A slider-crank mechanism can be used, which can generate a linear motion. However, revolute joints are more desirable than sliding joints, therefore a four bar mechanism - a crank-rocker in particular - should be used for longitudinal motion (see figure 2.6).

In the vertical direction, load handling and terrain adaptability characteristics are crucial. Therefore a hydraulic actuator fits best for these purposes (see figure 2.6).

Theoretically, increase in the overall length of a pantograph mechanism with an extra limb can allow the mechanism to be actuated by rotary motion, and the foot produce an approximate straight line during the support period. A model leg was built, and some simple experiments showed that the application is feasible.

2.7 Evaluation of the Buraq Leg Mechanism

The advantages of the Buraq leg mechanism can be listed according to the evaluation criteria as follows;

- The vertical actuation is done by a hydraulic cylinder, therefore the leg mechanism satisfies the minimum terrain adaptability requirement.
- Having the vertical actuation done by a hydraulic cylinder also satisfies the load handling characteristics from the actuation point of view. From the leg mechanism point of view, the ratios of L_1 and L_2 have the values of 0.23 and 0.33 respectively which is better than a pantograph leg mechanism (L_1 and L_2 are 0.20 and 0.25).
- Due to mechanical actuation in the longitudinal direction, the control task is easier, reliable and the dynamical characteristics are favourable unlike a pantograph mechanism.

- The leg mechanism is constructed completely by revolute joints except for one hydraulic actuator in its vertical direction. Hence there is one less sliding joint in the structure compared to a pantograph. Also having the sliding joint in the vertical direction is much better than having it in the longitudinal direction, because tension builds up much more in the longitudinal direction compared to the vertical direction due to the leg geometries of both leg mechanisms.

- Geometric work also can be removed by actuating legs in pairs through the same drive shaft in the longitudinal direction.

- From the inertial point of view, since all actuator units are concentrated on the vehicle body, the mechanism has similar advantages to a pantograph mechanism. From the actuation point of view, mechanical longitudinal actuation proves favourable for the Buraq leg mechanism compared to a pantograph while operating at high speeds.

- The amount of fluid that needs to be circulated in the vertical actuation the circuit is less, since the Buraq leg mechanism is much more sensitive to vertical displacements than a pantograph leg. Also having mechanical longitudinal actuators, much higher speeds can be achieved than it would be practical with hydraulic cylinders used in the longitudinal direction. However, by using the slider-crank mechanism for a pantograph this problem can be sorted out for operation at high speeds.

The disadvantages of the Buraq leg mechanism compared to a Pantograph leg are as follows;

- Simple experiments on a Buraq leg model have shown that it is possible to obtain only an approximate straight line foot trajectory during walking.

- The foot working envelope is smaller particularly in the vertical direction.

- The longitudinal motion is not fully controllable.

- The leg structure has more linkages which makes the construction of the leg relatively difficult, and also increases the backlash between the foot

and the actuated joints.

2.8 Conclusions

The new leg mechanism, Buraq, resembles a biological leg both for an insect and for a mammal when alternative versions are used (see figure 2.5). Also it inherits most of the advantages of a pantograph leg mechanism since it incorporates the same structure in its upper mechanism. Adding another limb to a pantograph mechanism is a promising development from the elastic energy point of view which is discussed in further detail in chapter 6.

Most of the disadvantages of the Buraq leg compared to a pantograph leg can be ignored considering that the leg is designed for high speed locomotion in obstacle free terrains.

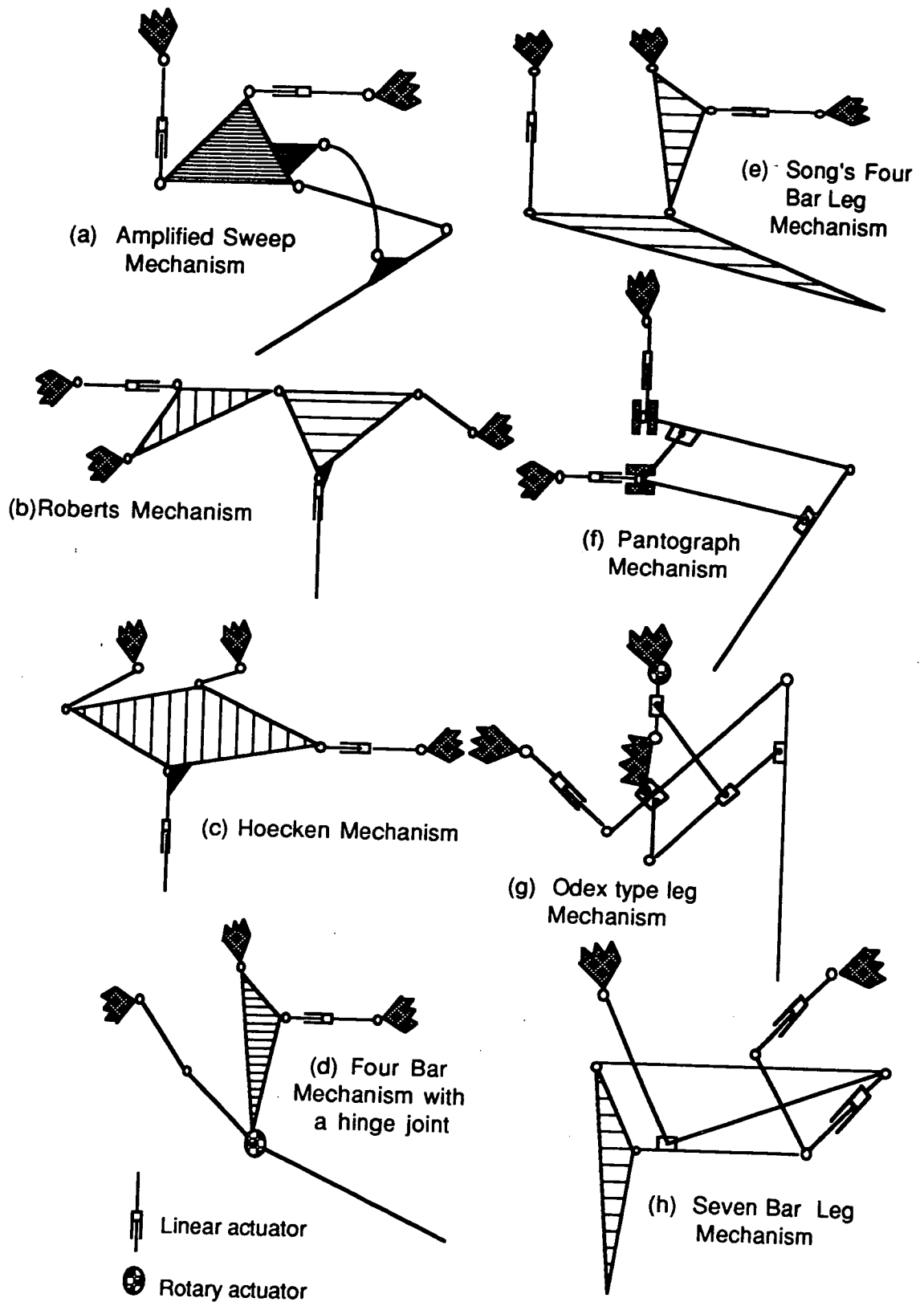


Figure 2.1 Some of the leg mechanisms studied in the previous research

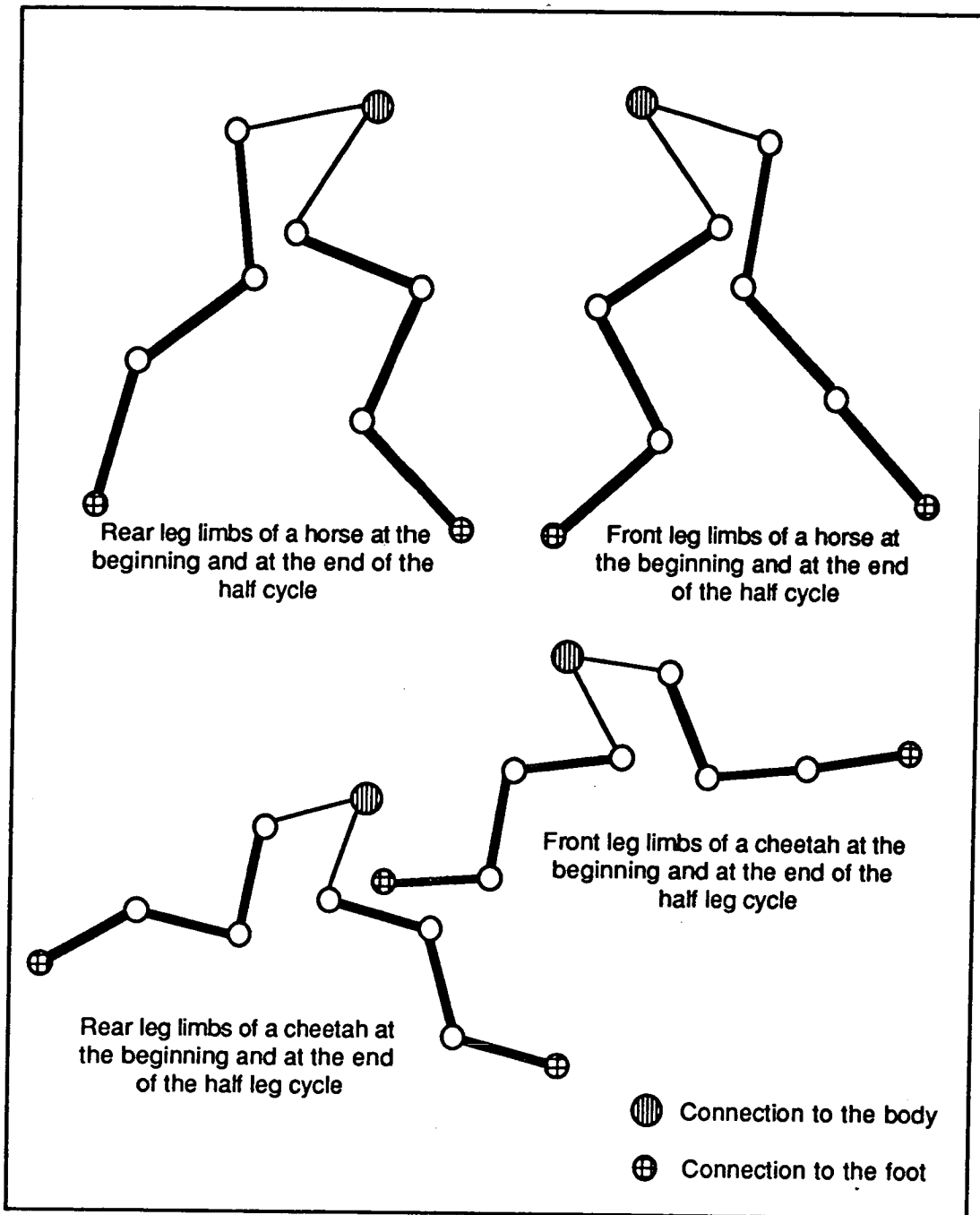


Figure 2.2 Leg limbs of a horse and a cheetah to show the limb configuration and movement during locomotion. Despite shorter legs, a cheetah has a longer forward leg stroke as the figure shows.



Figure 2.3 (a) Load handling characteristic: The parameter is the number of connections between the vehicle and the leg mechanism

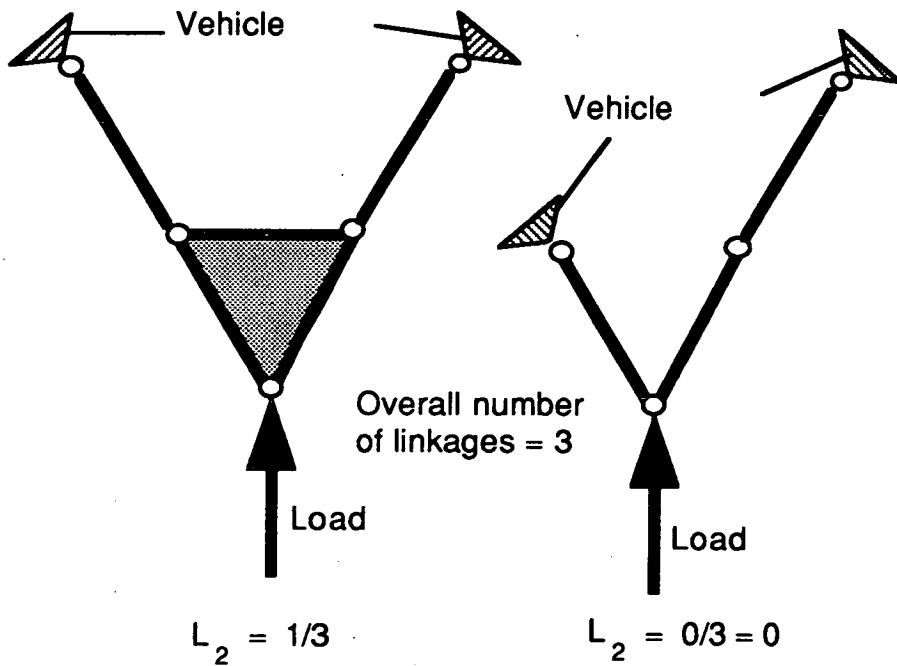
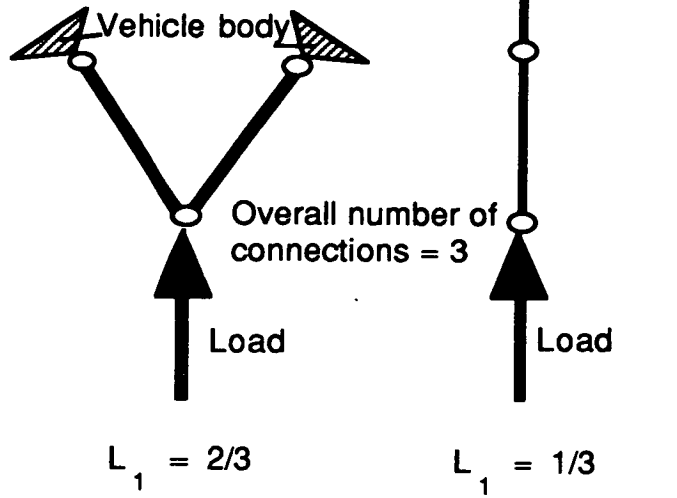


Figure 2.3 (b) Load handling characteristic: The parameter is the number of linkages with three connections

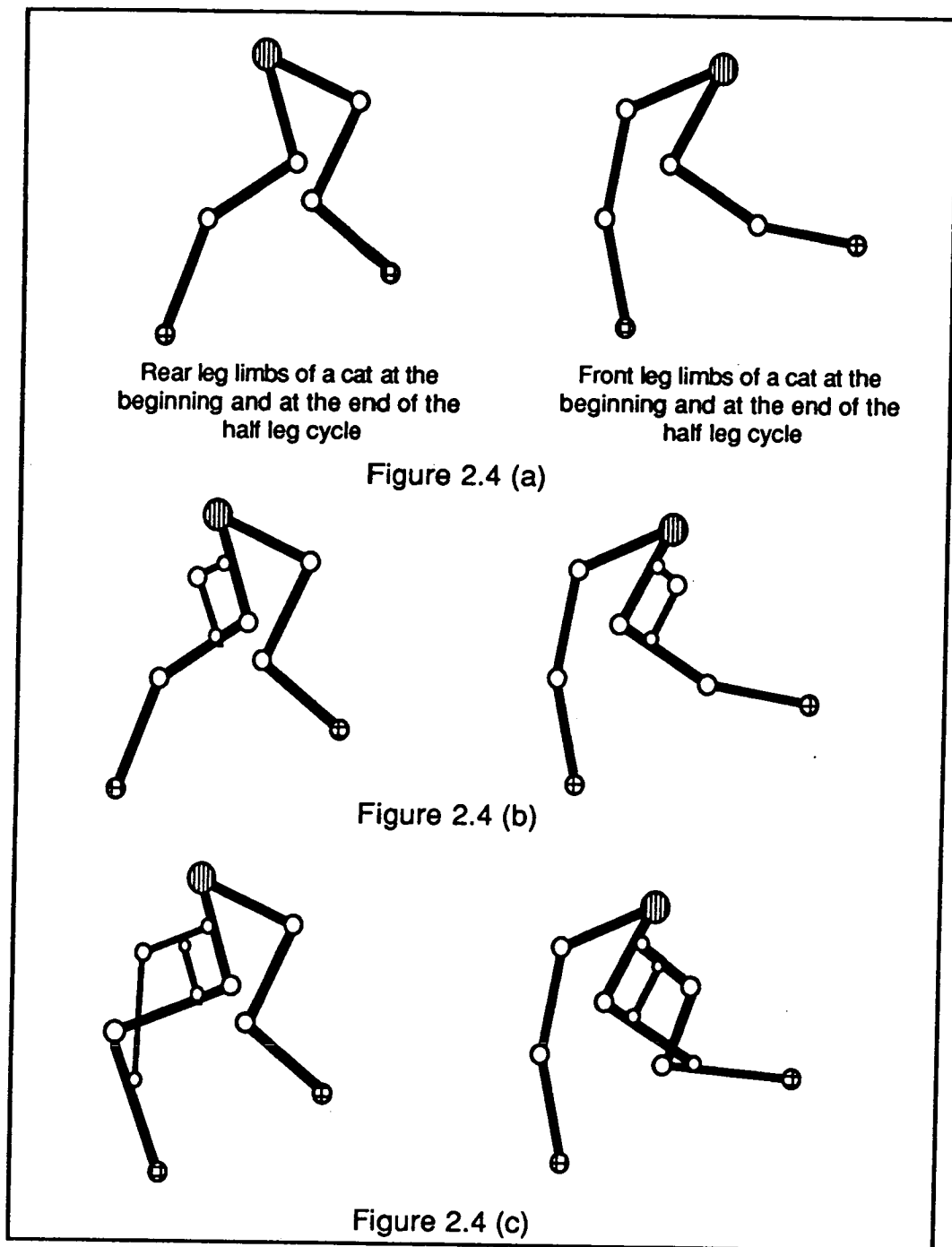


Figure 2.4 Development of a new leg mechanism starting with a pantograph fitting to the leg limbs of a cat, and further supporting the additional limb. Two different versions of the same leg mechanism are shown at the last stage (c).

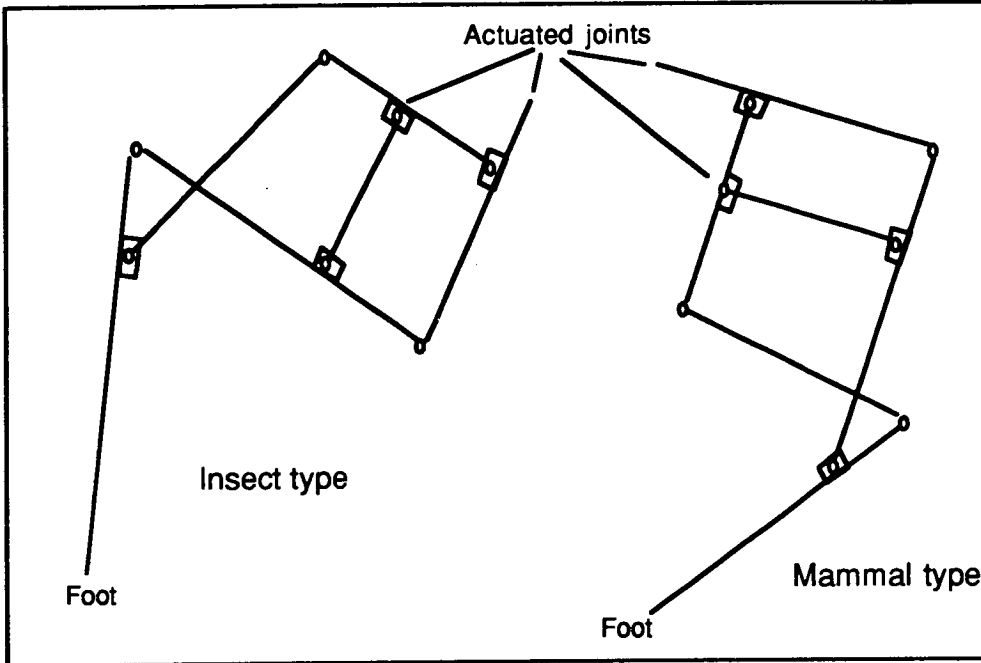


Figure 2.5 Two different applications of the Buraq Leg

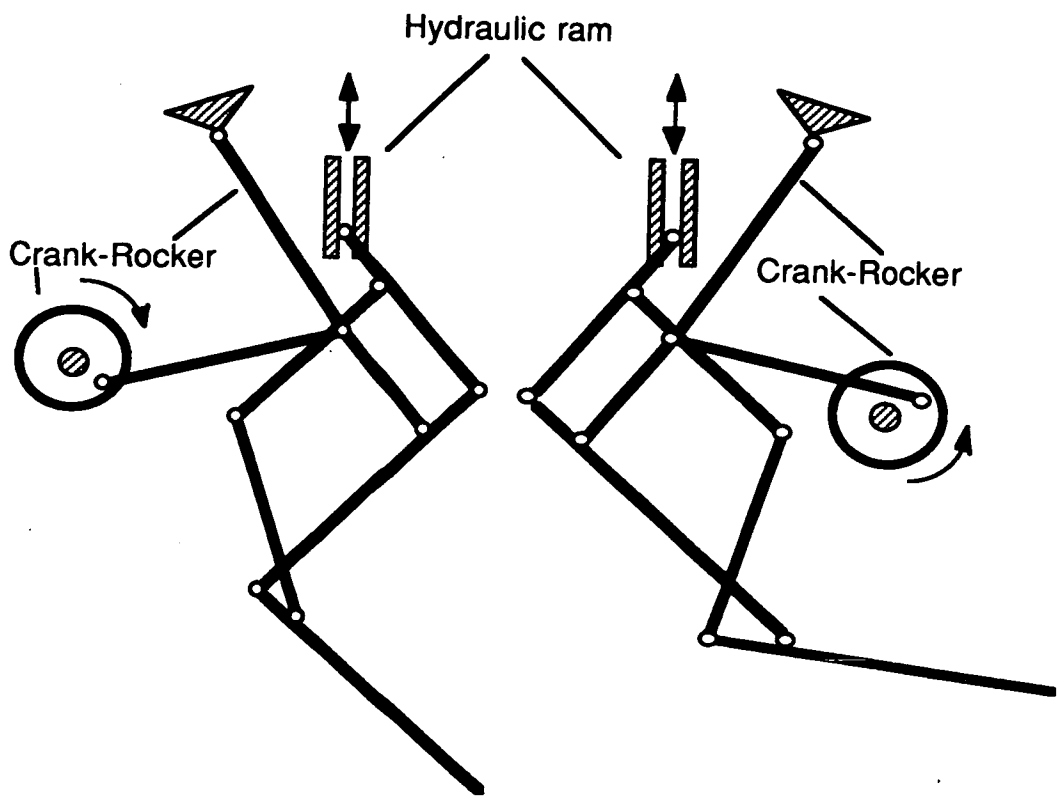


Figure 2.6 Actuation of two different applications of the Buraq Leg Mechanism

Chapter 3

Computer Simulation Studies of the Buraq Leg

Contents

3.1 Introduction

3.2 Definitions

3.3 Simulation Study

3.3.1 The Initial Position and Values

3.3.2 The Support Period

3.3.3 The Lower Actuator Positions

3.3.4 The Transfer Period

3.3.5 Crank-Rocker Mechanism Design

3.4 Effects of The Drive Parameters on the Leg Mechanism Motion

3.5 Kinematical Analysis of the Buraq Leg Mechanism

3.6 Simulation Results

3.7 Conclusions

3.1 Introduction

In this chapter, a computer simulation model for the Buraq leg mechanism is developed. The leg is considered to be actuated as proposed in chapter 2, that is, a crank-rocker is used for longitudinal drive, and a hydraulic ram is used for vertical drive (see figure 3.1). The procedure followed in this study can be briefly mentioned as follows;

1. The leg mechanism dimensions are calculated in such a way that when the leg mechanism is actuated in longitudinal direction from point Q, the foot produces a straight line trajectory.
2. A crank-rocker mechanism is designed to give the required trajectory of point Q.
3. Using the overall leg mechanism and its drives, a simulation program for the leg and its drives is written, so that velocity and acceleration profiles of the foot can be examined through kinematical analysis.

3.2 Definitions

A sketch of the Buraq leg mechanism is shown in figure 3.2. All motions can be considered to be in the plane shown. Parameters in the figure are explained as follows.

The upper actuated joint, 'U': This is point U in figure 3.2, where a hydraulic cylinder is applied for up and down motion of the foot. When the piston moves downwards, the foot raises up, and vice versa. During the support period, point U (U_x, U_y) is fixed and taken as the origin. During the transfer period, it is moved down and up along the y axis to raise and to lower the foot respectively.

The lower actuated joint, 'Q': This is point Q in figure 3.2, where a crank-rocker is applied for longitudinal motion of the foot. The point Q is represented as (Q_x, Q_y) in Cartesian coordinates.

The foot, 'P': This is point P in figure 3.2 representing the foot. In section 7.3.5 details of the foot structure are given. For the simulation study, a point representation of the foot is sufficient.

A, B, C, D, E, F, H, K : These letters represent the length of linkages used in the Buraq leg mechanism.

R₁, R₂, R₃ and R₄ : These numbered letters represent the linkage lengths of the crank-rocker used to drive the Buraq leg mechanism (see figure 3.1).

a, b, c and x : These letters represent the angular displacements shown in figure 3.2. The standard right hand rule is used for the orientation of angular displacements in Cartesian coordinates.

3.3 Simulation Study

The leg mechanism has four degrees of freedom in the plane, for example, knowing the position of one point and two angles is enough to calculate the position of any point on the mechanism. Following sections explain the simulation study carried out in sequential order.

3.3.1 The Initial Position and Values

A leg mechanism which was built as a small prototype model was used to assign the initial values of the linkage lengths of the leg mechanism.

The prime constraint on the mechanism is producing a straight line trajectory during the support period. Therefore the position with the tibia vertical is set as the start of the support period. The initial values of angles a and c are 0 and $-\pi/2$ shown in figure 3.3. Using the prototype linkage dimensions, the foot position and angle b (initially b_1) values are assigned.

3.3.2 The Support Period

The following steps are used during the simulation of the support period;

- Initial position and values are set as described in the previous section.
- As shown in figure 3.3, point U is fixed at the origin. Angular displacement b is given an increment. At this position, the foot (point P) is constrained to be on a perfect horizontal line as shown in the figure. Hence the position of point U, vertical position of the foot and angle b are known.

Horizontal position of point P and angles a and c need to be calculated.

- Following equations are derived (see appendix 1.1 for details);

$$U_X + (A+B)\cos a + (C+E)\cos b + K\cos c - P_X = 0 \quad (3-1)$$

$$U_Y + (A+B)\sin a + (C+E)\sin b + K\sin c - P_Y = 0 \quad (3-2)$$

$$2BH\cos(a-c) + 2H(E-D)\cos(b-c) + \\ - 2B(E-D)\cos(a-b) - (B^2 + H^2 + (E-D)^2 - F^2) = 0 \quad (3-3)$$

During the support period point U is fixed at the origin and the value of P_y is nil. There are three equations (3-1, 3-2 and 3-3) and three unknowns (P_x , a, c), hence the solution sets can be calculated for each b angular displacement value following the flow chart shown in figure 3.4. Angle b is increased until angle c variation changes its direction which means that the leg starts to lengthen to keep on a straight line foot trajectory instead of being shortened. Since this motion needs an action from the vertical actuator, and the support period is aimed to involve only the longitudinal actuator, the support period is considered to be finished at that point.

Another way could have been followed to solve the equations. Instead of incrementing angle b and finding the horizontal foot position (P_x), the foot position could be assigned and angle b could have been calculated. However, it is easier to calculate an unknown which has a unique solution compared to an angle which has at least two different solutions.

- Having calculated the angular positions, the trajectory of point Q for an exact straight line foot trajectory during the support period can be calculated using the following equations (see appendix 1.1 for details);

$$U_X + A\cos a + C\cos b - Q_X = 0 \quad (3-4)$$

$$U_Y + A\sin a + C\sin b - Q_Y = 0 \quad (3-5)$$

The trajectory of point Q is shown in figure 3.5.

3.3.3 Lower Actuator Positions

As figure 3.5 shows, the lower actuator positions, the trajectory of point Q,

is not an exact arc. Because the leg mechanism has been decided to be driven by a crank-rocker, the point Q should have a circular arc trajectory, since it refers to the end of the rocker.

An arc is fitted to the trajectory of point Q by using the following method;

- A curve is fitted to the trajectory of point Q using the standard least squares curve fit method (Faux and Pratt 1985).

- Three normals are drawn inward from the beginning, the middle and the end points of the curve as shown in figure 3.6.

- The arithmetic mean of the centre positions is calculated to find the average central point.

- The arithmetic mean of the distances between three assigned points on the curve and the average central point are calculated to find the average radius.

- Using the average central point and the average radius, the arc for the rocker arm is produced. To compare the errors obtained in the arc fitting procedure and the standard curve fitting procedure, both fittings are plotted in figure 3.7. As can be seen, the developed arc fitting method proves beneficial at least for this particular application since the errors are negligible.

Through application of the arc fitting procedure, the rocker positions for the crank-rocker have been calculated. These positions repeat themselves for both support and transfer trajectory when the crank radius is fixed.

3.3.4 The Transfer Period

The initial values of the transfer period can be assigned the same as the last solution for the support period. To raise and to lower the foot, point U is moved along y axis. Hence the position of U is known. Also the trajectory of point Q is known. However the foot position($P(x,y)$) and angular displacements (a, b, c) need to be calculated (see figure 3.8). The equations derived in section 3.3.2 are used to find the unknown values.

The flow chart of the calculation procedure is shown in figure 3.9.

The same algorithm can be used to find the foot positions during the support period simply by assigning position of point U as the origin.

Carrying out the calculations, the dimensions of the prototype leg mechanism are modified to obtain an approximate straight line mechanism. The non-dimensional figures adopted at the end of the several simulations can be listed as follows;

$$A = 1, B = 2, C = 1, D = 2, E = 3.5, F = 2.7, H = 0.8, K = 4.1.$$

The dimensions used in the simulation studies are 32 times of the non-dimensional figures in mm since this happens to be the exact length of the built model leg. Using the modified linkage lengths, the foot trajectory for a complete leg cycle can be calculated (see figure 3.10) which is discussed in detail in section 3.6.

3.3.5 Crank-Rocker Mechanism Design

Various crank-rocker mechanisms can be designed to drive point Q, and to generate the desired trajectory. In figure 3.11 a general four bar mechanism is shown with its parameters. The main constraint in design is to choose the transmission angle (γ in the figure) in the range of ($40^\circ - 140^\circ$) so that high forces can be transmitted by the mechanism (Mabie and Reinholtz 1987). Overall, during the design, the following criteria is used;

- The range of transmission angle is chosen in the range ($60^\circ - 100^\circ$) away from the critical values.

- The distance between the centres of the crank and the rocker (R_1) is chosen small to have a compact mechanism and to avoid buckling of linkages.

Using the triangles occurring at two singular position of the mechanism (shown in figure 3.12) equations of the mechanism are derived, and simulation studies are carried out (see appendix 1.2 for details). The crank-rocker has to be placed with some angular orientation to satisfy the desired criteria as shown in figure 3.13. The following non-dimensional figures are calculated for the linkage lengths;

$$R_1 = 3.5, R_2 = 1, R_3 = 2.5, R_4 = 3.2.$$

To confirm further, the calculated linkage lengths for a crank-rocker mechanism, *Grashof's Mobility Criteria* (see (Angelas and Bernier 1987) and (Angeles and Callejas 1984) for further detail) is applied. The criteria provide the necessary and sufficient conditions for the linkage lengths of a crank-rocker. The criteria were applied to the calculated set of the linkage lengths, and the set proved to be satisfactory (see appendix 1.3 for details).

Also, through simulation studies, the variations of the angular displacements of the crank-rocker mechanism are calculated and shown in figure 3.14 (see appendix 1.4 for details).

3.4 Effects of The Drive Parameters on the Leg Mechanism Motion

In this section, the effects of hydraulic ram displacements and crank radius variation on the leg trajectory are examined through simulation studies.

The hydraulic ram displacement is kept constant throughout the stroke, and the trajectory of the foot is calculated using the algorithm explained in section 3.3.4. Hence the figure 3.15 is produced which shows the leg trajectory with respect to the hydraulic ram displacement.

The simulation study explained in sections 3.3.4 and 3.3.5 is used to produce figure 3.16 which shows the foot stroke with respect to the crank radius variation.

The simulation study explained in section 3.3.5 is used, and the angular displacements of the crank-rocker mechanism for the whole leg cycle are calculated. Figure 3.17 is developed to show the rocker swing range and values with respect to the crank radius variation.

The results are evaluated in section 3.6.

3.5 Kinematical Analysis of the Buraq Leg Mechanism

The vectorial velocity and acceleration expressions are derived for the

foot and the rocker to examine the mechanism from kinematical point of view (see appendix 1.5). Using the simulation results, the angular speeds and accelerations for the joints of the mechanism are calculated using the method developed by (DiBenedetto and Pennestri, 1983). The results are shown in a series of figures starting with 3.18 (see appendix 1.5 for details).

3.6 Simulation Results

The Buraq Leg Mechanism Linkage Dimensions

Computer simulation studies have shown that the length of the additional limb, which can be called the tibia (see figure 3.2), affects the leg stroke, the magnification ratio, material strength and required power for the actuators. The longer the tibia length, the longer the leg stroke, however the higher the magnification ratio, the bigger the stress and the higher the required actuation power.

Actuation of the joint in the support period is another factor affecting the length of the tibia. According to the computer simulations when a linear actuator such as a hydraulic cylinder is used at point Q to generate a horizontal motion, then the length of tibia decreases to produce the desired straight line foot path. However, when an arc generator such as a four bar mechanism is used to actuate Buraq, then the length of tibia increases for production of straight line motion. Since a crank-rocker is chosen for the actuation of point Q, to keep the required actuation power and the stresses in material as low as possible, the smallest tibia length enabling a straight line motion has been computed through several simulation studies.

The pantograph mechanism which is inherited in the Buraq leg mechanism has the same linkage ratios as predicted in the studies done by Song and Waldron (refer to the papers dated 1987 (a) and (1989)).

Foot Trajectory

Even though the support period calculations were carried out for a straight line foot trajectory, the magnification of the errors, which are the

result of the fitting procedure, causes the foot to travel on an approximate straight line(see figure 3.10).

As figure 3.15 shows, the foot has an intrinsic ballistic foot trajectory. That is, the foot is much more sensitive toward the vertical actuation at the beginning of the transfer period compared to the end (see the leg orientation in figure 3.1).

The Effects of the Actuators

Figure 3.16 shows a directly proportional relation between the crank radius and the foot stroke. Figure 3.17 shows that the foot stroke shortens and lengthens symmetrically according to the rocker swing range.

Foot Velocity and Acceleration

A series of figures are produced while the angular velocity of the crank is set to a constant value, 2.123 rad/s in clock-wise direction.

Figure 3.18 shows the x and y components of the foot velocity with respect to the foot displacements along x axis (represented by f_x). As expected, x component of the foot velocity is greater than the y component. At the end of the support period the irregularities are due to sudden upward foot motion. However the landing occurs smoothly due to ballistic leg trajectory.

Figure 3.19 shows the y component of the foot acceleration with respect to the foot displacements along x axis. The irregularities when the foot is raised at the end of the support period are very clear. This figure also shows the smooth landing of the foot.

Figures 3.20 and 3.21 show the variation of the x and y components of the foot and the arm velocities respectively along the same longitudinal foot displacement axis. Since the rocker trajectory is the same for both support and transfer periods, the speed profiles of the rocker are also similar unlike the case for the foot.

Another significant point to note is the speed difference between the

support and the transfer periods. The calculated foot speed during the transfer period is recorded to be at least 15% higher than that of the support period while the crank speed is constant. This is due to the change in foot trajectory which is shorter during the support period.

3.7 Conclusions

The following conclusions can be drawn from the simulation studies carried out in this chapter;

1. The Buraq leg mechanism can produce an approximate straight line mechanism. It can be actuated either by two linear actuators or a linear actuator and a four bar mechanism in both cases producing an approximate straight line foot trajectory during the support period.

2. A four bar mechanism with approved mobility can be designed, hence allowing the mechanism to be actuated as it was proposed in the previous chapter.

3. Having analysed the kinematics of the mechanism, the speed and acceleration profiles showed a smooth landing which is suitable especially for fast running legged systems.

4. The leg trajectory was shown to be a ballistic one, similar to the leg trajectories of mammals.

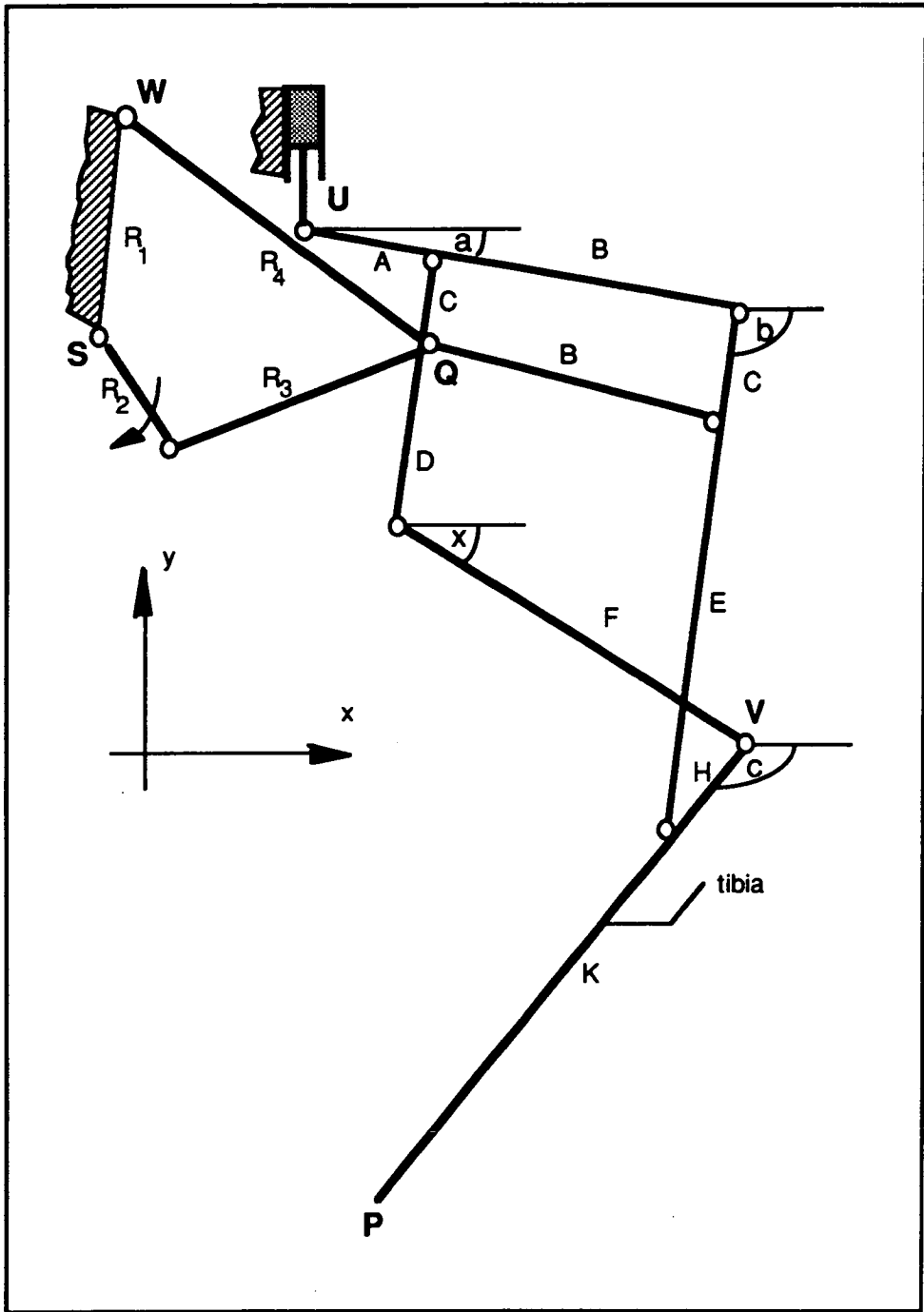


Figure 3.1 The Buraq leg driven by a crank-rocker in longitudinal direction, and driven by a hydraulic ram in vertical direction.

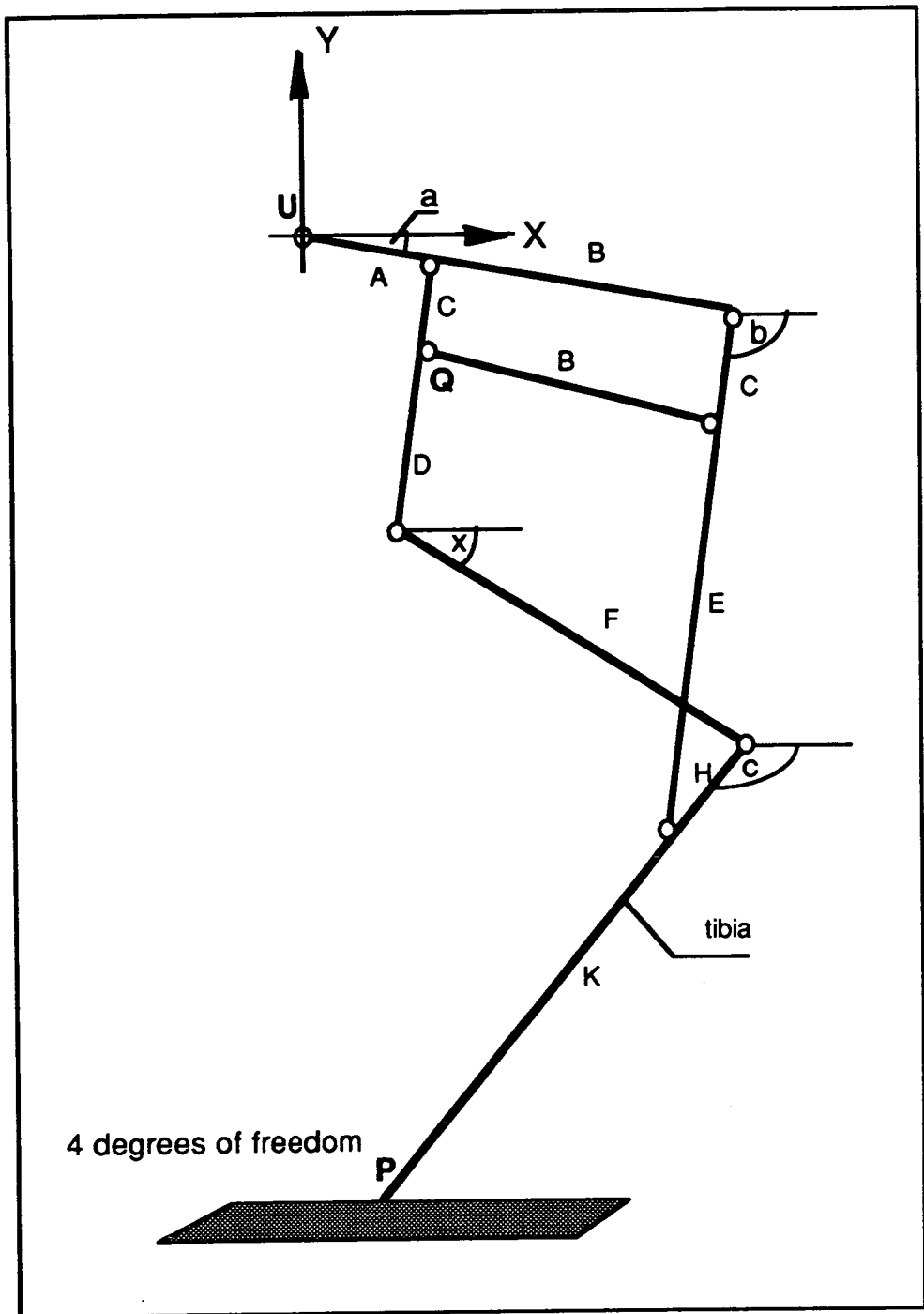


Figure 3.2 The Buraq leg with its parameters

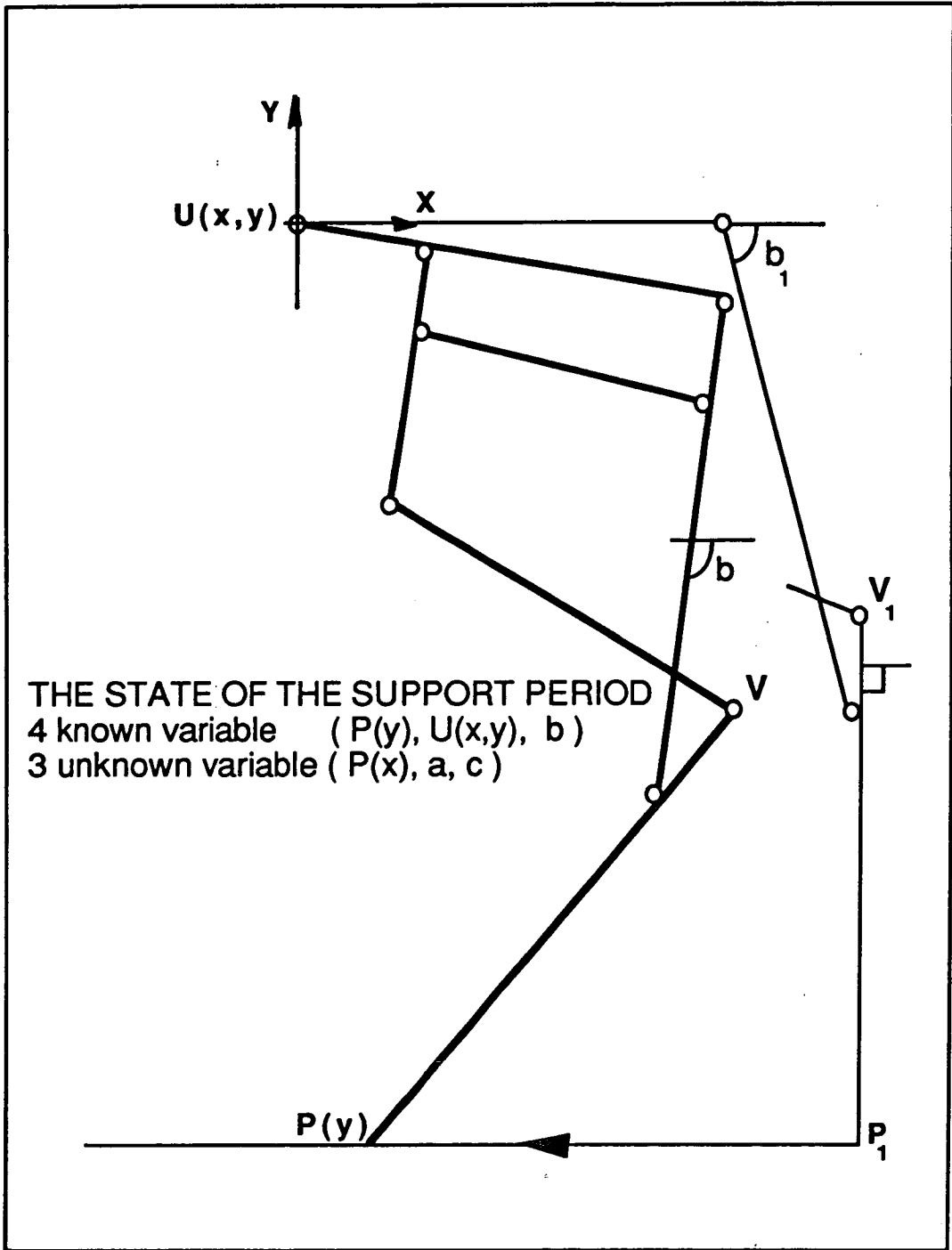


Figure 3.3 The state of the support period

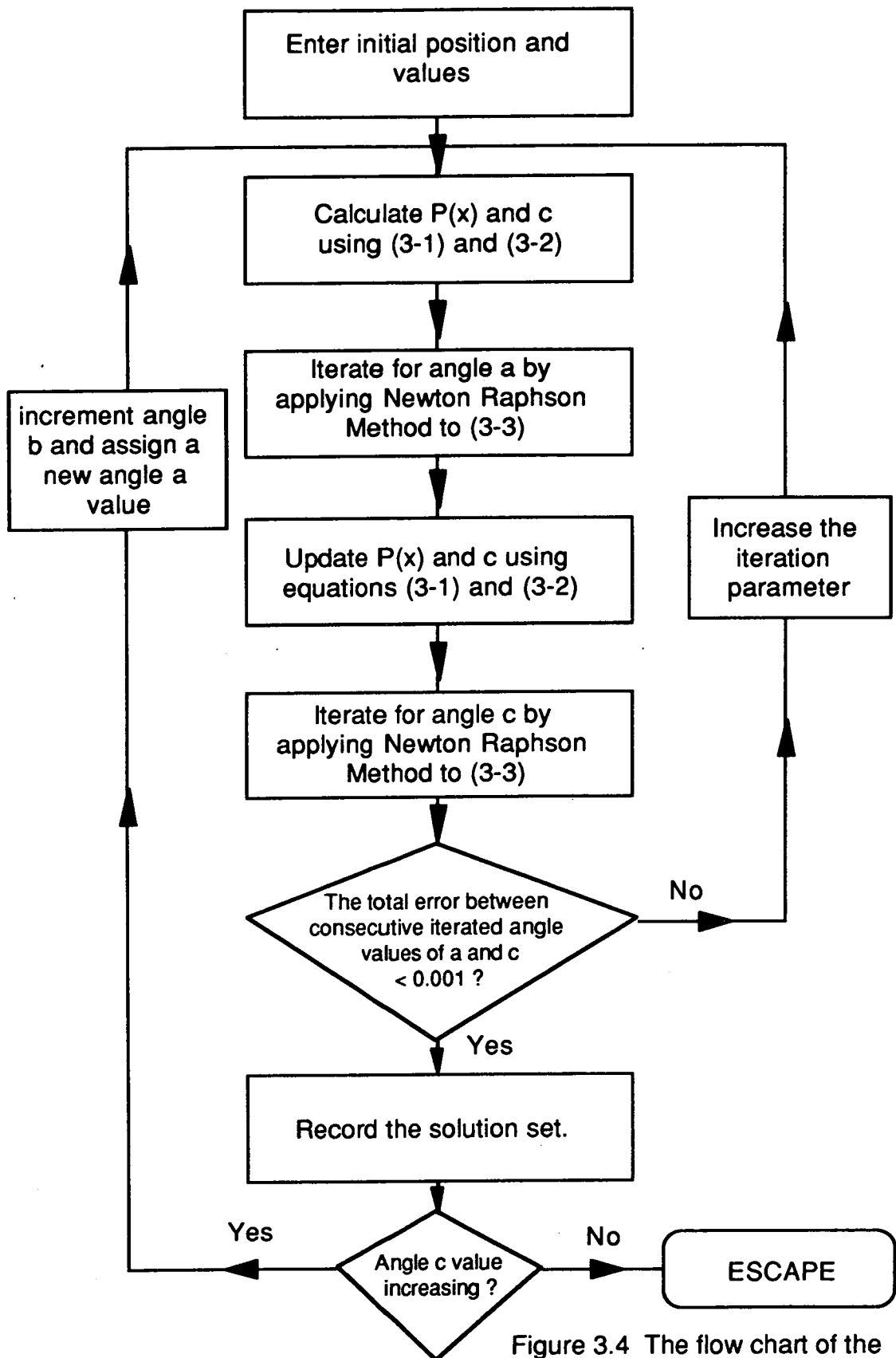


Figure 3.4 The flow chart of the subroutine calculating the leg parameters during the support period.

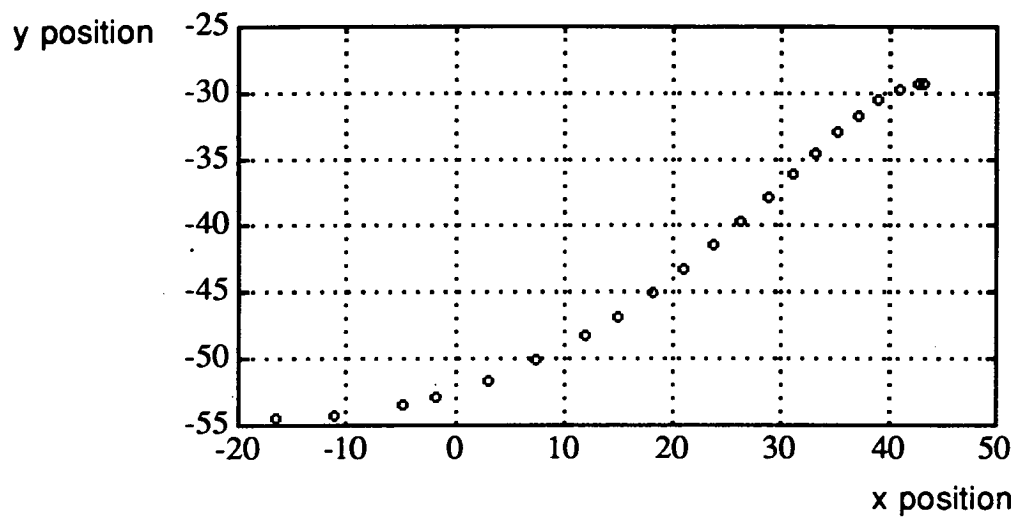


Figure 3.5 The trajectory of the point Q for an exact straight line foot trajectory

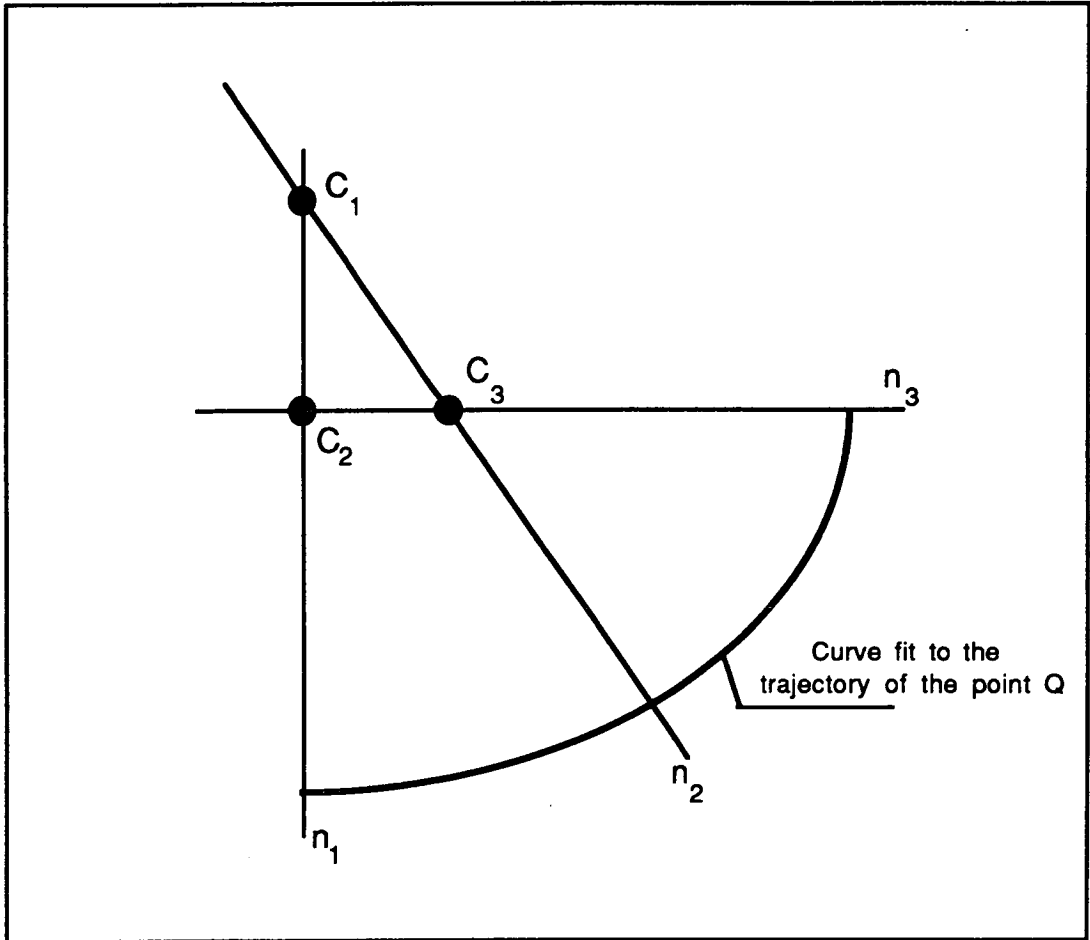


Figure 3.6 Fitting an arc to the trajectory of the point Q

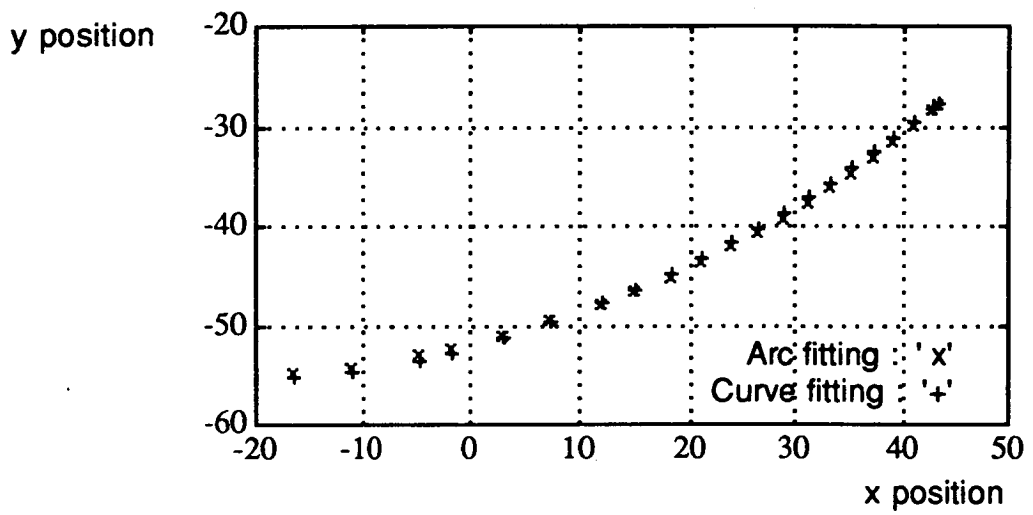


Figure 3.7 Comparison of the two fitting procedures to the trajectory of the points of Q

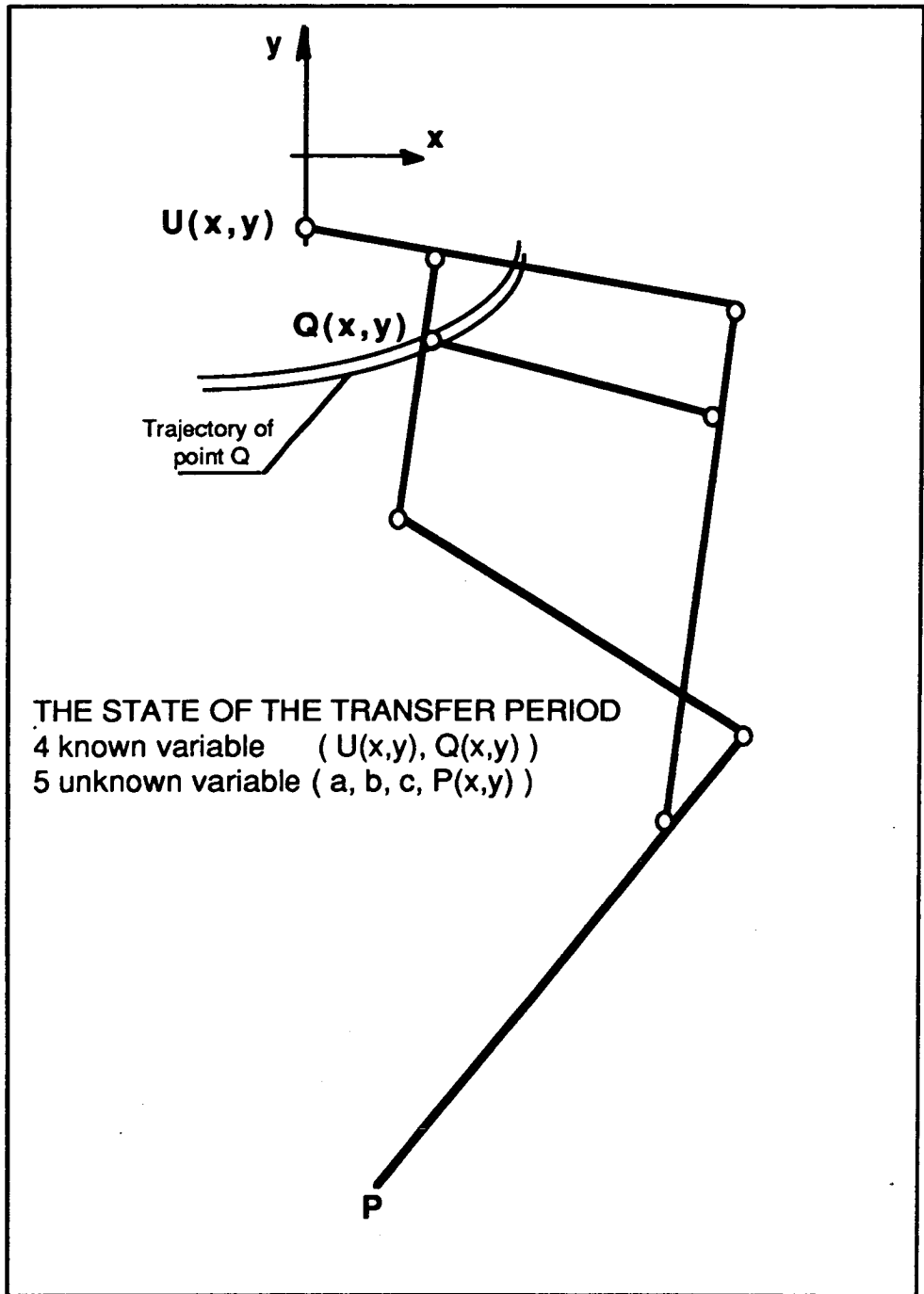


Figure 3.8 The State of the Transfer Period

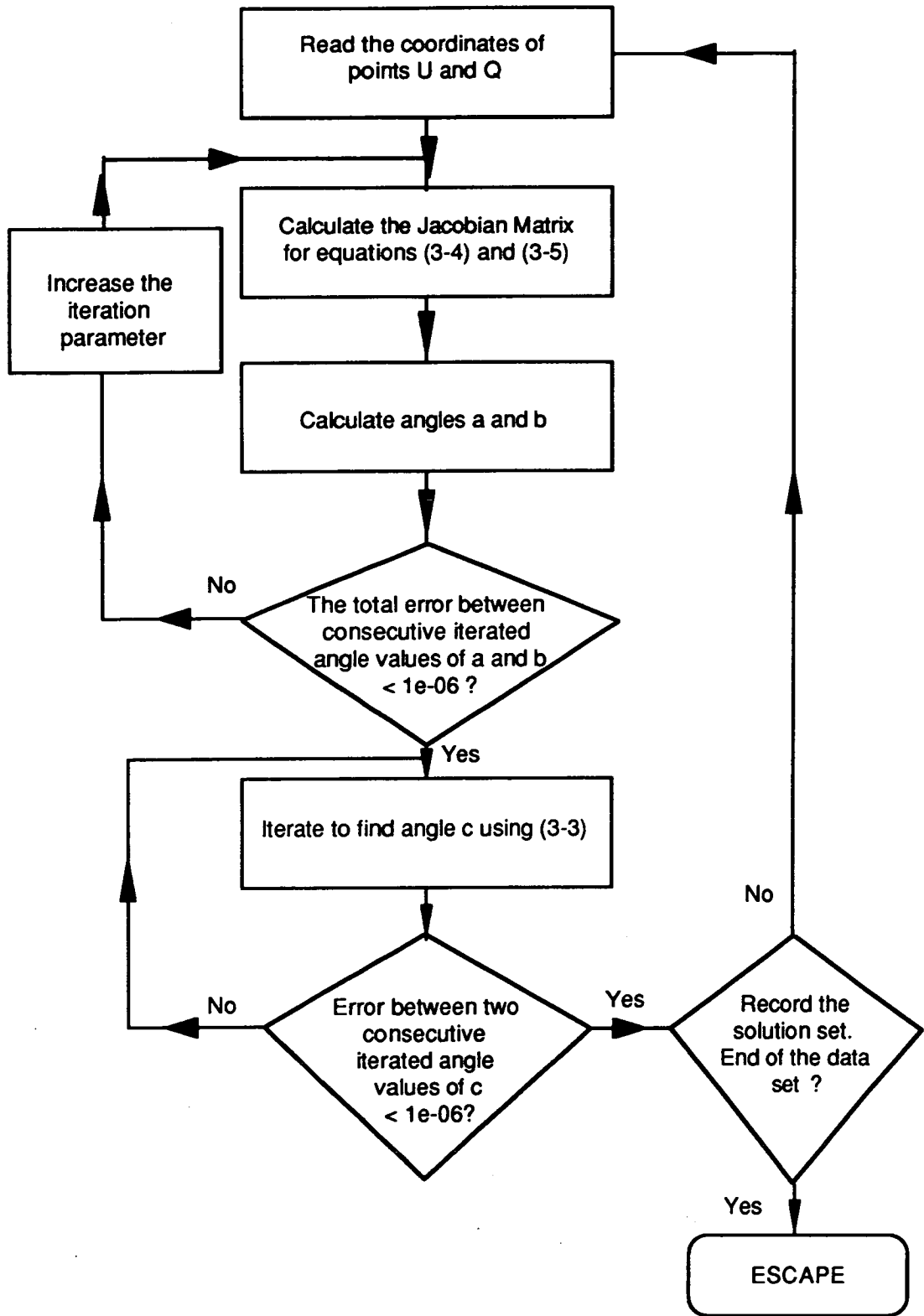


Figure 3.9 The flow chart of the subroutine calculating the leg parameters during the transfer period.

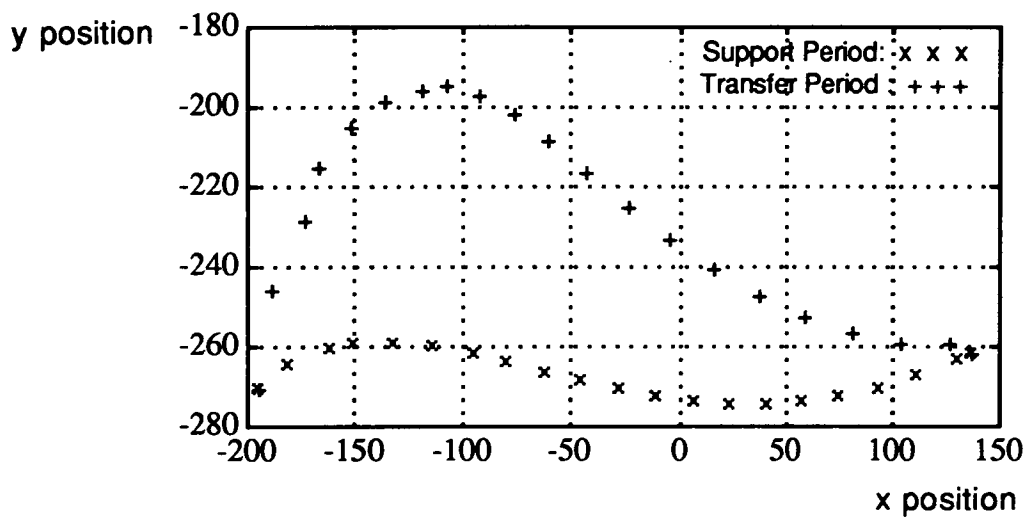


Figure 3.10 The simulation of the foot trajectory.

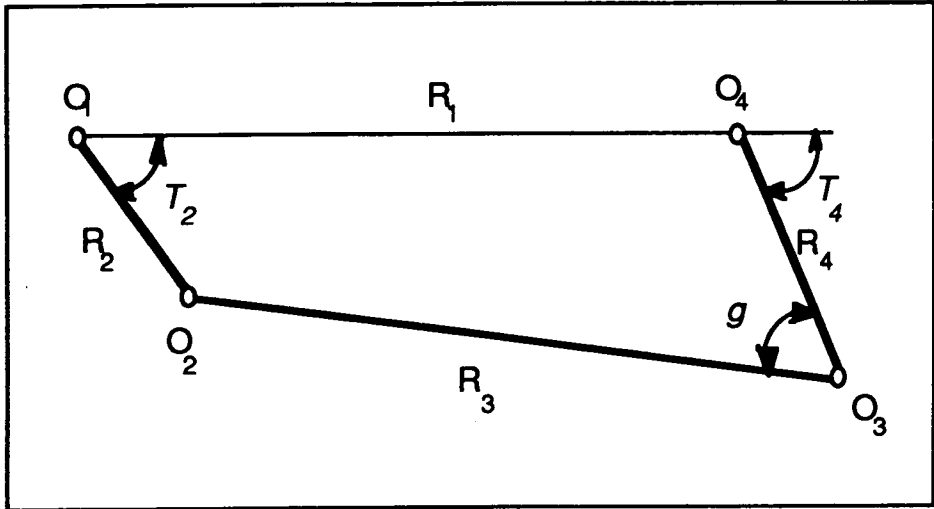


Figure 3.11 Schematic representation of a crank-rocker mechanism

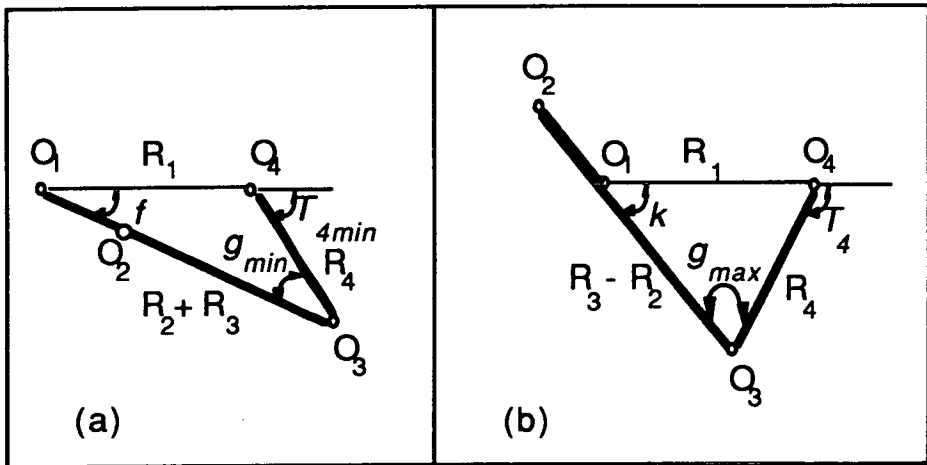


Figure 3.12 Singular positions of a crank-rocker

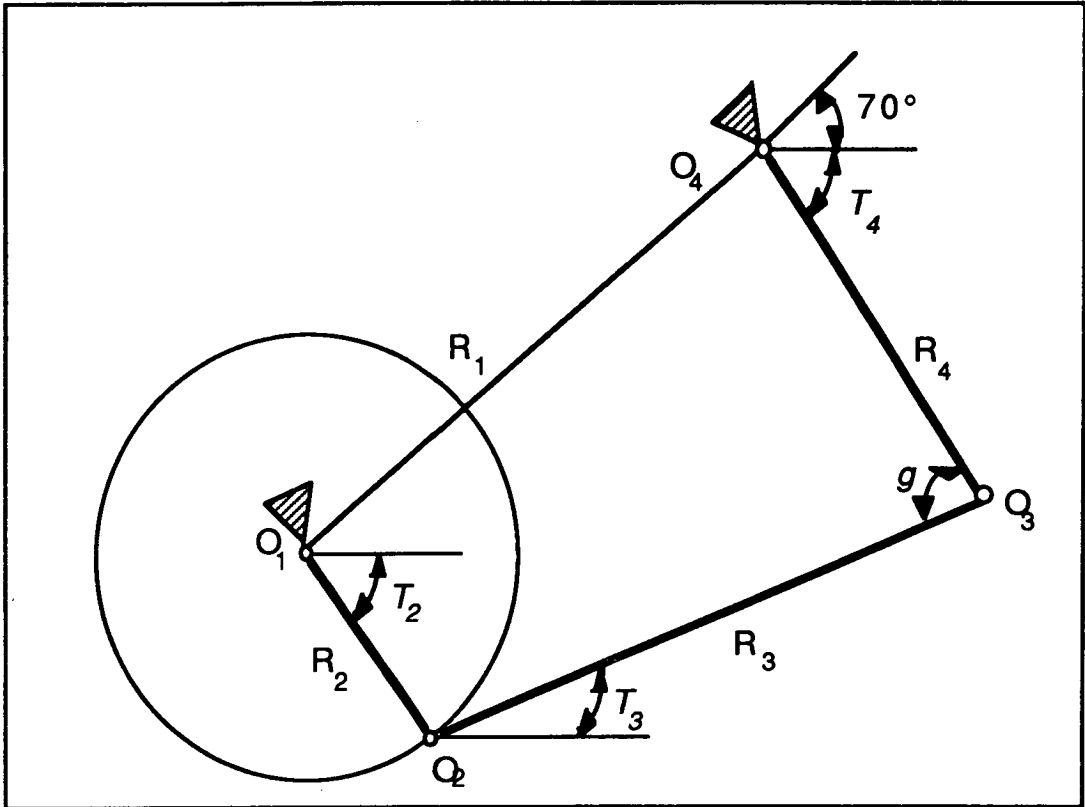


Figure 3.13 Angular analysis of the crank rocker mechanism

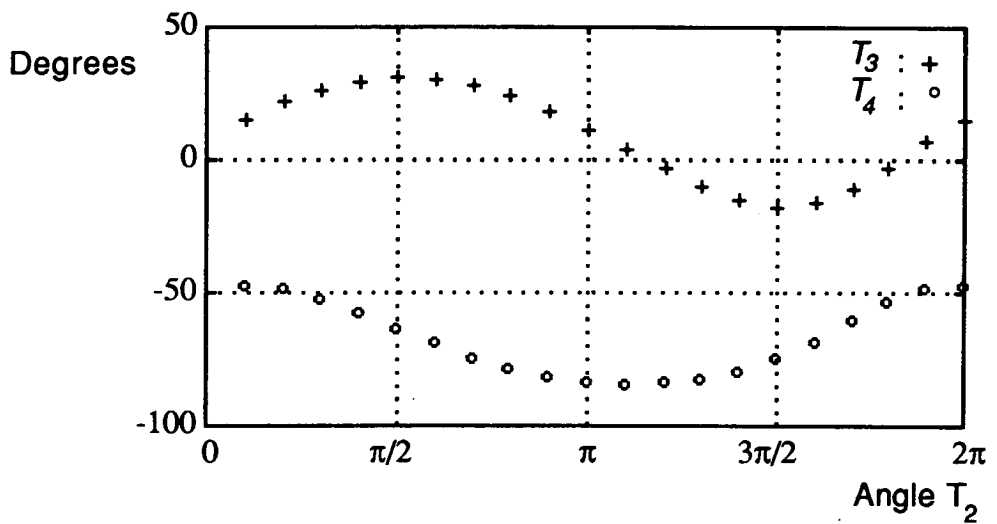


Figure 3.14 Angular displacement variations of the four bar mechanism during the complete leg cycle

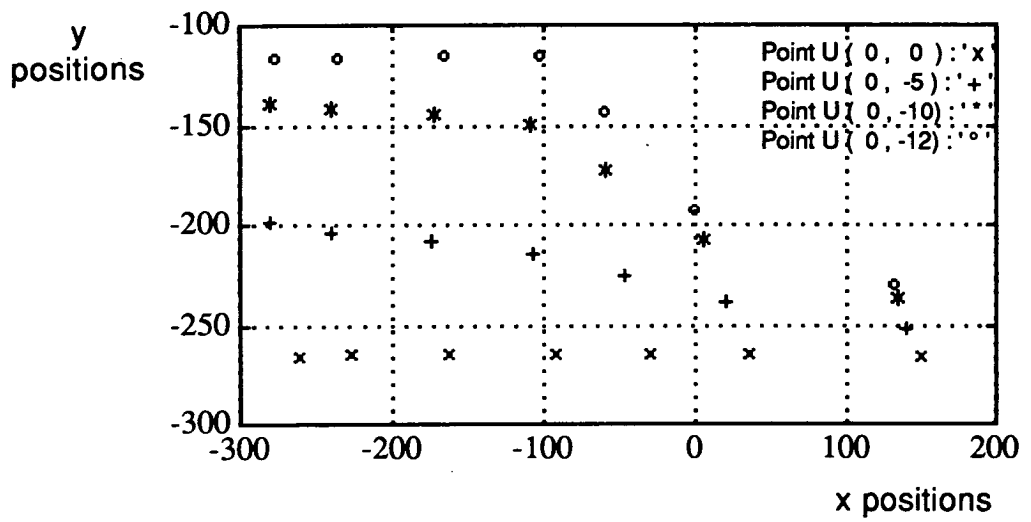


Figure 3.15 Effect of the upper actuated joint (point U) on the foot trajectory

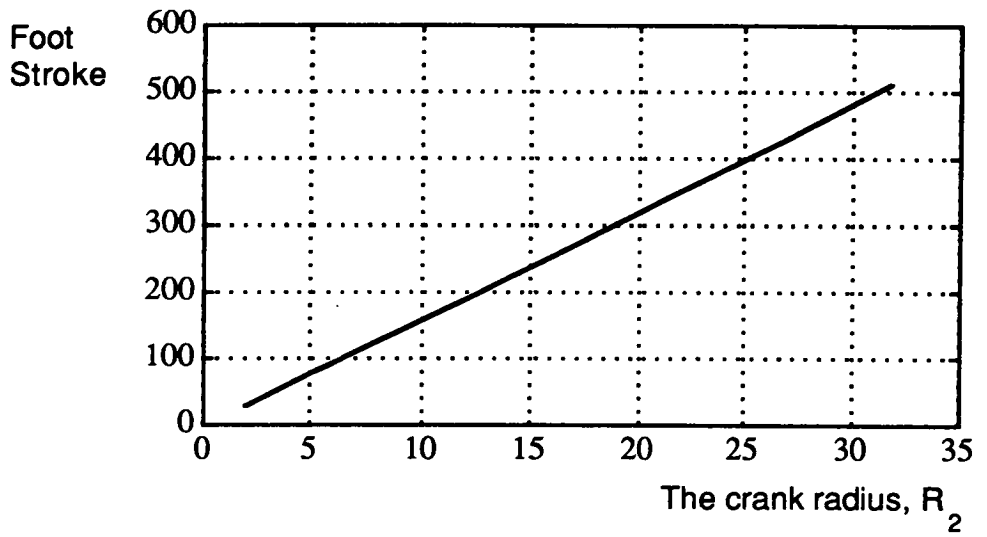


Figure 3.16 The variation effect of the crank radius on the foot stroke

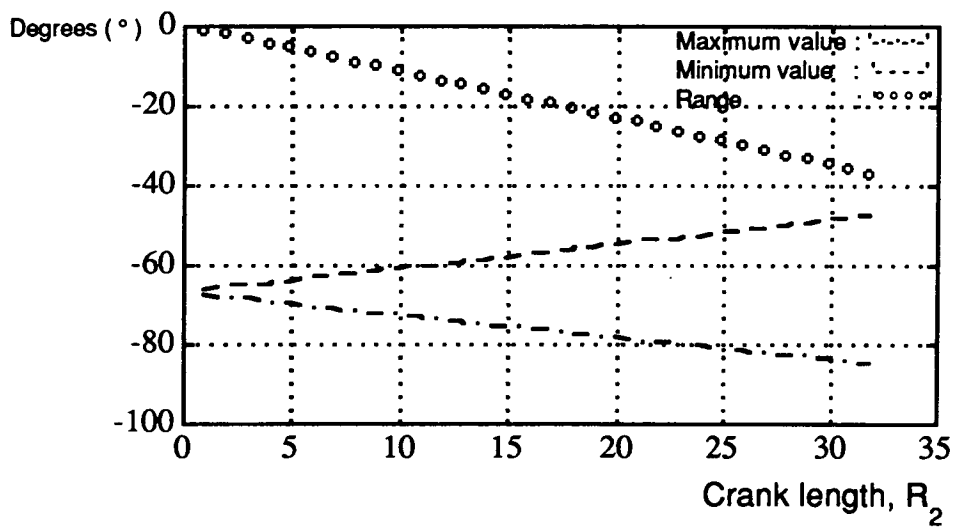


Figure 3.17 The crank variation effect on the range of the rocker swing

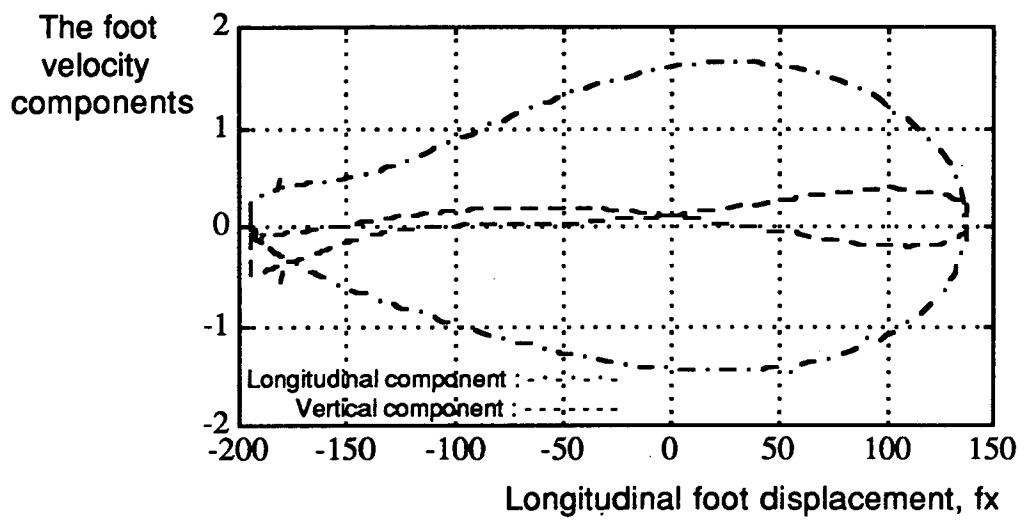


Figure 3.18 The foot velocity components with respect to the longitudinal foot displacement during the leg cycle.

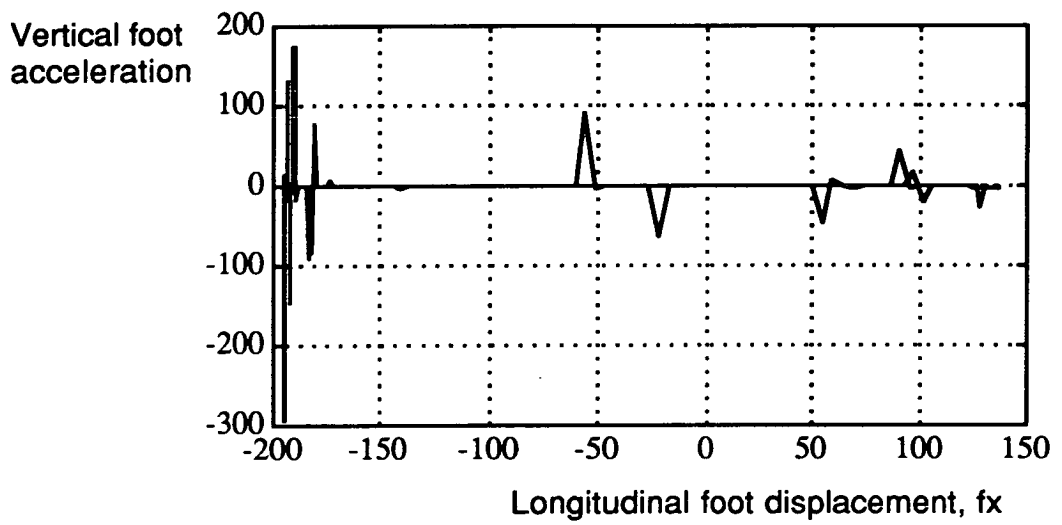


Figure 3.19 The vertical foot acceleration with respect to the longitudinal foot displacement

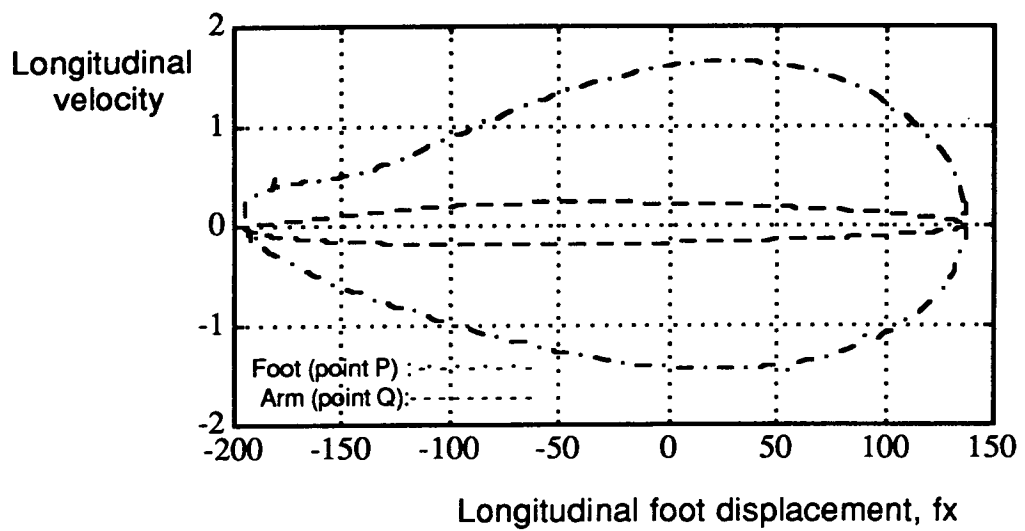


Figure 3.20 The longitudinal velocity components of the foot and the arm with respect to the longitudinal foot displacement.

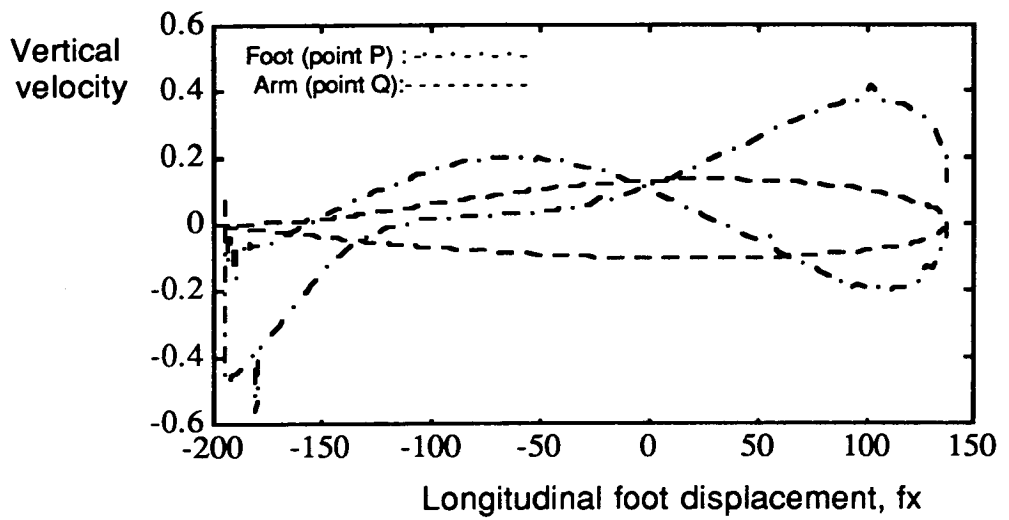


Figure 3.21 The vertical velocity components of the foot and the arm with respect to the longitudinal foot displacement.

Chapter 4

Experimental Study of the Buraq Leg Mechanism

Contents

4.1 Introduction

4.2 Design of a Model

4.2.1 Mechanical Design

4.2.2 Power System

4.2.2.1 Longitudinal Drive

4.2.2.2 Vertical Drive

4.2.3 Control

4.2.3.1 Logic Control

4.2.3.2 Computer Control

4.3 Experiments to Calculate Specific Resistance

4.3.1 Initial Assumptions and Instrumentation

4.3.2 Calibration of the Instruments

4.3.2.1 Strain-gauge calibration

4.3.2.2 Current transducer calibration

4.3.3 DC Motor Characteristics

4.3.3.1 Measuring stall torque

4.3.3.2 No load speed

4.3.3.3 Evaluations

4.3.4 Calculation of the Specific Resistance

4.3.5 Load Sensitivity of the Specific Resistance

4.4 Foot Trajectory

4.4.1 A Mechanical Constraint on the Foot Trajectory

4.4.2 Calibration of the Straight Line Potentiometer

4.4.3 Measurement of the Foot Trajectory

4.5 Observations

4.6 Conclusions

4.1 Introduction

In the field of legged vehicles, proposing a new design in a crucial subject such as leg design makes it essential to back the theoretical analysis with experimental study. Therefore a model leg was built and a series of experiments were conducted with the following objectives;

1 - To confirm the computer simulation results,

2 - To use the model leg as a design aid to observe some features which would be hard to imagine without seeing them in action, so that this experience could be used when a real leg is built,

3 - To produce some experimental data to compare the newly designed leg mechanism with previously built leg mechanisms.

4.2 Design of a Model

For practical reasons a single leg mechanism was built as a model leg instead of a complete legged vehicle. A picture of the model with the whole test rig is shown in photograph 4.1. Also the back view of the test rig is shown in photograph 4.2. More detailed pictures are presented in appendix 2. The following sections briefly describe the model.

4.2.1 Mechanical Design

Using the simulation results for the Buraq leg from the previous chapter a model leg was built as a prototype. The mm dimensions used were three times the lengths used in the computer simulation. Linkage lengths for both the computer simulation model and the model used in the experimental study are shown in figure 4.1.

For longitudinal drive a crank was used. To be able to change the longitudinal foot stroke, the crank length should be able to vary. To serve this purpose, a disk with four different crank position holes with different radii was used. The disk also helped to balance inertial loads. Hence the disk served two purposes, namely varying the crank length and balancing the inertial forces.

4.2.2 Power System

A hydraulic ram was used to actuate the foot up and down, and a four bar mechanism was used to actuate the leg forward and backward as shown in figure 4.1. In this section details of these actuators are presented.

4.2.2.1 Longitudinal Drive

The overall drive system for the longitudinal drive is shown in figure 4.2. A dc motor was used as the main drive unit. The power was supplied through a 3-phase variac and a diode-bridge to the motor. By changing the voltage setting from the variac, the dc motor could be operated at various speeds. To provide the necessary torque, a series of belt and chain drives formed a reduction gear. The manufacturer's advice and equations were followed in the selection and the sizing of drive train components.

4.2.2.2 Vertical drive

The overall drive system for the vertical drive is shown in figure 4.3. The pump was driven by the same motor which drove the crank. By operating the solenoid valves the foot could be moved up or down. Also foot motion could be stopped by selecting the stand-by position of the valves. Since no check valves are used in the system, reverse flow of the fluid in the hydraulic cylinder due to load could not be avoided. To keep a constant height during the support period, hydraulic pressure had to be used continuously causing extra power losses.

4.2.3. Control

To achieve high performance for a legged vehicle, the leg trajectory should be controlled effectively. The control of foot trajectory is mainly what distinguishes a legged vehicle from a traditional off-road vehicle.

The control of the foot trajectory can be done in various ways. However what is aimed at is basically the same. Assuming that the foot trajectory can

be symbolically represented as in figure 4.4;

The period $t_0 \rightarrow t_1$ represents foot lowering

$t_1 \rightarrow t_2$ represents foot on the ground (support period)

$t_2 \rightarrow t_3$ represents foot raising

$t_3 \rightarrow t_0$ represents foot on the air (transfer period)

The graphs shown in figure 4.4 refer to four different signals;

The signal at t_0 ends the transfer period, and starts the foot lowering action.

The signal at t_1 ends the foot lowering action, and starts the support period.

The signal at t_2 ends the support period, and starts the foot raising action.

The signal at t_3 ends the foot raising action, and starts the transfer period.

The following sections describe how sensor signals were used to control the actuators, and monitor the variables. The leg mechanism was originally driven by logic control. Then logic control was replaced by computer control.

4.2.3.1 Logic Control

The prototype model was driven purely by logic as a simple way of getting the model leg running. Digital signals (t_0, t_1, t_2, t_3) were generated using only microswitches to guide the foot along the leg cycle.

Due to mechanical actuation of the leg mechanism, the start and the end of the foot stroke are predictable. Therefore, the signals t_0 and t_2 can be generated using the particular crank positions. Hence the microswitches were placed behind the disk to signal the start and the end of the foot stroke as shown in figure 4.5.

Ideally a microswitch placed on the foot could be used to provide a signal (t_1) to stop lowering the foot, and another microswitch placed along the vertical drive could be used to provide a signal (t_3) to stop raising the foot. However, in the prototype model all four microswitches were placed behind the disk as shown in figure 4.5 to run the model leg in the simplest way.

The logic circuit used to control the leg cycle is shown in figure 4.7. The circuit uses flip flops (see Savant et al, 1987). Normally two signals are used (set/reset) in a flip flop circuit. Since four microswitch signals are involved in this experiment, the basic flip flop circuit was improved to accommodate 2 set and 2 reset signals working together. As can be seen from the truth table of the circuit either of the reset signals (B or Q) could be used to stop the flow (see figure 4.6) .

4.2.3.2 Computer Control

The prototype model was then modified so that it could be computer controlled. Analog and digital signals were generated using a straight line potentiometer to measure the vertical drive position, and microswitches to determine the crank position (see figure 4.8). The same microswitches A and P (see fig. 4.5) were used to generate the signals t_0 and t_2 . Using the straight line potentiometer, the foot height could be controlled accurately, and kept in prescribed limits by occasional corrections during the leg cycle.

The flow chart of the programme used to control the leg is shown in figure 4.9. The value 'X' refers to the hexadecimal value of the digital interface. The called subroutines and explanations are as follows;

Stand_by: When called by main programme it sent a signal through A/D board to the circuit setting stand_by value high and the rest low.

Foot_down: Used to set the valve which moves the foot downwards high and the rest low.

Foot_up: Used to set the valve which moves the foot upwards high and the rest low.

Set_values: Set the values used in the programme to adjust the foot height from the ground.

Get_values: Read the analog and digital values fed back to the computer from the test rig.

Corr_up: Corrected the foot upwards if vertical foot position was outside the prescribed limits ($value2 < uvl_val$) by set_values.

Corr_down: Corrected the foot downwards if vertical foot position was outside the prescribed limit (value2 > bvl_val) by set_values.

pdata: Printed the desired values on the screen.

4.3 Experiments to Calculate Specific Resistance

A set of experiments were carried out to calculate an approximate value of the specific resistance of a vehicle using Buraq legs. Specific resistance of a vehicle is described as expressed in the section 1.3.1;

$$\text{specific resistance} = \frac{\text{power input}}{\text{total weight} * \text{speed}}$$

The following sections describe the calculation method to determine the specific resistance.

4.3.1 Initial Assumptions and Instrumentation

Specific resistance is normally calculated for a complete vehicle according to its speed, power consumption and total weight. Since the prototype consisted of a single leg, a series of assumptions were made.

1. To simulate the leg during support period, a foot trail was fitted along the foot trajectory pushing the foot upwards by a spring as shown in figure 4.10. This gradual load on the foot was assumed to be due to the weight of the vehicle, and was measured by strain-gauges mounted on the critical point of the tibia of the leg as shown in the figure.

2. At the same time using a current transducer and a voltmeter, the amount of power sent to the leg mechanism could be calculated. Assuming a constant speed throughout a complete leg cycle, an average value for the foot speed was also calculated to substitute for the vehicle speed.

3. It was assumed that since the specific resistance value is non-dimensional, its calculation for a single leg would not make any difference to its calculation for a complete vehicle.

4.3.2 Calibration of the Instruments

4.3.2.1. Strain-gauge calibration

A pair of strain-gauges were fixed on the critical point of the tibia of the Buraq leg as shown in figure 4.11. The outputs of the strain-gauges were connected to the computer interface through a strain-gauge amplifier. A wooden board hinged from one end and suspended from another was placed as a foot trail. The foot was fitted with a pair of wheels which moved freely on the trail to simulate body motion. From the suspended end of the board, load was applied to the foot with a magnification ratio which was calculated using the ratio between the distances from hinged joint to the foot and to the suspended end. The leg mechanism was fixed to prevent vertical and longitudinal motion so that the foot could not move due to applied load as shown in the figure. That way a set of pairs, strain-gauge values with respect to particular foot positions along the foot trail, could be produced.

For different positions of the foot, various loads were applied to the track at its end point, and simultaneously the strain-gauge readings (sgv) were recorded from the screen. This produced the plot shown in figure 4.12 which shows the load values acting at the end of the foot trail (N) and relative strain-gauge recordings (sgv). When there was no weight acting on the foot, the strain-gauge reading (sgv) was adjusted using the amplifier to give a computer reading of 500. To determine the calibration, a straight line approximation was made through the least squares method as shown in figure 4.12.

4.3.2.2 Current transducer calibration

A current transducer, a device producing voltage proportional to current, was installed in the dc drive circuit. Also an ammeter was connected through the cable on the same line. The output of the device was sent to the computer interface. By gradually increasing the voltage fed to the dc motor, the readings from the screen and the ammeter were recorded as shown in figure 4.13. To determine the calibration, line fit approximation was made as shown in the figure.

4.3.3 DC Motor Characteristics

To find the input power term in the specific resistance expression, the dc motor characteristics were needed. Since the manufacturer's data was inadequate, some experiments and calculations were carried out to find the dc motor characteristics.

4.3.3.1 Measuring stall torque

The test rig was powered by a 180 V, 1.5 kW permanent magnet dc motor. The motor was disconnected from the test rig. A lever was attached to the motor shaft with a spring balance at its end. Varying the voltage from nil up to 14 V the ammeter and spring balance readings were recorded. Accordingly, using the length of the lever, the generated torque values (stall torque) were calculated. Hence, while dc motor shaft speed was zero, table 4.1 was obtained.

4.3.3.2 No load speed

The lever was disconnected from the motor, and the motor was run at various speeds under no load. Voltmeter and optical tachometer readings were recorded while torque applied to the shaft was zero. Hence table 4.2 was obtained.

4.3.3.3 Evaluations

Point 1: Using the data in tables 4.1 and 4.2, the plot in figure 4.14 was produced. The figure shows the constant voltage lines on the torque (T , Nm) versus angular speed (ω , rad/s) plot. Using stall torque values the points on the T axis was produced. Then corresponding angular speed values were calculated using no load speed values. Following equations were produced as explained in the parentheses;

$$T_o = 0.4768 V - 1.576 \quad (\text{from table 4.1}) \quad (4 - 1)$$

$$\omega_o = 1.5198 V - 1.279 \quad (\text{from table 4.2}) \quad (4 - 2)$$

$$\omega_r = \omega_o (1 - T_r / T_o) \quad (\text{from figure 4.15}) \quad (4 - 3)$$

Point 2: Using the torque and current values in table 4.1 the plot in figure 4.16 was produced. The relation between the torque, T, and current, i, was a linear one, and was expressed as follows;

$$T = 0.6325 i - 0.645 \quad (4 - 4)$$

4.3.4 Calculation of the Specific Resistance

The specific resistance of a vehicle is expressed as follows;

$$\text{specific resistance} = \frac{\text{power input}}{\text{total weight} * \text{speed}}$$

Power input represented the power supplied to the leg mechanism from the dc motor, and was expressed as follows;

$$\text{power input} = V i - R i^2 \quad (W) \quad (4 - 5)$$

where R represents the armature resistance of the dc motor, and was measured as 2Ω . Total weight was assumed to be the force imposed on the foot through the foot trail.

The speed was taken to be the average foot speed through a whole leg cycle. It was expressed as follows;

$$v_f = \frac{L}{f} \frac{360}{160} \quad (m/s) \quad (4 - 6)$$

where L represents the foot stroke length, and was measured to be 0.755 m. during the experiments. f represents the period of the leg cycle. The support and transfer trajectories of the foot are different, and transfer trajectory is longer. Also, the foot goes through transfer period faster than it does for support period (see also section 3.6). Therefore average foot speed is faster than simply $2L/f$ value. Nevertheless the ratio $360/160$ is an approximate value.

During the experiments voltage readings were recorded from the voltmeter. Also the period of the leg cycle was measured by a stop-watch. The values relating to current and load values were recorded from the computer screen. The following algorithm was used to calculate the specific resistance at various speeds;

1. Read the voltage (V), the leg cycle period(f), the strain-gauge recording (sgv) and current transducer recording (cur).

2. Calculate motor angular speed w_m (rad/s) using f .

$$w_m = \frac{2 \pi GR}{f}$$

where GR represents the gear ratio between the crank and the motor shaft.

3. Calculate current (i) and load (load) values using equations in figures 4.12 and 4.13;

$$\text{load} = 0.399 \text{ sgv} - 164.89 \quad (\text{N})$$

$$i = 0.0171 \text{ cur} - 0.005 \quad (\text{A})$$

4. Find the position in figure 4.15, T-w plot, by using equations (4-1) and (4-2), hence finding T_o and w_o .

5. Calculate the torque value, T, by inserting i value into equation (4-4).

4. Calculate the power input to the leg mechanism from the dc motor which was equal to $V i - R i^2$ by using equation (4-5).

7. Calculate the average foot speed (v_f) by using equation (4-6).

8. Calculate the specific resistance value which can be expressed as follows;

$$sr = \frac{V i - R i^2}{\text{load } v_f}$$

The algorithm is carried out for two cases, Case 1 and Case 2, so that the power loss due to not having check valves in the system can be taken into account. By evaluation of the results, a specific resistance value was obtained as explained in the following sections;

Case 1.

The pump was under full load and the hydraulic ram was active, applying force on the foot against the foot trail during the support period. The crank was rotating. Maximum values were recorded. The results are shown in table 4.3 where L represents the load acting on the foot, V represents the voltage value, i represents the current value, $V i$ represents the power drawn from the environment, $R i^2$ represents the power loss inside the dc, v_f

represents the average foot speed and sr represents the specific resistance value.

Case 2.

In this case only the crank was active and rotating under load; the hydraulic pump was disconnected. Maximum values were recorded. The results are shown in table 4.4.

Evaluation of both cases: When the foot made its first contact with the ground there was a sudden impulse acting on the foot. During the rest of the support period, the force started to drop after reaching a maximum value around the mid-stroke. Calculating the specific resistance according to the results in the Case 1 for the whole support period would be ignoring the fact that the recordings of the Case 1 were the maximum peak values. And also, by using check valves the power drain from the hydraulic circuit could be avoided soon after the foot contact with the ground, hence saving a considerable amount of energy. This was because, once the check valves were active, the fluid in the hydraulic ram would become blocked, and there would be no consumption of hydraulic power. When check valves were not used, hydraulic power was used continuously to overcome the ground reaction forces during the support period as in the Case 1.

The specific resistance of the vehicle was then calculated by taking the average specific resistance values between the Case 1 and the Case 2, assuming that during the support period, both cases had an equal share to play even though Case 2 could be even more dominant due to long foot stroke. Figure 4.17 shows calculated specific resistance values with respect to the speed for both cases. In figure 4.18 average values of both cases are used to produce an approximate curve representing specific resistance variation of the legged vehicle with Buraq mechanism with respect to vehicle speed.

4.3.5 Load sensitivity of the specific resistance

During the calculation of the specific resistance above, one of the assumptions made was that the specific resistance value did not change when the load conditions changed. This assumption played a significant role while taking the average curve between the Case 1 and the Case 2 (see figure 4.18). Each case represented a different loading condition for the same speed value. A set of experiments were carried out to find the load sensitivity of the specific resistance. By changing the load on the foot trail gradually and by keeping the speed and voltage constant, a set of results were produced as shown in table 4.5. The specific resistance values found were with $\pm 5\%$ variation as it can also be seen in figure 4.19 which is not a significant change.

The experiment confirmed that loading changes do not affect the specific resistance of the leg mechanism as long as power input can be supplied to produce enough current to overcome the loading. Hence the procedure carried out to find the average curve in section 4.3.4 was justified.

4.4 Foot Trajectory

4.4.1 A Mechanical Constraint on the Foot Trajectory

During simulation studies no solutions for the leg trajectory was found when the foot height value was specified higher than the knee at the beginning of the transfer period.

During the experimental studies, it was also confirmed that the foot should not be raised higher than the knee joint at the beginning of the transfer period. When the foot was raised higher than the knee at the beginning of the transfer period, the mechanism could not complete the transfer period, since mechanically this was impossible.

4.4.2 Calibration of the Straight Line Potentiometer

For various positions of the upper actuated joint, U, computer readings from the straight line potentiometer (mon) were recorded. Having scaled the

upper actuation positions according to the simulation model by dividing with three, figure 4.20 is produced showing computer readings of the potentiometer with respect to the scaled upper actuated point positions. As the figure shows, there is a directly proportional relation which is calculated to be as follows;

$$U_y = -0.770 \text{ mon} + 0.56 \quad [\text{mm}] \quad (4-7)$$

4.4.3 Measuring the Foot Trajectory

The leg was operated at slow speed under no load. In the mean time a marker was fixed to the foot point (P) in such a way that the foot trajectory could be drawn to a sheet of paper fixed behind the leg during operation. This procedure was repeated for various upper actuator positions while straight line potentiometer readings (mon) were recorded. Figure 4.21 shows the foot trajectories scaled down to the simulation model dimensions.

To compare the experimental results with the simulation results, potentiometer values referring to the each foot trajectory were converted into upper actuated point positions using equation (4-7). Afterwards the simulation model was executed for each upper actuated point. Two pairs of the experimental (*) and computational(o) foot trajectories are shown in figure 4.22. While the middle part of the foot trajectories fit well, the end parts seem to deviate slightly from each other which is likely to be due to backlash in the joints.

4.5 Observations

Some shortcomings were observed in the experimental model. Following are the proposed remedies;

1. High bending moments were observed on the shafts at the crank connection and at the ram connection to the leg due to unsymmetrical loading. Some extra fittings were made to strengthen the shafts especially at the rocker point to resist high moments. Therefore it was found to be essential that a real leg should be built with a complete symmetry on all its

joints. Later in chapter 7, a wooden legged vehicle model with completely symmetrical leg structure has been built (see photograph 7.2).

2. Considerable slackness in the joints resulted from the individual manufacture of the linkages since the holes did not align properly during assembly. While preparing the linkages for the wooden leg, the linkages were prepared in pairs keeping the holes aligned.

3. It was found to be essential that a real leg should accommodate bearings at joints where shaft contacts are kept as wide as possible to minimise the accumulation of slackness at the foot.

4.5 Conclusions

Building a model and conducting some experiments with it helped to achieve the objectives set out at the beginning of this chapter as follows;

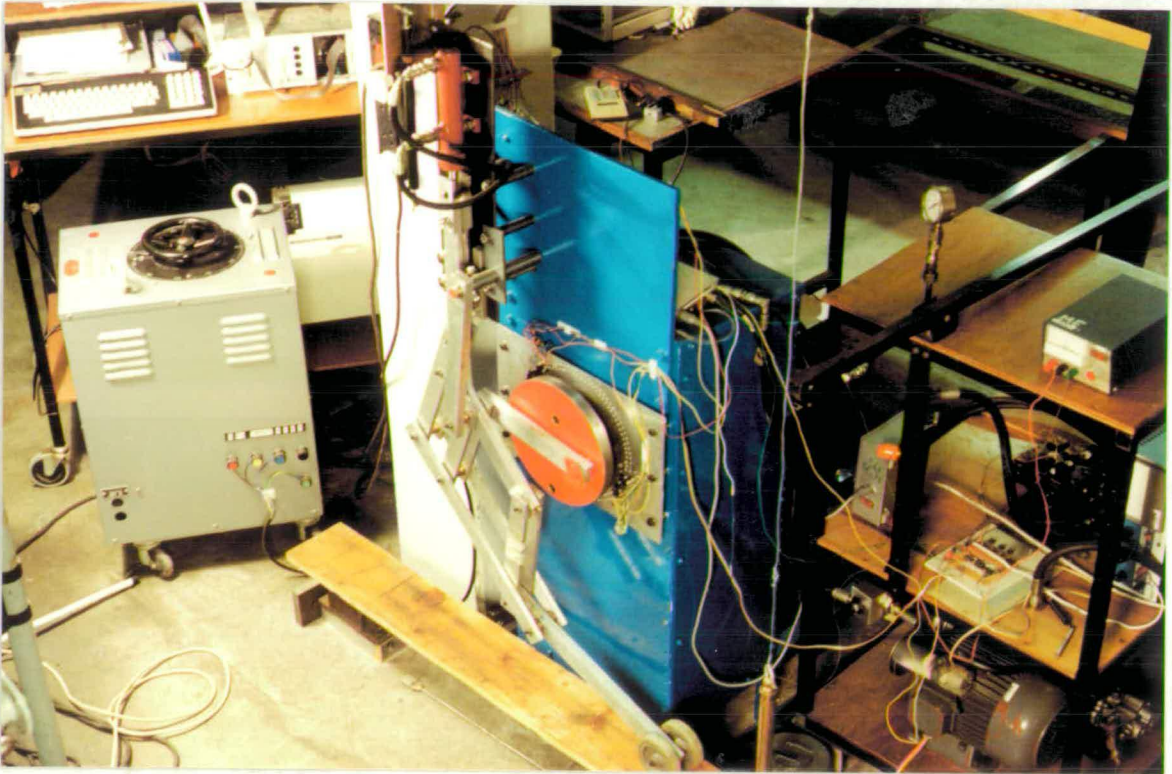
1. Computer simulation results were confirmed by seeing the model leg in action and observing it as being operational. Also the foot trajectory of the experimental model confirmed that of the simulation model (see figure 4.22). Experimentally it was proven that the Buraq leg provides an approximate straight line motion with a ballistic trajectory. Experiencing the mechanical constraint which was predicted during the simulation studies also helped the first objective to be achieved.

2. The second objective was achieved by recording the observations from the experimental study. This experience will be valuable if a complete legged vehicle is built.

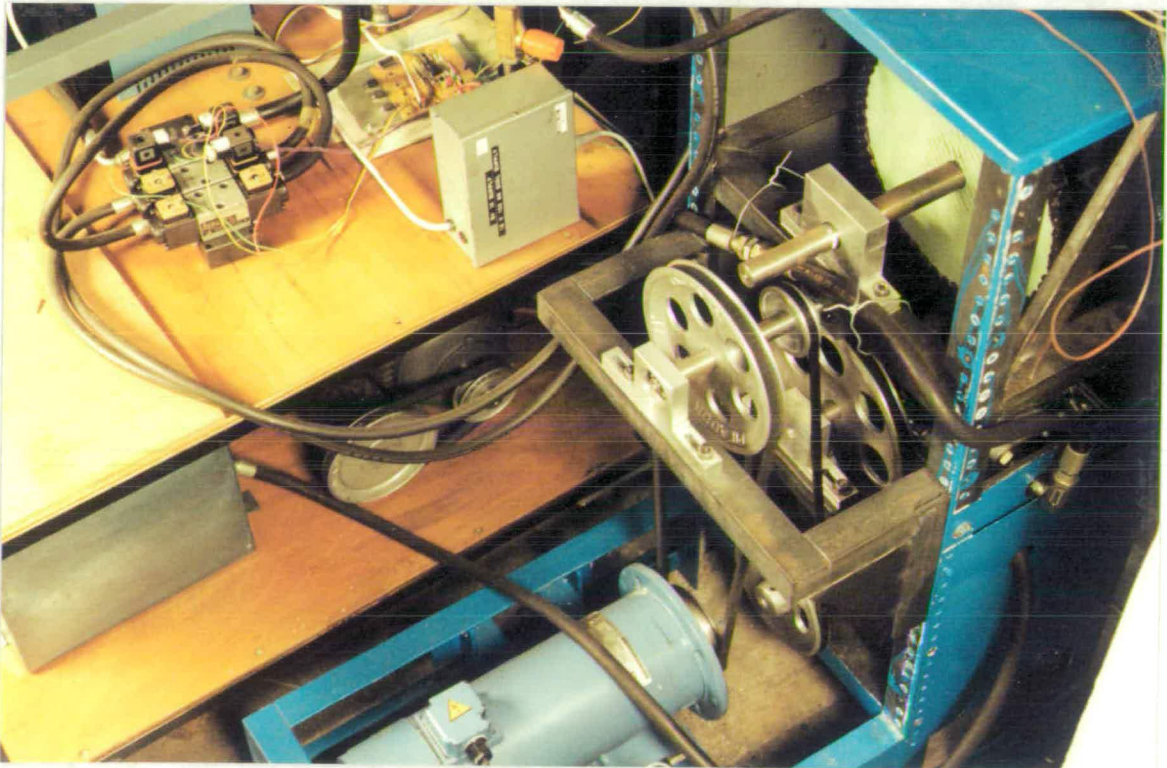
3. The third objective was achieved by carrying out a series of experiments to estimate the specific resistance of a vehicle with Buraq legs so that a legged vehicle with Buraq legs can be compared with other vehicles. Using the average curve obtained in figure 4.18, the legged vehicle with the Buraq legs, Buraq, is compared with previously built legged vehicles in figure 4.23. Figure 4.18 shows that Buraq has a good performance at low speeds, however, when the speed increases the performance decreases. Nevertheless it can be seen from figure 4.23 that it

is still in the average range of the tracked vehicles.

Figure 4.23 shows three previously built legged vehicles compared with Buraq, which are OSU Hexapod, GE Quadruped and Adaptive Suspension Vehicle (ASV) in addition to some biological and wheeled systems. The ideal for a legged vehicle is to be as efficient as a horse which is more efficient than any other system. Even though a Buraq legged vehicle is not comparable to a horse, it has a better efficiency at low speeds compared to other legged vehicles. It is expected that through elastic energy storage in the leg mechanism, a better performance can be achieved at high speeds as explained in chapter 6.



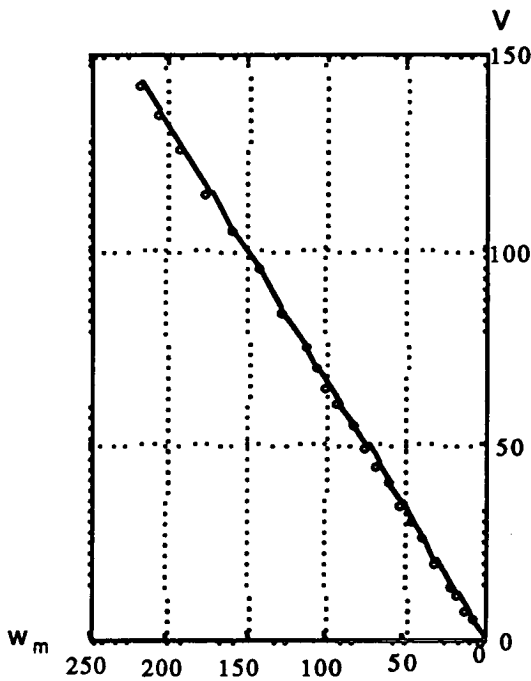
Photograph 4.1 An overall view of the experimental set-up.



Photograph 4.2 A back view of the test rig.

Voltage V	Torque Nm	Current A	Torque Current
5.0900	0.7684	2.4500	0.3136
5.6500	1.0245	2.7700	0.3699
7.2000	2.0491	4.0300	0.5085
8.9100	2.5614	4.9800	0.5143
10.4300	3.5859	6.4500	0.5560
13.9000	5.0225	9.1000	0.5519
14.5000	5.2508	9.4000	0.5586

Table 4.1 Measurement of the stall torque



1.0e-03 *	
Voltage V	Speed rad/s
0.0004	0
0.0052	0.0660
0.0083	0.1100
0.0121	0.1640
0.0141	0.1930
0.0205	0.2850
0.0267	0.3730
0.0310	0.4370
0.0351	0.4960
0.0409	0.5800
0.0455	0.6470
0.0500	0.7130
0.0561	0.8000
0.0609	0.8720
0.0659	0.9410
0.0706	1.0100
0.0754	1.0810
0.0851	1.2180
0.0954	1.3680
0.1054	1.5210
0.1154	1.6660
0.1260	1.8170
0.1355	1.9560
0.1430	2.0670

Table 4.2 and its plot

Measurement of the no load speed of the dc motor .

Line eq'n: $w_m = 1.5198 V - 1.2796$

w_m : motor angular speed (rad/s)

V : potential (V)

where 'o' represents experimental readings from the table 4.2

L	V	i	V i	R i²	v_f	sr
2.7640	35.6000	11.2000	398.7200	250.8800	0.1440	0.3715
2.7640	45.7000	11.4000	520.9800	259.9200	0.2145	0.4404
2.8530	56.6000	11.6000	656.5600	269.1200	0.2794	0.4860
2.8530	63.8000	11.8000	752.8400	278.4800	0.3242	0.5129
2.8530	73.4000	12.2700	900.6180	301.1058	0.3661	0.5740
2.8530	77.8000	12.5400	975.6120	314.5032	0.4164	0.5565
0.3200	35.7000	12.7000	453.3900	322.5800	0.5625	0.7267
0.3200	41.2000	13.4000	552.0800	359.1200	0.6795	0.8874

Table 4.3 The results of the processed data for the Case 1

L	V	i	V i	R i²	v_f	sr
0.8094	12.0100	3.0902	37.1133	19.0987	0.1798	0.1238
0.8094	17.0000	2.7311	46.4287	14.9178	0.2970	0.1311
0.7935	22.4000	2.7482	61.5597	15.1052	0.4174	0.1403
0.8094	27.4000	2.6627	72.9580	14.1799	0.5480	0.1325
0.8094	33.0000	2.6969	88.9977	14.5465	0.6410	0.1435
0.8094	38.6000	3.2441	125.2223	21.0484	0.7517	0.1712
0.8094	43.5000	3.6374	158.2269	26.4614	0.8327	0.1955
0.8094	48.6000	4.3556	211.6822	37.9425	0.9437	0.2274
0.8174	53.8000	3.7913	203.9719	28.7479	1.0960	0.1956
0.8154	59.6000	4.1846	249.4022	35.0218	1.2310	0.2136
0.8294	54.5000	4.1333	225.2648	34.1683	1.1176	0.2062
0.8294	49.0000	3.8768	189.9632	30.0592	0.9819	0.1963

Table 4.4 The results of the processed data for the Case 2

L	V	i	V i	R i²	v_f	sr
0.5461	20.4000	1.8419	37.5748	6.7852	0.3792	0.1487
0.6658	21.0000	2.2352	46.9392	9.9922	0.3817	0.1454
0.7955	21.1000	2.5601	54.0181	13.1082	0.3835	0.1341
0.8473	21.2000	2.7482	58.2618	15.1052	0.3742	0.1361
0.8932	21.0000	3.2612	68.4852	21.2709	0.3826	0.1382
0.9890	21.2000	3.9110	82.9132	30.5918	0.3669	0.1442
1.0867	21.6000	4.6805	101.0988	43.8142	0.3809	0.1384

Table 4.5 Load sensitivity of the specific resistance (± 5%)

L	V	i	V i	R i²	v_f	sr
kN	volt	Amper	Watt	Watt	m/s	—

U N I T S

Element #	Computer model [mm]	Experimental model [mm]
1+2	32+65	291
3+4	32+64	288
4+7	32+112	432
5	65	195
8	86	258
9+10	25+133	474
11	80.2	241
12	32	96
13	103	309

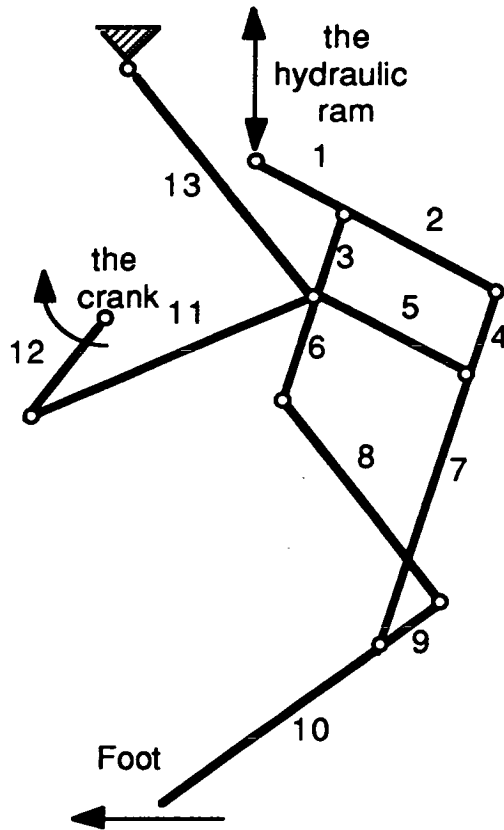


Figure 4.1 A sketch of the Buraq leg mechanism and a table containing its model dimensions

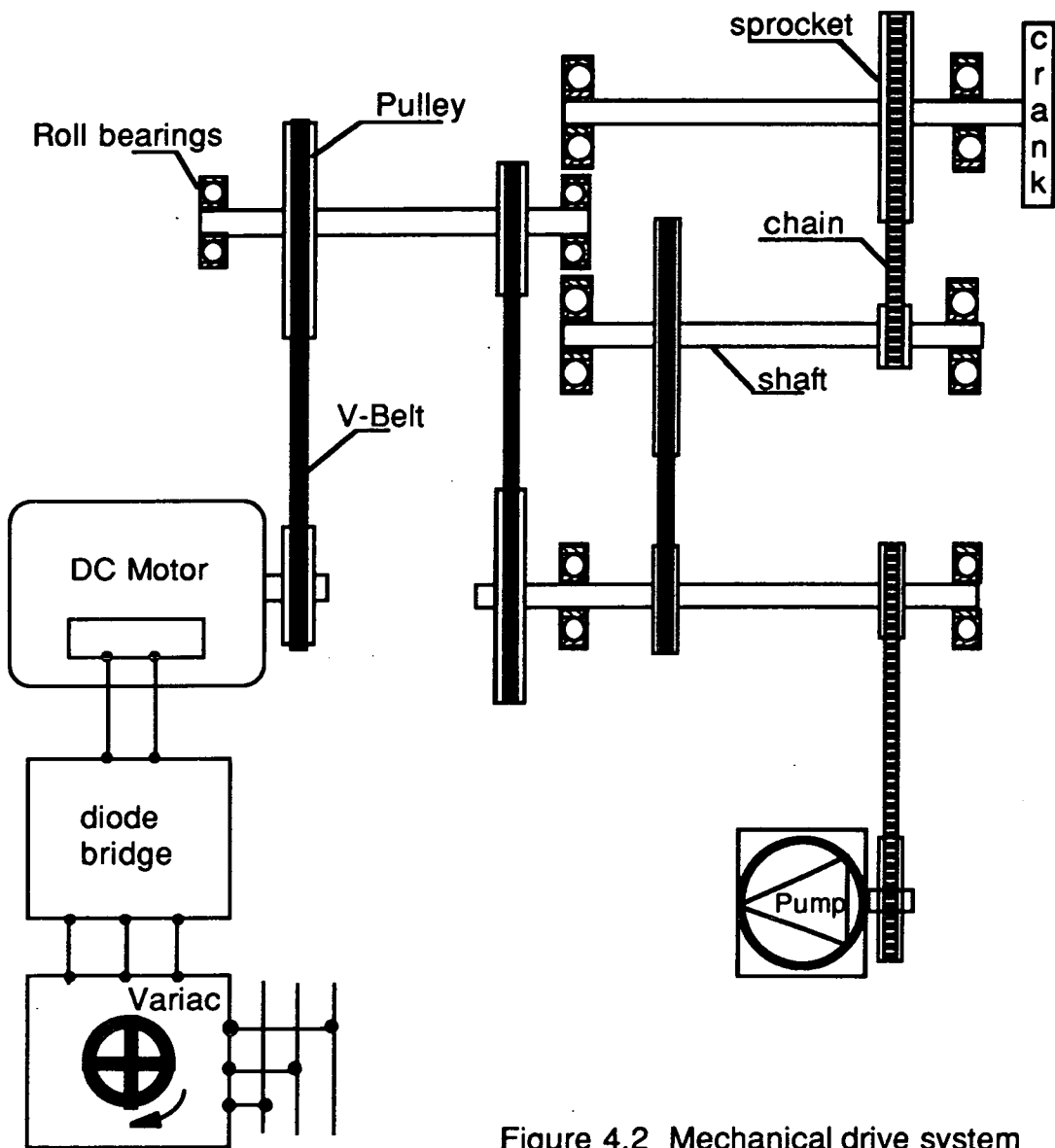


Figure 4.2 Mechanical drive system

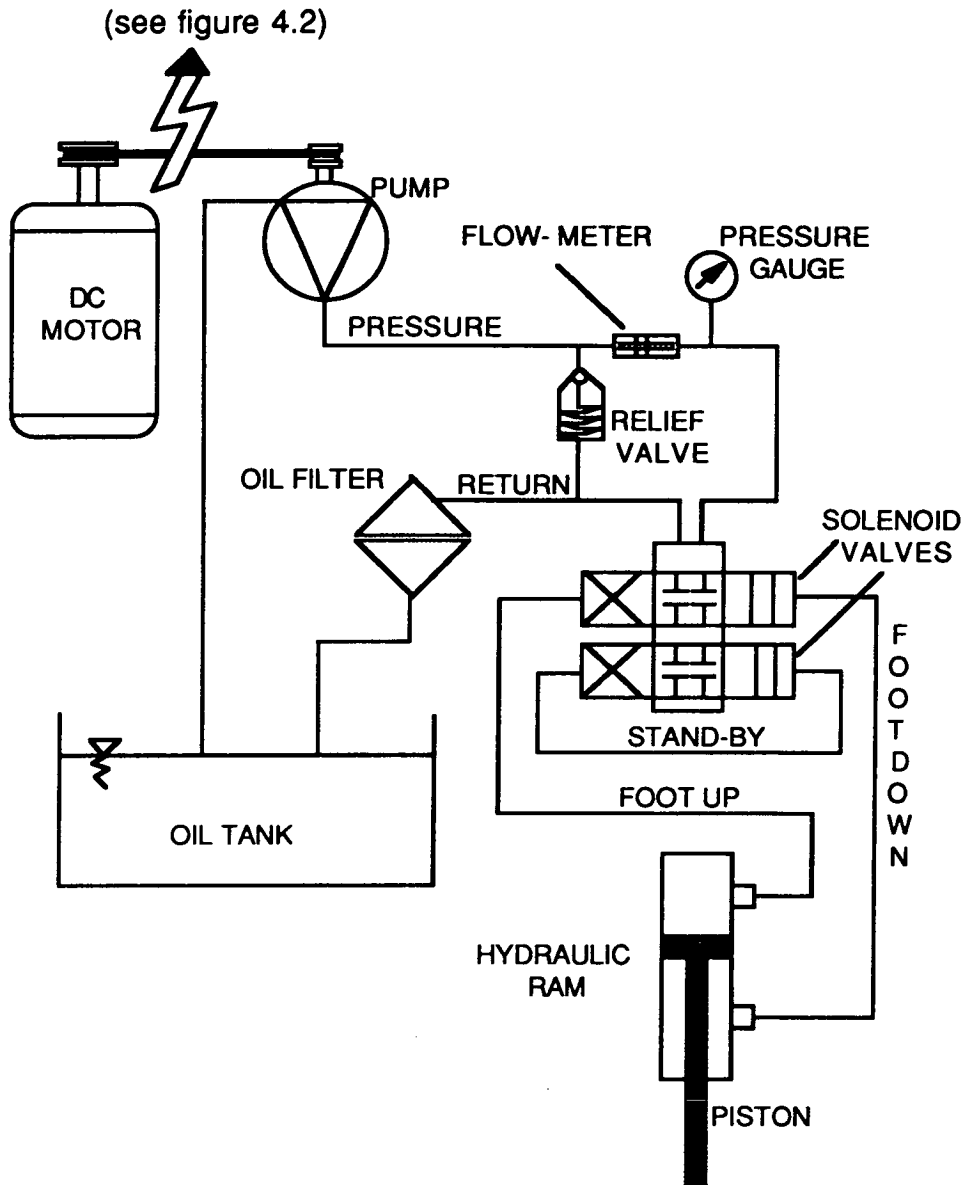


Figure 4.3 Hydraulic circuit operating the hydraulic ram for up and down motion of the foot

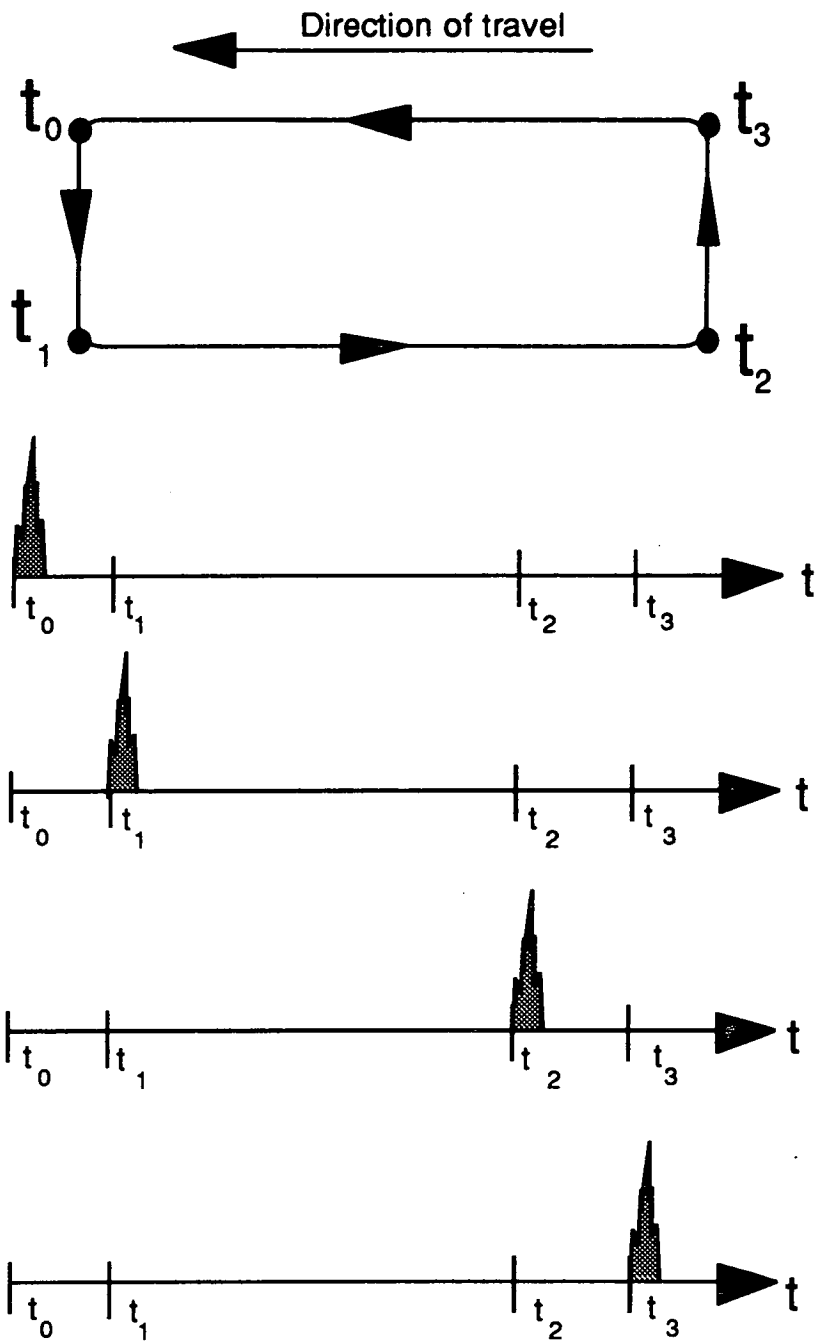
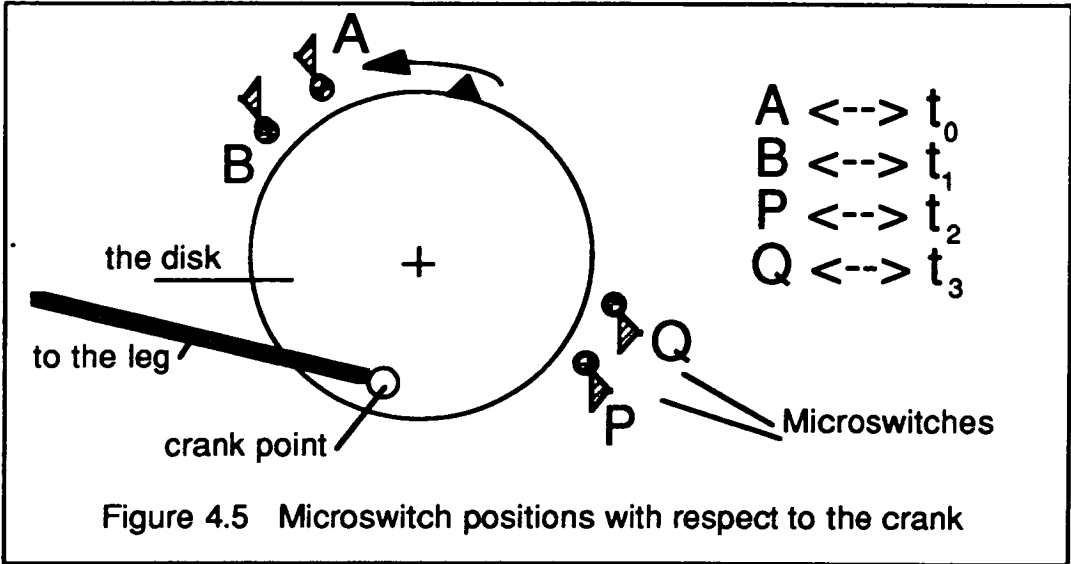


Figure 4.4 A symbolic representation of the foot trajectory and the order of the control signals driving the leg



A	B	P	Q	C	D	R	S	E	T	U	f l o w
0	1	1	1	0	1	1	0	0	1	0	+
1	1/0	1	0/1	1	0	1	0	0	0	1	STOP
1	1	0	1	1	0	0	1	1	0	0	-

Figure 4.6 The truth table for the logic circuit shown in figure 4.7.

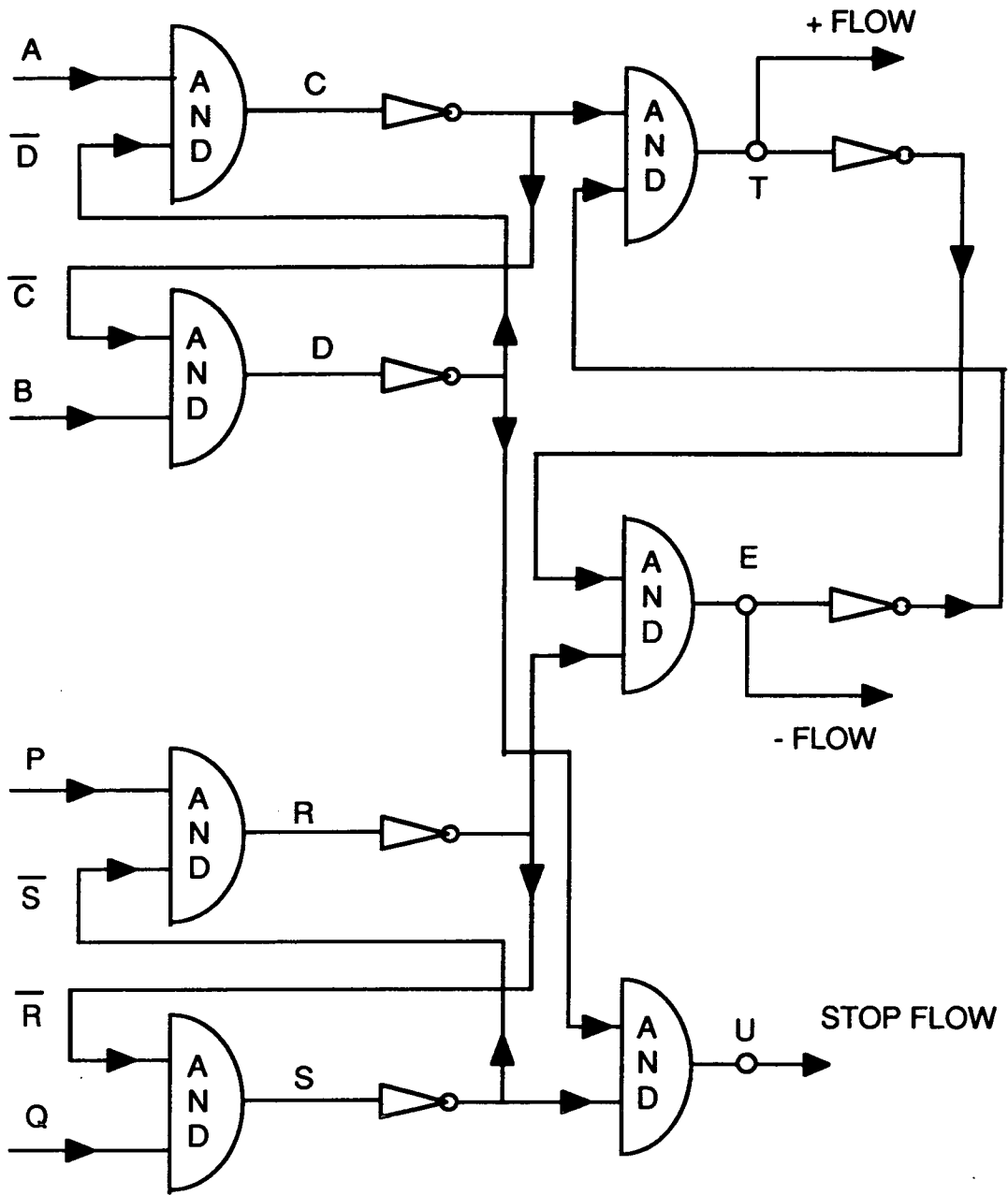


Figure 4.7 A schematic representation of the flip-flop circuit used to drive the leg purely by logic

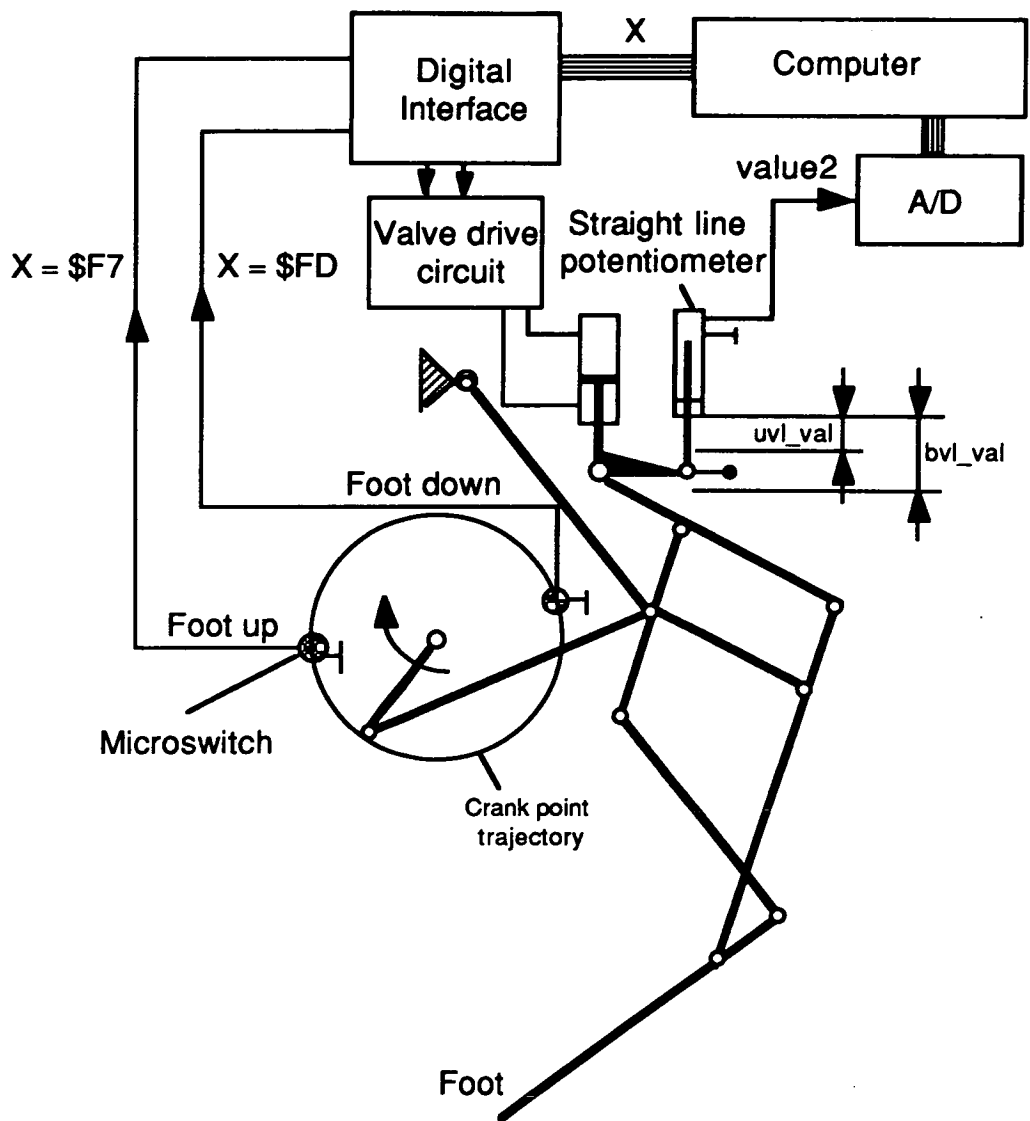


Figure 4.8 A sketch of the Buraq leg mechanism driven by computer control

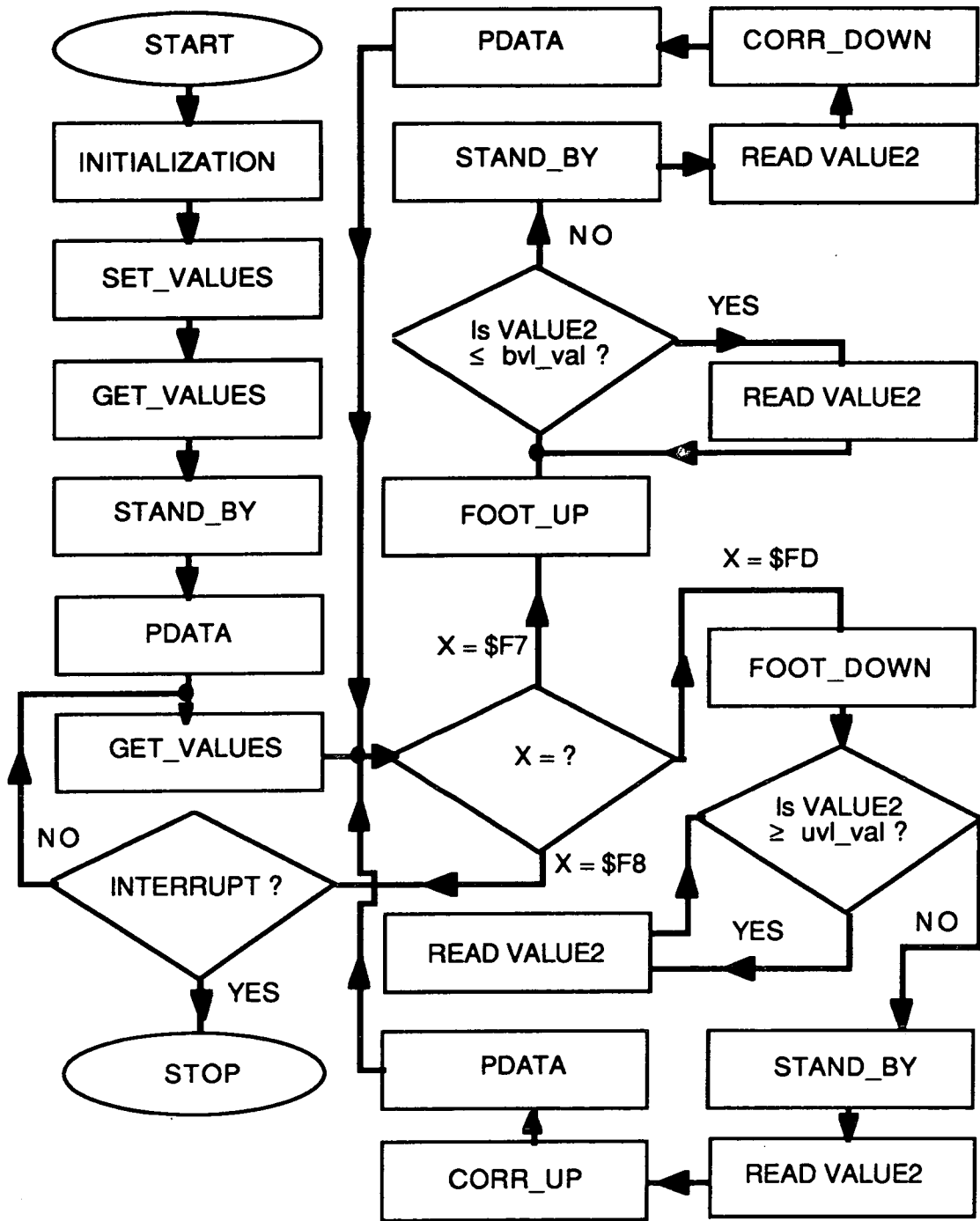


Figure 4.9 Flow chart of the program executed to drive the leg by computer

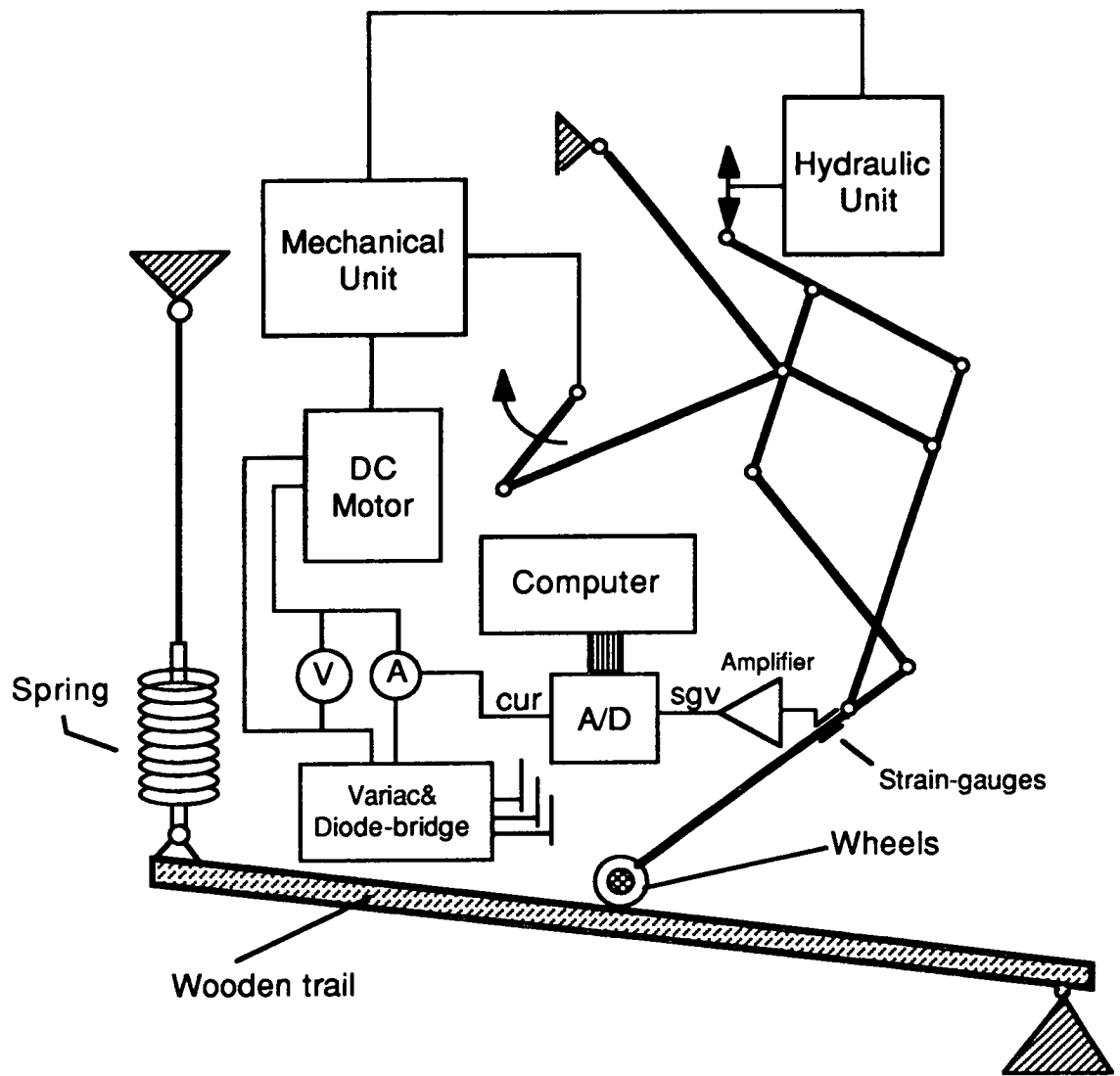


Figure 4.10 Experimental set up to measure the specific resistance

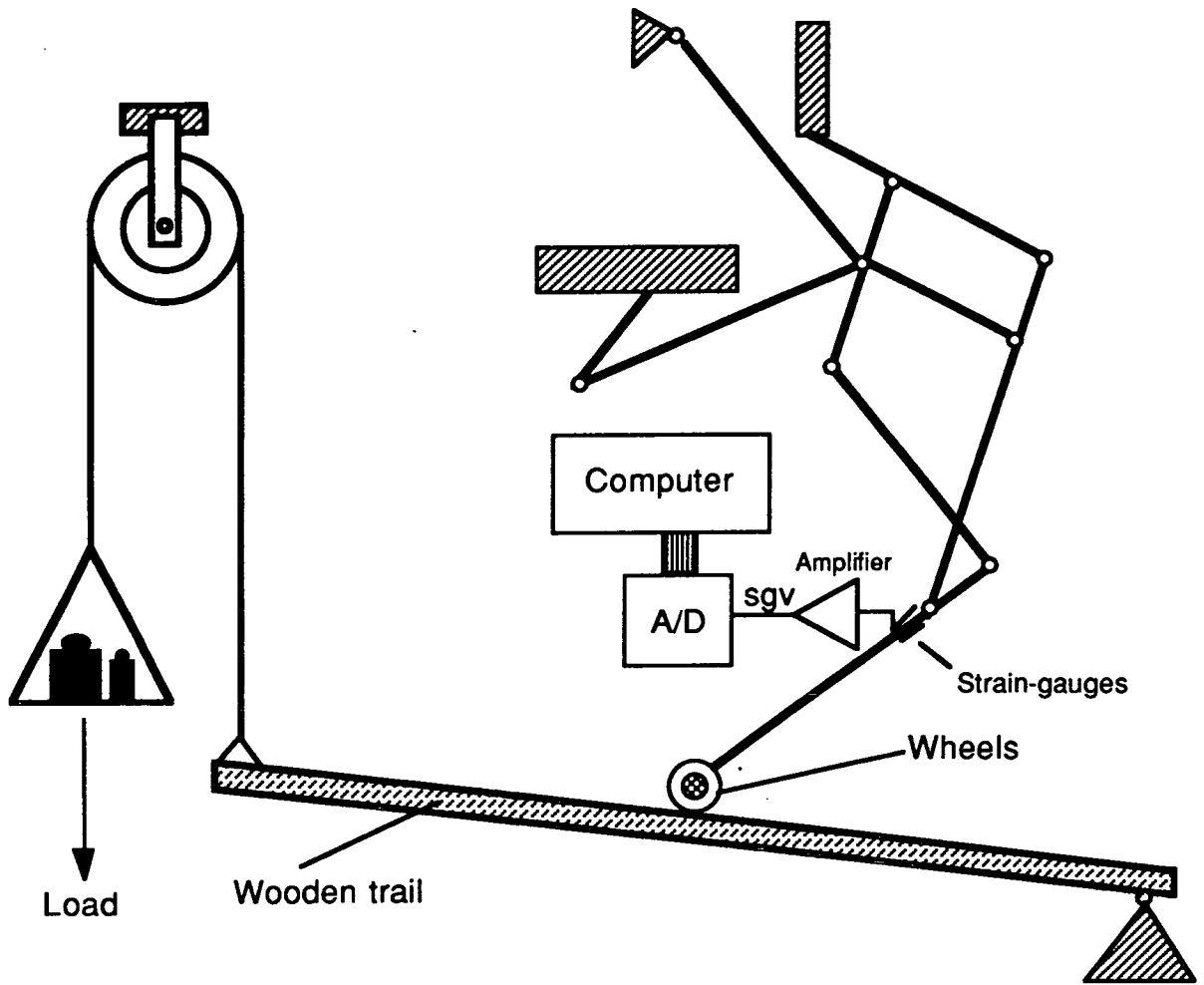


Figure 4.11 Calibration of the strain-gauge.

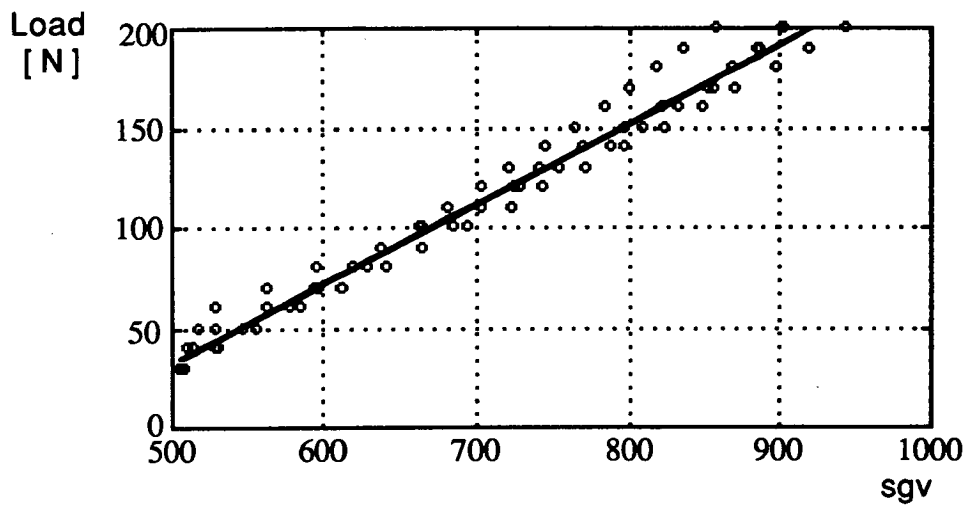


Figure 4.12 Strain-gauge amplifier output (sgv) versus load applied against the foot at the end of the foot trail
 The line eq'n: $load = 0.399 \text{ sgv} - 166.89$

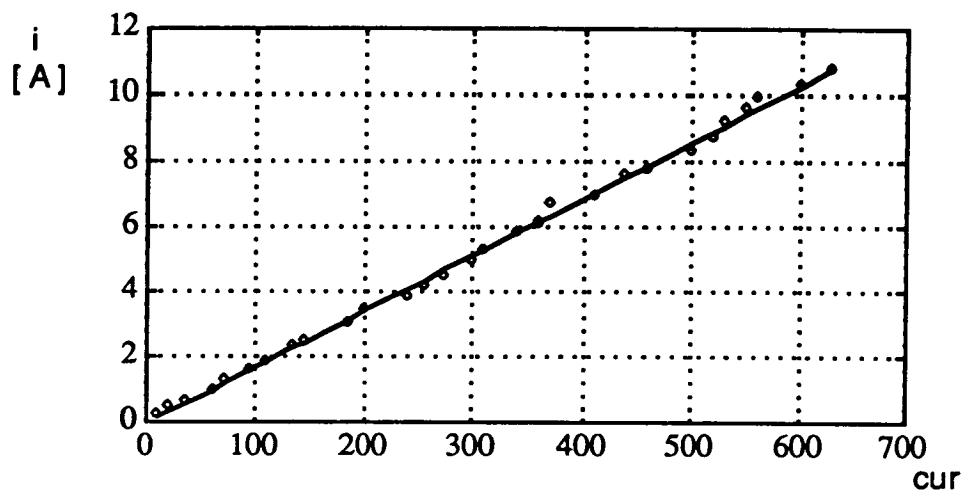


Figure 4.13 Current transducer output (cur) versus
Ammeter readings (i)

The line eq'n: $i = 0.0171 \text{ cur} - 0.0049$

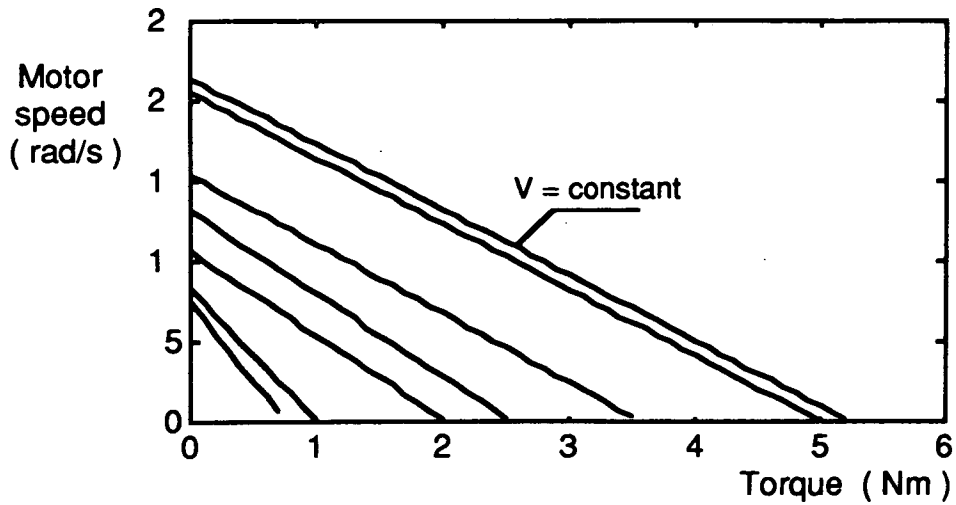


Figure 4.14 Torque vs dc motor speed variation with constant voltage lines produced using the data from tables 4.1 and 4.2. Constant voltage values and respective intersection points on both axis are given below.

torq = [0.7684 1.0245 2.0491 2.5614 3.5859 5.0225 5.2508]
 volt = [5.0900 5.6500 7.2000 8.9100 10.4300 13.9000 14.5000]
 wrad = [7.5151 8.3420 10.6305 13.1552 15.3994 20.5227 21.4086]

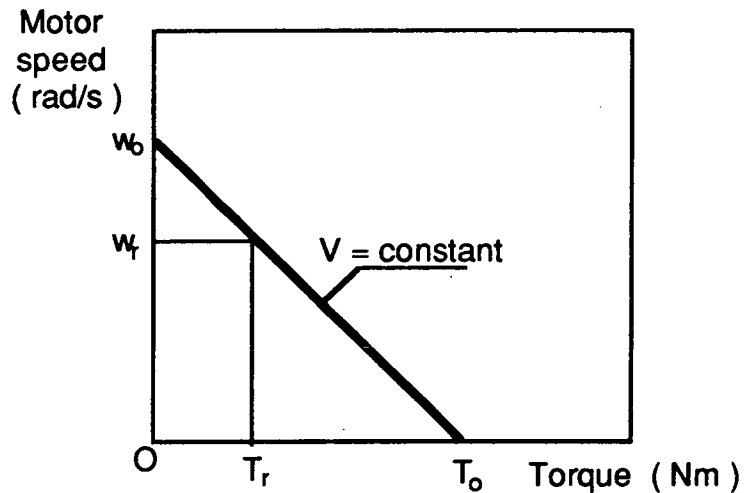


Figure 4.15 Torque, speed and voltage values of the dc motor during operation at an arbitrary point.

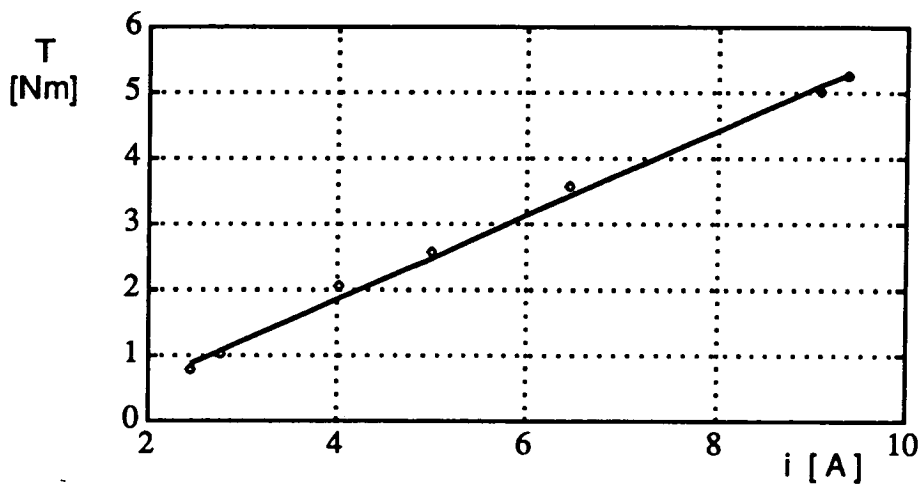


Figure 4.16 Current (i) vs torque (T) produced from table 4.1
 $T = 0.6325 i - 0.6446$

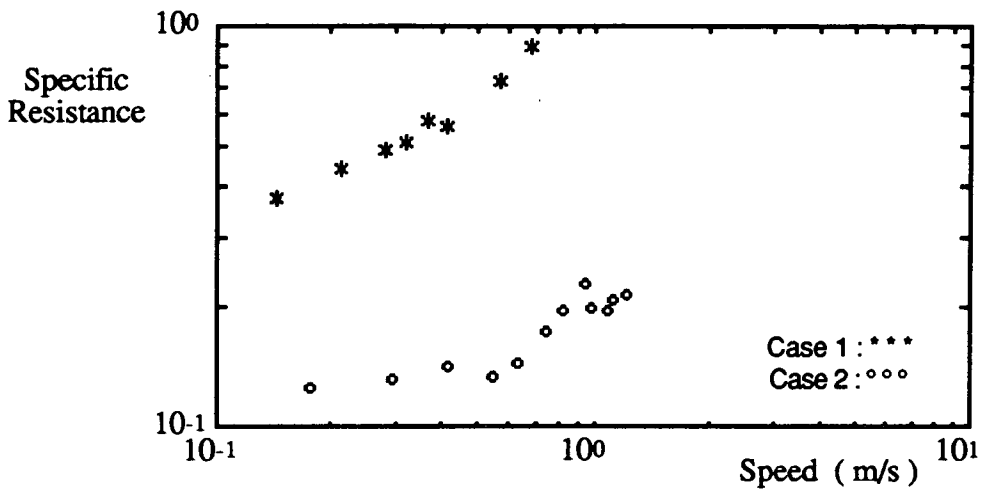


Figure 4.17 Variation of the specific resistance with respect to the average foot speed for case 1 and case 2.

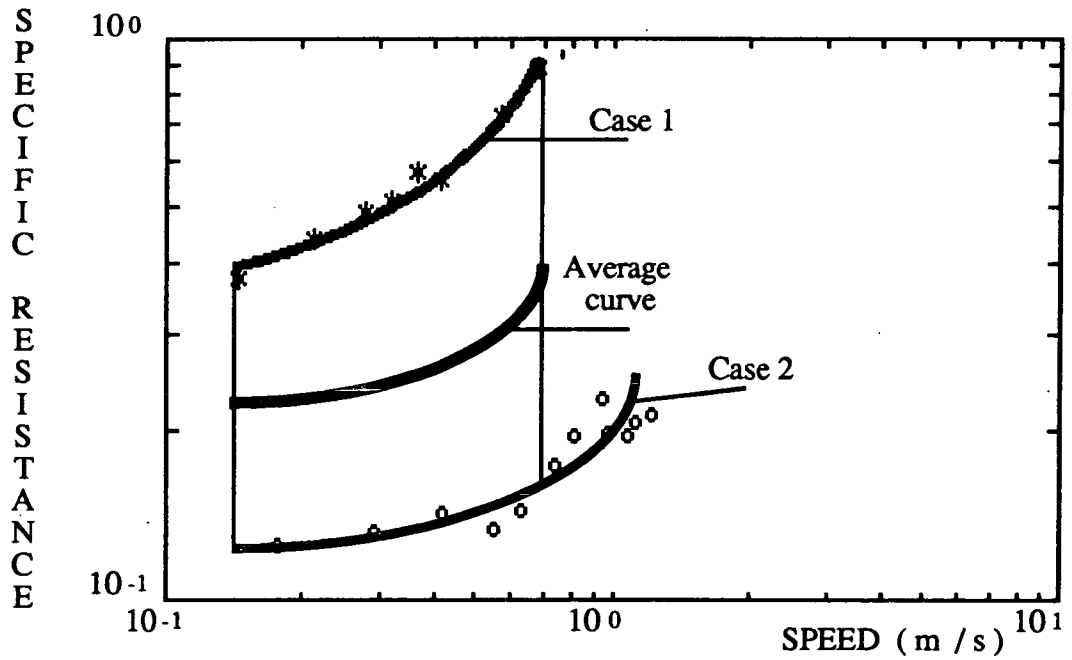


Figure 4.18 Finding an average curve as an approximation to the specific resistance variation of Buraq legged vehicle with respect to the vehicle speed.

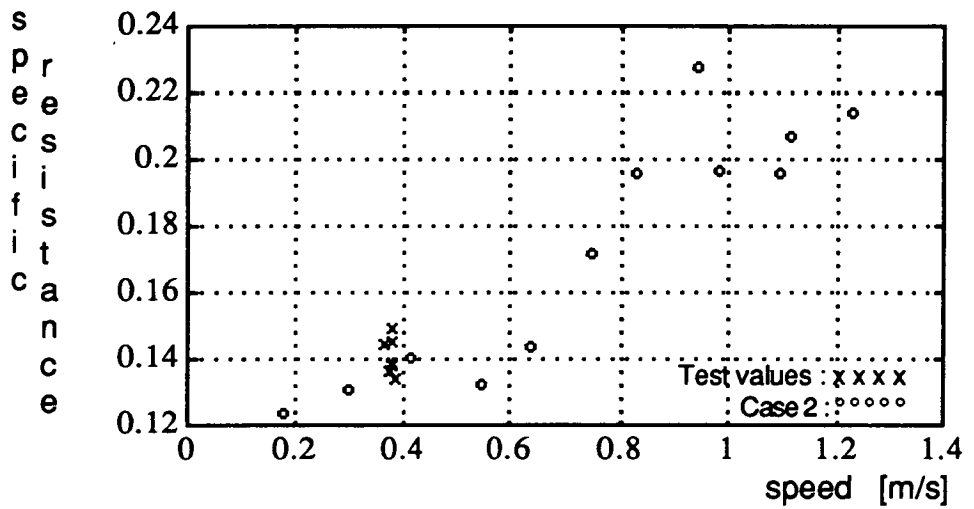


Figure 4.19 Testing the load sensitivity of the specific resistance. The test values are plotted with the values of study Case 2.

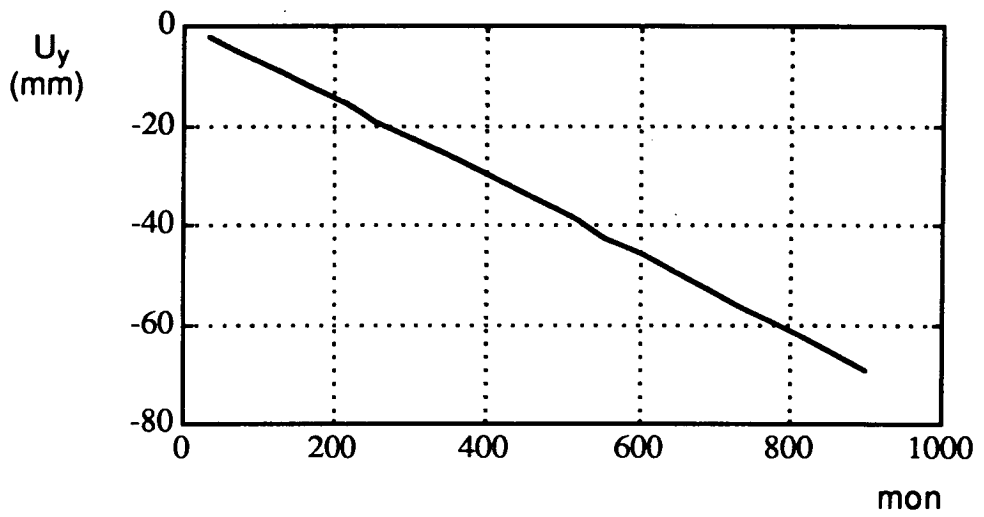


Figure 4.20 The upper actuated joint positions U_y with respect to the recorded values from the straight line potentiometer (mon).

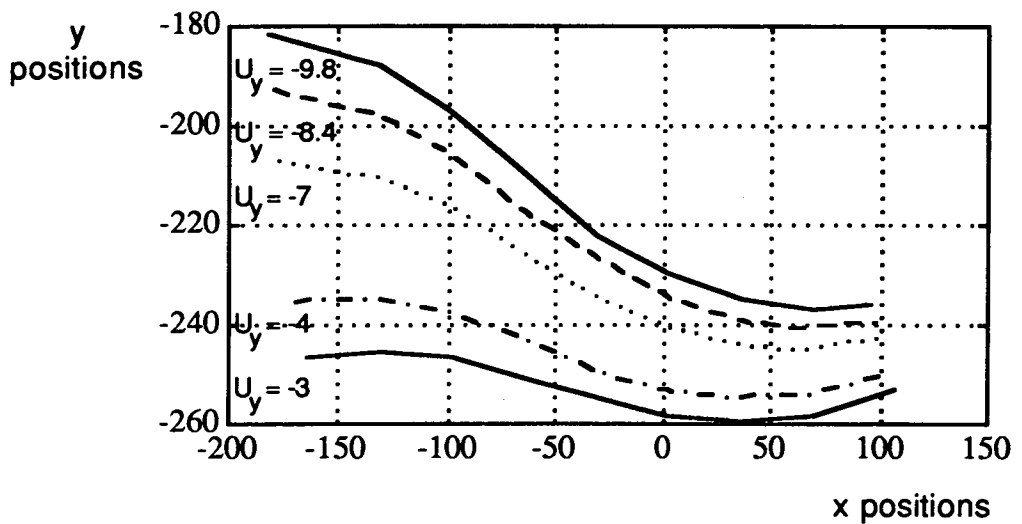


Figure 4.21 Experimental foot trajectories for various positions of upper actuated point U. The x and y components are scaled down to fit to the simulation model in chapter 3.

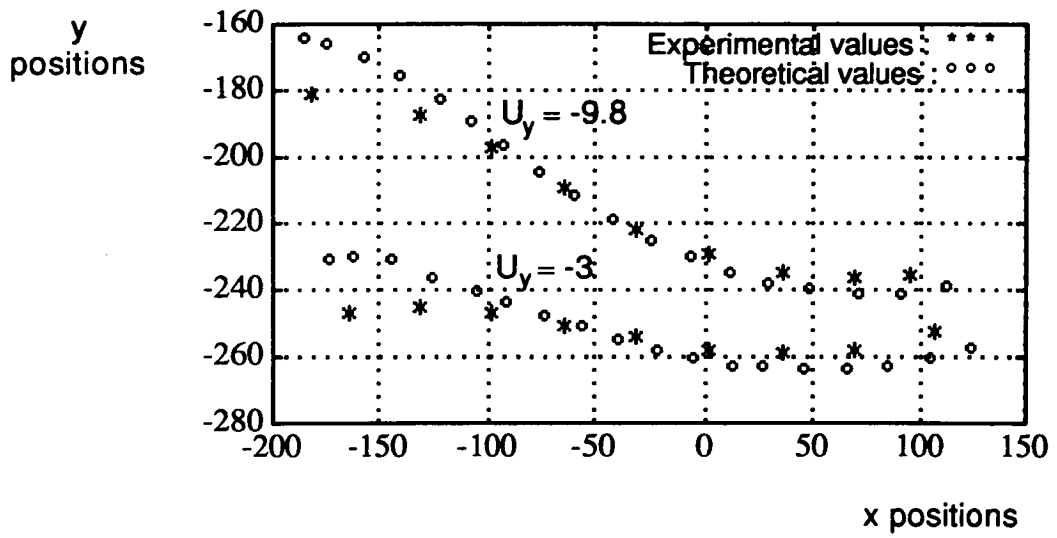


Figure 4.22 Comparison of the experimental and theoretical results for two arbitrary foot trajectories referring to the same upper actuated joint positions.

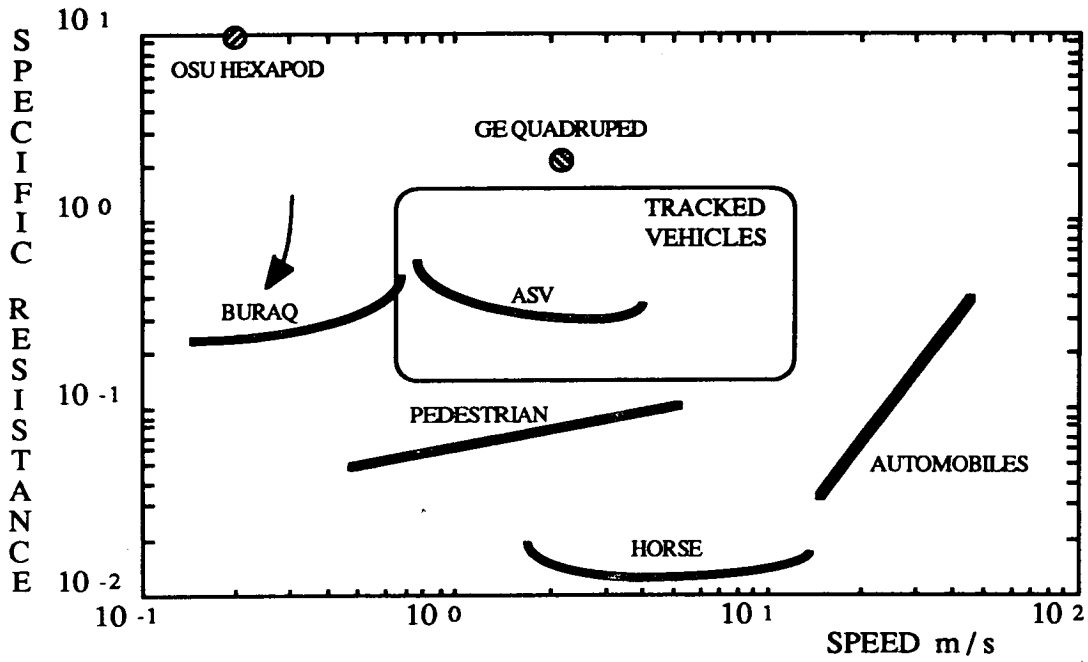


Figure 4.23 Comparison of the specific resistance values of various vehicles and systems with respect to Buraq legged vehicle (Some of the data is reproduced from (Waldron et al 1984(b))).

Chapter 5

Design and Application of a Mechanical Drive Mechanism with a Variable Stroke and Phase

Contents

5.1 Introduction

5.2 Change of The Foot Stroke

5.3 Change of Phase Between Two Parallel Driven Legs

5.4 The Proposed Method for Change of The Foot Stroke and Change of Phase

5.4.1 The Relation Between the Crank Point Position and the Crank Effective Length

5.4.2 The Relation Between the Crank Point Position and the Phase between Parallel Driven Legs

5.4.3 The Relation Between Phase and Gait

5.4.4 The Effect of the Crank Effective Length Variation on the Gait of the Vehicle

5.5 Characteristics of A Variable Crank Mechanism

5.5.1 A Mechanical Constraint

5.5.2 A Point to Consider in Control

5.5.3 The Crank Point Position on the Disk and Manouerebility of the Vehicle

5.5.4 Maximum Time to Change Phase

5.6 Simulation Results

5.7 Conclusions

5.1 Introduction

In this chapter gait shift and steering methods are developed for a legged vehicle with the Buraq legs.

To shift gaits, the design objective is to achieve the control of foot placement patterns during locomotion.

To steer, the design objective is to achieve not only the control of motion axis of the legs relative to the vehicle body, but also to achieve the control of foot strokes for each leg. In this chapter, the steering study is limited to the role of the crank which is the control of the foot strokes, and the control of motion axis of the legs is dealt with in section 7.3.3.

The following points need to be considered in the design process of the mechanisms to achieve above objectives;

1. The Buraq leg is actuated in the longitudinal direction by a crank mechanism which is purely a mechanical actuator. Mechanical actuators have very poor control characteristics compared to other actuators as was pointed out in section 2.4.1. Therefore an ordinary crank mechanism needs to be modified to control the foot stroke.

2. The Buraq legs are driven in pairs through the same drive shaft (*driven in parallel*) in longitudinal direction. Therefore a gait shift requires the control of the phase between parallel driven legs. Design of a mechanism to produce phase shift between parallel driven legs therefore becomes necessary.

5.2 Change of the Foot Stroke

Fundamental knowledge about a four bar mechanism shows that the foot stride can be changed by varying the crank radius. Since the rocker is fixed, the length of its circular trajectory can be adjusted through changing the crank radius. To change the length of the crank, the introduction of a hydraulic cylinder may be proposed. However, since the crank is an active element with repeated rotations, the fluid cannot be supplied from the vehicle body to the cylinder without high-speed rotating couplings. Traditionally the most convenient way to transfer energy from a stationary

element to a rotating element has been by slip rings conducting electrical energy. Hence, choosing slip rings allows the selection of an actuator with a lead-screw mechanism to be used to change the radius of the crank as shown in figure 5.1. Using either of the arrangements shown in the figure, a four bar mechanism can be designed with variable crank length, hence variable foot stride.

5.3 Change of Phase Between Two Parallel Driven Legs

To serve this aim a mechanism can be designed to allow a phase shift between two rotating cranks connected to the same drive shaft. A similar mechanism is used to change valve timing to increase fuel efficiency in car engines. The mechanism shown in figure 5.2(a) is proposed by Dr. J. Todd. Another mechanism is also designed to serve this particular purpose as shown in figure 5.2(b). Both mechanisms proposed in figure 5.2 are to be placed in the centre of the shaft which drives both cranks in parallel. In both mechanisms, the phase change is achieved by rotating one shaft with respect to the other one while the shaft is rotating.

5.4 The Proposed Method for Change of the Foot Stroke and Change of Phase

The methods to change the foot stroke and the phase examined in the previous sections 5.2 and 5.3 introduce additional actuators to the vehicle. It is possible to design a mechanism which can operate with a single actuator and yet cause similar effects on the foot stroke and phase. The proposed method is to build a crank on a disk in an off-centered position. The disk can be driven by the drive shaft. By rotating crank with respect to the rotating disk a 360 degrees phase change can be achieved. A sketch of the proposed design can be seen in figure 5.3. This new design is called *variable crank mechanism*. In the new mechanism, the crank is assembled off-centre on the disk so that the radius will be changing while the crank is rotating. The point where the crank is connected to the rocker is defined as *crank point*. . And the distance from the disk centre to the crank point is referred as the *crank effective length* (C_e). In this setting it can be seen

that the parameter which affects the rocker trajectory is not crank radius any more, and the crank effective length, C_e , replaces this parameter. The crank can be actuated by a lead-screw mechanism driven by a speed reducer. The power can be supplied to the electrical motor through slip rings which is a common and an effective method.

This simplification brings out the coordination requirement between the phase change and the foot stroke change, because both motions are no longer decoupled. In this chapter the simulation studies are aimed to show that coupled motion of the foot stroke and the phase change can be carried out for steering and phase-shift purposes.

5.4.1 The Relation Between the Crank Point Position and the Crank Effective Length

The relation between the crank point position and the crank effective length can be seen in figure 5.4. The figure consists of two columns, one of which shows crank point positions with respect to the disk, and the other column shows the crank point trajectory while the disk rotates. The radius of the crank point trajectory is the crank effective length as shown in the figure.

As the figure shows, while the crank point approaches to the centre of the drive shaft, the crank effective length (C_e) shortens, hence the foot stroke becomes shorter.

5.4.2 The Relation Between the Crank Point Position and the Phase in Parallel Driven Legs

Figure 5.5 consists of three columns, the first one shows the phase shift while the crank effective lengths for both parallel driven legs are equal. The second column shows the crank effective length change while the phase is constant and equal to π . The third column shows the change in the ratio of the crank effective lengths in relation to the second column.

As the figure shows, crank effective length ratios and phase variations can be expressed in the following ranges;

$$\frac{(C_e)_L}{(C_e)_R} = \left[\frac{(C_e)_{\min}}{(C_e)_{\max}} : \frac{(C_e)_{\max}}{(C_e)_{\min}} \right]$$

$$\text{Phase} = [0 : 2\pi]$$

Where subscripts L and R stand for "Left" and "Right". Furthermore figures 5.6 and 5.7 are produced from figure 5.5. Figure 5.6 shows the distances $(C_e)_{max}$, $(C_e)_{min}$ and d . Using figure 5.6, it can be shown that d is the geometric mean of $(C_e)_{max}$ and $(C_e)_{min}$, that is;

$$d = \sqrt{(C_e)_{max} (C_e)_{min}}$$

In figure 5.7, the analytical relation between both of the crank effective lengths is shown. As the figure shows, both crank effective lengths are equal when the phase between parallel driven cranks is nil. Also, due to the off-centered position of the crank on the disk, the function (Phase = π) is not a straight line.

5.4.3 The Relation Between Phase and Gait

Before studying the relation between phase and gait, running gaits should be examined in some detail. Gaits for running quadrupeds were mentioned in section 1.3.1 previously, and figure 1.1 was presented showing quadruped running gaits. In this study some running gaits for hexapods and octopods are proposed by using the quadruped running gaits. Even though no biological example exists running on more than four legs, the stabilisation problem is simpler when the number of legs gets bigger than four at walking speeds (see McGhee 1981).

The following method is proposed for running gaits of the hexapods and octopods; using two or more legs as virtual legs (refer back to the definition of virtual leg in section 1.3.1), hence reducing the total number of legs from 6 or 8 to 2 or 4 virtual legs. Since biped and quadruped running gaits have been studied in the previous research, the same running strategy can be applied to hexapods and octopods which are virtual quadrupeds and bipeds according to the adapted gait structure. The application of this method is shown in figure 5.8.

To understand the relation between phase and gait, the mechanical structure of the leg mechanism should also be examined; each leg is actuated by a variable crank mechanism in longitudinal direction. Variable crank mechanisms are connected to drive shafts in pairs, and the drive

shafts are connected to a main shaft driven by an engine.

Centre of the crank relative to the drive centre is fixed. Therefore the crank mechanisms can be constructed in various ways. Four different positioning of crank centre with respect to the drive shaft centre are examined (see figure 5.9).

The type of fixation of the crank centre with respect to the disk (N, S, W or E) affects the gaits of the vehicle. For example, if a vehicle was considered to have all the same type variable crank mechanisms, e.g. type N, then the vehicle would be travelling with trot gait at low speeds, and with pronk gait at high speeds. Figures 5.10 and 5.11 show this case for quadrupeds and hexapods respectively. The quadruped running gaits are very similar to octopods, since the octopods can be considered as virtual quadrupeds, therefore their phase-gait relation for an octopod can easily be figured out from the figure 5.10.

By changing the type of the variable crank mechanisms, different gaits can be adapted. For example figure 5.12 shows how a hexapod can change its gait from virtual trot at low speeds to bound at high speeds.

5.4.4 The Effect of Crank Effective Length Variation on the Gait of the Vehicle

The gaits are presented assuming that the vehicle travels along a straight line. However, while the vehicle has to change its direction, it has to change the crank effective lengths in longitudinal drives. This section investigates how the crank effective length can be changed without affecting the gaits.

In figure 5.13, the positions of crank points in variable crank mechanism pairs are shown for different turning angles at different vehicle operation speeds. The gaits are preserved by rotating both cranks simultaneously in symmetry to the drive shaft centre. Hence, the gait is preserved while changing the crank effective length for steering of the vehicle. As the figure shows, at walking speeds, the magnitude of angle α depends on the vehicle trajectory. The sharper the turn, the higher the value of angle α . At high speeds, the ratio of b/c depend on the vehicle trajectory. The sharper is the

turn, the higher is the angular ratio.

5.5 Characteristics of a Variable Crank Mechanism

In this section the characteristics of the variable crank mechanism are studied to lay a base for further studies.

5.5.1 A Mechanical Constraint

The leg mechanism has a mechanical constraint during the locomotion in the support period. The foot should be on the ground during the lower cycle of the crank point, and it should be off the ground during the upper cycle of the crank point as shown in figure 5.14.

5.5.2 A Point to Consider in Control

It is suggested that the crank should be driven only during the transfer period, and it should be kept locked during the support period. That way the electrical motor and the gears could be chosen to be smaller since they would not be subjected to heavy loads during operation.

5.5.3 The Crank Point Position on the Disk and Manoeuvrability

Instantaneous radius for the arc of the vehicle trajectory towards right or left, $(rot)_{RL}$ can be expressed as follows (see appendix 3.1 for details);

$$(rot)_{RL} = (C_e)_{RL} \frac{\text{width}}{|(C_e)_R - (C_e)_L|}$$

where width represents the distance between parallel driven legs and L represents the maximum foot stroke. Maximum crank effective length can be expressed as follows;

$$(C_e)_{\max} = r + y_0$$

$$(C_e)_{\min} = r - y_0$$

where r represents the radius of the crank and y_0 represents the distance between the centres of the drive shaft and the crank. The bigger the y_0 value, the smaller is the rot value which means sharper turns. To be able to provide 2π phase difference between parallel driven legs, r should be chosen bigger than y_0 value (see appendix 3.1).

5.5.4 Maximum Time To Change Phase

Following parameters are defined;

ω_ψ : Right leg crank speed with respect to the drive shaft

ω_θ : Left leg crank speed with respect to the drive shaft

$\omega_\psi = \dot{\psi}$, where ψ is angular displacement of the right leg crank

$\omega_\theta = \dot{\theta}$, where θ is angular displacement of the left leg crank

During locomotion, drive shaft operates at various speeds. In the mean time, the crank operates with respect to the disk during transfer period to change the foot stroke and phase. To find the longest time that will take the crank to change phase (which is equivalent to π phase difference) following equation can be used (see appendix 3.2 for details);

$$g \equiv \frac{2\pi}{|\omega_\psi - \omega_\theta|} \text{ where } \omega_\psi \text{ and } \omega_\theta \text{ are in [rad/s].}$$

As the equation shows, when the crank angular speeds are the same, no phase change takes place which is a reasonable and expected result.

5.6 Simulation Results

In this section the phase between parallel driven legs and variation of crank effective length are examined during locomotion. Simulation results are presented in figures 5.15-17.

Both crank points are symbolically shown in the same crank to clarify the relative positions of the crank points. Also an additional plot shows the states of left and right feet (support or transfer period) for each foot. While left foot is on the ground, 'o' symbol is printed on ($y=1$) line. And while the right foot is on the ground, '+' symbol is printed on ($y=-1$) line. While the feet are off the ground, y value is assigned as 0.5 for the left foot and -0.5 for the right foot. The phase difference can be recognised by looking at the upper plot. The lower plot shows values of the crank effective lengths for left and right legs with respect to the time.

Figure 5.15 shows the case when the crank effective lengths of both legs take the same value. As the upper plot show, there is no phase difference,

and lower plot shows that the crank effective lengths take their maximum values.

Figure 5.17 shows the case when the right leg crank effective length takes the maximum value while the left leg crank effective length takes the minimum value. The lower plot confirms the crank point positions. Also upper plot shows phase difference of π between legs.

Figure 5.16 shows one of the intermediate positions between the two cases discussed above.

5.7 Conclusions

To collect the results obtained in this chapter, two tables are produced. The tables should be used with figure 5.18. Figure 5.18 shows various crank point positions on a single crank. These positions are used in the tables to specify the crank effective length and the phase. In table 5.1 phase-gait-speed relation is shown. According to the crank point positions for left and right legs, phase, gait and speed of the leg pair are given for two extreme cases. Table 5.2 shows the relation between the phase and the direction examining all the possible crank point positions for both legs.

The study presented in this chapter shows that it is possible to get use of the dynamical superiority of a crank mechanism even for systems which require certain degree of control, by introducing a method to change its stroke length. Moreover, it has been shown that the newly developed *variable crank mechanism* can be used to change gait and stroke lengths simultaneously in a legged vehicle.

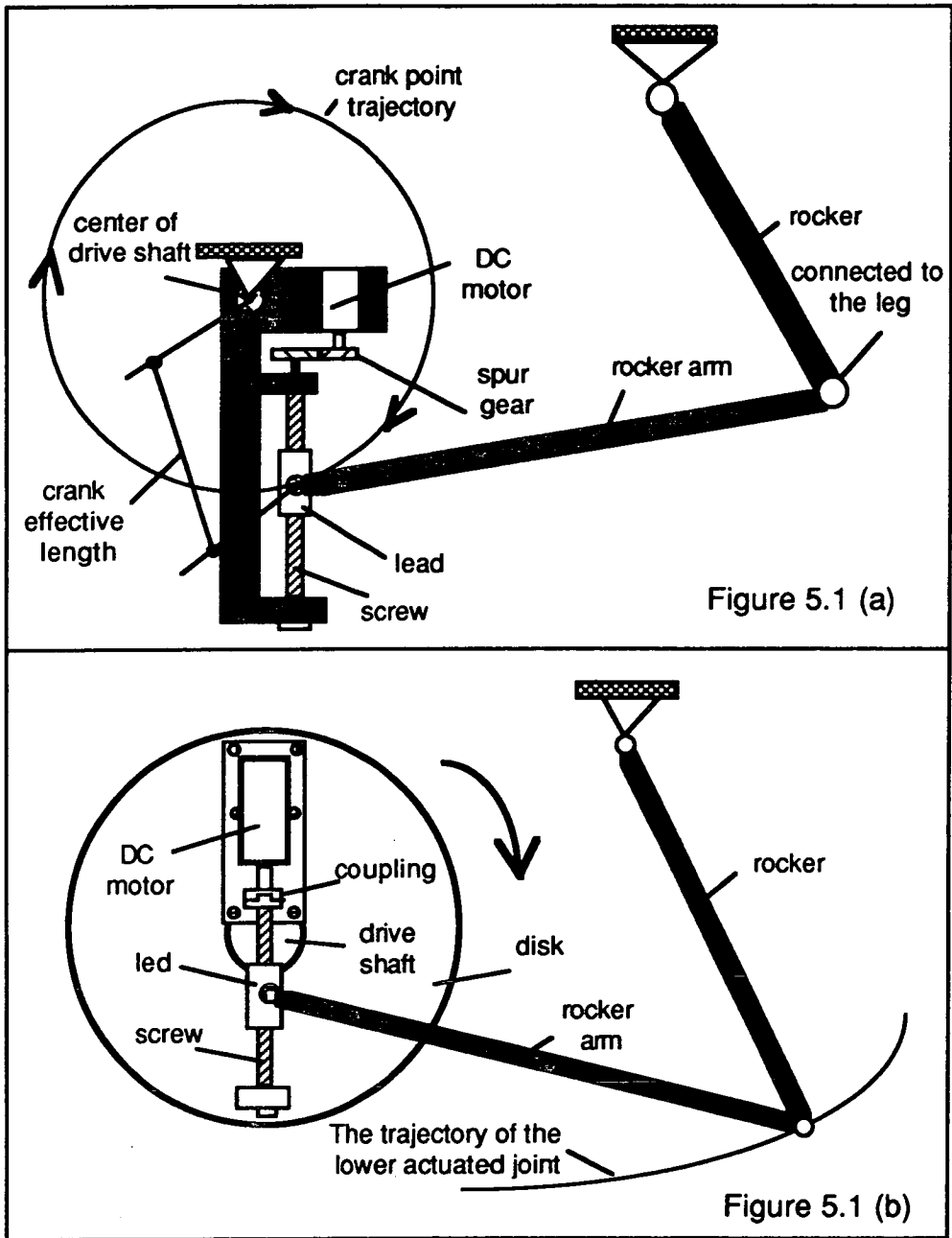


Figure 5.1 Variation of the crank length by lead screw mechanism powered by a dc motor with two similar applications

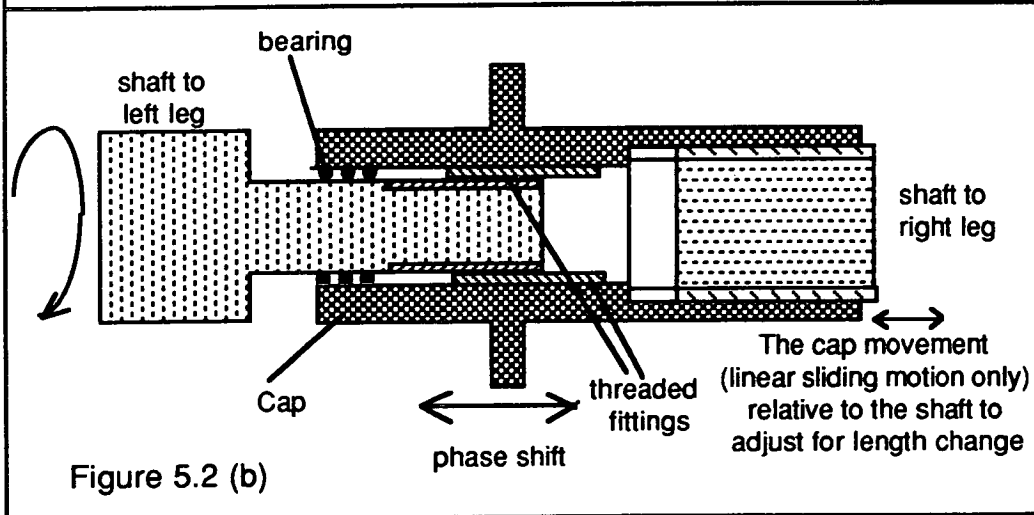
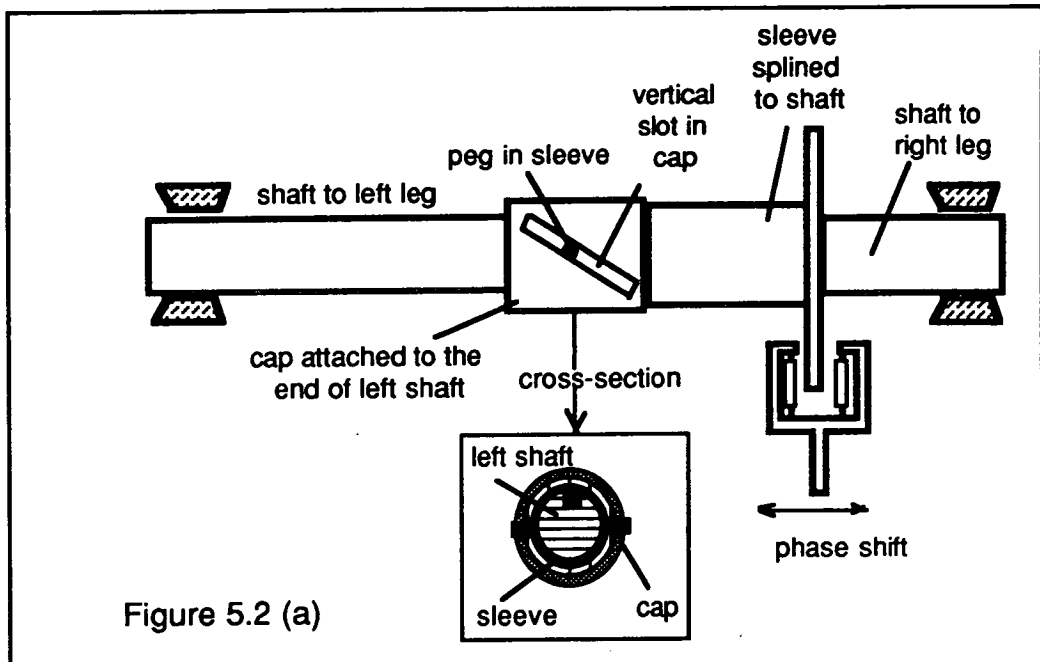


Figure 5.2 Two similar applications of phase variation between two parallel driven legs by rotating one shaft with respect to the other during operation

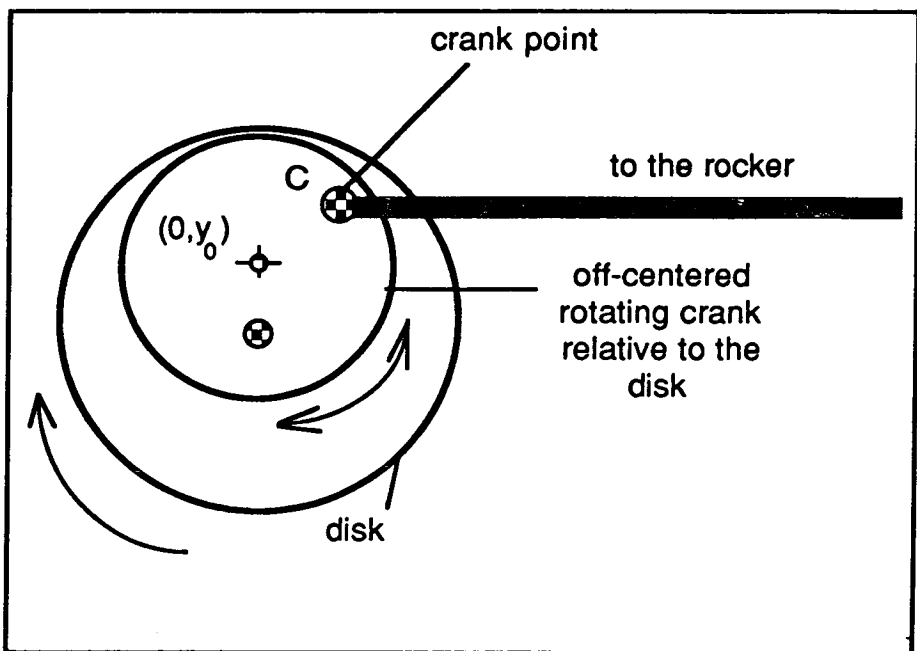


Figure 5.3 A sketch of the variable crank mechanism

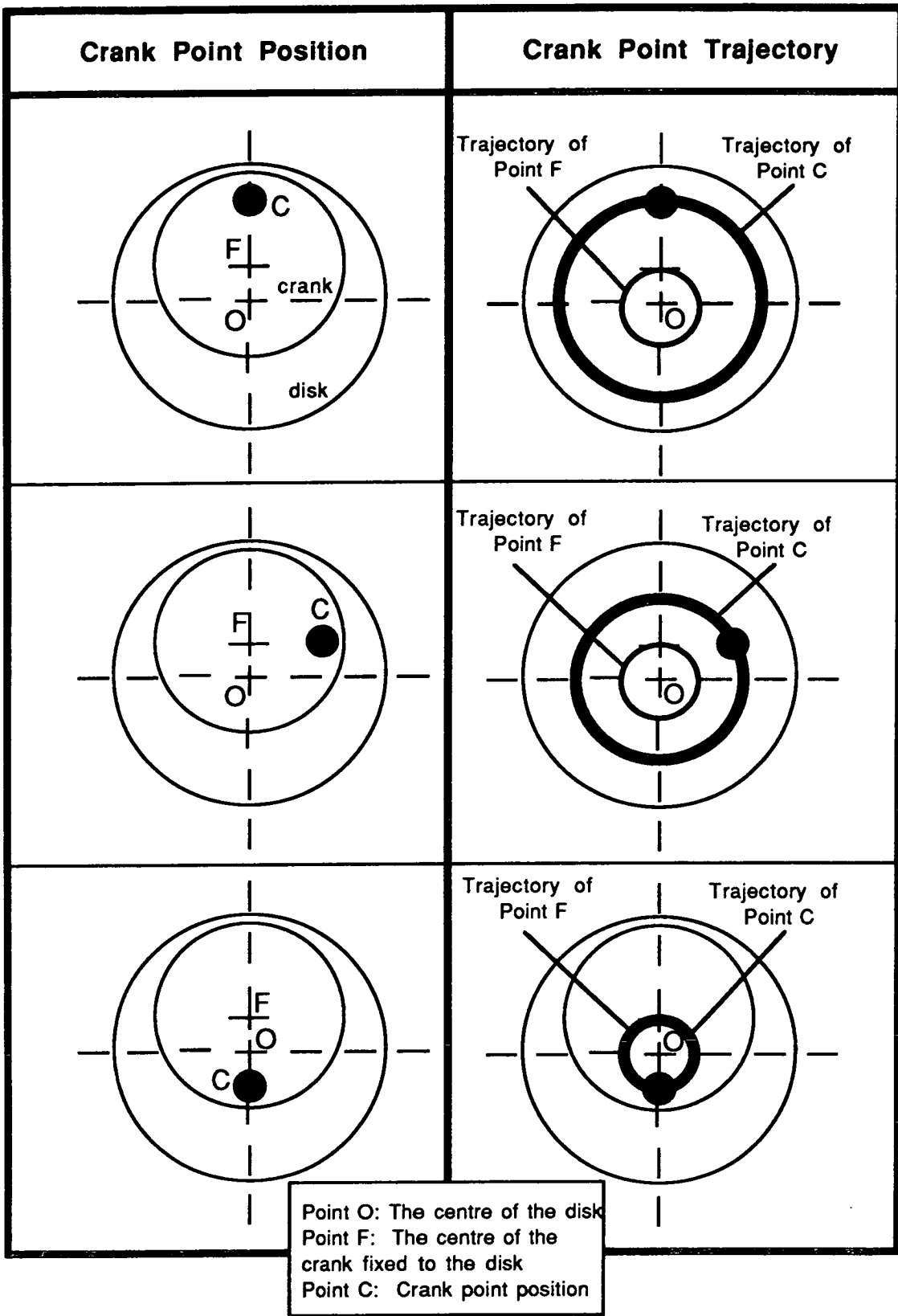


Figure 5.4 The relation between the crank point position and the crank effective length. Realise the variation of the radius of the crank point trajectory which is equal to the crank effective length

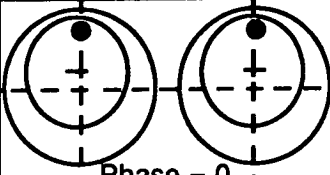
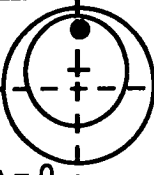
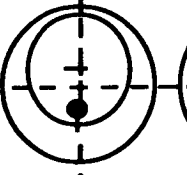
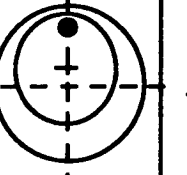
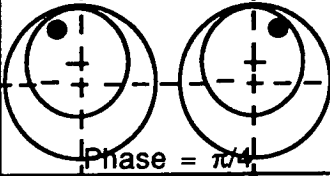
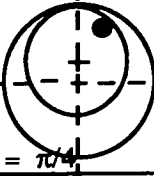
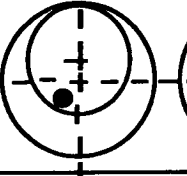
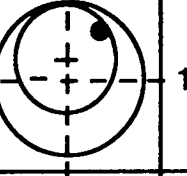
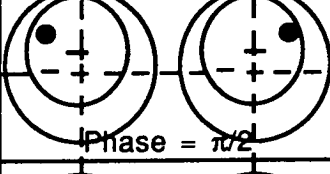
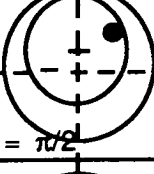
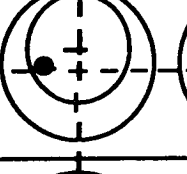
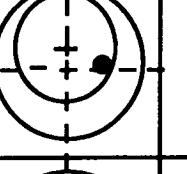
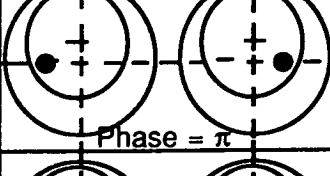
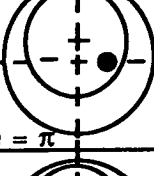
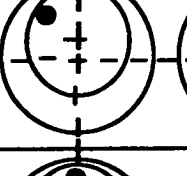
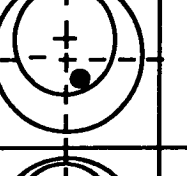
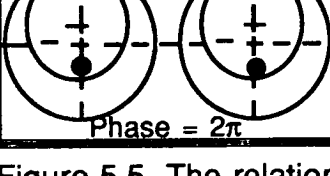
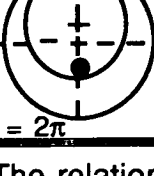
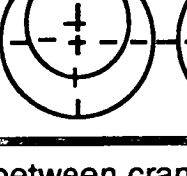
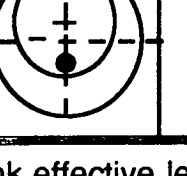
Case 1: Both crank effective lengths are equal		Case 2: The phase difference is π		The relation between the crank effective lengths for Case 2.
Left	Right	Left	Right	
				$\frac{(C_e)_R}{(C_e)_L} = \frac{(C_e)_{\max}}{(C_e)_{\min}}$
				$1 < \frac{(C_e)_R}{(C_e)_L} < \frac{(C_e)_{\max}}{(C_e)_{\min}}$
				$\frac{(C_e)_R}{(C_e)_L} = 1$
				$\frac{(C_e)_{\min}}{(C_e)_{\max}} < \frac{(C_e)_R}{(C_e)_L} < 1$
				$\frac{(C_e)_R}{(C_e)_L} = \frac{(C_e)_{\min}}{(C_e)_{\max}}$

Figure 5.5 The relation between crank effective length and phase in parallel driven variable crank mechanisms

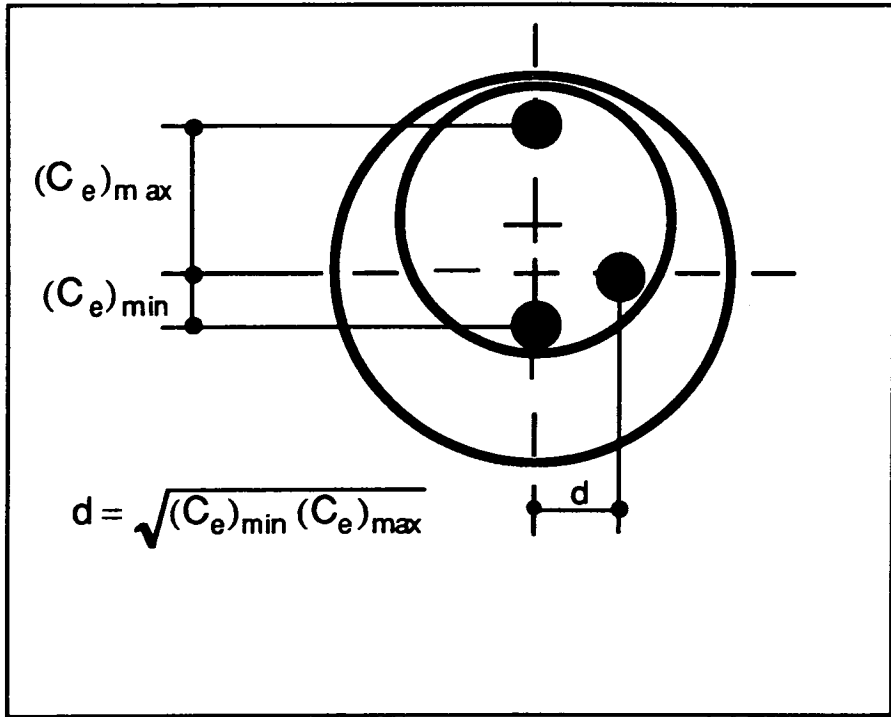


Figure 5.6 The relation between the maximum and minimum crank effective lengths and the crank position on the disk

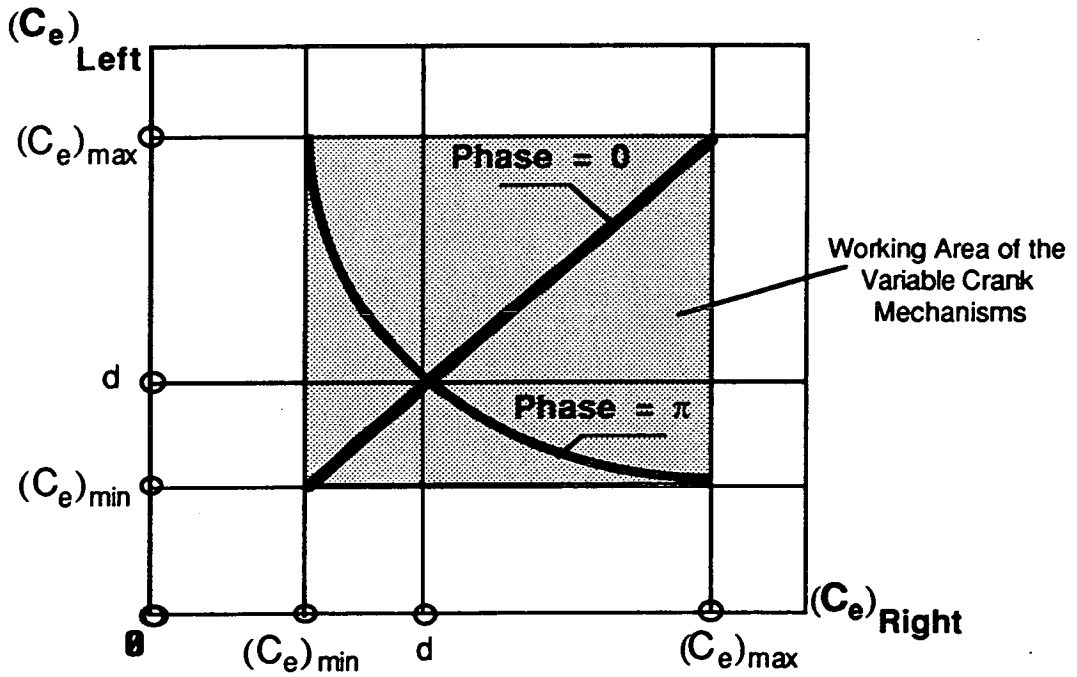


Figure 5.7 The analytical relation between the crank effective lengths of parallel driven legs.

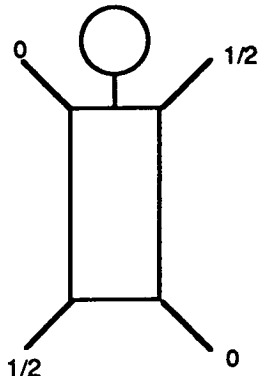
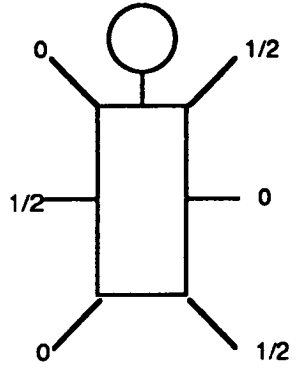
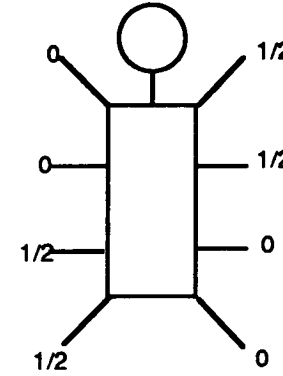
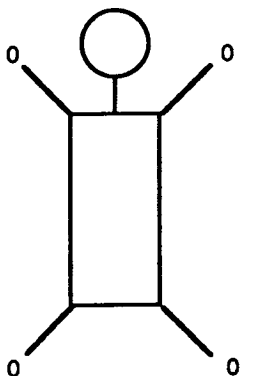
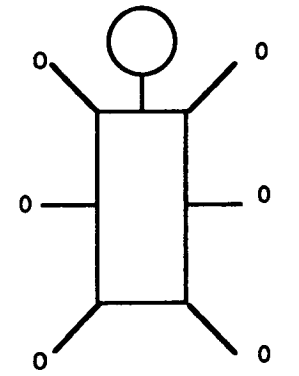
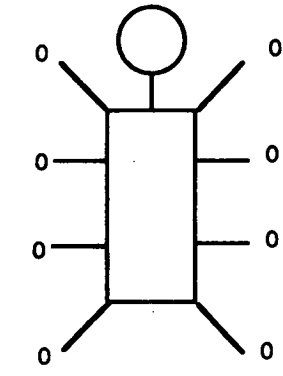
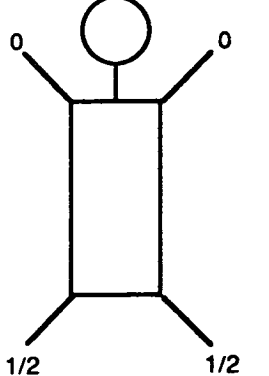
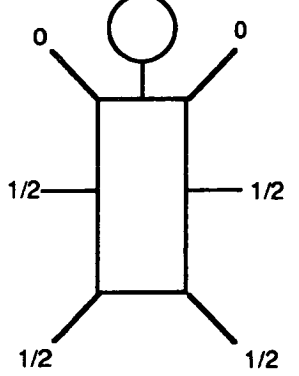
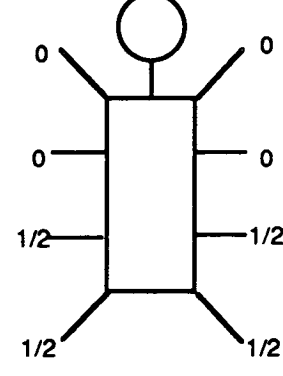
gait	QUADRUPED Configuration	HEXAPOD Configuration	OCTOPOD Configuration
T R O T			
P R O N K			
B O U N D			

Figure 5.8 Some running gaits with relative phase descriptions

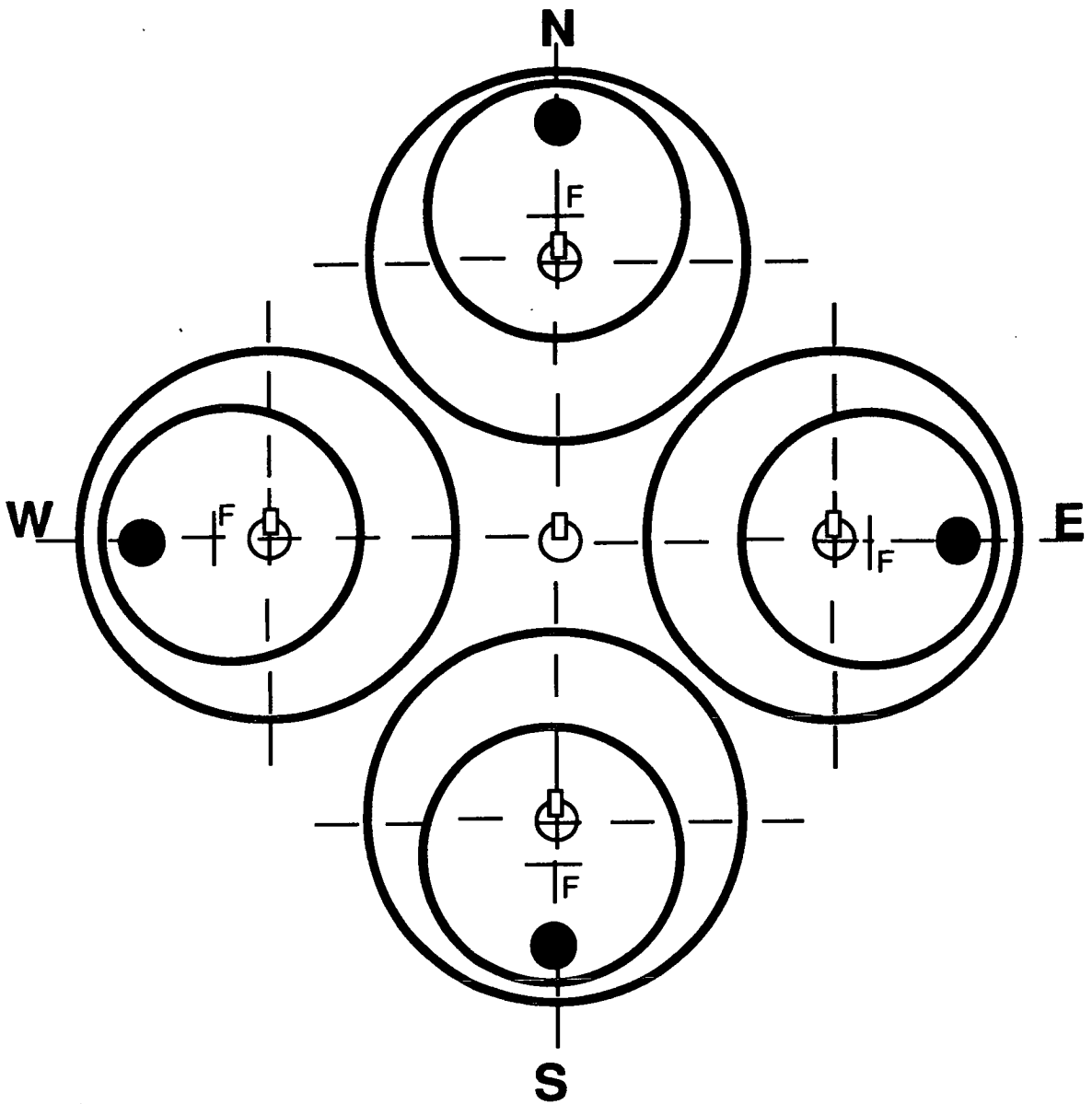



Figure 5.9 Four types (N, W, S, E) of variable crank mechanism; realise the orientation according to the drive shaft centre ().

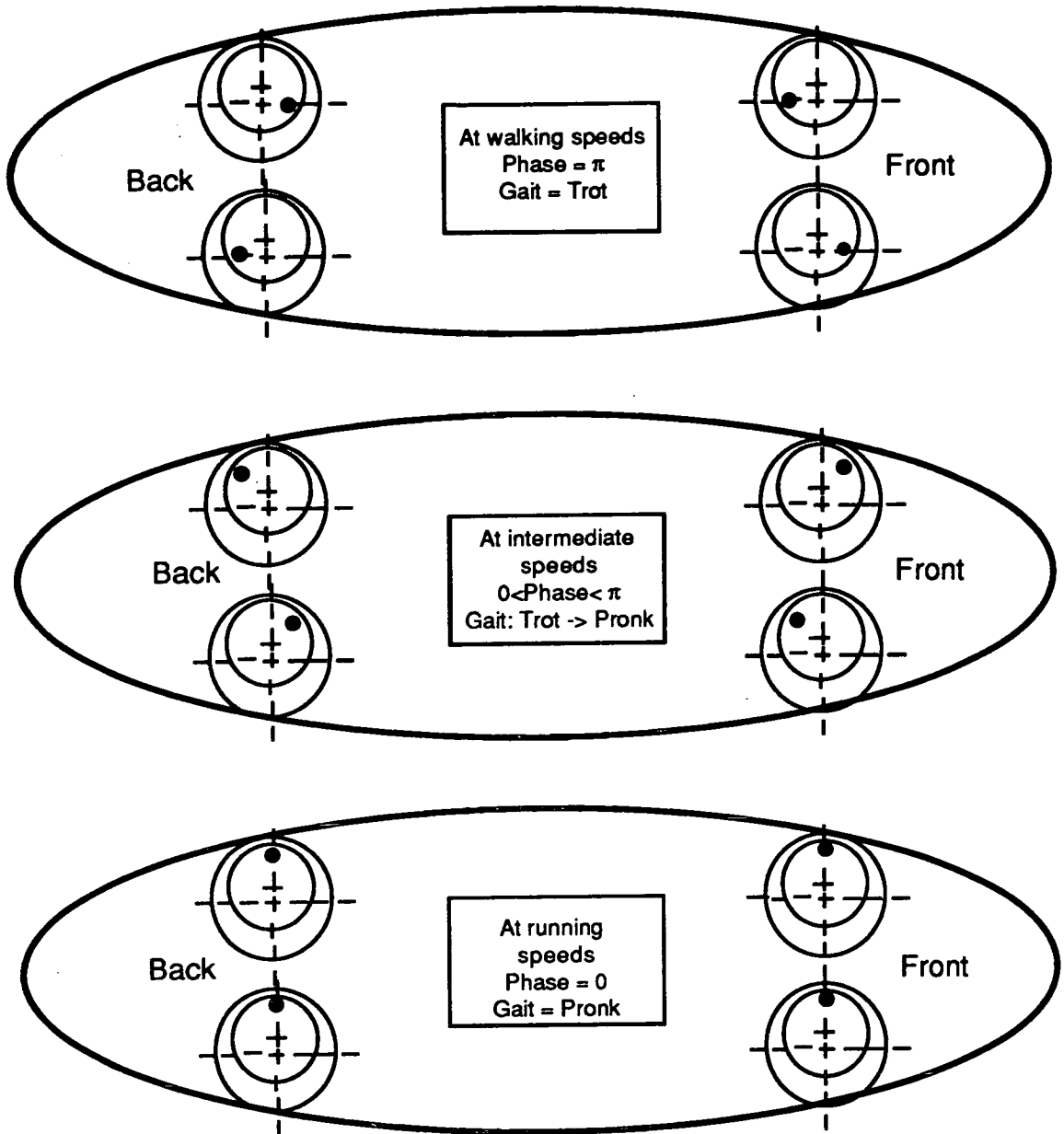


Figure 5.10 A quadruped case: The effect of the variable crank mechanism type on the gaits of a vehicle. Variable crank mechanisms are all the same type, therefore the gaits are trot and pronk.

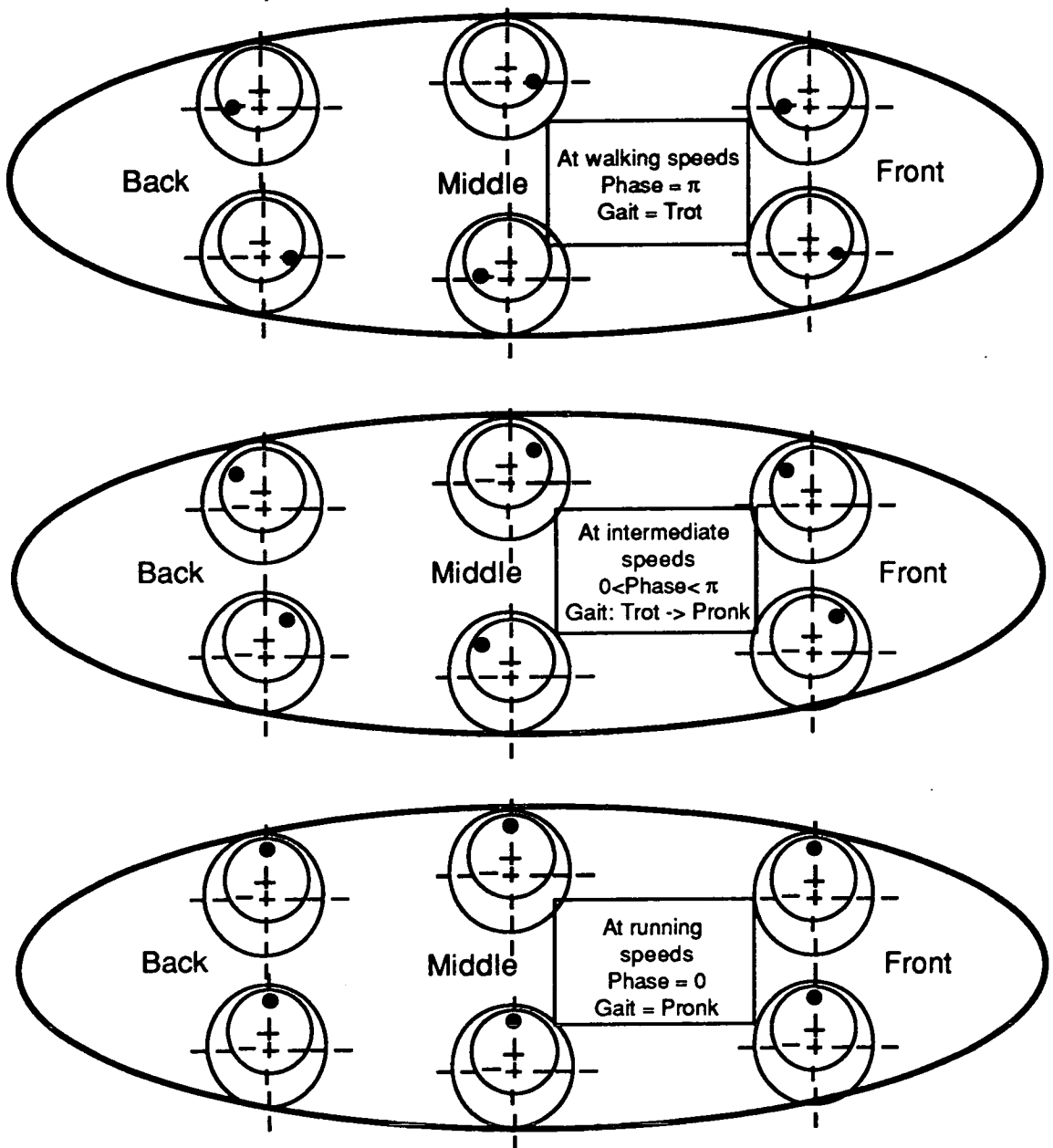


Figure 5.11 A hexapod case: The effect of the variable crank mechanism type on the gaits of a vehicle. Variable crank mechanisms are all the same type, therefore the gaits are trot and pronk.

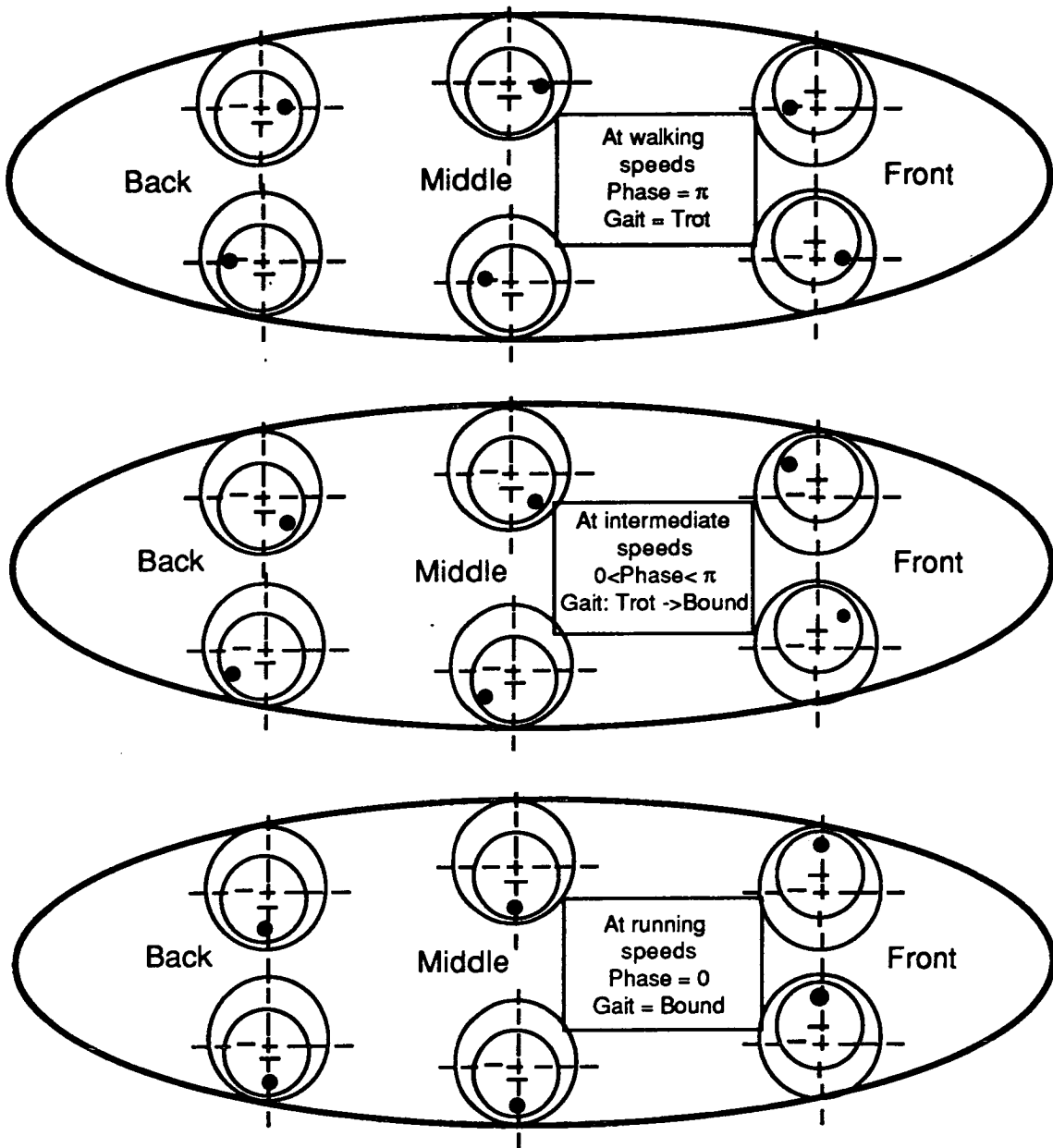


Figure 5.12 A hexapod case : The effect of the variable crank mechanism type on the gaits of a vehicle. Types of variable crank mechanisms are: The front pair (N), The middle and back pairs (S). Therefore the gaits are trot and bound.

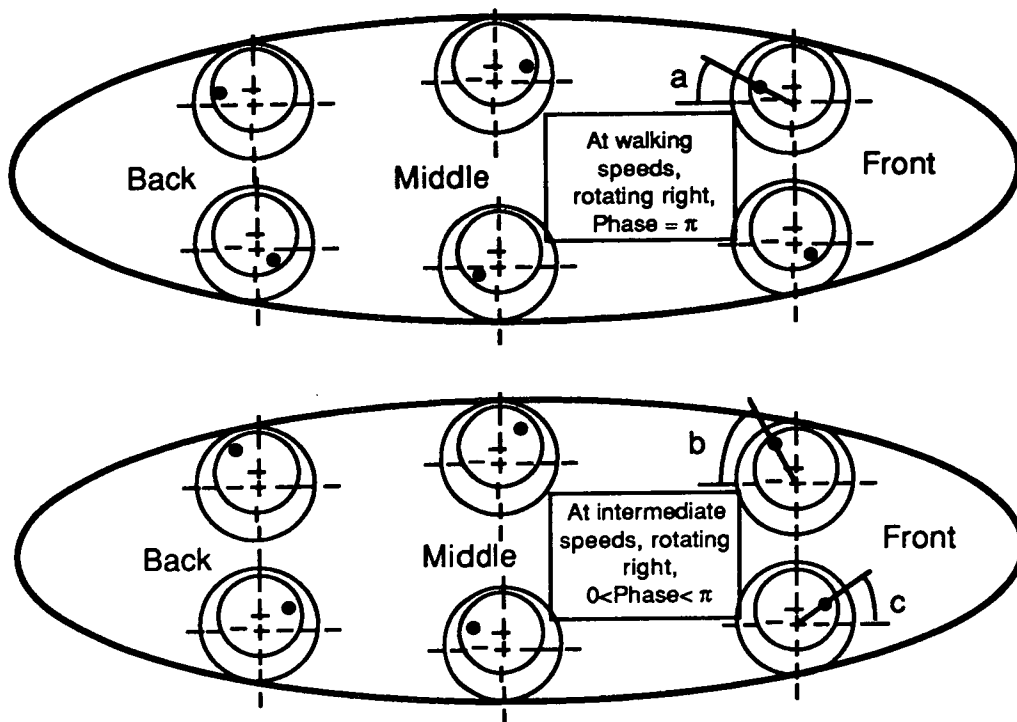


Figure 5.13 A hexapod case: Preservation of the gait structure during rotation.

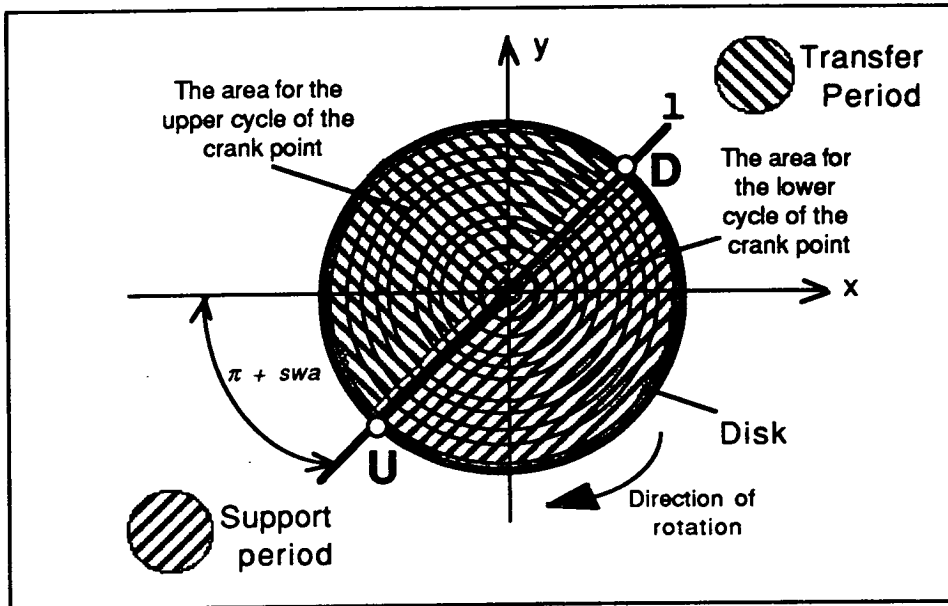
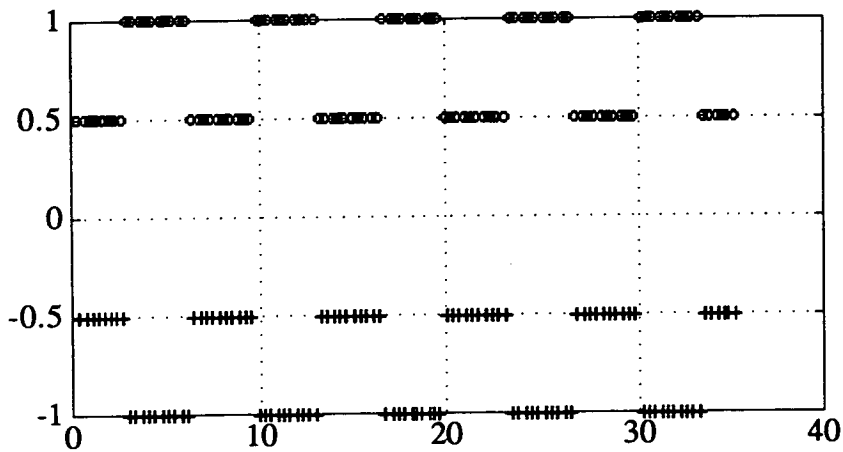
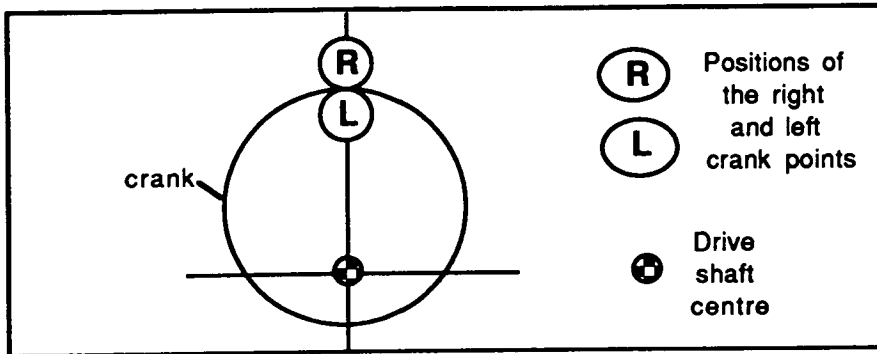
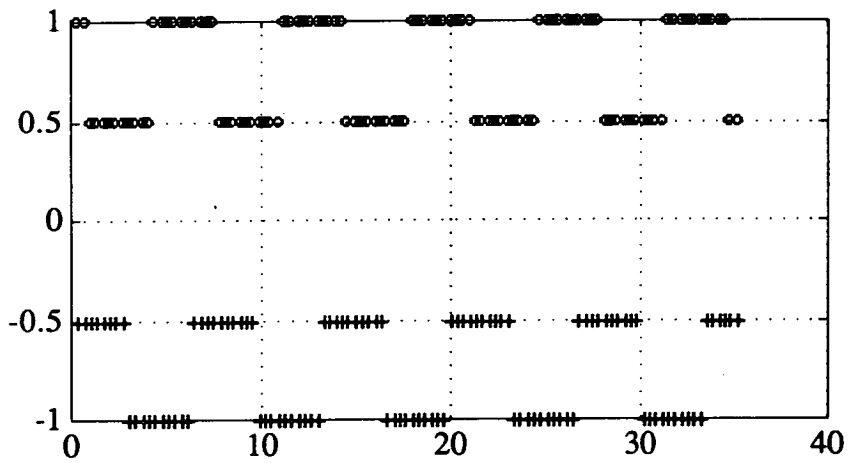
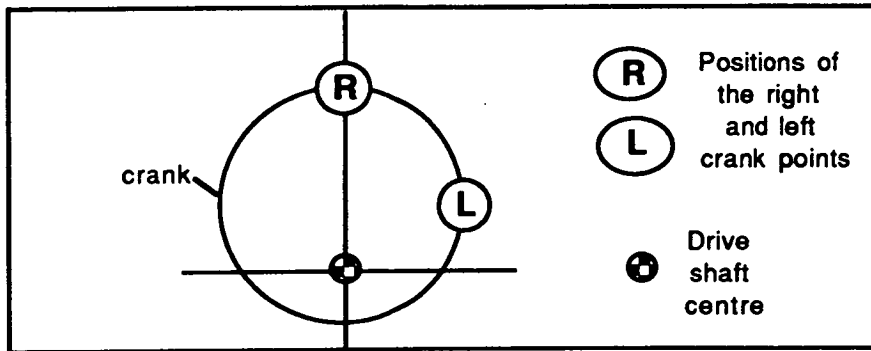


Figure 5.14 Mechanical constraint on the crank point positions with respect to the leg cycle periods. Point U marks where foot must be raised up, and point D marks where foot must be lowered down.



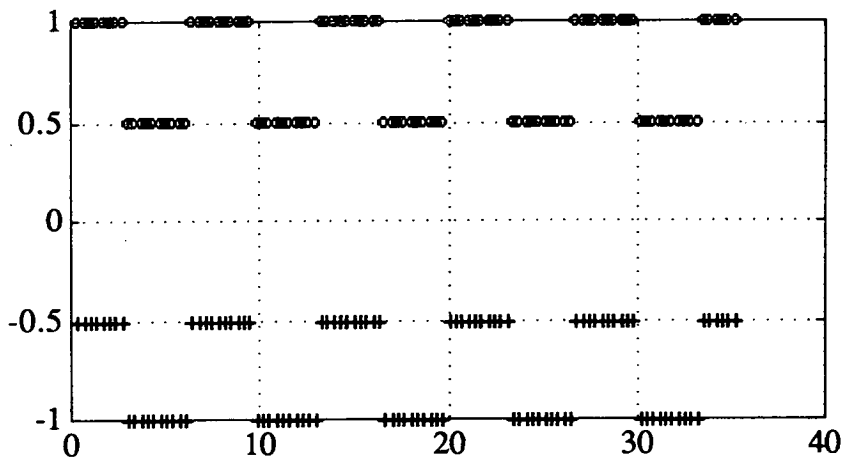
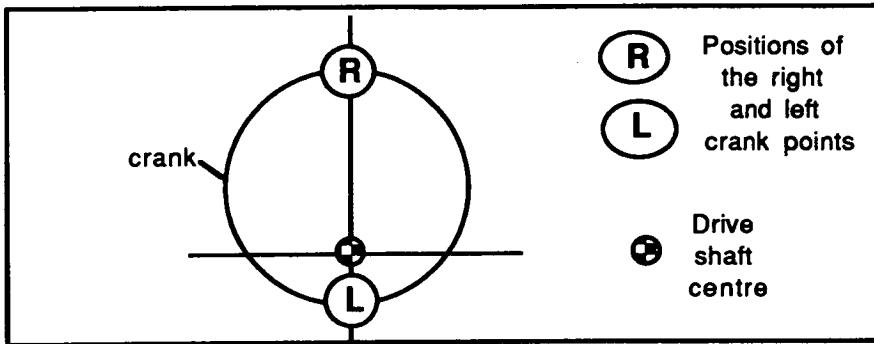
Left Leg: 'o' $\text{tet}0 = \pi/2$ $C_e = 96$
 Right Leg: '+' $\text{ksi}0 = \pi/2$ $C_e = 96$

Figure 5.15 Both cranks operating with no phase and with maximum crank effective length.



Left Leg: 'o' $tet0 = 0.0$ $C_e = 72$
 Right Leg: '+' $ksi0 = \pi/2$ $C_e = 96$

Figure 5.16 Keeping the right crank effective length at maximum length, operating with a phase difference.



Left Leg: 'o' $\text{tet}0 = -\pi/2$ $C_e = 32$
 Right Leg: '+' $\text{ksi}0 = \pi/2$ $C_e = 96$

Figure 5.17 Keeping the right crank effective length at its maximum value, operating with π phase value

Position		Condition	Phase	Gait	Speed
Left Leg	Right Leg				
A_i	B_j	$i = j$	π	Trot	Slow
B_i	A_j				
A_i	A_j	$i = j$	0	Gallop / Prong	Fast
B_i	B_j				

Table 5.1 Phase-Gait-Speed relation of the parallel driven legs

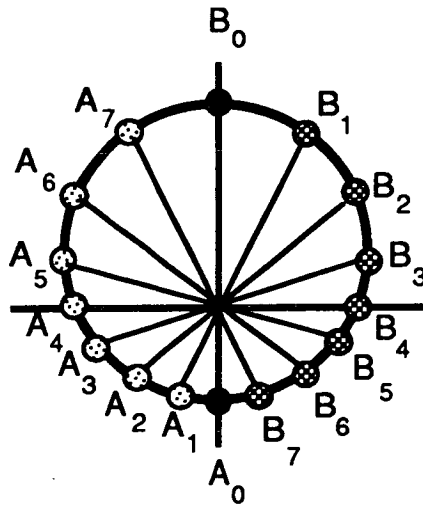


Figure 5.18 Various crank point positions on the crank and crank effective lengths

Position		Condition/s	Phase ϑ	Direction
Left Leg	Right Leg			
A_i	B_j	$0 \leq i < 4$ $0 \leq j \leq 4$	$\pi/2 < \vartheta < \pi$	Rotation to left
B_i	A_j			Rotation to right
A_i	B_j	$i = j = 4$	$\vartheta = \pi$	Straight
B_i	A_j			
A_i	B_j	$0 < i \leq 7$ $0 < j \leq 7$ $i = 8 - j$	$0 < \vartheta < \pi$	Straight
B_i	A_j			
A_i	B_j	$4 < i < 8$ $4 < j < 8$	$\pi/2 < \vartheta < \pi$	Rotation to left
B_i	A_j			Rotation to right

Table 5.2 Phase-Direction relation of the parallel driven legs

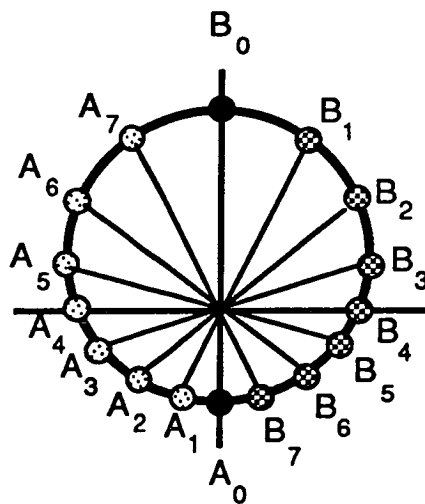


Figure 5.18 Various crank point positions on the crank and crank effective lengths

Chapter 6

Elastic Energy Storage in the Buraq Leg Mechanism for High Speed Legged Locomotion

Contents

6.1 Introduction

6.2 How Elastic Energy is Stored and Contributed Into the Leg Energy Cycle

6.3 Ground Reaction Forces During High Speed Legged Locomotion and the Need for the Elastic Energy Storage

6.4 Force Analysis of the Buraq Leg Mechanism for Elastic Energy Storage

6.5 Evaluation of Results and Conclusions

6.1 Introduction

Previously in section 1.5 the need for practical applications of elastic energy storage in legged vehicles was briefly discussed. For this chapter the following objectives are set out;

- To investigate the way elastic energy is stored and is contributed back into leg cycle
- To show the necessity of elastic energy storage for high speed legged vehicle applications
- To carry out a feasibility study of the Buraq leg as a potential leg mechanism for elastic energy storage purposes.

6.2 How Elastic Energy is Stored and Contributed Into the Leg Energy Cycle

While running, the body is propelled into the air at an angle, using vertical actuation to push the foot against the ground during the support period. After the flight period, landing generates a ground reaction force. This force is directed to deform the springs in the linkages of the leg mechanisms. When the foot passes through the mid-stroke in the support period, the spring force changes direction, and tends to produce enough energy to supply the body with the necessary thrust force to continue running. Due to the vertical actuation input, repeating the above process builds up energy, and gradually the speed of the vehicle increases. Storing the increasing energy in the springs, and putting this energy back into cycle paves the way for very high speeds.

6.3 Ground Reaction Forces During High Speed Legged Locomotion and The Need For Elastic Energy Storage

While walking, it is assumed that a multi-legged vehicle uses one leg from each pair of legs for a better balance. Hence the payload, the body weight and the weight of the legs in the air are carried by the legs which are supporting the vehicle. It should also be remembered that each leg has its

own weight to support. Hence, the maximum ground reaction force can be expressed as follows during walking on flat terrain assuming that all ground reaction forces are acting in vertical direction;

$$F_{\max} = \frac{\frac{n}{2} W_{\text{leg}} + W_{\text{body}} + W_{\text{payload}}}{\frac{n}{2}} + W_{\text{leg}} \quad (6-1)$$

where W_{leg} represents weight of a leg unit, W_{body} represents weight of the body, W_{payload} represents weight of payload, and n represents number of legs.

Unlike walking, while running, the maximum ground reaction forces are caused by the landing of the body on the ground after its flight on the air. An expression for the maximum ground reaction force (F_{\max}) can be obtained in terms of a vehicle's total weight (W_{tot}) and its speed (V) by using the data in (Munro et al 1987);

$$F_{\max} = W_{\text{tot}} [0.15 (V - 3) + 2.5] \quad (6-2)$$

For running speeds, V value is either equal or bigger than 3 m/s.

The maximum speed of a battle tank is around 12.5 m/s. Having this speed value substituted in equation (6-2), the following is obtained;

$$F_{\max} = 3.925 W_{\text{tot}} \quad (6-3)$$

The equation (6-3) shows a directly proportional relation between the maximum ground reaction force and the vehicle's weight at a constant speed.

Assuming that no elastic energy storage takes place, to start the vehicle's flight period, a thrust force should be applied to the vehicle, and this thrust force should be less than or equal to the maximum ground reaction force. Hydraulic actuators are commonly used for load handling. Using an ordinary hydraulic ram operating at 200 bar, a basic relationship can be obtained from the manufacturer's data between thrust force and cross-sectional area of the ram as follows [see (Webtec Hydraulics Catalogue, 1988)] ;

$$F_{\text{thrust}} = 2,035 A \quad (6-4)$$

where F_{thrust} represents the thrust force (N) that the ram is able to stand at 200 bar pressure, and A represents cross-sectional area (cm^2).

The Buraq leg mechanism has an average magnification ratio of 10 between the foot and the vertically actuated joint. This factor can be contributed into the equation (6-3) as follows;

$$F_{\text{thrust}} = 10 F_{\text{max}} = 39.25 W_{\text{tot}} \quad (6-5)$$

Combining equations (6-4) and (6-5), and by cancelling out F_{thrust} , following equation can be obtained;

$$W_{\text{tot}} = 51.85 A \quad (6-6)$$

where W_{tot} is in (N) and A is in (cm^2). In terms of the diameter of the cross-sectional area, D (cm), equation (6-6) can be rewritten as follows;

$$W_{\text{tot}} = 40.72 D^2 \quad (6-7)$$

If $W_{\text{tot}} = 10,000$ N, then $D = 15.67$ m.

This huge diameter of the hydraulic ram to provide the necessary thrust force to start the flight period proves the necessity of the elastic energy storage to be incorporated into the leg cycle for running legged vehicles.

6.4 Force Analysis of the Buraq Leg Mechanism for Elastic Energy Storage

While running the total forces exerted on the body totals up to about 4 times of the body weight as shown in equation (6-3). To be on the safe side, the maximum ground reaction force during running is taken as 5 times of the body weight for calculations while assuming that the vehicle's total weight is $W_{\text{tot}} = 10,000$ N. Hence;

$$F_{\text{max}} = 5 W_{\text{tot}} = 50,000 \text{ N} = 50 \text{ kN}$$

The aim of the force analysis is to find the suitable linkages which can be accommodated as springs in the leg structure. In the leg mechanism only those linkages which are free of any bending moment can be accommodated as springs to avoid complications in manufacturing. The forces on the springy linkages should act similar to the spring forces of a

basic mass-spring model (see figure 6.1). These similarities are as follows;

- The maximum force is achieved around the middle of the support period,

- A sign change takes place as soon as the force achieves its maxima.

The linkages carrying purely compression or extension forces are TQ, WQ, QN and JV (see figure 6.2). A sample linkage for elastic energy storage is shown in figure 6.3.

For a complete support period, the internal forces acting on linkages are calculated by statical analysis, and ground reaction forces are exerted for the cases of flat terrain, 60° uphill and 60° downhill conditions (see figure 6.4).

The calculations are carried out while the ground reaction force is 50 kN and the terrain is flat. The force variation on the specified linkages are shown in figures 6.5 through 6.8. To show the sign changes taking place, x and y components of the forces are shown separately.

6.5 Evaluation of Results and Conclusions

The force variation results are found similar to those of a mass-spring model. It can also be observed that the maximum spring force occurs at the linkage WQ, which is about 40 times the ground reaction force value.

Using the force variation results, sign changes are recorded in figure 6.9. It can be seen from the figure that for all terrain conditions (flat, uphill and downhill) QN and JV linkage pair shift sign in opposite with TQ and WQ linkage pair while positive sign represents extension forces.

Legs can be placed in either directions on the body (see also section 7.3.2). However the leg placement should be done in a such a way that the linkages with springs should be those going through compression cycle first, so that elastic energy can be stored.

While running at high speeds, hydraulic rams can be used for two purposes

1. During flight period, to raise and to lower the foot,

2. In the mid-support to increase the thrust on the springy linkages by pressing the foot towards the ground. The rest of the time the valves can be kept shut.

The crank however should act continuously so that the speed of the vehicle can be maintained.

The magnitude of forces on linkage WQ is calculated for three different terrain conditions (see figure 6.10). Since the highest peak force is achieved during downhill locomotion, it can be said that maximum vehicle speeds can be achieved during downhill locomotion which is an expected result.

Through this research, the Buraq leg mechanism has been justified to be a convenient leg mechanism for elastic energy storage purposes as the force results confirmed. During the calculations of the specific resistance in section 4.3.4, the force variation was experimentally observed to be maximum around the mid-stroke which confirms the simulation results.

The study also showed that it is feasible to build self-sufficient legged vehicles for off-road transport to operate at various speeds.

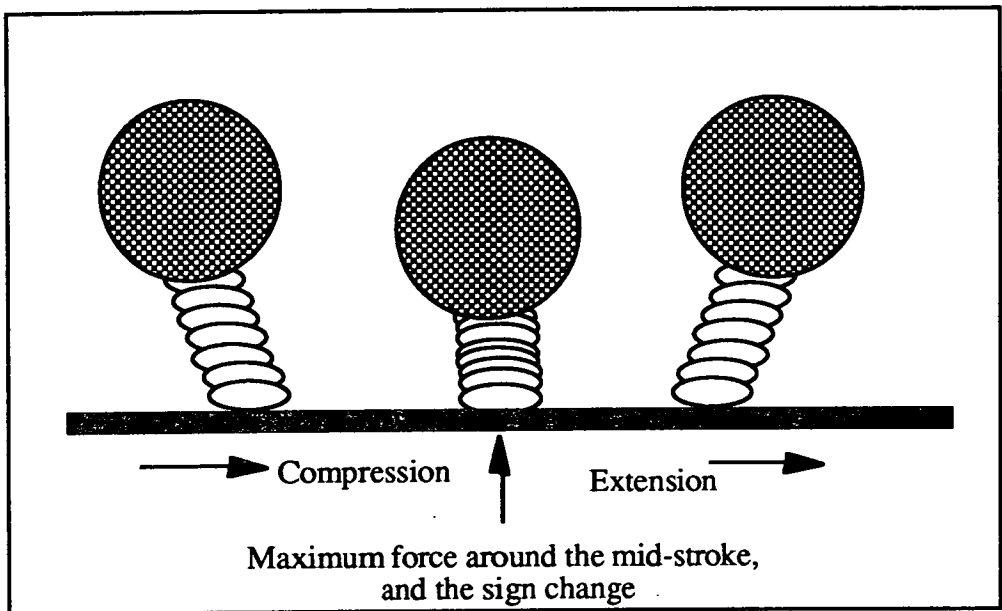


Figure 6.1 The Spring Force Variation in a mass-spring model

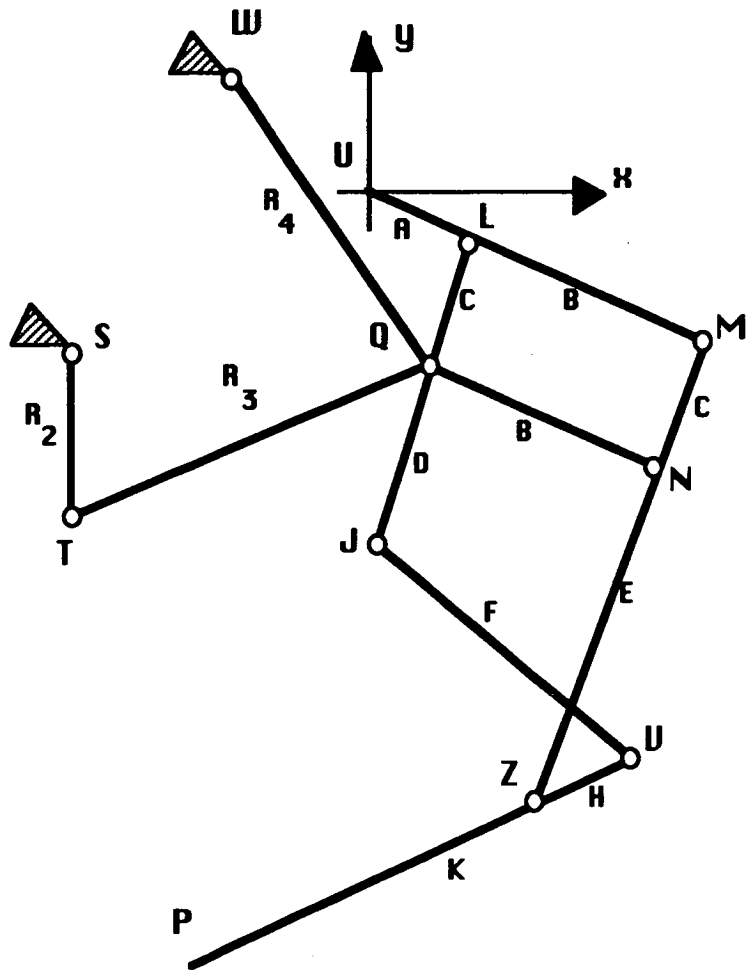


Figure 6.2 The Buraq Leg Mechanism with the crank-rocker



Figure 6.3 A sample springy linkage

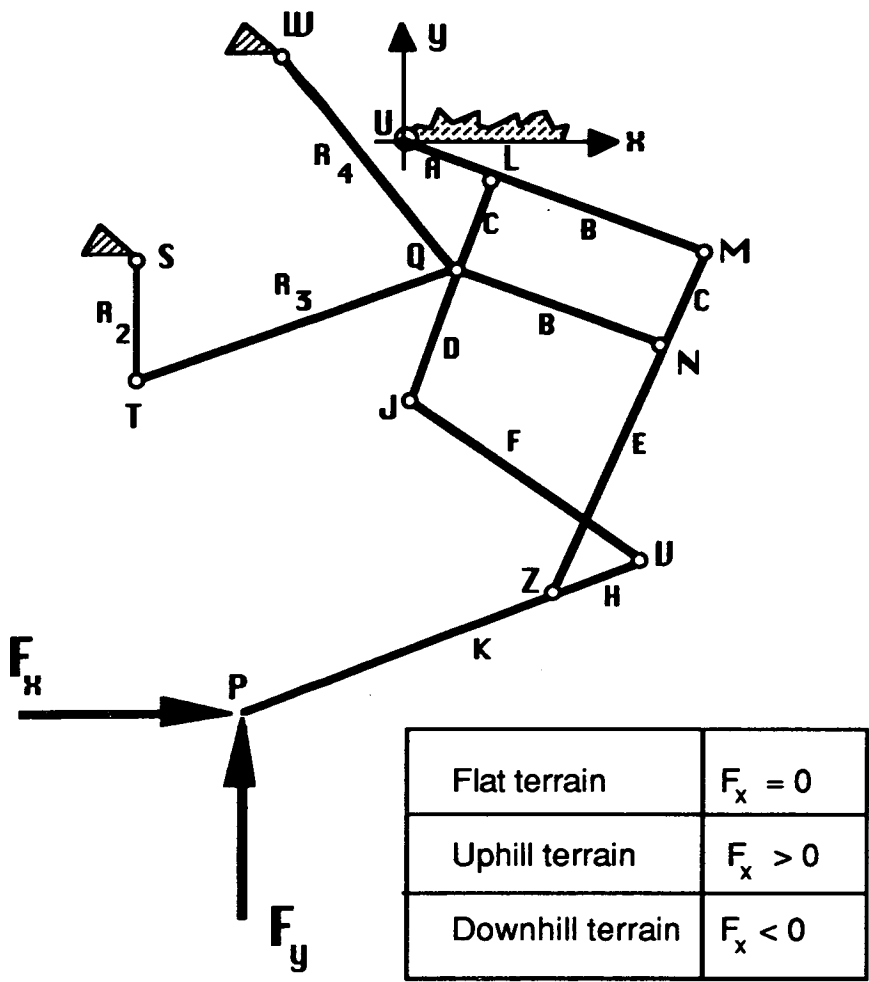


Figure 6.4 Ground reaction forces acting on the Buraq leg mechanism at various terrain conditions during support period

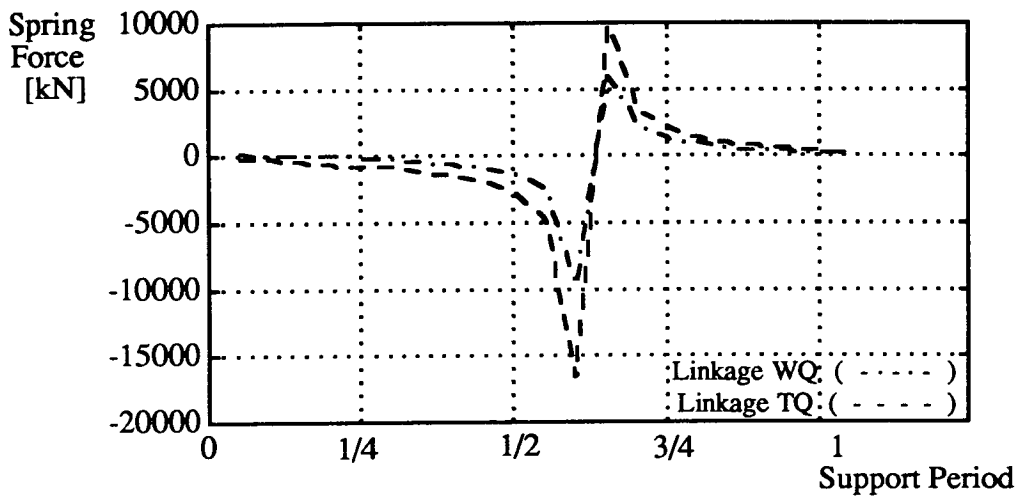


Figure 6.5 Variation of spring force in the -x- direction on the linkage TQ and WQ during support period (See the orientation of the leg in figure 6.2).

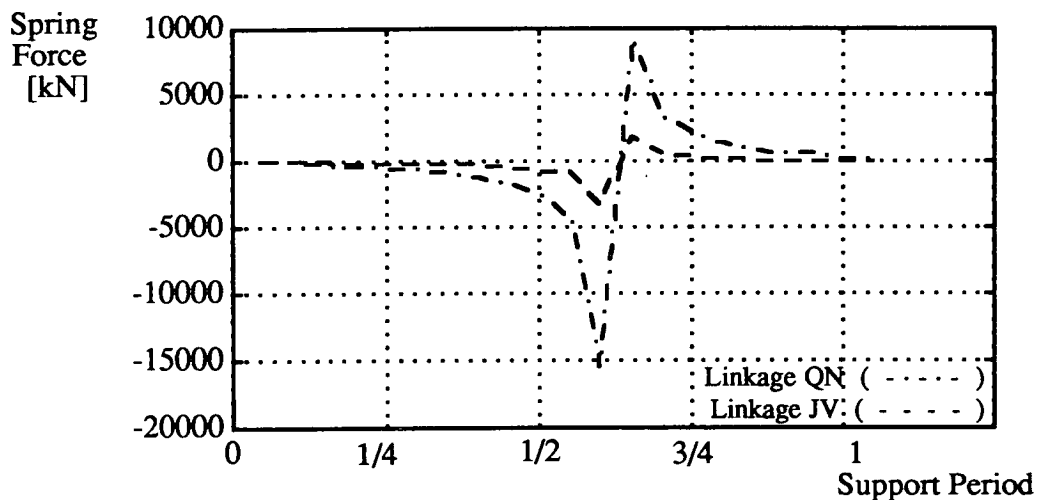


Figure 6.6 Variation of spring force in the -x- direction on the linkages QN and JV during support period (See the orientation of the leg in figure 6.2).

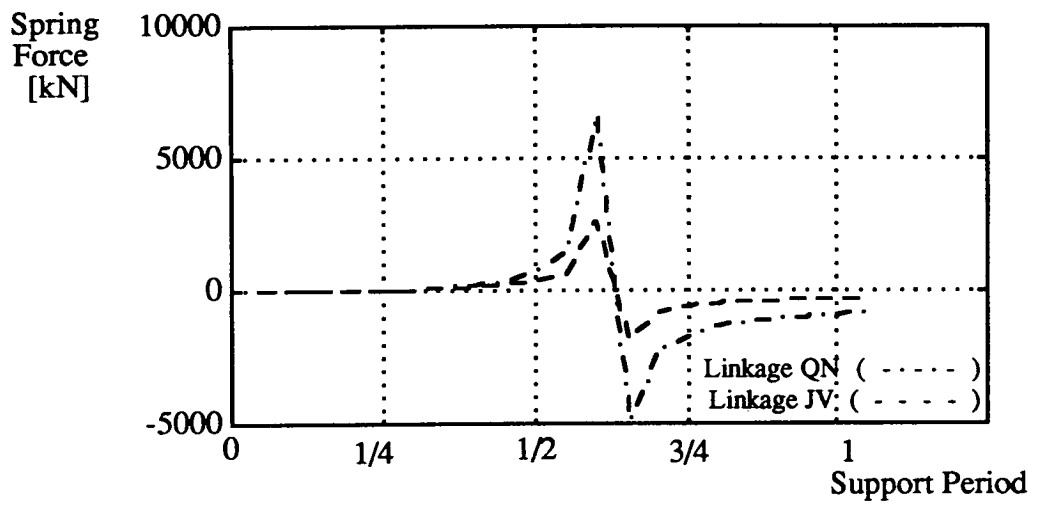


Figure 6.7 Variation of spring force in the -y- direction on the linkages QN and JV during support period (See the orientation of the leg in figure 6.2).

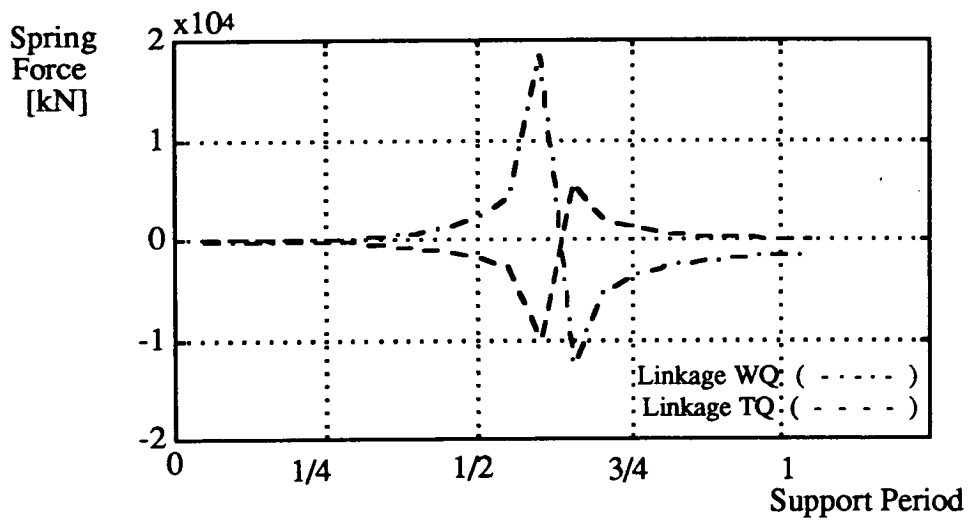


Figure 6.8 Variation of spring force in the -y- direction on the linkages TQ and WQ during support period (See the orientation of the leg in figure 6.2).

Terrain ==>	Flat		60° up-hill		60° down-hill	
	<i>Mid stroke</i>		<i>Mid stroke</i>		<i>Mid stroke</i>	
Linkage QN	+	-	+	-	+	-
Linkage JV	+	-	+	-	+	-
Linkage TQ	-	+	-	+	-	+
Linkage WQ	-	+	-	+	-	+

Figure 6.9

Force Variation around the leg mid-stroke
 Extension forces are represented by plus '+' sign
 where compression forces are represented by minus '-' sign
 Orientation of the leg is as shown in figure 6.2.

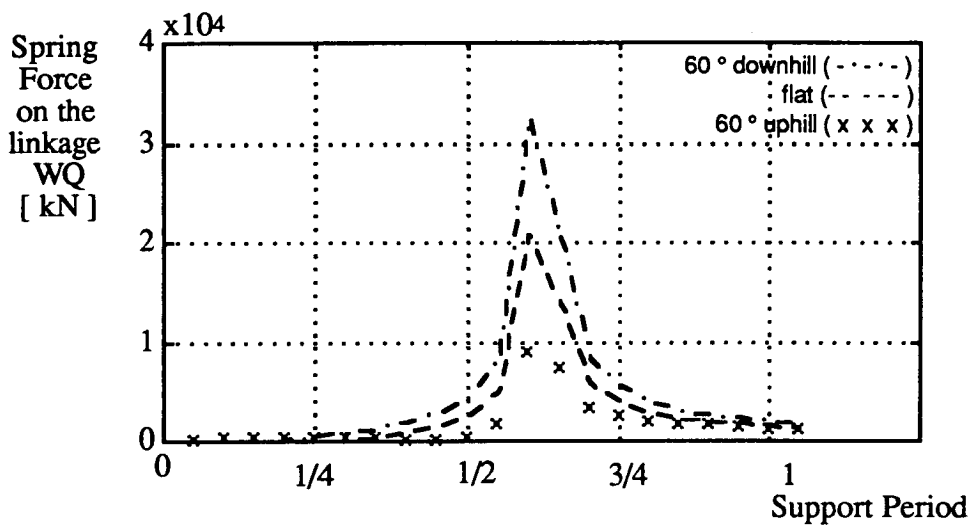


Figure 6.10 Variation of spring force on the linkage WQ during support period for three different terrains.

Chapter 7

Proposed Mechanical Design for a Legged Vehicle with the Buraq Legs

Contents

7.1 Introduction

7.2 Setting the Terrain and the Performance Characteristics

7.3 A Mechanical Design Proposal

7.3.1 Leg Mechanism

7.3.2 Vehicle Body

7.3.3 Steering

7.3.4 Brake and Suspension Systems

7.3.5 Foot Design

7.4 Power Transmission

7.4.1 Longitudinal Drive

7.4.2 Vertical Drive

7.4.3 Steering

7.5 Conclusions

7.1 Introduction

In this chapter a hybrid type legged vehicle with the Buraq leg mechanisms is examined. The design parameters are specified for a case study. Some proposals are presented for the mechanical design of the legged vehicle. The study is not only expected to set a foundation for a real vehicle to be built in the future, but also serves as a medium to examine the feasibility of a legged vehicle with the Buraq legs.

7.2 Setting the Terrain and the Performance Characteristics

As it was mentioned in the first chapter, the motivation behind this thesis is to design a legged vehicle with competent performance to be used instead of traditional off-road vehicles due to the harm that they cause to the environment. Keeping this basic principle in mind, the legged vehicle proposal for off-road transportation represents the off-road vehicle with the best performance. Since a competitive legged vehicle is aimed to be designed, the obstacle crossing characteristics of a battle tank, and the ground traverse and performance characteristics of a motor cycle are taken as desired design parameters which are described as follows (The data is reproduced from (Bryson 1988) and (Larminie 1988));

Desired parameters for obstacle crossing:

Minimum ground clearance: 480 mm

Maximum height : 3 m

Fording depth: 1.5 m

Length to breadth ratio (limits) : [1.2 - 1.8]

Stability tilt angle : 40 degrees

Desired parameters for ground traversing:

Mean Maximum Ground Pressure < 140 kPa

Ground pressure is the ratio of weight to the area of the track in contact with the ground. The motion of a wheeled or a tracked vehicle depends on

the friction force that treads or palettes provide. Whereas a legged vehicle moves by pushing its foot against the ground. According to the characteristics of the ground, a legged vehicle can adjust the reaction forces on its feet according to the necessary ground pressure unlike a wheeled or a tracked vehicle.

Desired parameters for performance:

Power to weight ratio: 22.5 kW/t (approx. 2.25×10^8 W/N)

Turning circle: Pivot turn

Speed: 12.5 m/s

Gearbox: 30:1 - 4:1

Brake: Able to stop on a 60 degree slope

Suspension period: Bounce, min: 0.75 s.

Pitch, min : 1.5 s.

Damping < Critical

Available bump deflection from static, minimum : 210 mm

7.3 A Mechanical Design Proposal

In table 7.1 the performance (P.C.) and the terrain (T.C.) characteristics affecting the mechanical design process are shown. As it can be seen from the figure, the crucial part of mechanical design is the leg design. The leg should be designed by taking into account both terrain and performance characteristics unlike other steps of the mechanical design. The leg design is also affected by the number of legs from the strength point of view. The rest of the mechanical design, in sequence namely, vehicle body, steering, brakes, suspensions and foot can be designed according to required characteristics.

7.3.1 Leg Mechanism

The primary constraints on the leg structure are terrain characteristics. Maximum height of the vehicle has been specified as 3 m. in section 7.2.

There are a few methods to proceed from this point;

1- the leg mechanism can be designed as high as 3 m. and the rest of the vehicle can be placed in between leg pairs.

2- the leg mechanism can be designed as small as possible, so that the vehicle body can be placed over the leg mechanism, the same as in a car, where the body is over the wheels.

3- the leg mechanism can be designed with an intermediate height. Part of the vehicle body can then be accommodated in between leg pairs, and the remainder over the legs.

The third way is followed in this study.

The Buraq leg mechanism is drawn in figure 7.1. Wooden model dimensions (WM) and non-dimensional figures are both shown for linkages, as well as along x and y axes. Non-dimensional figures are produced by dividing all dimensions to the crank length (R_2) which is 32 mm. according to the built wooden model.

By calculation of the crank length under prescribed constraints, the dimensions of the rest of the mechanism can be calculated.

The leg mechanism is designed to have an intermediate height. The overall height of the leg is set to be less than 2 m. As shown in figure 7.1, the leg height is represented in the table about the distances along y axis; "PW" which is also equal to $9.71 R_2$ refers to the leg height. Hence, the following inequality can be written;

$$\begin{aligned} Y_{PW} &< 2 \text{ m} \\ 9.71 R_2 &< 2 \text{ m} \\ R_2 &< 0.206 \text{ m} \end{aligned}$$

R_2 is chosen as 0.2 m. Since R_2 is known, the rest of the leg dimensions can be found using non-dimensional figures from the tables in figure 7.1.

$$\text{Leg stroke length } (P_{\min}P_{\max}) = 10.19 R_2 = 2.038 \text{ m}$$

7.3.2 Vehicle Body

To find the body dimensions, the following constraints should be taken into account;

-Avoid the leg trajectories intersecting at any point

-Lower body (the part of the body which takes place between legs) should allow the leg to rotate for steering. Maximum steering angle should ensure pivot turn capability.

-Body form should have its centre of gravity on the longitudinal symmetry axis to ensure balance

The leg unit is connected to the vehicle along the vertical axis that pass through the drive shaft which also goes through point S in figure 7.1. The foot reaching length about point S is not symmetrical as can be seen by comparing to $P_{min}S$ to SP_{max} along x axis in the figure. SP_{max} is more than 1.5 times greater comparing to $P_{min}S$.

A star form is proposed for the body. This has its centre of gravity in the centre of the star while all legs are on the ground. The body and its dimensions are shown in figure 7.2. Parameter μ is used to ease the design process. μ represents the side length of the equilateral triangle used to form the vehicle body. For a pivot turn with a star form body, the front and rear legs require 60 degrees turning capability (see figures 7.3 and 7.4).

To be able to come up with the shortest vehicle body, the leg placement on the vehicle is done as shown in figure 7.5 (see also photograph 7.1). The difference between $P_{min}S$ and SP_{max} is exaggerated in the figure. As the figure shows, this set of leg orientations avoids the feet interferences during steering. If the leg orientations were all the same, the vehicle body would need to be bigger.

Using the guidelines set above, and using figure 7.1, following equation can be written;

$$\begin{aligned}x : \quad SP_{min} &< \mu / 3 \\ &4.07 R_2 < \mu / 3 \\ &2.442 \text{ m} < \mu\end{aligned}$$

When $\mu = 2.5$ m, the body dimensions can be expressed as follows:

Length = 3.333 m.

Width = 2.887 m.

Height = 3.000 m.

Turning circle = Pivot turn

Leg swing angle = $\pm 60^\circ$

Full reaching length = $\mu + 12.26 r_2 = 4.952$ m.

Full reaching length refers to the distance between the front and the rear feet when they are stretched away from the body.

7.3.3 Steering

It was already dealt with the change of foot stroke for steering purposes in chapter 5. In this section, variation of the motion axis of the legs relative to the body is studied. Some steering mechanisms of off-road vehicles have been investigated widely by Dudzinski (1983,1986 and 1989). In this section a new mechanism is proposed. The proposed mechanism can be used for any type of multi-legged vehicle as long as leg placements on the vehicle body allows the mechanism to operate as it is described below.

The mechanism involves a single linear drive actuator. The top view of the mechanism is shown in figure 7.6. The front and back are marked in the figure. The mechanism is symmetric according to y axis at all times. The leg units which are connected to the vehicle body from their centre are represented simply by a line which is $2b$ unit long.

In case of a quadruped application, the leg positions are clear. In case of a hexapod application the middle pair legs are placed along the y axis, in the middle of the vehicle. Middle legs are not rotated relative to the body assuming that they are always in the centre of the vehicle trajectory. However, during steering the foot stroke change applies to all legs, front, middle and back pairs.

The drive shaft and supports have to be placed all in the same line where the leg unit is connected to the vehicle body, so that a rotation can take

place (see photograph 7.1). The front and back leg unit pairs are connected by two linkages which are also joined to the actuated point in their centre point. The length of each linkage is $2a$.

Movement of the leg units relative to the vehicle body is achieved by positive or negative displacement of the actuated point along y axis. Due to mechanical constraint the actuated point cannot move along x axis. A positive displacement along y axis results in a right turn, and a negative displacement along y results in a left turn.

Using the mechanical constraint of the mechanism, the minimum value of arc radius that the vehicle can travel through (R_{min}) can be calculated to predict the manoeuvrability of the mechanism (see appendix 4 for further detail);

$$R_{min} = \frac{a \cos \Omega_o + b}{\sin \varphi_M}$$

where

$$\varphi_M = \cos^{-1} \left[\frac{a \cos \Omega_o + b}{a + b} \right]$$

a and b are linkage lengths, and Ω_o is the angular value measured while the vehicle travels along a straight line trajectory. φ_M is the maximum value of angle φ . Note that when non-dimensional a and b values are used, φ_M is found to be greater than 60° which satisfies pivot turn condition (refer back to section 7.3.2).

A more elaborate steering mechanism can be designed as shown in figure 7.7. Steering arrangements are added for different modes of operation. The steering mechanism working according to the *basic operation mode* is explained above. During basic operation mode, all four points (A,B,C and D) are driven by a single actuator. Through this mode, pivot turn can be achieved around the left or right middle leg as shown in figure 7.4.

Two more operation modes are added to the mechanism provided that all four points can be driven independently as shown in figure 7.7.

Through this proposed drive mechanism, during *sharp action mode*, front and rear leg units can be driven separately to change position suddenly.

Also, *pivot turn* around the centre can be achieved if points A and B and points C and D can be driven in pairs as shown in the figure which also can be referred to figure 7.3.

7.3.4 Brake and Suspension Systems

To ease the production and the maintenance, a standard car brake mechanism is proposed as seen in figure 7.8. A disc with a pair of shoes is fitted on each drive shaft. A hydraulic system consisting of a servo, a master cylinder and a pressure control valve provide all three pairs of shoes.

For the suspension of the vehicle, a similar approach followed. A typical spring damper pair is fitted to each leg unit as shown in figure 7.9.

7.3.5 Foot Design

To have a high performance of ground traversing, the mean maximum pressure (MMP) of the vehicle should be not more than 140 kpa on any terrain (see section 7.2). For a legged vehicle MMP value should be defined. Hence for a leg it can be written as follows;

$$\text{MMP} = \frac{\text{Ground Reaction Force}}{\text{Area of Contact}}$$

Ground reaction force for a leg was calculated as 3270 N while walking for the speeds up to 2.5 m/s. Hence area of contact for the foot of a legged vehicle can be expressed as follows;

$$\text{Area of contact} > \frac{3270 \text{ N}}{140 \text{ kPa}} = 233.57 \text{ cm}^2$$

Assuming a square foot form and complete contact between the foot and the ground, foot dimensions can be chosen as 16 x 16 (256) cm². It should be realised that this foot area has been calculated for walking speeds. Therefore, foot area for running speeds is required to be bigger to have the same MMP value. The side of the square foot needs to be at least

twice longer for running speeds.

A sketch of the proposed foot design is shown in figure 7.10. The foot is equipped with a pair of microswitches to sense the foot contact. A piston head keeps pressing on the microswitches through the spring force under no-load conditions. When load is applied on the foot the spring is compressed, and microswitches are released. Two microswitches are used in case one fails to operate. The bellows and the cylinder cover are to protect the switch mechanism from the environment. The spring and the bellows also serves as a padding surface along rubber sole especially during high landing impulses. In similar way, various designs and sense mechanisms for the foot can be developed.

7.4 Power Transmission

The main power source of the vehicle is a 35 kW engine. The engine supplies a battery and the main drive shaft similar to a car example. A sketch of the power circuit is shown in figure 7.11. As the figure shows, the engine feeds the battery and its shaft is connected to the gear box. The gear box provides the pump and the main drive shaft. While pump actuates the vertical drives of the leg mechanisms, the power is further distributed to the front and the rear shafts so that the cranks can be actuated. The battery provides for the main steering motor in addition to high torque speed reducers which are mounted on variable crank mechanisms in each leg unit.

In the following sections, more detailed description of the power transmission is given.

7.4.1 Longitudinal Drive

A sketch of the power transmission for longitudinal drive is shown in figure 7.12. For longitudinal drives variable crank mechanisms are used. The power, transmitted to the main drive shaft from the engine via the gear box, is further transmitted to the front and the rear shafts through chain drives. From each drive shaft, the power is further transmitted to 3 pairs of

variable crank mechanisms through universal joints.

7.4.2 Vertical Drive

A sketch of the power transmission for vertical drive is shown in figure 7.13. The power, transmitted to the pump from the engine via the gear box, is further transmitted to six pairs of valves. Each valve pair is situated by the leg it drives, so that minimum flow losses can be achieved. Each pair consists of a three-way valve and a check valve. Check valves are used to minimise the hydraulic energy losses during support period as mentioned in section 4.3.4.

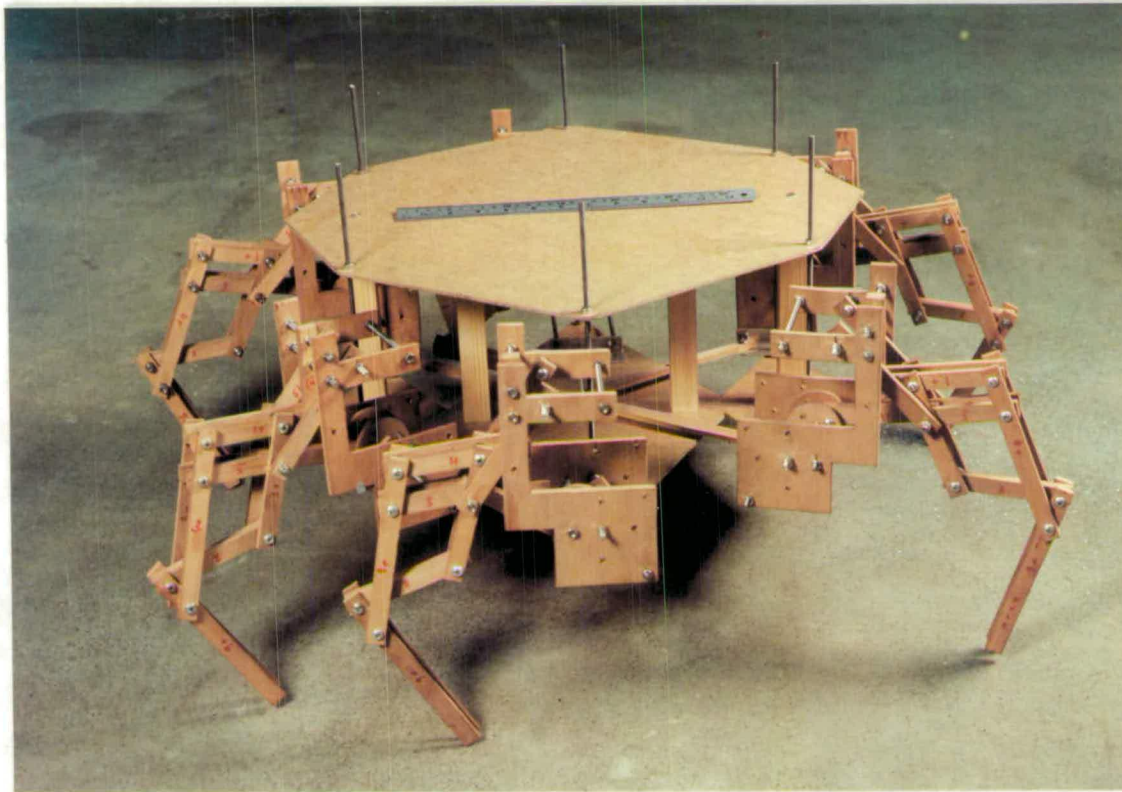
7.4.3 Steering

A sketch of the power transmission for steering is shown in figure 7.14. The power transmitted to the battery from the engine is further transmitted to the main steering motor and the six high torque speed reducers each mounted on variable crank mechanisms in leg units. The transmission of electrical energy from the leg unit to the rotating crank is carried out by using brushes and slip-rings as shown in the figure.

7.5 Conclusions

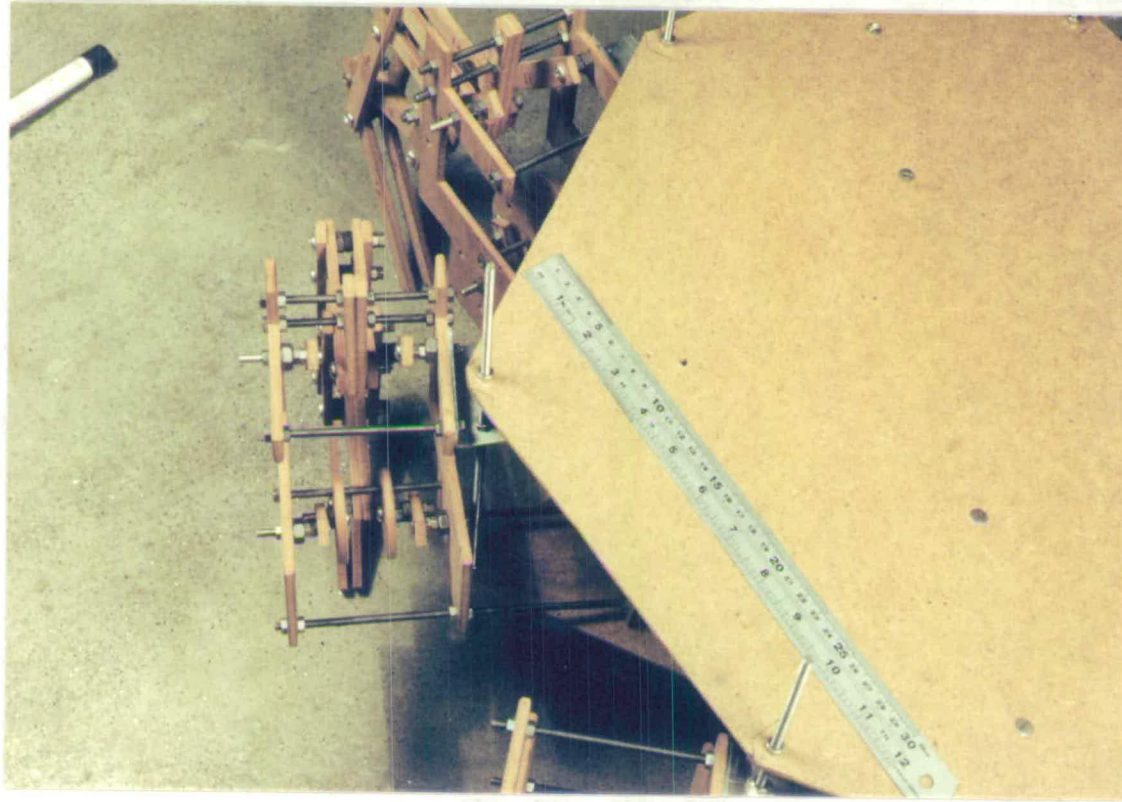
The studies conducted in this chapter have helped to examine the mechanisms designed throughout this research. Also additional questions such as steering and power transmission are answered relating to a legged vehicle with Buraq legs. According to the conducted study in this chapter, a wooden prototype legged vehicle is built which consists of a body and six legs (see photograph 7.1). Also a simplified wooden model of the leg driven by the variable crank mechanism is shown in photograph 7.2.

Surely, there needs to be further study in the area to design a real legged vehicle. However, the study has served to give a rough idea about what the real vehicle should look like.



Front ←----- Back

Photograph 7.1 A wooden model of the legged vehicle
-while a 30 cm. ruler is placed on- to give an idea about its size
which is about 1/8 of the proposed vehicle in this chapter.



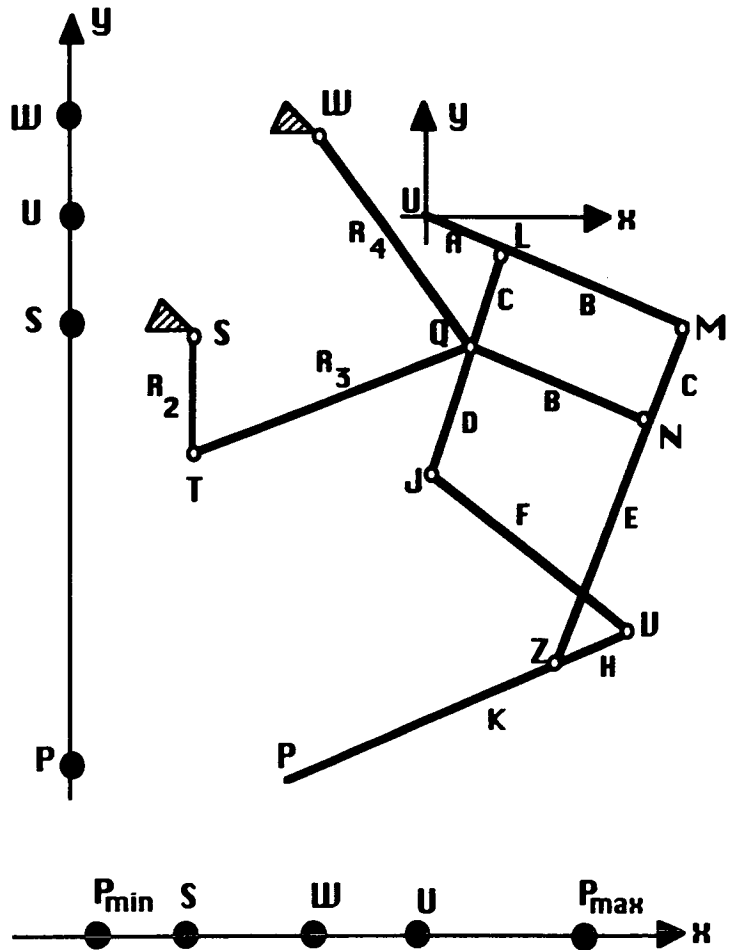
Photograph 7.2 The detail of the variable crank mechanism driving the leg in the wooden model leg unit built with completely symmetric linkages with respect to the leg vertical axis.

Steps in Mechanical Design	Constraints	Type of Constraint
Leg and Body Design	Ground Clearance, fording depth, length to breadth, stability tilt angle, available bump deflection	T.C
	Number of legs, Gait Structures	L.C
	Turning Circle	P.C
Engine, Actuators, Power Transmission	Speed, Power/Weight, Gearbox ratio	P.C
Foot Dimensions	Mean Maximum Pressure	T.C
Brake Design	Brake Requirements	P.C
Suspension Design	Suspension Requirements	P.C

Table 7.1 The performance characteristics (P.C.), the terrain characteristics (T.C.) and the locomotion characteristics (L.C.) affecting the mechanical design process

	WM	ND
A	32	1
B	65	2.03
C	32	1
D	64	2
E	112	3.5
F	86	2.69
H	25	0.78
K	133	4.16
R ₂	32	1
R ₃	80.2	2.51
R ₄	103	3.22

Linkage Dimensions



x	WM	ND
P P _{min} P _{max}	326.3	10.19
P _{min} S	130.22	4.07
S P _{max}	196.08	6.13
S U	64.68	2.02
U P _{max}	131.4	4.11
S W	38.26	1.19
W U	26.4	0.83

Distances along x axis

y	WM	ND
S W	105.18	3.29
P S	205.52	6.42
S U	57.48	1.79
U W	47.7	1.49
P U	263	8.22
P W	310.7	9.71

Distances along y axis

Figure 7.1 The Buraq Leg Mechanism with the crank-rocker
WM refers to the dimensions of the wooden model leg in mm.
ND column refers to non-dimensional figures produced by dividing
WM dimensions to the crank length which is 32mm.

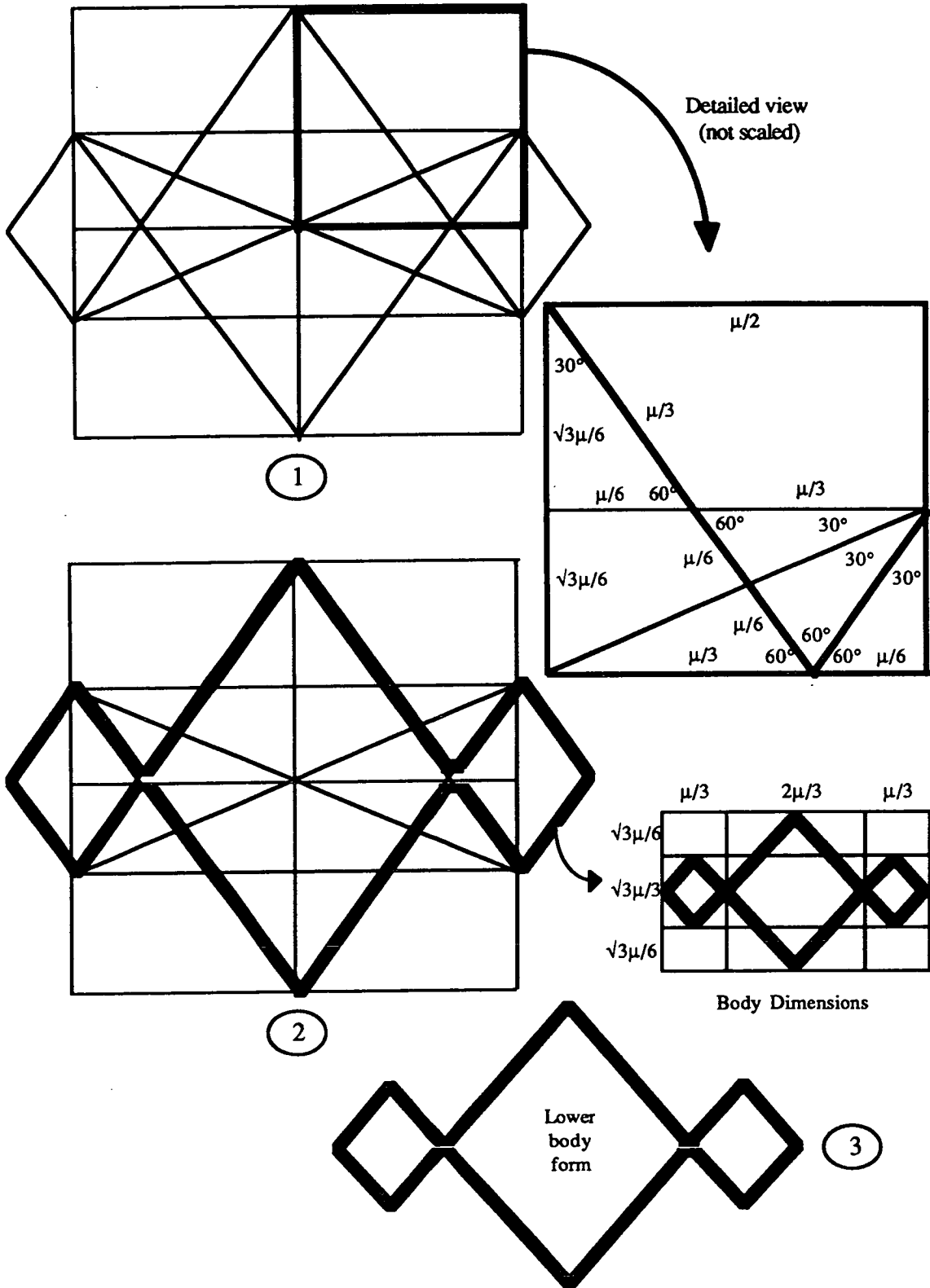


Figure 7.2 Steps in the lower body design

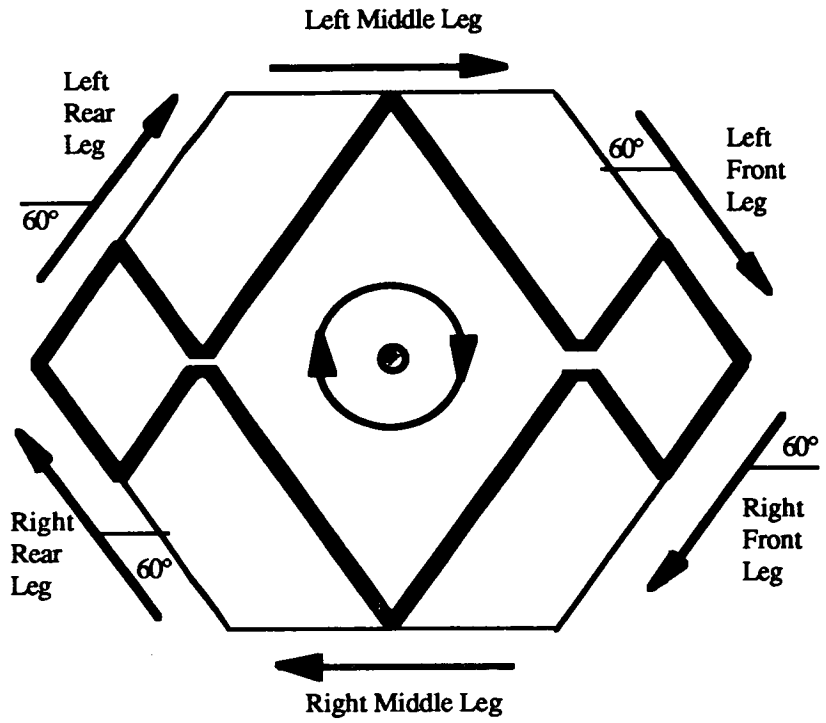


Figure 7.3 Pivot turn around the center towards right

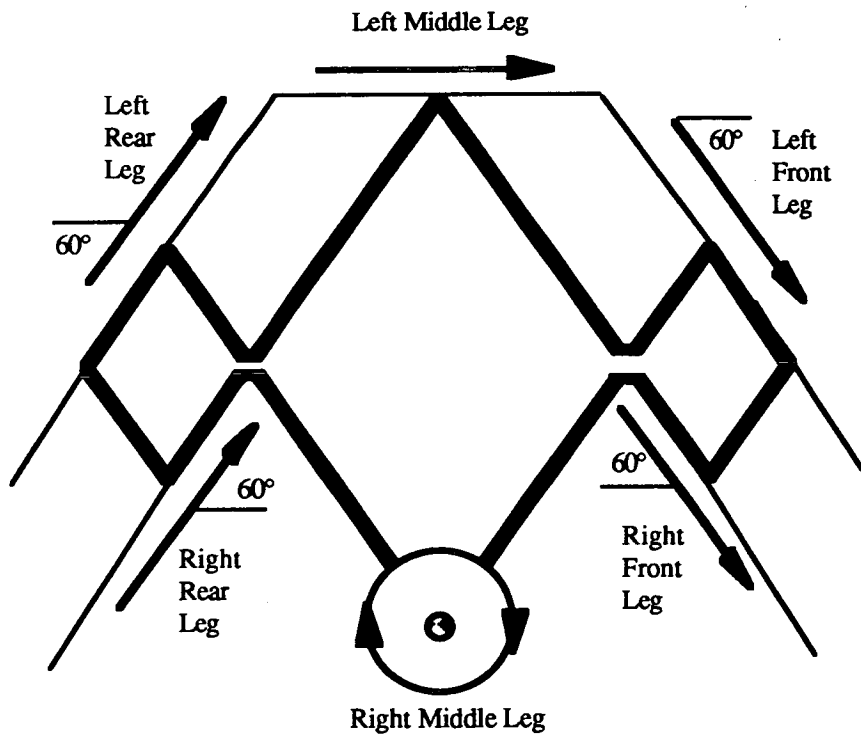
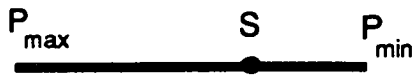


Figure 7.4 Pivot turn around right middle leg towards right



Leg reaching length with respect to the point S

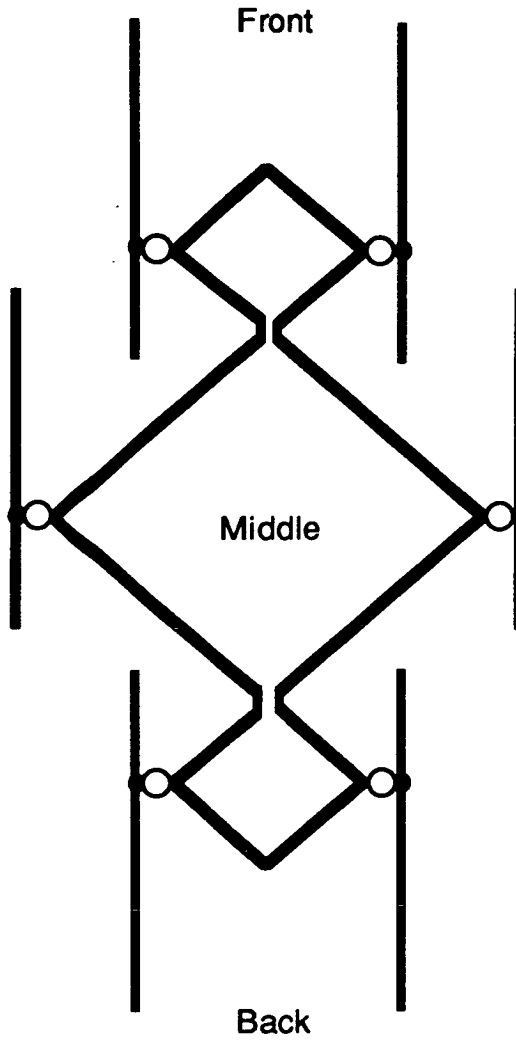


Figure 7.5 Leg placements according to the vehicle orientation

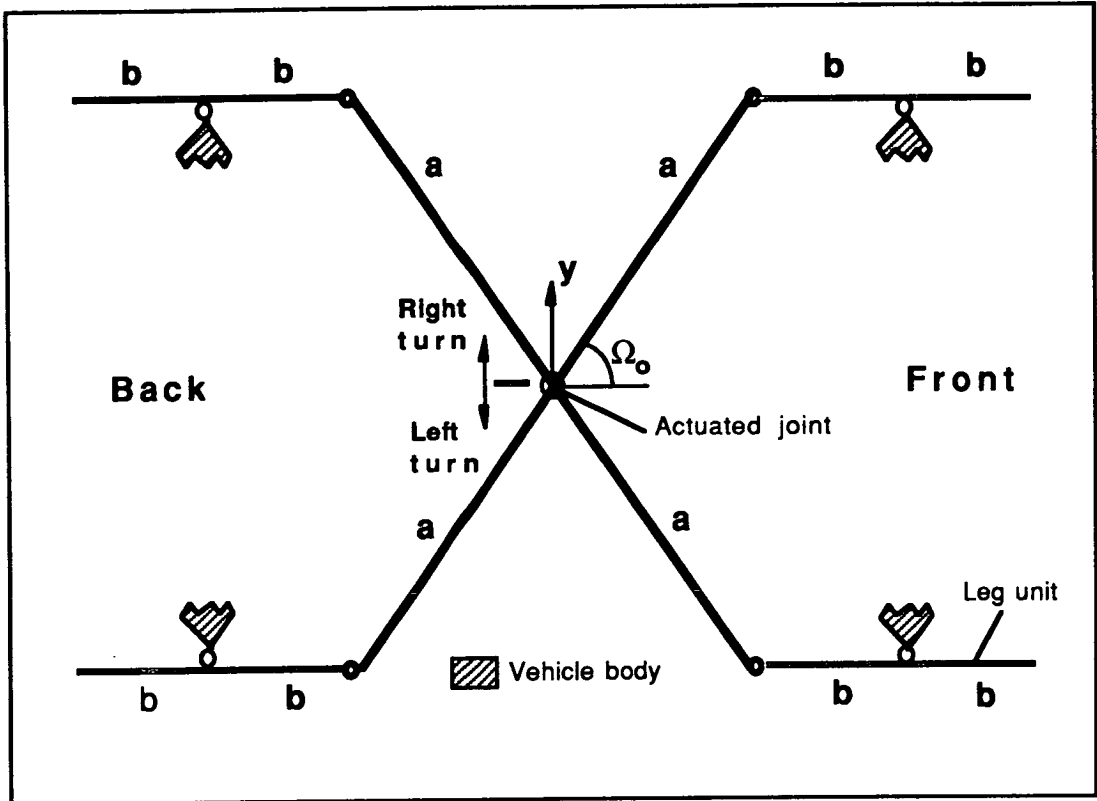
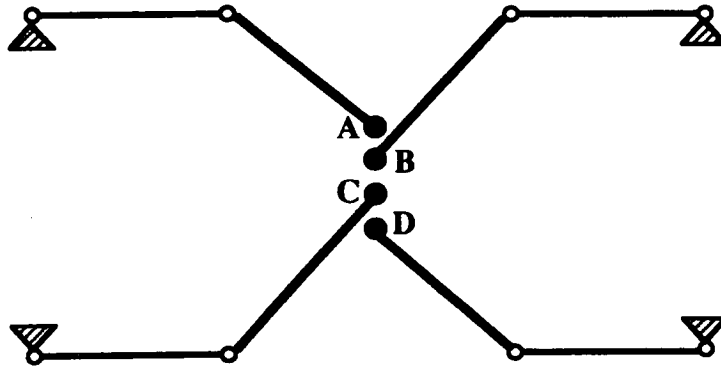
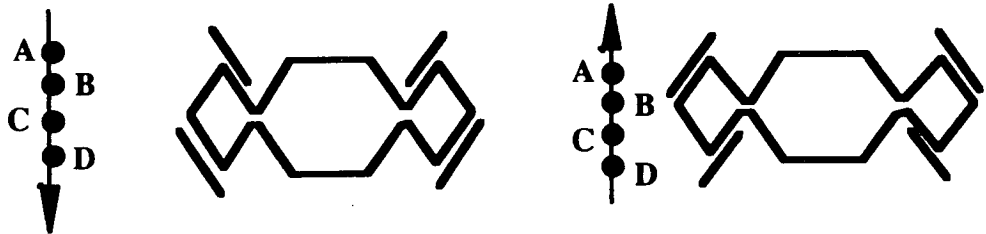


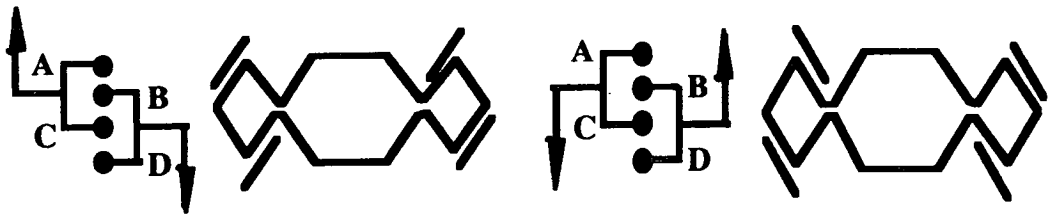
Figure 7.6 Steering Mechanism



Sketch of the Steering Mechanism



Basic Operation Mode



Sharp Action Mode

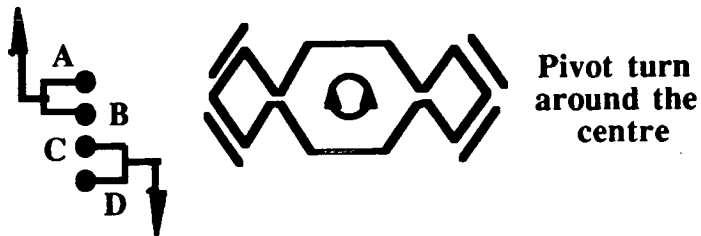


Figure 7.7 Steering modes

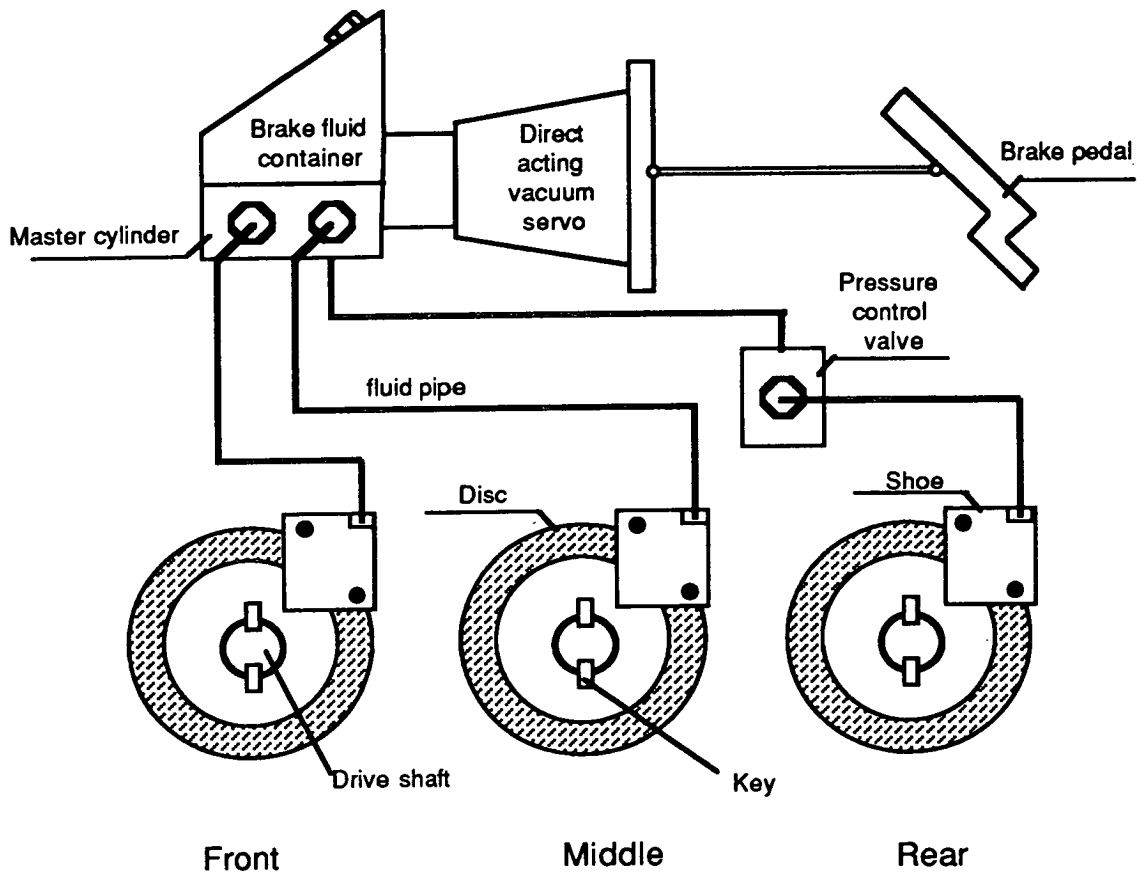


Figure 7.8 Brake system of the vehicle

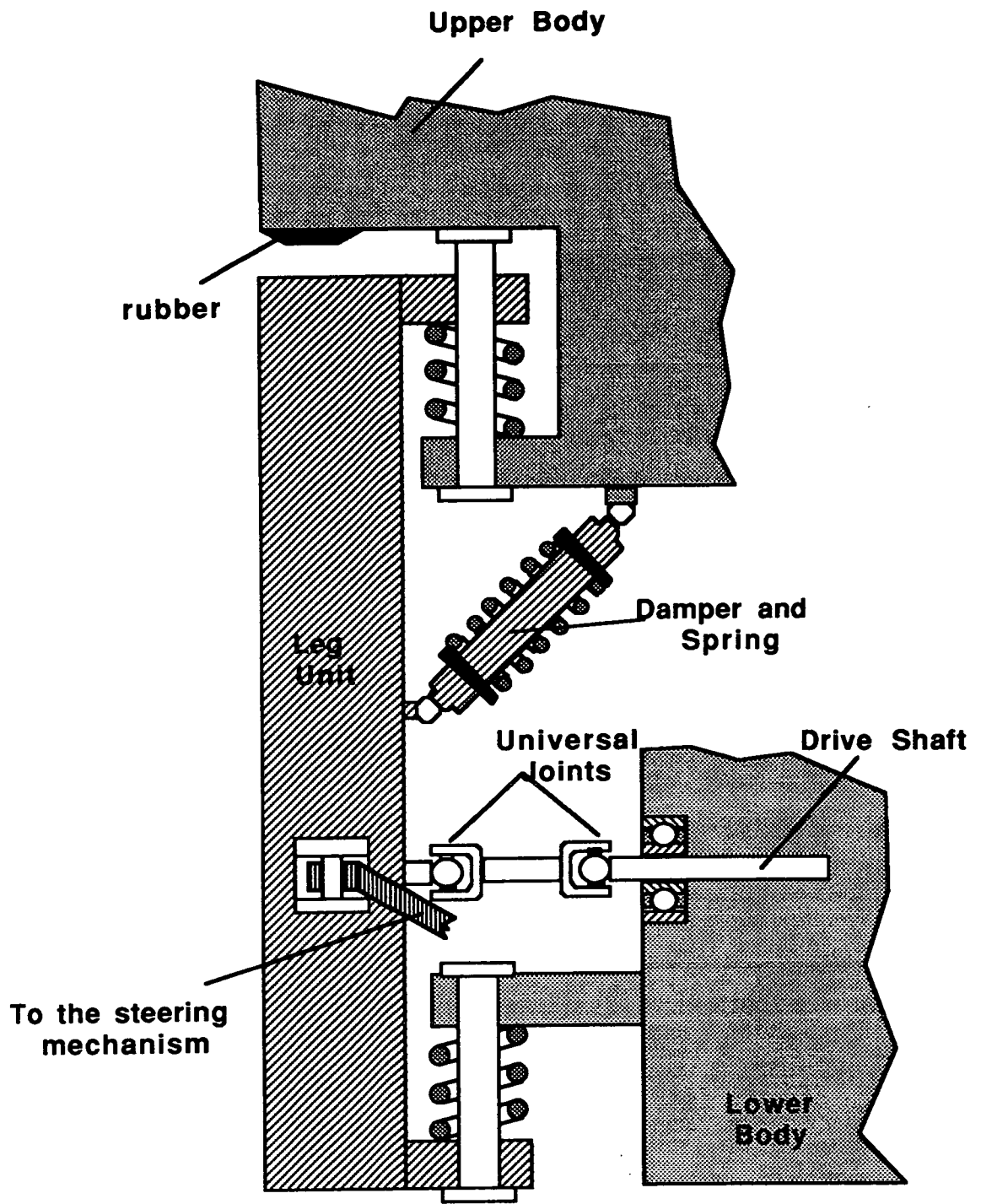


Figure 7.9 The suspension system

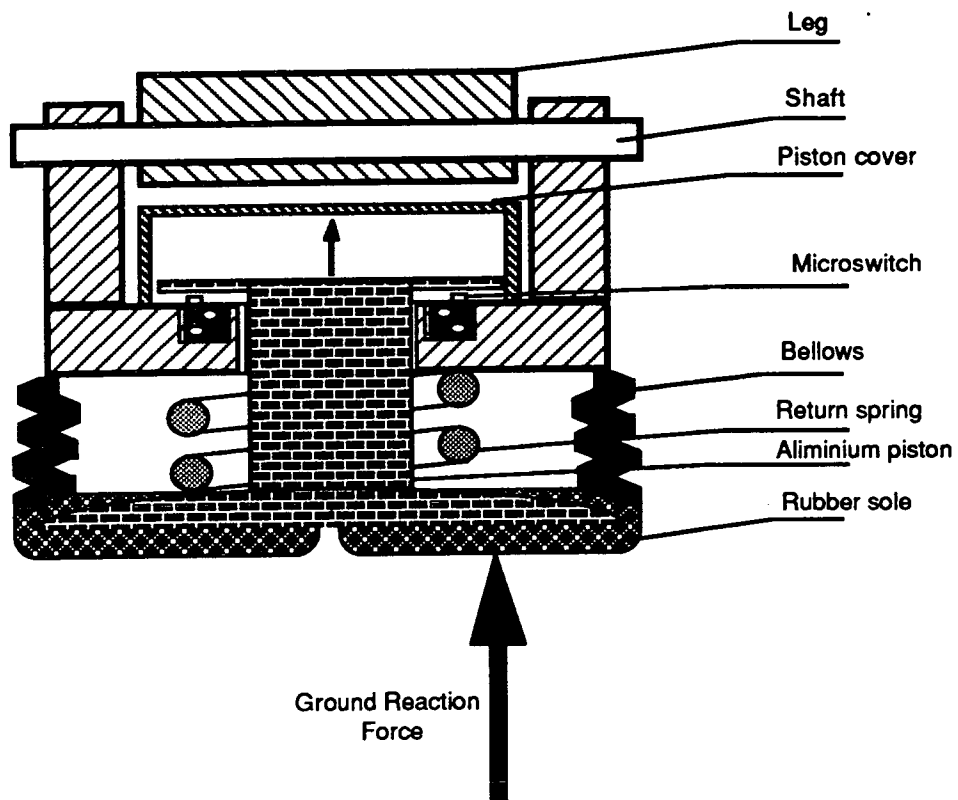


Figure 7.10 Unscaled representation of the foot cross-section under load.

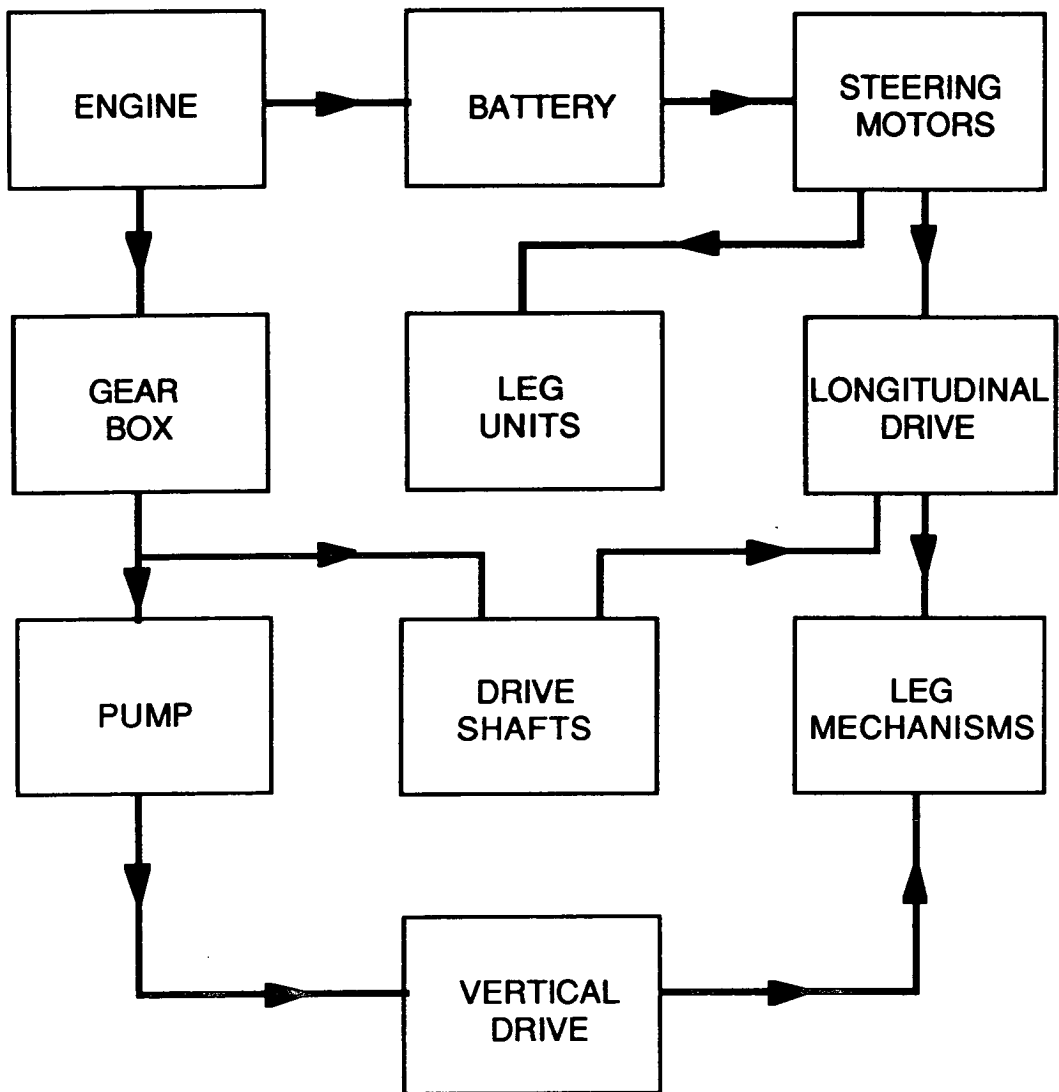


Figure 7.11 Power Flow in the Legged Vehicle

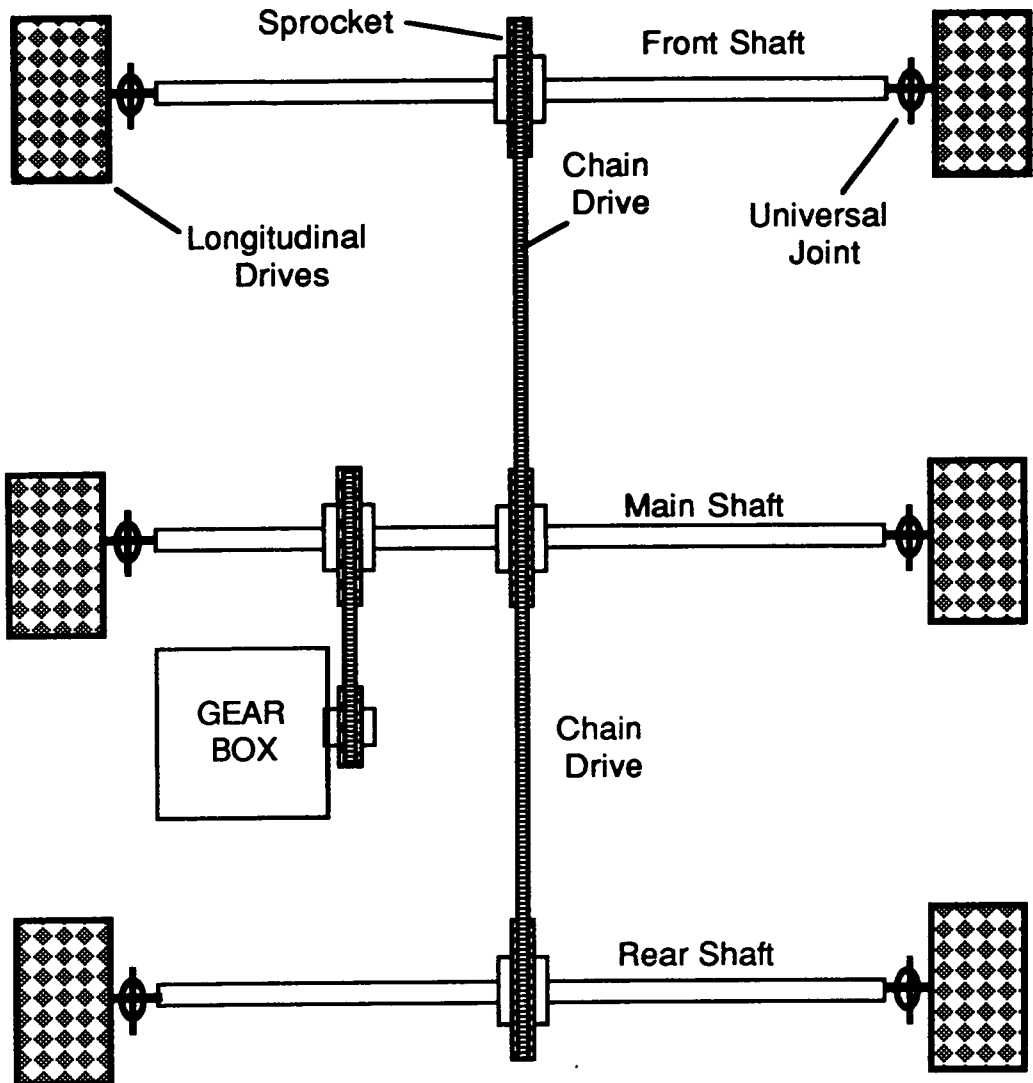


Figure 7.12 A symbolical representation of the mechanical power transmission for longitudinal drives (tension sprockets are not shown).

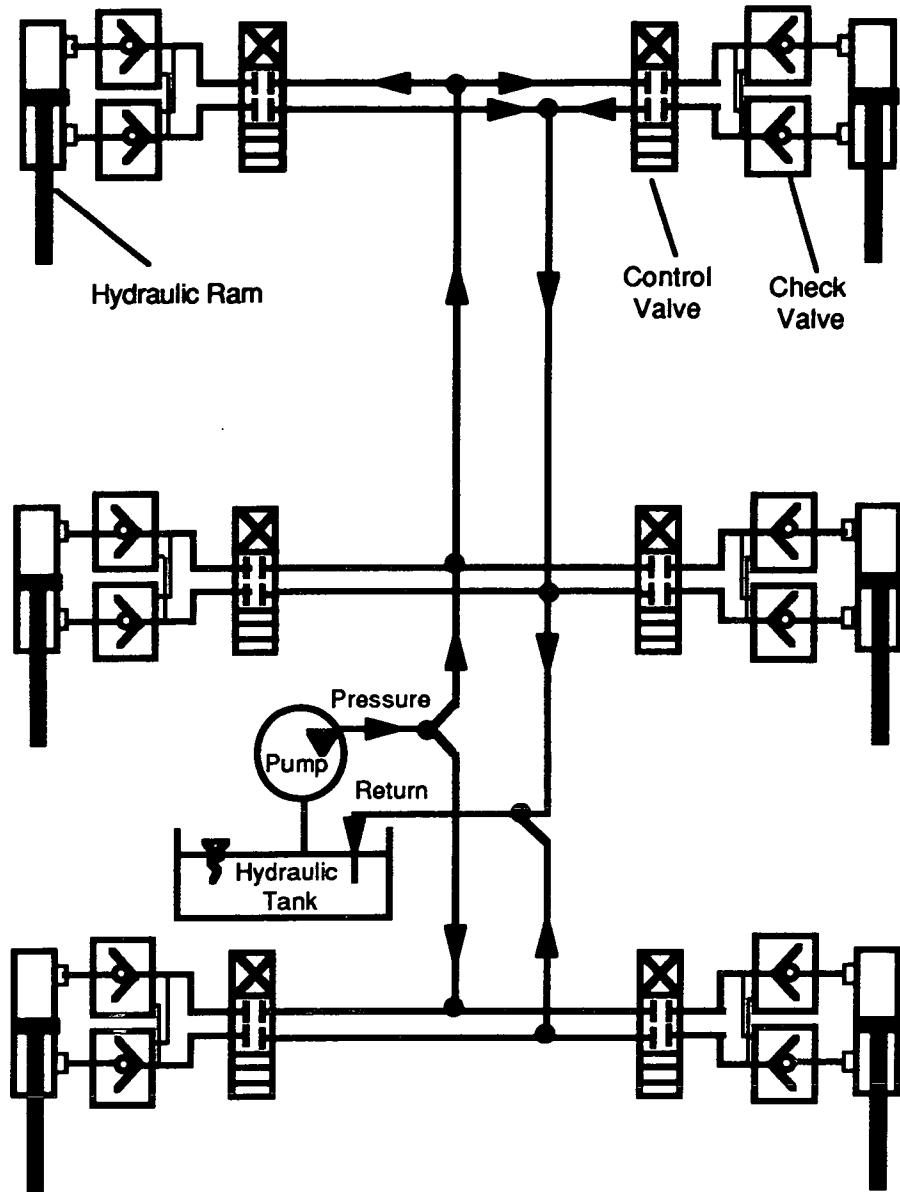


Figure 7.13 A symbolic representaton of the hydraulic power flow

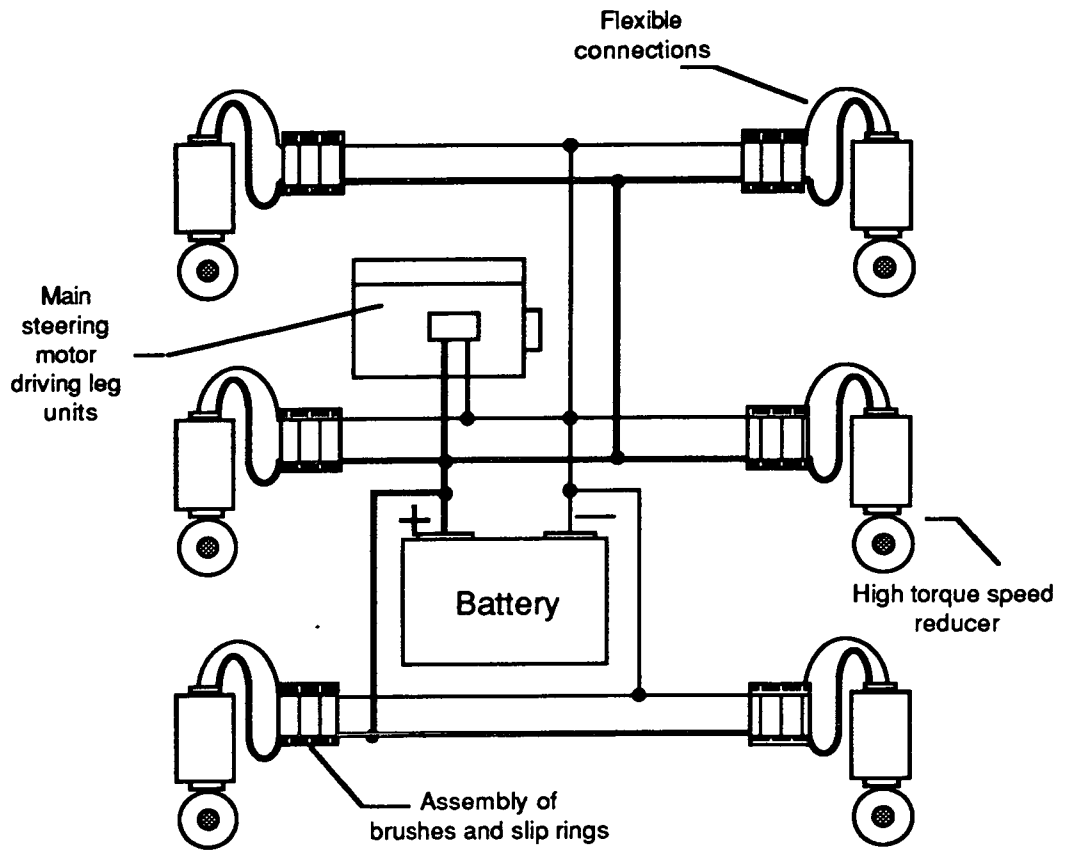


Figure 7.14 A sketch of the power transmission for steering; High torque speed reducers are used to activate the cranks in variable crank mechanisms. The main steering motor is used to drive the leg units as proposed in figure 7.7 according to the basic operation mode.

Chapter 8

A Summary and Evaluation of the Overall Research

Contents

8.1 Introduction

8.2 A Summary and Evaluation of the Overall Research

8.2.1 Design of the New Leg Mechanism

8.2.2 Choice of the Actuation Method

8.2.3 The Leg Unit Consisting of the Buraq Leg and Actuators

8.2.4 The Legged Vehicle with Prescribed Leg Units

8.2.5 Future Study

8.1 Introduction

In this chapter, the overall work carried out through out the thesis is evaluated according to the set objectives in section 1.6. These objectives includes designing a leg mechanism, developing an actuation strategy, studying the means for elastic energy storage and mechanical design of a legged vehicle.

Looking through the chapter headings from chapter 2 up to chapter 7, all the topics included among objectives are dealt with. Since each chapter contains a conclusion set at the end, some comments relating to the objectives are already covered. However, the aim in this chapter is to give a complete picture of the research described in the thesis, so that its evaluation can be carried out to see to what extend the set objectives are achieved.

8.2 A Summary and Evaluation of the Overall Research

The whole thesis is devoted to showing the availability of a new leg mechanism for a high speed leg locomotion to be used in obstacle free terrain. The research study can be examined around this point under the following sub-titles;

- 1- Design of the New Leg Mechanism
- 2- Choice of the Actuation Method
- 3- The Leg Unit Consisting of the Buraq Leg and Actuators
- 4- The Legged Vehicle with Prescribed Leg Units
- 5- Future Study

Each topic can be explained as follows;

8.2.1 Design of the New Leg Mechanism

The new leg mechanism, Buraq, has the following characteristics;

- a. It has a long horizontal stroke compared to its height which is a positive attribute for a leg mechanism to be used for high speed legged locomotion.

- b. It has no sliding joints in its structure which makes it reliable and easy to design.
- c. It can be actuated by various means; the linkage dimensions can be adjusted to allow either linear or rotary actuators.
- d. The experimental study has shown that the leg mechanism is structurally sound, and able to handle loads in the vertical direction.
- e. The magnification ratio between the foot and the actuated joints is quite high (max: 13/1) which makes the mechanism quite a compact one.
- f. The leg mechanism can be used as either an insect type or a mammal type leg due to its geometric characteristics.

8.2.2 Choice of the Actuation Method

- a. Due to the dynamic superiority of mechanical actuation, the leg can achieve high speeds without requiring huge hydraulic circuits which avoids considerable hydraulic energy conversion losses.
- b. Despite mechanical actuation, varying the foot stroke, steering and gait shift are possible by using the variable crank mechanism.
- c. In the vertical direction the use of a hydraulic cylinder enables the terrain adaptability and load handling, while in the longitudinal direction the use of a mechanical crank-rocker provides dynamic superiority, reliability and ease in control.
- d. The compactness of the leg mechanism minimises the hydraulic energy conversion losses since the transferred amount of fluid in the hydraulic circuit becomes less.

8.2.3 The Leg Unit Consisting of the Buraq Leg and Actuators

- a. The leg mechanism and its particular actuation method have been specifically chosen for an obstacle free terrain and high speed legged locomotion.
- b. A detailed comparison of the Buraq leg and a pantograph leg (see section 2.7) has shown that the Buraq leg fits better for high speed legged

locomotion despite its disadvantages.

c. The number of sliding joints is minimised through the usage of a crank-rocker mechanism in longitudinal direction.

d. The leg mechanism has an approximate straight line foot trajectory during the support period, and has a ballistic foot trajectory during the transfer period.

e. Compared to other artificial legged systems, experimentally a smaller specific resistance value has been found for the Buraq leg with the way it is actuated which means a higher performance.

8.2.4 The Legged Vehicle with Prescribed Leg Units

a. By carrying out a design study of a legged vehicle with the Buraq legs, the possibility of such an application for high speed legged locomotion has shown to be feasible.

b. A gait shift strategy during locomotion is introduced using a variable crank mechanism driving Buraq legs.

c. A steering strategy with three different modes including pivot turn capability is introduced using Buraq legs.

d. For running applications, in addition to existing quadruped running gaits, hexapod and octopod running gaits are introduced to ease the stability problem at walking speeds.

e. For efficient running, compliance is introduced to the Buraq leg mechanism, and a feasibility study of the Buraq leg with proposed compliance method has given a positive result.

f. A strong similarity has been revealed through kinematical analysis of the Buraq leg mechanism between the speed profiles of the foot driven by a crank-rocker and the mass of a basic mass-spring model. This is another positive point which makes the Buraq leg mechanism favourable for elastic energy storage.

g. The vehicle with Buraq legs looks promising for both low and high speed applications for an obstacle free terrain. This is mainly because the

vehicle inherits the energy saving mechanisms which are used at low as well as at high speeds. At low speeds, an approximate straight line foot trajectory, avoidance of geometric work through driving legs across more than one joint and hence a low specific resistance value are energy savers. At high speeds, avoidance of hydraulic actuation in the longitudinal direction, usage of dynamically superior crank mechanisms, long foot stroke and elastic energy storage characteristics are energy savers.

8.2.5 Future Study

The objectives set out at the beginning of the thesis in chapter 1 have all been discussed through out the thesis. While experimental studies have also been carried out for the designed leg mechanism, the rest of the research such as variable crank mechanism for gait shift and foot stroke variation, steering mechanism, elastic energy storage and mechanical design of the legged vehicle depends on the theoretical calculations and computer simulations. A wooden prototype model of the legged vehicle with variable crank mechanisms has been built enabling to visualise all the mechanisms. However, to be able to build a real legged vehicle, future work should be concentrated on experimental studies of what has been already explained theoretically in the thesis.

First, an experimental study of the variable crank mechanism should be carried out to further examine its characteristics. A prototype vehicle with a pair of parallel driven legs in front axis and a castor wheel in the centre of rear axis can be built to confirm the behaviour of the variable crank mechanism with the simulation study, while the balance problem is eliminated to ease the experimental procedure.

Then, a multi-legged vehicle can be built, and various gaits can be adopted as prescribed in chapter 5.

A leg mechanism with elastic energy storage elements can be built and tested with the legged vehicle as proposed in chapters 6 and 7.

The question of timing to change gaits with respect to the speed can be

answered by various trials of gait shifts during locomotion at different speeds while energy consumption is recorded for further evaluation.

Finally, having completed all the steps satisfactorily, a real legged vehicle can be designed and built.

References

(in alphabetical order)

- Abele, G. et al 1984. "Long Term Effects of Off-road Vehicle Traffic on Tundra Terrain," *Journal of Terramechanics*, vol.21, no.3, pp.283-294.
- Ackland, T.R. et al 1988. "Inertial Characteristics of Adolescent Male Body Segments," *Journal of Biomechanics*, vol.21, no.4, pp.319-327.
- Alexander, R.McN. 1980. "Optimum walking techniques for quadrupeds and bipeds," vol.192, pp.97-117, London.
- Alexander, R.McN. 1982. "The role of tendon elasticity in the locomotion of the camel(*Camelus dromedarius*)," *Journal of Zoology*, vol.198, pp.293-313, London.
- Alexander, R.McN. 1984(a). "The gaits of bipedal and quadrupedal animals," *The International Journal of Robotics*, vol.3, no.2, pp.49-59, MIT.
- Alexander, R.McN. 1984(b). "Elastic energy stores in running vertebrates," *American Zoology*, vol.24, pp.85-94.
- Alexander, R.McN. 1988. "Elastic Mechanisms in animal movement," Cambridge Univ. Press, Great Britain.
- Alexander, R.McN. 1989. "Optimization and gaits in the locomotion of vertebrates," *Physiology Reviews*, vol.69, no.4, pp.1199-1227.
- Alexander, R.McN. 1990. "Three uses for springs in legged locomotion," *The International Journal of Robotics Research*, vol.9, no.2, pp.53-61, MIT.
- Alexander, R.McN. and Goldspink, G. 1977. "Mechanics and energetics of animal locomotion", Chapman and Hall, London.
- Alexander, R.McN. and Jayes, A.S. 1978. "Vertical movements in walking and running," *Journal of Zoology*, vol.185, pp.27-40, London.
- Alexander, R.McN. and Jayes, A.S. 1980. "Fourier analysis of forces exerted in walking and running," *Journal of Biomechanics*, vol.13, pp.383-390, Pergamon Press Ltd, Great Britain.
- Alexander, R.McN. and Jayes, A.S. 1983. "A dynamic similarity hypothesis for the gaits of quadrupedal mammals," *Journal of Zoology*, vol.201, pp.135-152, London.
- Alexander, R.McN. and Vernon, A. 1975. "The mechanics of hopping by kangaroos (*Macropodidae*)," *Journal of Zoology*, vol.177, pp.265-303, London.

Alexander, R.McN. et al 1980. "Estimates of energy cost for quadrupedal running gaits," *Journal of Zoology*, vol.190, pp.155-192, London.

Alexander, R.McN. et al 1985. "Elastic structures in the back and their role in galloping in some mammals," *Journal of Zoology*, vol.207, pp.467-482, London.

Alexander R.McN. et al 1986. "Mechanical properties and function of the paw pads of some mammals," *Journal of Zoology*, vol.209, pp.405-419, London.

Angeles, J. and Bernier, A. 1987. "A general method of four-bar linkage mobility analysis," *Journal of Mechanisms, Transmissions, and Automation in Design*, vol.109, pp.197-203, June.

Angeles, J. and Callejas, M. 1984. "An algebraic formulation of Grashof's mobility criteria with application to linkage optimization using gradient-dependent methods," *Journal of Mechanisms, Transmissions, and Automation in Design*, vol.106, pp.327-332, September.

Ashman, R.B. and Rho, J.Y. 1988. "Elastic Modulus of Trabecular Bone Material," *Journal of Biomechanics*, vol.21, no.3, pp.177-181.

Baldwin, M.F. and Stoddard, Jr.D. 1973. "The Off-road Vehicle and Environmental Quality," *The Conservation Foundation*, pp.14-27, Washington D.C., U.S.A..

Bennett, M.D. 1987. "A possible energy-saving role for the major fascia of the thigh in running quadrupedal mammals," *Journal of Zoology*, vol.219, pp.221-230, London.

Bobbert, M.F. and Schenare, G. 1988. "Coordination in Vertical Jumping," *Journal of Biomechanics*, vol.21, no.3, pp.249-262.

Bobbert, M.F. et al 1991. "Calculation of Vertical Ground Reaction Force Estimates During Running From Positional Data," *Journal of Biomechanics*, vol.24, no.12, pp.1095-1105.

Bodner, A. 1989. "Adding flexibility to the links of a rigid-link dynamic model of an articulated robot," *Robotica*, vol.7, pp.165-168.

Braunack, M.V. 1986. "The Residual Effects of Tracked Vehicles on Soil Surface Properties," *Journal of Terramechanics*, vol.23, no.1, pp.37-50.

Brown, H.B. and Raibert, M.H. 1987. "Legs that Deform Elastically," Sym. Theory and Practice Robots and Manipulators 6th Cracow, Kogan Page Ltd, pp.436-443, London.

Bryant, J.D. et al 1987. "Forces exerted on the ground by galloping dogs(*Canis familiaris*)," Journal of Zoology, vol.213, pp.193-203, London.

Bryson, R.A. 1988. "Quantifying Battle Tank Mobility - A Manufacturer's View," Journal of Terramechanics, vol.25, no.1, pp.57-67.

Byrd, J.S. and DeVries, K.R. 1990. "A Six Legged Telerobot for Nuclear Applications Development," The International Journal of Robotics Research, vol.9, no.2, pp.43-52, April.

Cavagna, G.A. 1985. "Force Platforms as Ergonometers," Journal of Applied Physiology, vol.39, no.1, pp.174-179, July.

Cavagna, G.A. et al 1977. "Mechanical Work and Efficiency in Level Walking and Running," Journal of Physiology, no.268, pp.467-481.

Cavanagh, P.R. and LaFortune, M.A. 1980. "Ground Reaction Forces in Distance Running," Journal of Biomechanics, vol.13, pp.397-406.

Choi, B.S. and Song, S.M. 1988. "Fully Automated Obstacle Crossing Gaits for Walking Machines," Proceedings of 1988 IEEE International Conference on Robotics and Manipulators, pp.802-807.

Coates, D.R. 1981. "Environmental Geology," John Wiley and Sons, Inc.

DiBenedetto, A. and Pennestri, E. 1983. "Analysis of angular velocities and accelerations in plane linkages by means of numerical procedure," Journal of Mechanisms, Transmissions, and Automation in Design, vol.105, pp.624-630, December.

Dickinson, J.A. et al 1985. "The Measurement of Shock Waves Following Heel Strike While Running," Journal of Biomechanics, vol.18, no.6, pp.415-422.

Dimery, N.J. and Alexander, R.McN. 1985. "Elastic properties of the hind foot of the donkey, *Equus asinus*," Journal of Zoology, vol.207, pp.9-20, London.

Dimery, N.J. et al 1986(a). "Elastic properties of the feet of

- deer(Cervidae)," *Journal of Zoology*, vol.208, pp.161-169, London.
- Dimery, N.J. et al 1986(b). "Elastic extension of leg tendons in the locomotion of horses(equus caballus)," *Journal of Zoology*, vol.210, pp.415-425, London.
- Dudzinski, P.A. 1983. "Problems of Turning Process in Articulated Terrain Vehicles," *Journal of Terramechanics*, vol.19, no.4, pp.243-256.
- Dudzinski, P.A. 1986. "The Problem of Multi-Axle Vehicles," *Journal of Terramechanics*, vol.23, no.2, pp.85-93.
- Dudzinski, P.A. 1989. "Design Characteristics of Steering Systems for Mobile Wheeled Earthmoving Equipment," *Journal of Terramechanics*, vol.26, no.1, pp.25-82.
- Dwyer, M.Y. 1984. "The Tractive Performance of Wheeled Vehicles," *Journal of Terramechanics*, vol.21, no.1, pp.19-34.
- Elftman, H. 1939. "Forces and Energy Changes in the Leg during Walking," *American Journal of Physiology*, vol.125, pp.339-356.
- Faux, I.D. and Pratt, M.J. 1985. "Computational Geometry for Design and Manufacture," Ellis Harwood Ltd., England.
- Gardner, J.F. et al 1983. "Design and Testing of a Digitally Controlled Hydraulic Actuation System for a Walking Vehicle Leg Mechanism," *Applied Mechanics Conference*, St.Louis, Missouri, September 19-21.
- Gorinevsky, D.M. and Shneider, A.Y. 1990. "Force Control in Locomotion of Legged Vehicles over Rigid and Soft Surfaces," *The International Journal of Robotics Research*, vol.9, no.2, pp.4-23, April.
- Gray, J. 1968. "Animal Locomotion," William Clowes and Sons Ltd., London.
- Greene, P.R. 1985. "Running on Flat Turns: Experiments, Theory and Applications," *Journal of Biomechanical Engineering*, vol.107, pp.96-103, May.
- Hay, J.G. and Nohara, H. 1990. "Techniques Used by Elite Long Jumpers in Preparation for Takeoff," *Journal of Biomechanics*, vol.23, no.3, pp.229-239.
- Hirose, S. and Kunieda, O. 1991. "Generalised Standard Foot

Trajectory for a Quadruped Walking Vehicle," *The International Journal of Robotics Research*, vol.10, no.1, pp.3-12, February.

Hirose, S. and Umetani, Y. 1978. "Some Considerations on a feasible Walking Mechanism as a Terrain Vehicle," 3rd Symposium on Theory and Practice of Robots and Manipulators, pp.357-376, Udine-Italy, September 12-15.

Hirose, S. and Umetani, Y. 1980. "The Basic Motion Regulation System for a Quadruped Walking Vehicle," *Trans. ASME*, no. 80-DET-34, pp.1-6.

Hirose, S.H. et al 1984. "Titan III: A Quadruped Walking Vehicle," 2nd International Symposium of Robotics Research, Kyoto, Japan, August 20-23.

Hoyt, D.F. and Taylor, C.R. 1981. "Gait and the energetics of locomotion in horses," *Nature*, vol.292, pp.239-240.

Jayes, A.S. and Alexander, R.McN. 1982. "Estimates of mechanical stress in leg muscles of galloping Greyhounds(*Canis familiaris*)," *Journal of Zoology*, vol.198, pp.315-328, London.

Jones, J.R. 1983. "Vibration due to Motion Discontinuities in Hydraulically Actuated Robots," *Robotica*, vol.1, pp.211-215.

Kaneko, M. et al 1985. "A Hexapod Walking Vehicle with Decoupled Freedoms," *IEEE Journal of Robotics and Automation*, vol. RA-1, no.4, pp.183-190, December.

Kemp, H.R. 1990. "Climbing Ability of Four-Wheel-Drive Vehicles," *Journal of Terramechanics*, vol.27, no.1, pp.7-23.

Ker, R.F. et al 1986. "The role of tendon elasticity in hopping in a wallaby (*Macropus rufogriseus*)," *Journal of Zoology*, vol.208, pp.417-428, London.

Kirby, R.L. et al 1988. "The effect of Locomotion Speed on the Anterior Tibial Intramuscular Pressure of Normal Humans," *Journal of Biomechanics*, vol.21, no.5, pp.357-360.

Klein, C.A. and Briggs, R.L. 1980. "Use of Active Compliance in the Control of Legged Vehicles," *IEEE Transactions on Systems, Man, and Cybernetics*, vol.SMC-10, no.7, pp.393-400, July.

Klein, C.A. et al 1983. "Use of Force and Attitude Sensors for Locomotion of a Legged Vehicle for Irregular Terrain," *The*

- International Journal of Robotics Research, vol.2, no.2, pp.3-17, Summer.
- Lapskin, V.V. 1991. "Motion Control of a Legged Machine in the Supportless Phase of Hopping," The International Journal of Robotics Research, vol.10, no.4, pp.327-337, August.
- Larminie, J.C. 1988. "Standards for the Mobility Requirements of Military Vehicles," Journal of Terramechanics, vol.125, no.3, pp.171-189.
- Liston, R.A. 1967. "Walking Machine Studies," Army Research and Development News Magazine, pp.22-24, April.
- Mabie, H.H. and Reinholtz, C.F. 1987. "Mechanisms and dynamics of machinery," John Wiley and Sons, New York.
- Majeed, K.N. 1990. "Dual-Processor Controller with Vehicle Suspension Applications," IEEE Transactions on Vehicular Technology, vol.39, no.3, pp.271-276, August.
- McCloy, D. 1989. "The effects of Foot Trajectory on the Power Required to Swing a Mechanical Leg," Journal of Mechanical engineering Science, vol.203, pp.419-428.
- McCloy, D. 1990. "Step Lengths and Efficiencies of Serial Operated and Parallel Operated Mechanical Legs," Robotica, vol.8, pp.23-29.
- McGeer, T. 1989 (a). "Powered Flight, Child's Play, Silly Wheels and Walking Machines," IEEE, pp.1592-1597.
- McGeer, T. 1989 (b). "Passive Bipedal Running," Center for Systems Science, ref.no. CSS-IS TR 89-02, Simon Fraser University, Burnaby, B.C., Canada.
- McGhee, R.B. 1977. "Control of Legged Locomotion," Proceedings of the 18th Joint Automation Control Conference, San Francisco, California, pp.205-215.
- McGhee, R.B. 1981. "Walking Machines," Spenry-Univac Seminar on "The Next Ten Years - The Unprecedented Opportunities," 20-24 July, SE Paul de-Vince.
- McGhee, R.B. and Orin, D.E. 1976. "A Mathematical Programming Approach to Control of Joint Positions and Torques in Legged Locomotion Systems," Theory and Practice of Robots and Manipulators, 2nd International CISM-IFTOMM Symposium, Warsaw,

Poland, september 14-17.

McGhee, R.B. et al 1978. "Real time computer control of a hexapod vehicle," Proceedings from the 3rd CISM-IFTOMM International Symposium on Theory and Practice of Robots and Manipulators, pp.323-339.

McKerrow, P.J. 1990. "Introduction to Robotics," Addison-Wesley Publ. Co., pp.420-431.

McMahon, T.A. 1984. "Muscles, Reflexes and Locomotion," Princeton Univ. Press, New Jersey.

McMahon, T.A. and Cheng, G.C. 1990. "The Mechanics of Running: How does Stiffness Couple with Speed?", Journal of Biomechanics, vol.23, Suppl., pp.65-78.

McMahon, T.A. et al 1987. "Groucho Running," American Physiological Society, pp.2326-2337.

Mochon, S. and McMahon, T.A. 1980 (a). "Ballistic Walking," Journal of Biomechanics, vol.13, pp.49-57.

Mochon, S. and McMahon, T.A. 1980 (b). "Ballistic Walking: An Improved Model," Mathematical Biosciences, vol.52, pp.241-260, N.Y.

Moorehead, A. 1965. "The Desert War. The North African Campaign 1940-1943," pp.196-197, Sphere Books Ltd. G.B..

Munro et al 1987. "Ground Reaction Forces in Running: A Reexamination," Journal of Biomechanics, vol.20, no.2, pp.147-155.

Orin, D.E. et al 1976. "Interactive Computer Control of a six-legged robot vehicle with optimization of stability, terrain adaptability and energy," Proceedings from the 1976 IEEE Conference on Decision and Control, pp.382-389.

Ozguven, H.N. and Berme, L.N. 1988. "An Experimental and Analytical Study of Impact Forces During Human Jumping," Journal of Biomechanics, vol.21, no.12, pp.1061-1066.

Pugh, D.R. et al 1990. "Technical description of adaptive suspension vehicle," The International Journal of Robotics Research, vol.9, no.2, MIT.

Raibert, M.H. 1986 (a). "Legged robots that balance," The MIT Press,

London.

Raibert, M.H. 1986 (b). "Running with symmetry," *The International Journal of Robotics Research*, vol.5, no.4, pp.3-19, MIT.

Raibert, M.H. et al 1986. "Running of Four Legs As Though They were One," *IEEE Journal of Robotics and Automation*, vol.RA-2, no.2, pp.70-82, June.

Raibert, M.H. 1990, "Trotting, Pacing and Bounding by a Quadruped Robot," *Journal of Biomechanics*, vol.23, Suppl. 1, pp.79-98.

Russel, Jr. M. 1983. "Odex I: The First Functionid," *Robotics Age*, vol.5, no.5, pp.12-18, USA.

Salathe, E.P. et al 1990. "The Foot as a Shock Absorber," *Journal of Biomechanics*, vol.23, no.7, pp.655-659.

Savant et al 1991. "Electronic Desing," *The Benjamin/Cummings Publ. Co., Inc.*, pp.737, California, U.S.A..

Seireg, A. and Arvikar, R.J. 1973. "A Mathematical Model for Evaluation of the Forces in Lower Extremities of the Musculo-Skeletal System," *Journal of Biomechanics*, vol.6, pp.313-326.

Song, S.M. and Chen, Y.D. 1991. "A Free Gait Algorithm for Quadrupedal Walking Machines," *Journal of Terramechanics*, vol.28, no.1, pp.33-48.

Song, S.M. and Lee, J.K. 1988. "The Mechanical Efficiency and Kinematics of Pantograph Type Manipulators," *IEEE International Conference on Robotics and Automation*, vol.1, pp.414-420, Pennsylvania.

Song, S.M. and Waldron, K.J. 1987 (a). "Geometric Design of A Walking Machine for Optimum Mobility," *Journal of Mechanisms, Transmissions and Automation in Design*, vol.109, pp.21-28, March.

Song, S.M. and Waldron, K.J. 1987 (b). "An analytical approach for gait study and its applications on wave gaits," *The International Journal of Robotics Research*, vol.6, no.2, pp.60-71, MIT.

Song, S.M. and Waldron, K.J. 1989. "Machines that Walk: The Adaptive Suspension Vehicle," MIT Press, Cambridge, Mass., London.

Song, S.M. et al 1981. "Computer Aided Design of a Leg for an

- Energy Efficient Walking Machine," 7th Applied Mechanisms Conference, no.7, pp.1-7, St. Louis.
- Song, S.M. et al 1983. "Computer Aided Design of Legs for a Walking Vehicle," Applied Mechanics Conference, St. Louis, Missouri, September 19-21.
- Tanaka, T. 1984. "Operation in Paddy Fields," Journal of Terramechanics, vol.21, no.2, pp.153-179.
- Todd, D.J. 1985. "Walking Machines," Kogan Page Ltd., London.
- Tsai, C.K. et al 1987. "Modified Hybrid Control for an Electro-Hydraulic Robot Leg," IEEE Control Systems Magazine, pp.12-19.
- Waldron, K.J. 1986. "Force and Motion Management in Legged Locomotion," IEEE Journal of Robotics and Automation, vol.RA-2, no.4, pp.214-220, December.
- Waldron, K.J. and Kinzel, G.L. 1981. "The Relationship between Actuator Geometry and Mechanical Efficiency in Robots," Proceedings of 4th Romancy Symposium on Theory and Practice of Robots and Manipulators, pp.305-316, September 8-12, Zaborow, Poland.
- Waldron, K.J. and McGhee, R.B. 1986 (a). "The Adaptive Suspension Vehicle," IEEE Control System Magazine, pp.7-12, December.
- Waldron, K.J. and McGhee, R.B. 1986 (b). "The Mechanics of Mobile Robots, Robotics2, pp.113-121, North Holland.
- Waldron, K.J. et al 1984 (a). "Mechanical and Geometric Design of the ASV," Theory and Practice of Robot Manipulators, Proceedings of RomanSy 84, The Fifth CISM-IFTToMM Symposium, pp.295-306.
- Waldron, K.J. et al 1984 (b). "Configuration Design of the ASV," The International Journal of Robotics Research, vol.3, no.2, pp.37-48, Summer.
- Webtec Hydraulics 1988. "Webtec Hydraulic Catalogue," Webtec Hydraulics, Cambridgeshire, England.
- Weiss, P.L. et al 1988. "Human Ankle Joint Stiffness Over the Full Range of Muscular Activation Levels," Journal of Biomechanics, vol.21, no.7, pp.539-544.

APPENDICES

Contents

- 1. Computer Simulation Studies of the Buraq Leg**
 - 1.1 Derivation of equations for the Buraq leg mechanism**
 - 1.2 Derivation of equations for the linkage lengths of the crank-rocker drive mechanism**
 - 1.3 Application of Grashof's Mobility Criteria**
 - 1.4 Calculation of angular displacement values for the crank-rocker drive mechanism**
 - 1.5 Kinematical analysis of the Buraq leg mechanism**
- 2. The Experimental Set up**
- 3. Design and Application of A Variable Crank Mechanism with a Variable Stroke and a Phase**
 - 3.1 The Significance of the Crank Position on The Disk**
 - 3.2 Variable Crank Mechanism and the Leg Cycle**
- 4. Steering Mechanism**

Appendix 1.1

Derivation of equations for the Buraq leg mechanism

Using figure 3.2, the distance between the point U and the point Q can be projected on the x axis and y axis as follows;

$$U_x + A\cos a + C\cos b - Q_x = 0 \quad (\text{A-1})$$

$$U_y + A\sin a + C\sin b - Q_y = 0 \quad (\text{A-2})$$

The distance between the point U and the point P can also be projected the same way;

$$U_x + (A+B)\cos a + (C+E)\cos b + K\cos c - P_x = 0 \quad (\text{A-3})$$

$$U_y + (A+B)\sin a + (C+E)\sin b + K\sin c - P_y = 0 \quad (\text{A-4})$$

Following a different path from the figure, the same distance can be projected using angular displacement x . Hence the following equations can be written;

$$(A+B)\cos a + (C+E)\cos b + K\cos c = A\cos a + (C+D)\cos b + F\cos x + (H+K)\cos c \quad (\text{A-5})$$

$$(A+B)\sin a + (C+E)\sin b + K\sin c = A\sin a + (C+D)\sin b + F\sin x + (H+K)\sin c \quad (\text{A-6})$$

Equations (A-5) and (A-6) can be used to eliminate the angular displacement x from the equations by following procedure;

From the equation (A-5):

$$F\cos x = B\cos a + (E-D)\cos b - H\cos c \quad (\text{A-7})$$

From the equation (A-6):

$$F\sin x = B\sin a + (E-D)\sin b - H\sin c \quad (\text{A-8})$$

Adding (A-7)² to (A-8)²:

$$2BH\cos(a-c) + 2H(E-D)\cos(b-c) - 2B(E-D)\cos(a-b) = B^2 + H^2 + (E-D)^2 - F^2 \quad (\text{A-9})$$

Note that equations (A-3, 4, 9, 1 and 2) refer to equations (3-1) through (3-5) respectively.

Appendix 1.2

Derivation of equations for the linkage lengths of the crank-rocker drive mechanism

Four bar mechanism inherits two singular positions. Using these positions trigonometric equations can be written (See figure 3.12).

From figure 3.12(a), the following equations can be written;

$$(R_1)^2 = (R_4)^2 + (R_2+R_3)^2 - 2(R_2 + R_3)R_4 \cos g_{\min} \quad (\text{A-10})$$

$$(R_4)^2 = (R_1)^2 + (R_2+R_3)^2 - 2(R_2+R_3) R_1 \cos f \quad (\text{A-11})$$

$$(R_2+R_3)^2 = (R_1)^2 + (R_4)^2 - 2 R_1 R_4 \cos(\pi - g_{\min} - f) \quad (\text{A-12})$$

From the figure 3.12(b), the following equations can be written;

$$(R_1)^2 = (R_4)^2 + (R_3 - R_2)^2 - 2(R_3 - R_2)R_4 \cos g_{\max} \quad (\text{A-13})$$

$$(R_4)^2 = (R_1)^2 + (R_3 - R_2)^2 - 2(R_3 - R_2)R_1 \cos k \quad (\text{A-14})$$

$$(R_3 - R_2)^2 = (R_1)^2 + (R_4)^2 - 2 R_1 R_4 \cos(\pi - g_{\max} - k) \quad (\text{A-15})$$

Subtracting the equations (A-13), (A-14) and (A-15) from (A-10), (A-11) and (A-12) the following set of equations are obtained:

$$4 R_2 R_3 - 2 a_0 R_4 (R_2 + R_3) + 2 d_0 R_4 (R_3 - R_2) = 0 \quad (\text{A-16})$$

$$4 R_2 R_3 - 2 b_0 R_1 (R_2 + R_3) + 2 e_0 R_1 (R_3 - R_2) = 0 \quad (\text{A-17})$$

$$4 R_2 R_3 - 2 c_0 R_1 R_4 + 2 f_0 R_1 R_4 = 0 \quad (\text{A-18})$$

where a_0 represents $\cos g_{\min}$, b_0 represents $\cos f$, c_0 represents $\cos(\pi - g_{\min} - f)$, d_0 represents $\cos g_{\max}$, e_0 represents $\cos k$ and f_0 represents $\cos(\pi - g_{\max} - k)$. Also, it should be clear that minimum and maximum values of angle T_4 are equal to $(g_{\min} + f)$ and $(g_{\max} + k)$ respectively. Using equation (A-18) following equation can be derived;

$$R_1 = 2 R_2 R_3 / [R_4 (c_0 - f_0)] \quad (\text{A-19})$$

Substituting equation (A-19) into (A-17), the following equation can be found:

$$R_3 = [(e_0 + b_0) R_2 - (c_0 - f_0) R_4] / (e_0 - b_0) \quad (\text{A-20})$$

Substituting equations (A-19) and (A-20) into equation (A-16), the following equation can be obtained:

$$P (R_2)^2 + Q R_2 + S = 0 \quad (A-21)$$

where $P = 2 (e_0 + b_0)$

$$Q = 2 (f_0 - c_0 - a_0 e_0 + d_0 b_0)$$

$$S = (c_0 - f_0)(a_0 - d_0) (R_4)^2$$

Since all the variables in the equation (A-21) are known except R_2 , by solving equation (A-21), R_2 value can be found. And also, by substituting value of R_2 into equations (A-19) and (A-20), R_3 and R_1 also can be calculated. Thus, the length of the four bar linkages are calculated.

Appendix 1.3

Application of Grashof's Mobility Criteria

Grashof's Mobility criteria are applied to the mechanism to check that the calculated crank-rocker linkage dimensions satisfy necessary and sufficient conditions for the mobility. Following quantities have been defined (Angeles, Callejas 1984);

$$k_1 = [(R_1)^2 + (R_2)^2 - (R_3)^2 + (R_4)^2] / (2 R_2 R_4) \quad (\text{A-22})$$

$$k_2 = R_1 / R_2 \quad (\text{A-23})$$

$$k_3 = R_1 / R_4 \quad (\text{A-24})$$

Numerical values are as follows;

R_1	=	111.93	k_1	=	2.69
R_2	=	31.87	k_2	=	3.51
R_3	=	80.22	k_3	=	1.085
R_4	=	103.10			

According to Grashof's Mobility Criteria; if the set $\{ k_1, k_2, k_3 \}$ verifies either set of inequalities, then the link lengths R_i ($i=1, 2, 3, 4$) do not define a linkage. These inequalities are as follows:

$$\begin{aligned} (k_2 - k_1 k_3)^2 &\geq (k_3)^4 \\ [(k_1)^2 - (k_2)^2 + (k_3)^2 - 1]^2 &> 4 (k_2 - k_1 k_3)^2 \\ (k_1)^2 - (k_2)^2 - 1 &> (k_3)^2 \\ (k_2 - k_1 k_3)^2 &\leq (k_3)^4 \\ (k_2 - k_1 k_3)^2 &< (k_3)^2 [(k_1)^2 - (k_2)^2 - 1] \end{aligned}$$

The necessary and sufficient conditions to produce an input crank is that both of the following inequalities hold;

$$2(k_2 - k_1 k_3)^2 - (k_3)^2 [(k_1)^2 - (k_2)^2 + (k_3)^2 - 1] > 0$$

$$[(k_1 - k_3)^2 - (k_2 - 1)^2] [(k_1 + k_3)^2 - (k_2 + 1)^2] > 0$$

Calculations prove that predicted values of R_1, R_2, R_3 do not satisfy the first set of inequalities, and satisfy the second set of inequalities. That way predicted results of linkage lengths in the section 3.3.5 have been verified.

Appendix 1.4

Calculation of angular displacement values for the crank-rocker drive mechanism

To find the angular displacements of each linkage (T_1 , T_2 , T_3 and T_4), following equations are generated by projecting the crank-rocker linkage lengths on the axis x and y (see figure 3.13);

$$f_1 : R_1 \cos T_1 - R_2 \cos T_2 - R_3 \cos T_3 + R_4 \cos T_4 = 0$$

$$f_2 : R_1 \sin T_1 + R_2 \sin T_2 + R_3 \sin T_3 - R_4 \sin T_4 = 0$$

Partial derivatives of these functions can be calculated as follows;

$$\frac{\partial f_1}{\partial T_3} = R_3 \sin T_3, \quad \frac{\partial f_1}{\partial T_4} = -R_4 \sin T_4, \quad \frac{\partial f_2}{\partial T_3} = R_3 \cos T_3, \quad \frac{\partial f_2}{\partial T_4} = -R_4 \cos T_4$$

T_1 is known, changing T_2 in small steps T_3 and T_4 can be calculated using Jacobian method which leads to the following matrix equation;

$$\begin{bmatrix} \frac{\partial f_1}{\partial T_3} & \frac{\partial f_1}{\partial T_4} \\ \frac{\partial f_2}{\partial T_3} & \frac{\partial f_2}{\partial T_4} \end{bmatrix} \cdot \begin{bmatrix} \partial T_3 \\ \partial T_4 \end{bmatrix} = \begin{bmatrix} -f_1 \\ -f_2 \end{bmatrix}$$

Using the Cramer's rule following equations can be written;

$$\partial T_3 = - \left(\frac{\partial f_2}{\partial T_4} f_1 - \frac{\partial f_1}{\partial T_4} f_2 \right) / \text{DET}$$

$$\partial T_4 = \left(\frac{\partial f_2}{\partial T_3} f_1 - \frac{\partial f_1}{\partial T_3} f_2 \right) / \text{DET}$$

where DET (the coefficients matrix's determinant) is as follows;

$$\text{DET} = \frac{\partial f_1}{\partial T_3} \frac{\partial f_2}{\partial T_4} - \frac{\partial f_1}{\partial T_4} \frac{\partial f_2}{\partial T_3}$$

Final T_3 and T_4 values can be calculated after a series of iterations while the increase in the value becomes nil.

$$T_3 = T_3 + \partial T_3$$

$$T_4 = T_4 + \partial T_4$$

The angular displacement results are shown in figure 3.14 during the complete leg cycle.

Appendix 1.5

For kinematical analysis of the Buraq leg, general expressions of the velocity and the acceleration of the foot are derived. The figures 3.1, 3.13 and 6.2 can be used for the derivation of vectorial expressions. The point W, which is the centre of the rocker, has the coordinates of (W_X, W_Y) . Hence, the coordinates of point S can be calculated as follows;

$$S_X = W_X + R_1 \cos T_1, \quad S_Y = W_Y + R_1 \sin T_1$$

The velocity of the foot can be obtained by the following vectorial equation. Superscript 'o' denotes the first derivative of the angular displacements;

$$\vec{V}_P = a \overset{o}{k} \times \vec{UM} + b \overset{o}{k} \times \vec{MZ} + c \overset{o}{k} \times \vec{ZP}$$

where;

$$\vec{UM} = (A+B) (\cos a \vec{i} + \sin a \vec{j}), \quad \vec{MZ} = (C+E) (\cos b \vec{i} + \sin b \vec{j}),$$

$$\vec{ZP} = K (\cos c \vec{i} + \sin c \vec{j})$$

Velocity of the foot in Cartesian coordinates can be obtained from the following equation;

$$\vec{V}_P = \vec{V}_{Px} + \vec{V}_{Py}$$

where;

$$\vec{V}_{Px} = - [a \overset{o}{(A+B)} \sin a + b \overset{o}{(E+F)} \sin b + c \overset{o}{K} \sin c] \vec{i}$$

$$\vec{V}_{Py} = [a \overset{o}{(A+B)} \cos a + b \overset{o}{(E+F)} \cos b + c \overset{o}{K} \cos c] \vec{j}$$

Also, the acceleration of the foot can be calculated as follows;

$$\vec{A}_P = a \overset{oo}{k} \times \vec{UM} + a \overset{o}{k} \times (\overset{o}{a} \overset{o}{k} \times \vec{UM}) +$$

$$b \overset{oo}{k} \times \vec{MZ} + b \overset{o}{k} \times (\overset{o}{b} \overset{o}{k} \times \vec{MZ}) +$$

$$c \overset{oo}{k} \times \vec{ZP} + c \overset{o}{k} \times (\overset{o}{c} \overset{o}{k} \times \vec{ZP})$$

where 'oo' superscript denotes the second derivative of the angular

displacements. Acceleration of the foot in Cartesian coordinates;

$$\vec{A}_P = \vec{A}_{Px} + \vec{A}_{Py}$$

where;

$$A_{Px} = - (A+B) (a \sin \alpha + a^2 \cos \alpha) - (E+F)(b \sin \beta + b^2 \cos \beta) - K(c \sin \gamma + c^2 \cos \gamma)$$

$$A_{Py} = (A+B) (a \cos \alpha - a^2 \sin \alpha) + (E+F)(b \cos \beta - b^2 \sin \beta) + K(c \cos \gamma - c^2 \sin \gamma)$$

Using above derived equations, velocity and acceleration of the foot can be calculated according to given angular displacement values and derivatives.

DiBenedetto and Pennestri (1983) in their paper about analysis of angular velocities and accelerations in plane linkages have derived the following equations for numerical calculations;

The total time of one cycle is calculated as t;

$$t = \frac{60 * \text{GEAR}}{\text{RPM}}$$

where GEAR is the gear ratio between the motor and the crank, and RPM is the motor speed. Also, time difference between iterations is represented by ∂t . c_N being a common coefficient and k being step number, the following formulas are derived for angular velocity (w) and accelerations (β) of the joints.

$$\partial t = \frac{t}{N}$$

$$c_N = \frac{t}{12N}$$

$$t_k = k \partial t \quad k = 1, 2, 3, \dots, N$$

Hence, angular velocities of a specific joint (j) can be calculated at any moment (k) during the operation cycle using following equations;

$$w_{j,k} = \frac{1}{72 c_N} (2 T_{j,k+3} - 9 T_{j,k+2} + 18 T_{j,k+1} - 11 T_{j,k}) \quad k = 0, 1, \dots, N-3$$

$$w_{j,k} = \frac{1}{72 c_N} (11 T_{j,k} - 18 T_{j,k-1} + 9 T_{j,k-2} - 2 T_{j,k-3}) \quad k = N-2, \dots, N$$

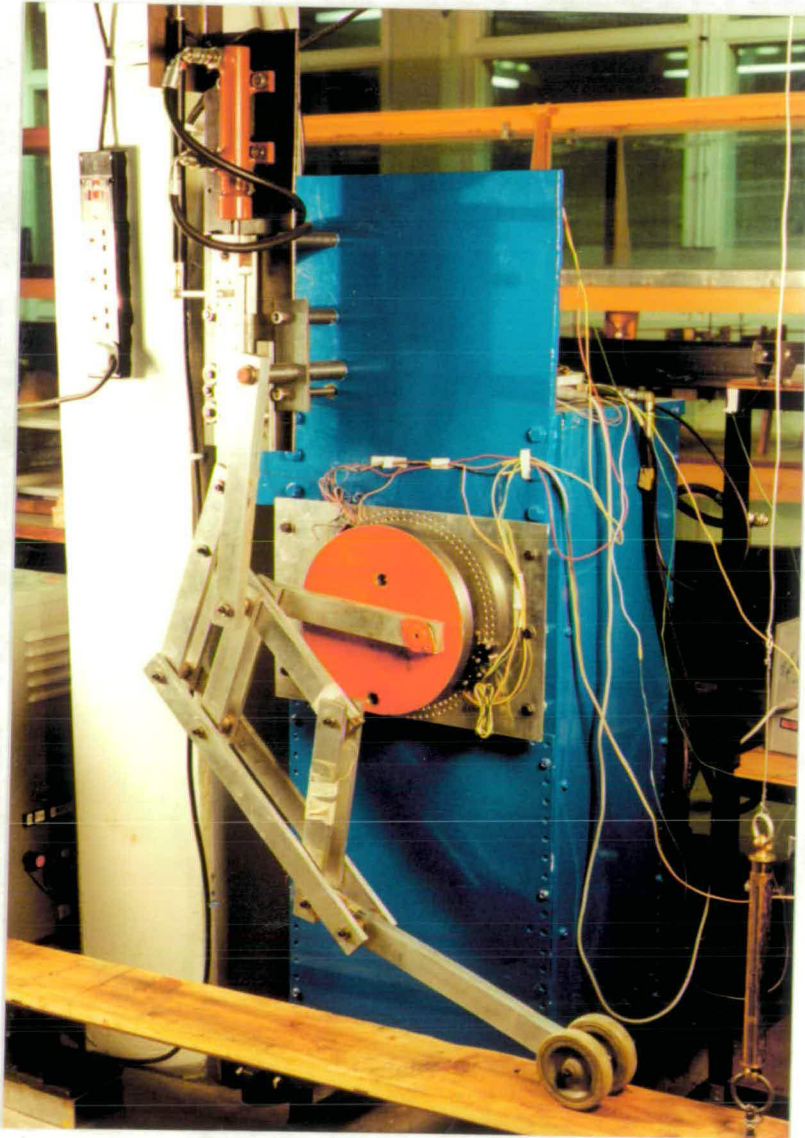
Also, angular accelerations of a specific joint (j) can be calculated at any moment (k) during the operation cycle similarly;

$$\beta_{j,k} = \frac{1}{72 c_N} (2 w_{j,k+3} - 9 w_{j,k+2} + 18 w_{j,k+1} - 11 w_{j,k}) \quad k = 0, 1, N-3$$

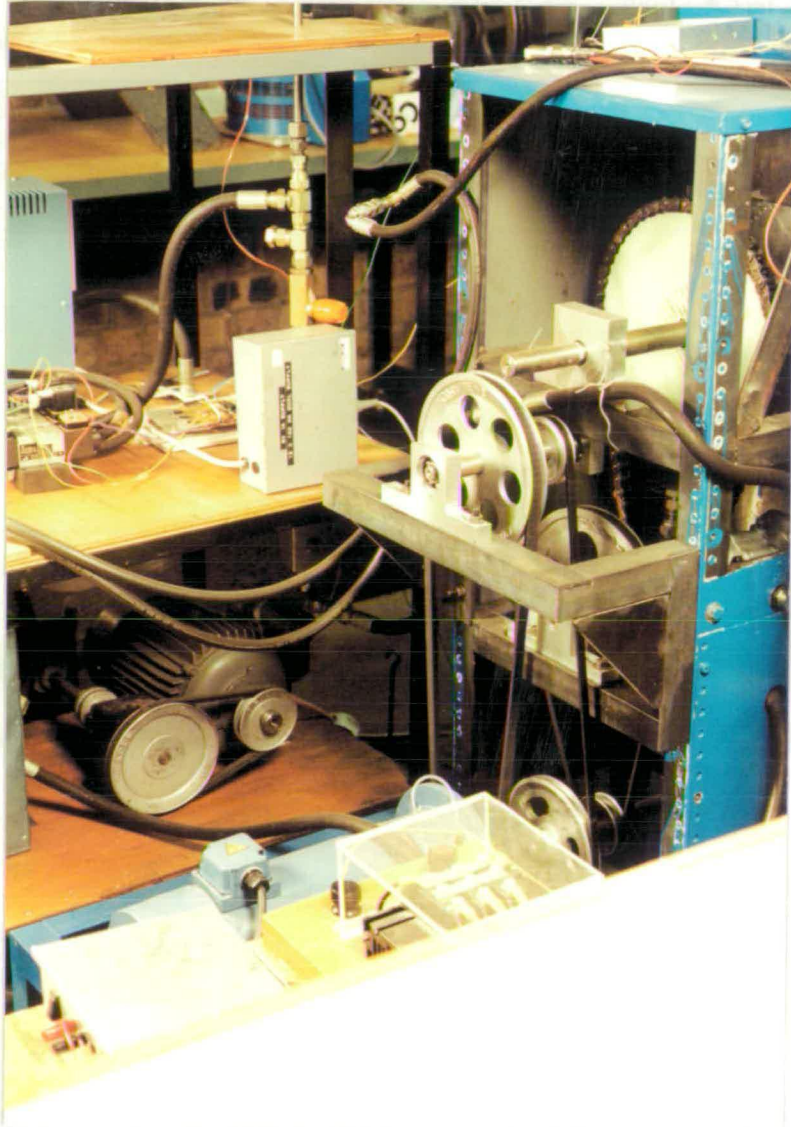
$$\beta_{j,k} = \frac{1}{72 c_N} (11 w_{j,k} - 18 w_{j,k-1} + 9 w_{j,k-2} - 2 w_{j,k-3}) \quad k = N-2, \dots, N$$

Appendix 2

The Experimental Set up



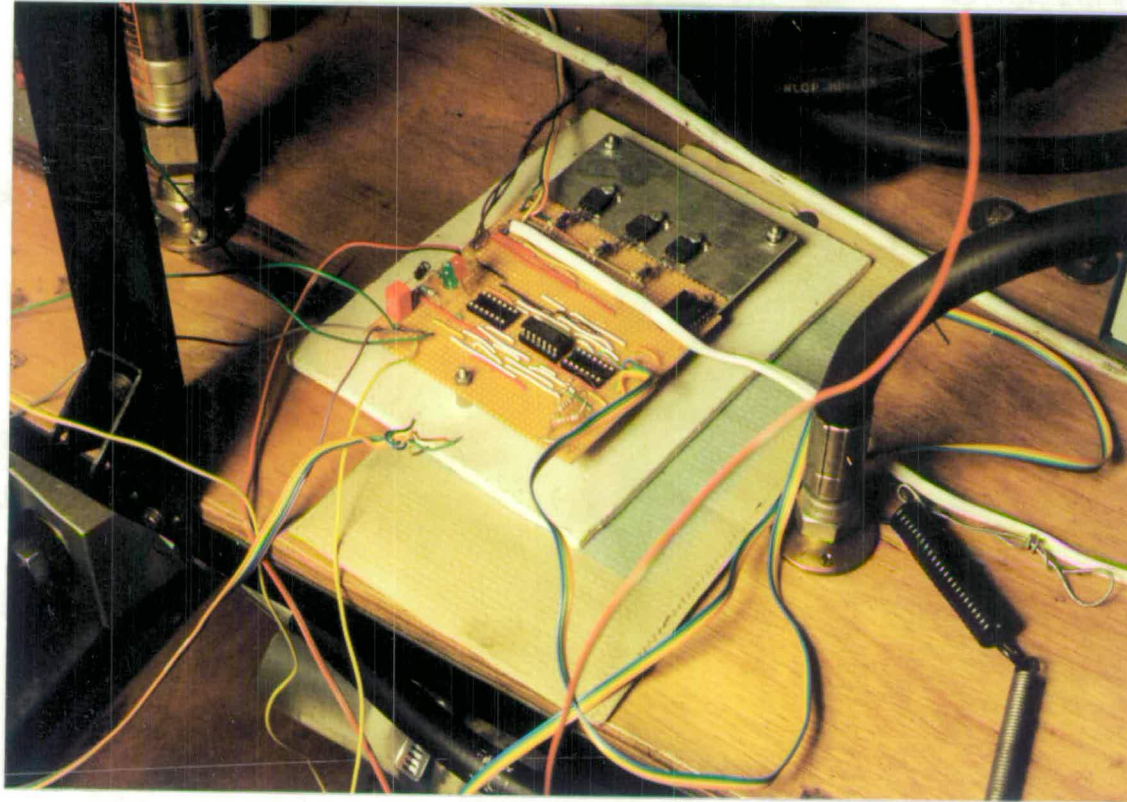
Photograph A2.1 The prototype leg mechanism driven by a crank-rocker in longitudinal direction, and by a hydraulic ram in vertical direction.



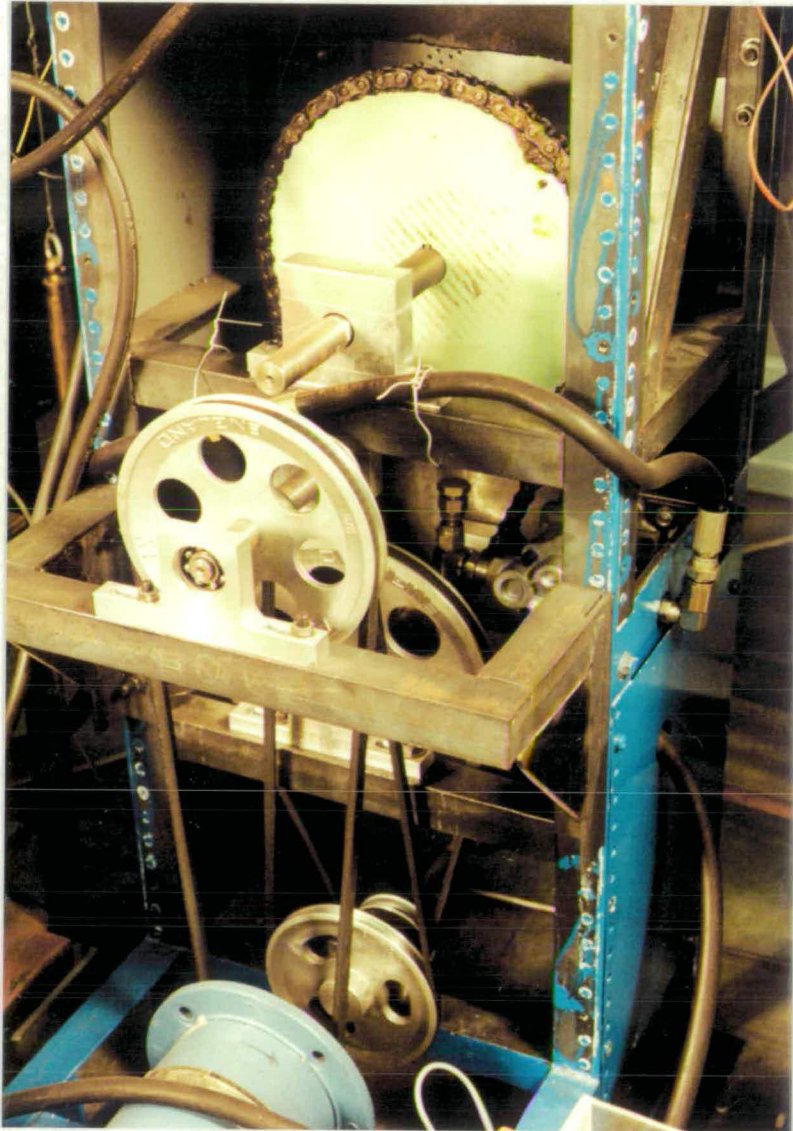
Photograph A2.2 A back view of the test rig; the DC motor driving the crank and the pump through a series of V-Belt and chain drives can be seen. Also solenoid valves controlling the flow and the diode bridge feeding the DC motor can be seen.



Photograph A2.3 The leg mechanism driven by computer control. The 3-phase variac supplying power to the test rig and the straight line potentiometer in parallel to the hydraulic ram can also be seen.



Photograph A2.4 The logic control circuit driving the transistors which are used to turn on/off the solenoid valves.



Photograph A2.5 The mechanical drive system in detail
(realise the hydraulic pump with hose connections).

Appendix 3.1

The Significance of the Crank Position on The Disk

Derivation of equations of motion for the crank point is necessary to understand the significance of the crank point position on the disk.

From figure A3.1 the following equations can be written;

$$\vec{i} = \cos\alpha \vec{e}_t - \sin\alpha \vec{e}_n \quad \text{and} \quad \vec{j} = \sin\alpha \vec{e}_t + \cos\alpha \vec{e}_n$$

$$\text{Hence, } \vec{e}_t = \cos\alpha \vec{i} + \sin\alpha \vec{j} \quad \text{and} \quad \vec{e}_n = -\sin\alpha \vec{i} + \cos\alpha \vec{j}$$

where α represents the angle between the unit vectors \vec{i} and \vec{e}_t . Also following equations can be written for the vectorial quantities \vec{R} , \vec{r} and \vec{a} ;

$$\vec{a} = \vec{R} + \vec{r}, \quad \vec{R} = y_0 \vec{e}_n, \quad \vec{r} = r \cos\theta \vec{e}_t + r \sin\theta \vec{e}_n$$

$$\text{where } r \text{ represents the radius of the crank. Hence,}$$

$$\vec{a} = y_0 \vec{e}_n + r \cos\theta \vec{e}_t + r \sin\theta \vec{e}_n = r \cos\theta \vec{e}_t + (y_0 + r \sin\theta) \vec{e}_n$$

$$\text{Using the equivalent unit vectors } \vec{i} \text{ and } \vec{j}, \vec{a} \text{ can be expressed as follows;}$$

$$\vec{a} = [r \cos(\theta + \alpha) - y_0 \sin\alpha] \vec{i} + [r \sin(\theta + \alpha) + y_0 \cos\alpha] \vec{j}$$

For the crank point coordinates (X_C, Y_C) following equations can be written using the vector \vec{a} ;

$$X_C = r \cos(\theta + \alpha) - y_0 \sin\alpha \quad \text{and} \quad Y_C = r \sin(\theta + \alpha) + y_0 \cos\alpha$$

where r represents the radius of the crank, y_0 represents the distance between the shaft centre and the crank centre. Angle α represents the angular displacement of the disk while angle θ represents the angular displacement of the crank relative to the disk.

Crank is placed in such a way that it is off-centered. This allows the crank effective length to change. The distance between the crank centre and the disk centre (which is also the centre of the drive shaft) is y_0 . In case the crank effective length is represented by C_e , it can be shown that y_0 is directly related to it as shown in the following equation;

$$\vec{a} = X_C \vec{i} + Y_C \vec{j}$$

$$(C_e)^2 = \sqrt{X_C^2 + Y_C^2} \Rightarrow (C_e)^2 = r^2 + y_0^2 + 2 r y_0 \sin\theta$$

reminder : $\sin\theta = \sin(\theta+\alpha) \cos\alpha - \sin\alpha \cos(\theta+\alpha)$

Therefore y_0 plays a prime factor in the manoeuvrability of the vehicle.

The maximum manoeuvrability of the vehicle depends on the maximum value of C_e , which can be calculated as follows;

$$\text{when } \theta = \frac{\pi}{2} \text{ then } C_e = \sqrt{r^2 + y_0^2 + 2 r y_0 \sin\left(\frac{\pi}{2}\right)} = \sqrt{(r + y_0)^2}$$

$$\text{hence } (C_e)_{\max} = r + y_0$$

For the minimum manoeuvrability of the vehicle a similar method can be followed;

$$\text{when } \theta = -\frac{\pi}{2} \text{ then } C_e = \sqrt{r^2 + y_0^2 + 2 r y_0 \sin\left(-\frac{\pi}{2}\right)} = \sqrt{(r - y_0)^2}$$

$$\text{hence } (C_e)_{\min} = |r - y_0|$$

As can easily be seen, while $r = y_0$ the minimum crank effective length, $(C_e)_{\min}$ becomes zero. However, while $r \leq y_0$ phase change characteristic of the mechanism becomes constrained. As it can be seen in figure A3.2(a), while $r=y_0$, the maximum phase is limited to π between right and the left leg. However, in figure A3.2(b), it is clear that the phase value is not limited and can be as big as 2π , which gives more potential to the mechanism to adjust the gaits during the locomotion.

Hence, the choice of y_0 affects the vehicle trajectory. In figure A3.3 the trajectories of the left foot and right foot are represented symbolically.

s_1 and s_2 can be represented as follows;

$$s_1 = \frac{(C_e)_L}{(C_e)_{\max}} L \quad \text{and} \quad s_2 = \frac{(C_e)_R}{(C_e)_{\max}} L$$

where;

$(C_e)_L$ represents the left crank effective length

$(C_e)_R$ represents the right crank effective length

L represents the maximum foot stroke

and $(C_e)_{\max}$ represents the maximum crank length.

For a left turn, the ratio of the arc lengths can be expressed as follows;

$$\frac{\text{rot}}{\text{rot} + \text{width}} = \frac{s_1}{s_2}$$

where rot represents the radius of the vehicle trajectory and width represents the distance between the pair of legs. Following equations can be written for the vehicle trajectory during a left turn;

$$\text{rot} = \frac{s_1 \text{ width}}{s_2 - s_1} \quad \text{and} \quad \tan \frac{\theta}{2} = \frac{\frac{s_1}{2}}{\text{rot}}$$

For a right turn, similarly following equations can be written for the vehicle trajectory (hint : shift s_1 by s_2 and vice versa).

$$\text{rot} = \frac{s_2 \text{ width}}{s_1 - s_2} \quad \text{and} \quad \tan \frac{\theta}{2} = \frac{\frac{s_2}{2}}{\text{rot}}$$

Appendix 3.2

Variable Crank Mechanism and the Leg Cycle

The variables used in this section can be defined as follows,

ω_s : Shaft speed which is also equal to disk speed.

$\omega_s = \dot{\alpha}$ where α is angular displacement of the shaft

ω_ψ : Right leg crank speed with respect to the shaft

$\omega_\psi = \dot{\psi}$ where ψ is angular displacement of the right leg crank

ω_θ : Left leg crank speed with respect to the shaft

$\omega_\theta = \dot{\theta}$ where θ is angular displacement of the left leg crank

Support Period

As it was explained in section 5.5.2, the crank is locked while the leg is in support period. And the crank is activated only during the transfer phase. This implies that the support period for both legs is the same, and also is equal to half of the period of the shaft rotation.

Assuming the time $t = t + i dt$ while $i = 0, 1, 2 \dots$

Hence for the support period at the moment of t , following equations can be written;

For left leg: $\theta_{i+1} = \theta_i$, For right leg: $\psi_{i+1} = \psi_i$

For the shaft (disk) : $\alpha_{i+1} = \alpha_i + \omega_s dt$

The period of the support period, T_{sup} can be written as follows;

$$T_{sup} = \frac{T_s}{2} = \frac{\pi}{\omega_s} \Rightarrow T_{sup} = \frac{\pi}{\omega_s}$$

where T_s represents the period of the shaft motion.

Transfer Period

Unlike the support period, during the transfer period the cranks are not kept locked, according to the gait, direction and speed requirements, they are rotated with respect to the disks;

For left leg: $\theta_{i+1} = \theta_i + \omega_\theta dt$

For right leg: $\psi_{i+1} = \psi_i + \omega_\psi dt$

For the shaft (disk) : $\alpha_{i+1} = \alpha_i + \omega_s dt$

Hence the period of the left leg during the transfer period;

$$T_{trf}^{\theta} = \frac{2\pi}{2(\omega_s + \omega_{\theta})} \Rightarrow T_{trf}^{\theta} = \frac{\pi}{\omega_s + \omega_{\theta}}$$

And the period of the right leg during the transfer period;

$$T_{trf}^{\psi} = \frac{2\pi}{2(\omega_s + \omega_{\psi})} \Rightarrow T_{trf}^{\psi} = \frac{\pi}{\omega_s + \omega_{\psi}}$$

To find the period that the leg takes to complete one whole revolution, the time values calculated for support and transfer periods can be added together. The period for a complete revolution of the right leg, T_R , can be expressed as follows;

$$T_R = T_{sup}^{\psi} + T_{trf}^{\psi} = \frac{\pi}{\omega_s} + \frac{\pi}{\omega_s + \omega_{\psi}}$$

The period for a complete revolution of the left leg, T_L , similarly, can be expressed as follows;

$$T_L = T_{sup}^{\theta} + T_{trf}^{\theta} = \frac{\pi}{\omega_s} + \frac{\pi}{\omega_s + \omega_{\theta}}$$

Effect of the Crank Speed on the Leg Cycle

Leg cycle period is the time that the leg takes to complete a whole revolution.

It is clear that if crank speed is zero, the leg cycle period is the same as the shaft period or the disk period.

From the transfer period expression, it is clear that if the angular velocities of the shaft and the crank are in the same direction (speeds having the same sign), the transfer period gets shorter than the support period. This implies that it takes a shorter time for the foot to travel on the air than to support the body on the ground. Also the leg cycle period becomes shorter than the shaft period, that is, it takes less time for the leg to complete a whole revolution than the shaft to complete a whole revolution.

In opposite, if the angular velocities of the shaft and crank are in opposite direction (speeds having opposite sign), the transfer period takes longer than the support period. This implies that it takes a longer time for the foot to

travel on the air than to support the body on the ground. Also the leg cycle period becomes longer than the shaft period, that is, it takes longer time for the leg to complete a whole revolution than for the shaft to complete a whole revolution.

Speed of the phase change

It is clear that the phase shift takes place gradually unless high speed actuators are used to rotate the crank with respect to the disk. In this section the relation between the crank speed and the time that it takes for the crank point to shift its position 180 degrees is studied in detail considering the simultaneous rotation of the shaft. Thus, the potential of the mechanism to adapt itself to phase changes can be estimated.

g is defined as the period for the crank point to change its position π radians phase change. π radian is chosen because this is the longest possible change. Considering that both crank points motions can be incorporated to shorten the time for the necessary change, g value should be considered for the longest possible phase shift.

The gait change takes place gradually by changing the phase. As it was mentioned previously, the support period takes the same time for both legs. However it is possible to change the time of the transfer period by changing the phase.

The following equation can be written for the number of times that the shaft has to rotate - which is represented by c -, so that the difference between two cranks transfer periods becomes equal to the time that will take the crank point to rotate π radians, which takes half of the period of the rotation of the shaft, T_s ;

$$c \left| [T_{trf}^{\theta} - T_{trf}^{\psi}] \right| = \frac{T_s}{2}$$

If the left and right leg periods' expressions are opened

$$c \left\| \left[\frac{\pi}{\omega_s + \omega_{\theta}} - \frac{\pi}{\omega_s + \omega_{\psi}} \right] \right\| = \frac{T_s}{2}$$

Hence for c the following statement can be obtained;

$$c = \frac{(\omega_s + \omega_\theta) (\omega_s + \omega_\psi)}{\omega_s |\omega_\psi - \omega_\theta|}$$

Then the maximum time to change phase with the value of π , g , can be expressed as follows;

$$g = \frac{2\pi (\omega_s + \omega_\theta) (\omega_s + \omega_\psi)}{\omega_s^2 |\omega_\psi - \omega_\theta|}$$

which can also be expressed as follows;

$$g = 2\pi \left[\frac{1}{|\omega_\psi - \omega_\theta|} + \frac{1}{\omega_s^2} \left(\frac{(\omega_\psi \omega_s + \omega_\theta \omega_s + \omega_\theta \omega_\psi)}{|\omega_\psi - \omega_\theta|} \right) \right]$$

if we define the expression in the smaller parenthesis with the following;

$$v = \frac{(\omega_\psi \omega_s + \omega_\theta \omega_s + \omega_\theta \omega_\psi)}{|\omega_\psi - \omega_\theta|}$$

expression of g can be restated as follows;

$$g = 2\pi \left[\frac{1}{|\omega_\psi - \omega_\theta|} + \frac{v}{\omega_s^2} \right]$$

Since;

$$\omega_s^2 \gg v \Rightarrow \frac{v}{\omega_s^2} \cong 0$$

Therefore it can be concluded that

$$g \cong \frac{2\pi}{|\omega_\psi - \omega_\theta|} \text{ where } \omega_\psi \text{ and } \omega_\theta \text{ are in [rad/s].}$$

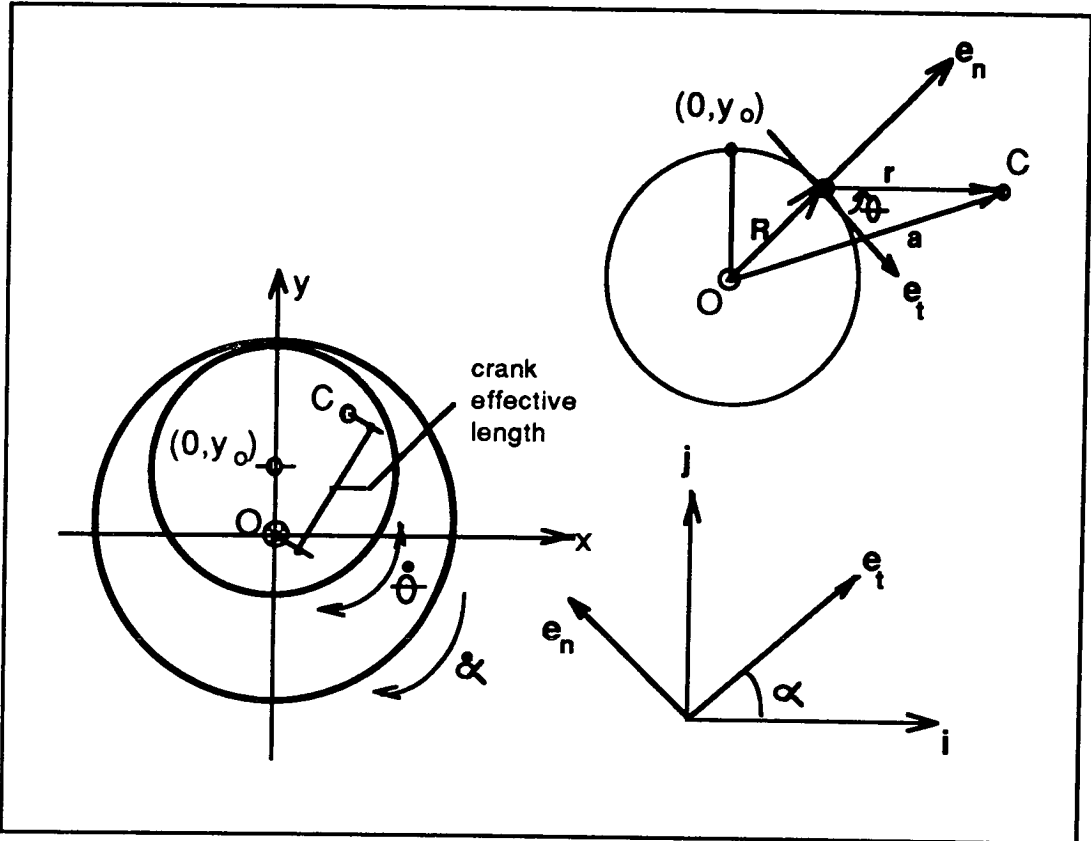


Figure A3.1 The parameters of the variable crank mechanism

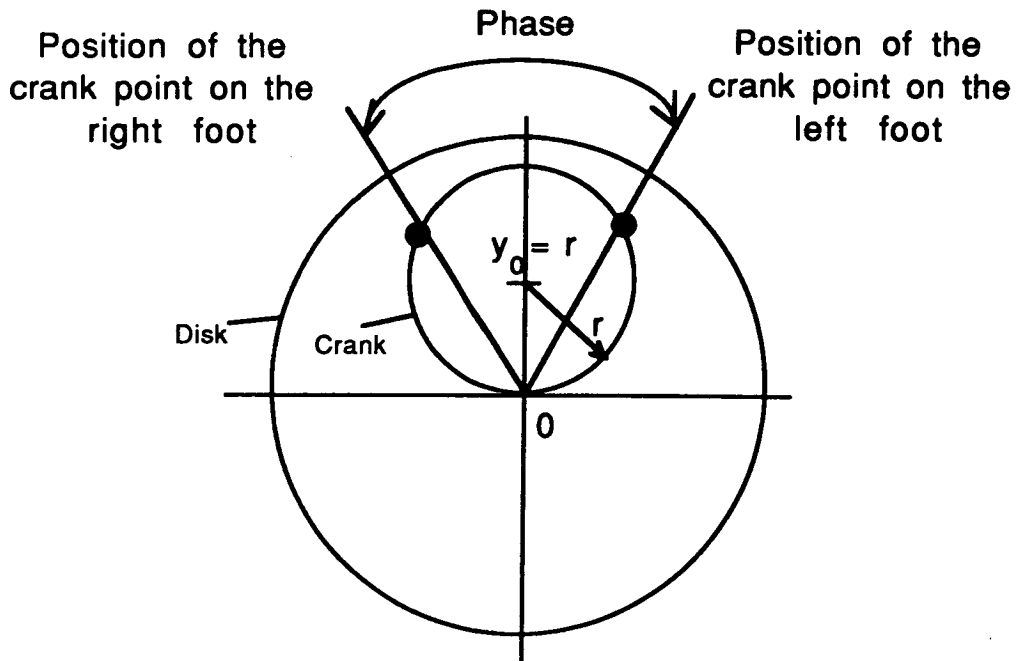


Figure A3.2 (a)

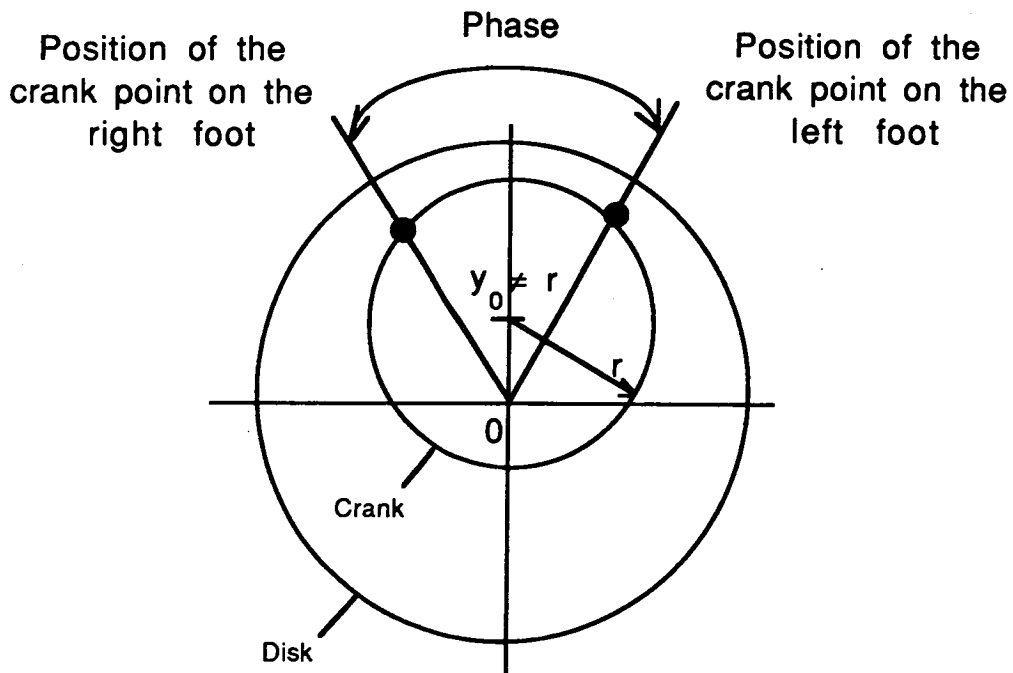


Figure A3.2 (b)

Figure A3.2 The relation between the crank position on the disk and the phase

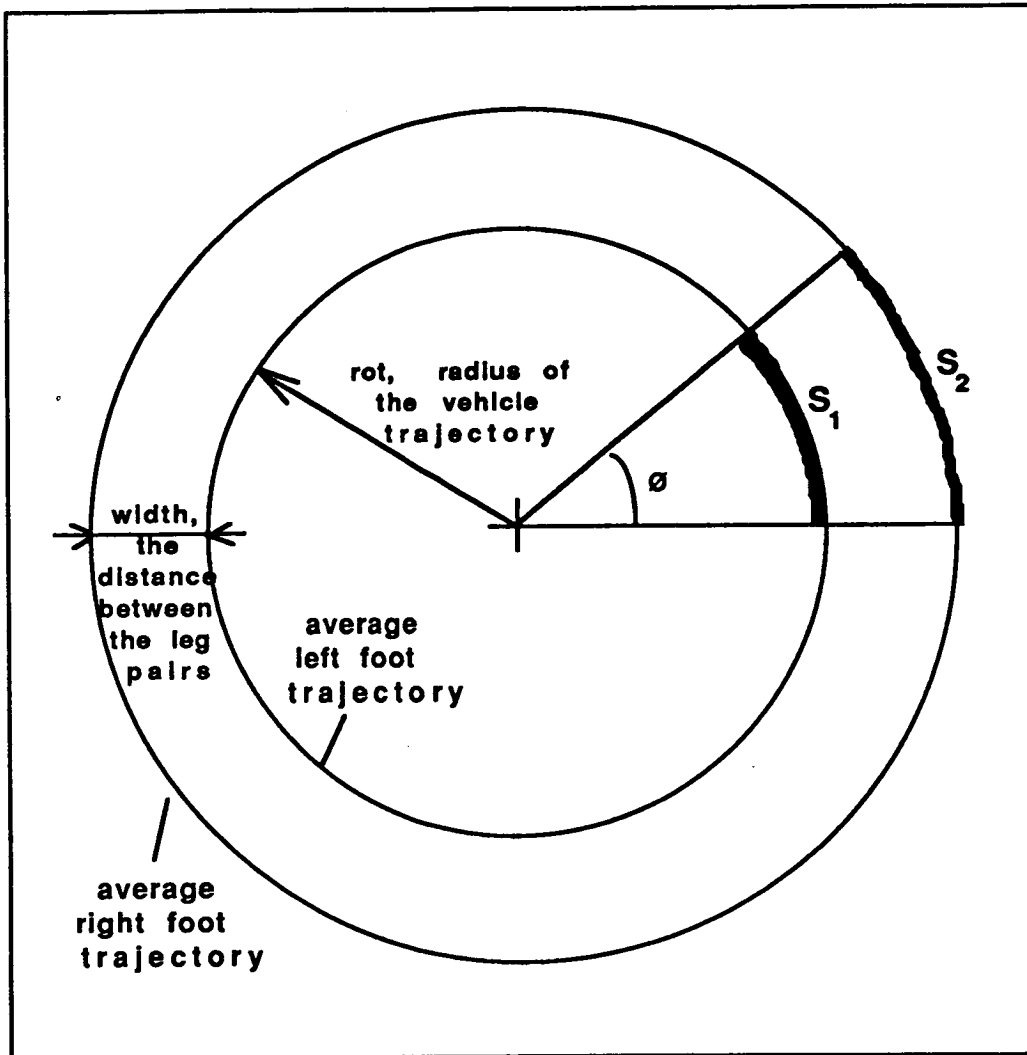


Figure A3.3 A symbolic representation of the vehicle's trajectory while rotating around a central point.

Appendix 4

Analysis of Steering Mechanism

Figure A4.1 represents two events in the same time; while $y = 0$, and while $y = y$, meaning any value. In the figure only a part of the picture is shown, since it is easy to figure out the whole picture due to symmetry about the location of the actuated point.

The quantities of a , b and Ω_0 are constant, unlike y , Ω and \forall . From figure A4.1, using the equality of the parallel sides of a rectangle, following equations can be written;

$$a \sin \Omega + y = b \sin \forall + a \sin \Omega_0$$

(Realise that while $y = 0$, $\forall = 0$; and hence $\Omega = \Omega_0$)

$$a \cos \Omega + b \cos \forall = a \cos \Omega_0 + b$$

While \forall_{\max} is specified and quantities of a , b and Ω_0 are known, using above equations maximum Ω and y values can be found.

Mechanical Constraint of the Mechanism

In figure A4.2 the mechanism is shown when angle \forall takes its maximum value, \forall_M . As a characteristics of the mechanism, Ω value takes its minimum value in this limit position, Ω_m . Since the distance between leg-vehicle connections is fixed the same as the distance between the centres of two wheels of a car, maximum value of the turning angle, \forall_M , can be calculated using this mechanical limitation;

$$2 (a + b) \cos \Omega_m + b (\cos \Omega_m + \cos \forall_M) = 2 (a \cos \Omega_0 + b)$$

Considering the symmetry of the mechanism, Ω_m is equal to \forall_M .

Therefore above equation can be rewritten;

$$2 (a + b) \cos \forall_M = 2 (a \cos \Omega_0 + b)$$

For \forall_M the following statement can be obtained;

$$\Psi_M = \cos^{-1} \left[\frac{a \cos \Omega_o + b}{a + b} \right]$$

Manoeuvrability of the Vehicle

Using the maximum turning angle of the vehicle minimum radius for the arc trajectory of the vehicle can be calculated to have an idea about the manoeuvrability performance of a vehicle using this particular mechanism for body steering.

The angular positions of the vehicle front and back leg units are shown in figure A4.3 while turning. R represents the radius of the vehicle arc trajectory. To find the minimum value of the R , R_{\min} , Ψ_M can be substituted in stead of Ψ in the figure. Using the right triangle in the figure, the following equation can be obtained for R_{\min} ;

$$R_{\min} = \frac{a \cos \Omega_o + b}{\sin \Psi_M}$$

The same equation can be used to calculate the radius of the arc trajectory at any time using the value of Ψ . In the equation, value of Ψ can be substituted in stead of Ψ_M .

The Foot Stroke Variation with respect to the Steering of The Vehicle Body

While the body of the vehicle is steered to anticipate turns, the foot stroke lengths of the legs of the vehicle also should be adjusted accordingly.

Between the crank effective length and the produced foot stroke, there is a direct proportion. There is also a direct proportion between the radius of the leg arc trajectory and the arc length. Therefore the crank effective length of a leg is directly proportional to the radius of the leg arc trajectory. Moreover, it can be concluded that the ratio of crank effective lengths of parallel driven legs is equal to the ratio of the radii of leg arc trajectories.

Hence following equation can be written;

$$\frac{R + \partial R}{R} = \frac{(C_e)_{out}}{(C_e)_{in}}$$

where ∂R represents the distance between the inner leg and outer leg during the rotation. And C_e represents the crank effective length for outer and inner legs.

The figure A4.1 shows that the distance between the vehicle axis and the leg unit is equal to $a \sin \Omega_0$. Therefore ∂R can be calculated;

$$\partial R = 2a \sin \Omega_0$$

Hence, the equality of the ratios can be restated as follows;

$$\frac{R + 2a \sin \Omega_0}{R} = \frac{(C_e)_{out}}{(C_e)_{in}}$$

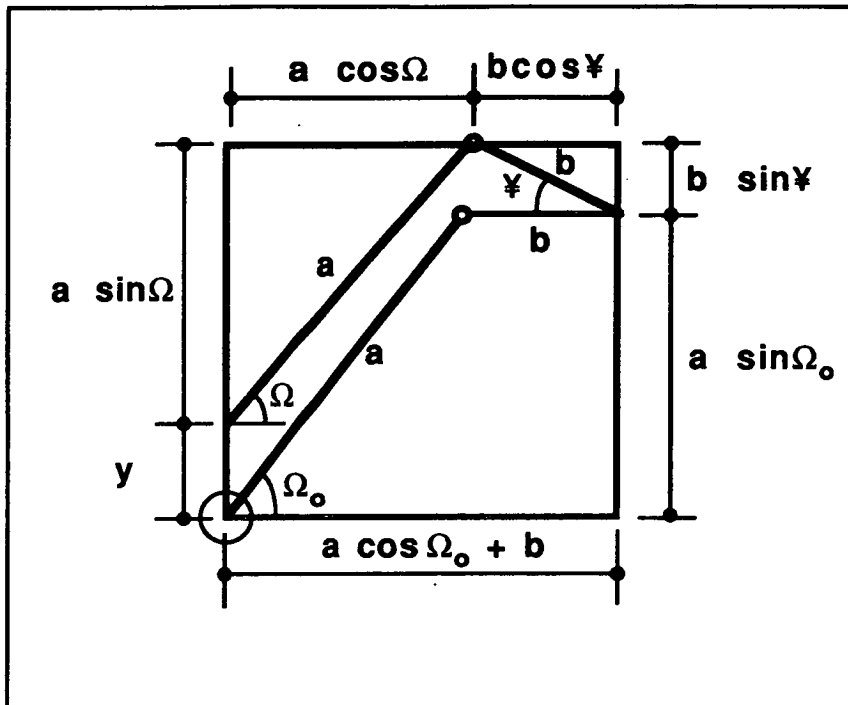


Figure A4.1 Geometric relations in the steering mechanism